Neutrophil Tissue Inhibitor of Matrix Metalloproteinases-1 (TIMP-1): Novel localisation, mobilisation and possible role

by

BRENDON PRICE

B.Sc. (*summa cum laude*), B.Sc. (Hons) (*cum laude*) (Natal)

Submitted in fulfilment of the
academic requirements for the degree of
Doctor of Philosophy
in the School of Molecular and Cellular Biosciences
University of Natal
Pietermaritzburg
February 2002

PREFACE

The experimental work described in this thesis was carried out in the Department of Biochemistry, University of Natal, Pietermaritzburg from January 1997 to October 2000 and in the Department of Biochemistry, University of Bielefeld, Germany from September 1997 to November 1997, under the supervision of Dr. Edith Elliott and Prof. Dr. Harald Tschesche, respectively.

These studies represent original work by the author and have not been submitted in any other form to another university. Where use was made of the work of others, it has been duly acknowledged in the text.

Brendon Price
February 2002

ABSTRACT

At the beginning of this study, the granule localisation and regulation of release of human neutrophil (PMNL) precursor collagenases, proMMP-8 and -9 (type I and type IV/V collagenases, respectively), enzymes highly active against the extracellular matrix (ECM) and thought to be relevant in invasion and inflammation, had been established while that of their inhibitor, tissue inhibitor of matrix metalloproteinases-1 (TIMP-1), had not.

Electron microscopy immunogold labelling of cryoultramicrotomy sections for granule marker proteins, lysosome-associated membrane proteins (LAMPs) and endocytosed bovine serum albumin-coated gold probes, followed by stereology, established that TIMP-1 was mainly located in a distinct oval, electron translucent organelle, a little larger than azurophil granules. A lack of labelling for endocytic markers and for glycosylphosphatidylinositol-anchored proteins, established using granule fractionation and immunolabelling to be markers for the secretory vesicles, and LAMPs-1 and -2, indicated the non-endosomal, non-secretory and non-lysosomal nature of this organelle. Density gradient cofractionation with the least dense secretory vesicle population and some pleiomorphism of the organelle suggested that it is a "vesicle" rather than a "granule" population. Colocalisation with proMMP-9 in minor subpopulations suggests that TIMP-1 vesicle biogenesis occurs between metamyelocytic and termination differentiation, but before secretory vesicle synthesis.

Immunolabelling of phagocytosed and pulse-chased IgG-opsonised latex beads showed that specific and azurophil granules and a small number of proMMP-8-containing granules (a specific granule subpopulation) fuse with the phagosome whereas the TIMP-1 vesicle and proMMP-9-containing granules do not, suggesting that the latter play no role in phagosomal destruction of IgG-opsonised bacteria and that their phagosomal release is not calcium regulated. However, studies using the calcium ionophore, ionomycin, and monitoring extracellular granule marker protein release upon addition of increasing levels of extracellular calcium, showed that all granules, except the TIMP-1 vesicle, appeared to be calcium regulated. This suggests that the regulation of proMMP-9 release is not exclusively via calcium and that TIMP-1 vesicle release is not calcium regulated.

Whereas most granules were shown to be associated with microtubule-like structures, the TIMP-1 vesicle and proMMP-9-containing granules were shown to associate with two morphologically different cytoskeletal elements, neither resembling actin nor tubulin. These elements, and the release of the TIMP-1 vesicle and proMMP-9-containing granules, need to be studied further, but results achieved to date may explain the observed differential mode of release of TIMP-1 relative to proMMP-9.

The proMMP-9-binding and inhibitory capacity of a 66 kDa high molecular mass form of TIMP-1 was demonstrated in PMNL homogenates and plasma using western ligand blots and a novel reverse zymography method. The role and relevance of this form remains unknown as does the relevance and potential role of proMMP-9/TIMP-1 complexes seen during isolation procedures. The proMMP-9/TIMP-1 complex may occur *in vivo*, as evidenced by immunolocalisation studies, and, together with TIMP-1 released from its own discrete vesicle population, may be responsible for the fine regulation of extracellular proteolysis.

ACKNOWLEDGEMENTS

I would like to express my appreciation and thanks to the following people for their contribution to this thesis and my sanity:

My supervisor, Dr. Edith Elliott, for allowing me to work independently and pursue the areas of neutrophil cell biology that I found both interesting and relevant, and for constant support and enthusiasm especially during the writing up of this thesis. In addition, many thanks for initiating contact with Prof. Tschesche's lab and providing the opportunity to work in his laboratories for 6 weeks.

Prof. Clive Dennison and Dr. Edith Elliott, for giving me the freedom to attend conferences both locally and abroad and for introducing me to prominent scientists in the field of proteolysis and cell biology.

Prof. Dr. Harald Tschesche, for allowing me to work in his laboratory and interrogate his students mercilessly about practical peculiarities of MMP biochemistry that do not appear in text.

Frau Margot Müller and her husband for their hospitality during my stay in Bielefeld and helping me find more suitable attire when I experienced my first European winter.

Volker Zölzer, Christian Kopp and Marc Luther, students of Prof Tschesche, for showing me around Germany and Nord-Rhein Wesfahlien over weekends and for introducing me to Weißbier.

Prof. Theresa Coetzer, for her generous donations of MMP references and her interest in my studies and for organising chickens for immunisations.

The Staff of the Centre for Electron Microscopy. To Tony Bruton for his assistance and advice; Vijay Bandu, for all his help on the TEM and the practical tricks of EM work. Thanks for all your patience and encouragement! Priscilla Donnelly, for sorting out all the darkroom

procedures and developing prints in a hurry when abstracts were due in yesterday; Belinda White, for all her help with SEM.

Dr. Richard Kirsch, Liver Research Unit, UCT for the donation of phalloidin, and for discussions and rantings and ravings about neutrophils.

Fellow past postgraduates, especially Nicollette Shearer and Kerry Taylor for their encouragement and positive thinking when my reserves were on empty. Thanks for Touchwood lunches, movies, nights out and tequila!

Nic Scholfield, for all her support and understanding of issues both academic and other (wink!). Thanks for providing many laughs and for all your suggestions regarding future DNA work and PCR and for making the Table of Contents a breeze and making me see the light of master documents and styles.

The students in Lab 44, Ché, Lizette, Thunicia and Dr. Frieda Dehrmann, for providing a fantastic environment for work and discussion and for laughing at my jokes.

AJ, for all your support and encouragement in the last few months of writing up when life, the universe and everything seemed too overwhelming.

Mrs Lesley Brown, for being the epitome of efficiency and ordering all my obscure chemicals and being the provider of caffeine! Thanks too for organising bank drafts for the Brdo Conference and for organising car hire on numerous occasions.

Ms Jenny Schwartz, for organising all things administrative.

Ms Melody Webber, for organising and preparing the third year Biochemistry Pracs and making my job of coordinating the pracs a great deal easier.

The University of Natal and the National Research Foundation (NRF), for bursaries and scholarships throughout my entire academic career, thereby allowing me to focus entirely on my studies.

Prof. Gillian Murphy (School of Biological Sciences, University of East Anglia, UK), for organising a full rebate on airfare and conferences fees to attend the 2000 Gordon Research Conference in New Hampshire, USA.

The German government and the NRF for funding the exchange visits and equipment as part of a bilateral scientific collaboration. The assistance of the Research Centre (Jülich, Germany) and in particular, Dr. U. Breuer, Dr. CH Manthem and Frau Wieland for administering the collaborative funds (Grant 396K0A6A) is greatly appreciated. In addition, thanks go to Prof. Drs. Hans Fritz and Harald Tschesche for organising this bilateral collaboration.

Jacqui and Margie, my two best friends, for the last 7 years and those to come.

EH and KS, for providing escapism.

My parents, Dave, Deidré, Dawn and Bobby for all your love, support and encouragement throughout my University career and for understanding when my work kept me away longer than I would have liked.

My grandparents, Joan and John Abbott, for all your love, encouragement and interest in my work.

My late grandmother, Amy Jane Price, to whom this thesis is dedicated, for the time we had together.

TABLE OF CONTENTS

CHAPTER 6

LIST OF FIGURES

LIST OF TABLES

LIST OF ABBREVIATIONS AND SYMBOLS

α_2-M	alpha$_2$-macroglobulin
ϕ	diameter
λ	wavelength
λ_{em}	emission wavelength
λ_{ex}	excitation wavelength
λ_{max}	wavelength of maximal absorbance
ρ	density/specific gravity
ζ	zeta potential
%C	monomer crosslinking concentration
%T	total monomer concentration
$[Ca^{2+}_i]$	intracellular calcium concentration
$[Ca^{2+}_{ex}]$	extracellular calcium concentration
[X]	concentration of compound X
A_x	absorbance at x nm
ABTS	2,2'-azino-di-(3-ethyl)-benzthiozoline sulfonic acid
AEBSF	4-(2-aminoethyl)-benzenesulfonyl fluoride
AMC	7-amino-4-methylcoumarin
APC(s)	antigen presenting cell(s)
ATP	adenosine 5'-triphosphate
BCA	bicinchoninic acid
B-cell	bone-marrow-derived lymphocyte
BCIP	5-bromo-4-chloro-3-indolyl phosphate
bp	base pairs
BPI	bactericidal/permeability-inducing protein
Brij 35	polyoxyethylene (23) lauryl alcohol
BSA	bovine serum albumin
C3a, C5a, C3b, C3bi, C1q	complement components
CAM	chorioallantoic membrane
CD	cluster determinant/cluster of differentiation
cDNA	complementary/copy DNA
CMC	critical micelle concentration
CPD	critical point drying
CTAB	cetyltrimethylammonium bromide
Da	dalton(s)
DAB	diaminobenzidine/3,3',4,4'-tetraaminobiphenyl
DAF	complement decay-accelerating factor
DAG	diacylglycerol
dist.H_2O	distilled water
dd.H_2O	MilliQ distilled, deionised water
DMF	dimethylformamide
DMSO	dimethylsulfoxide
DNA	deoxyribonucleic acid
DOC	deoxycholic acid
DTT	dithiothreitol
ECL	enhanced chemiluminescence
ECM	extracellular matrix

EDTA	ethylene diamine tetraacetic acid
EDX	energy dispersive X-ray microanalysis
EGTA	ethylene glycol-bis(β-aminoethyl ether) *N*,*N*,*N'*,*N'*-tetra acetic acid
ELISA	enzyme linked immunosorbent assay
EM	electron microscope/microscopy
EPA	erythroid potentiating activity
F-actin	filamentous actin (actin polymer)
Fc	fragment crystallisable
FcγR, FcεR	receptors binding the Fc region of the indicated Ig molecule (γ for IgG, ε for IgE)
FCA	Freund's complete adjuvant
FIA	Freund's incomplete adjuvant
FITC	fluorescein isothiocyanate
fMLP	*N*-formyl-L-methionyl-L-leucyl-L-phenylalanine
FSG	fish skin gelatin
g	relative centrifugal force
G3PDH	glyceraldehyde 3-phosphate dehydrogenase
G-actin	gel actin (actin monomer)
GAG	glycosaminoglycan
G(M)-CSF	granulocyte(macrophage) colony stimulating factor
GPI	glycosylphosphatidylinositol
G-protein	guanosine triphosphate binding protein
GTP	guanosine 5'-triphosphate
h	hour(s)
H_2O_2	hydrogen peroxide
HEPES	*N*-2-hydroxy-piperazine-*N'*-2 ethane sulfonic acid
HNE	human neutrophil elastase
HOCl	hypochlorous acid
HRP(O)	horseradish peroxidase
HSA	human serum albumin
IC_{50}	concentration resulting in 50% inhibition
ICAM-1/2	intercellular adhesion molecule-1/2
IgE, IgG, IgM, IgY	immunoglobulins E, G, M, Y
IL	interleukin
Ins 1,4,5 P_3	inositol 1,4,5 trisphosphate
IVVM	intravital video microscopy
k_{cat}	turnover number
kDa	kilodalton(s)
K_m	Michaelis constant
l	litre
LAMP	lysosome-associated membrane protein
Levamisole	L[-]-2,3,5,6-tetrahydro-6-phenylimidazo-[2,1-b] thiazole
LPS	lipopolysaccharide/endotoxin
LTB_4	leukotriene B_4
MDPF	2-methoxy 2,4 diphenyl-3(2*H*) furanone
MeOSuc	methoxysuccinyl
MHC	major histocompatibility complex
min	minute(s)
MMP	matrix metalloproteinase/matrixin
mOsm	milliosmols

MPO	myeloperoxidase
M_r	relative molecular mass
mRNA	messenger ribonucleic acid
MT-MMP	membrane-type MMP
NADP(H)	nicotinamide adenine dinucleotide phosphate
NBT	nitroblue tetrazolium
NGAL	neutrophil gelatinase-associated lipocalin
nm	nanometer (10^{-9} meter)
nM	nanomolar
NSF	*N*-ethylmaleimide-sensitive factor
o/n	overnight
$^1O_2$	singlet oxygen
O_2^-	superoxide free radical
$^\bullet OH$	hydroxyl free radical
P_2, P_3, P_4	bis-, tris-, and tetrakisphosphate
PA	phosphatidic acid
u/tPA	urokinase/tissue-type plasminogen activator
PAI	plasminogen activator inhibitor
PAF	platelet activating factor
PAGE	polyacrylamide gel electrophoresis
PBS(G)	phosphate buffered saline (with glucose)
PBS-Tween	Tween 20 dissolved in PBS
PC	phosphatidylcholine
*p*CMPSA	*para*-chloromecurophenylsulfonic acid
PCR	polymerase chain reaction
PE	phosphatidylethanolamine
PEG	polyethylene glycol
PFA	paraformaldehyde
pI	isoelectric point
PI	phosphatidylinositol
PI-PLC	phosphatidylinositol-specific phospholipase C
PIPES	piperazine-*N*,*N*'-bis(2-ethanesulfonic acid)
pKa	dissociation constant
PKC	protein kinase C
PLA_2, PLC, PLD	phospholipase A_2, C and D
PLT	progressive lowering of temperature
pM	picomolar (10^{-12} molar)
PMA	phorbol 12-myristate-13-acetate
PMNL(s)	polymorphonuclear leukocyte(s)/neutrophil(s)
PMSF	phenylmethylsulfonyl fluoride
PNH	paroxysmal nocturnal haemoglobinuria
*p*NP(P)	*para*-nitrophenyl (phosphate)
Ponceau S	3-hydroxy-4-[2-sulfo-4(sulfo-phenylazo)phenylazo]2,7-naphthalene disulfonic acid
PS	phosphatidylserine
PVDF	polyvinyldifluoride
-R	receptor
ROS	reactive oxygen species
RPMI	Roswell Park Memorial Institute
RT	room temperature
RTK	receptor tyrosine kinase

RT-PCR	reverse transcription PCR
s	second(s)
SCAMP	secretory carrier membrane protein
SDS	sodium dodecyl sulfate
SEM	scanning electron microscopy
serpin	serine proteinase inhibitor
sn	stereospecific numbering
SNAP	soluble NSF attachment protein
SNARE	soluble NSF attachment protein (SNAP) receptor
TAPS	*N*-tris(hydroxymethyl)methyl-3-amino-propanesulfonic acid
TBS	tris buffered saline
t-BuOH	tertiary butanol
TC	tropocollagen
TCA	trichloroacetic acid
T-cell	thymus-derived lymphocyte
TEM	transmission electron microscopy
TEMED	*N*,*N*,*N'*,*N*,'-tetramethyl ethylenediamine
TEN	tris-EDTA-NaCl
TIMP	tissue inhibitor of the MMPs
™	trademark
T_m	melting temperature
TNFα	tumour necrosis factor-α
TPP	three phase partitioning
Tricine	*N*-[2-hydroxy-1,1-bis(hydroxymethyl)ethyl]glycine
Tris	2-amino-2-(hydroxymethyl)-1,3-propandiol
TRITC	tetramethyl rhodamine isothiocyanate
Triton X-100	polyoxyethylene (9-10) *p*-*t*-octyl phenol
Triton X-114	polyoxyethylene (7-8) *p*-*t*-octyl phenol
UV	ultraviolet
VAMP	vesicle associated membrane protein
μm	micrometer (10^{-6} meter)

"The joy of discovery is certainly the liveliest that the mind of man can ever feel."

Claude Bernard (1813-78). French physiologist

CHAPTER 1

Introduction

1.1 Invasion

Throughout the life of an organism, a complex balance of protein anabolism and catabolism is required for the maintenance and turnover of cells, tissues and organs. During development, various cells and organs may override the protein turnover balance in order to invade or pass through a local protein barrier. Examples of this invasion process are found in blastocyst implantation into the uterine wall and angiogenesis - processes that are (temporarily) catabolic, yet essential for survival. Further examples of cellular invasion include the extravasation of immune cells into the perivascular tissue during infection and inflammation and the metastatic movement of malignant cancers to distant sites. Apart from sharing the common feature of invasion, these processes seem largely reliant on enzymatic destruction of tissues. Members of the proteinase family of enzymes have attracted interest and have been implicated in such invasive behaviour, although other non-proteolytic enzymes and growth factors are known to contribute to the entire process (Mignatti and Rifkin, 1993).

Invasion from the bloodstream into the perivascular stromal tissue occurs in both metastatic spread of malignant cells and during normal tissue migration by phagocytes during chemotaxis towards a site of infection or inflammation. For the purposes of this study, the mechanisms involved in the invasive movement of the neutrophilic polymorphonuclear leukocyte (PMNL) during inflammation and tumour metastasis are of interest as common proteinases may be involved. The main barrier to cell invasion (malignant or normal immune) into the perivascular stromal layer and underlying tissue, is the extracellular matrix (ECM). This multi-protein complex provides a support framework for endothelial cells (i.e. the basement membrane component of the ECM) and elastic, compressive and tensile strength to the tissue. The protein components of the ECM vary with respect to charge, glycosylation, tertiary structure and amino acid composition. Therefore, it would seem that destruction and migration through the ECM would require one or more highly specific and active enzyme species. Among these, the matrix metalloproteinases (MMPs), found in a variety of human tissues and cell types [e.g. monocytes and macrophages (Campbell *et al.*, 1991), lymphocytes (Goetzl *et al.*, 1996) and PMNLs (Murphy *et al.*, 1980; Hasty *et al.*, 1990; Edwards, 1994)], have the widest specificity for ECM

components.

1.2 The ECM and invasion

The ECM is responsible for the separation of tissue and organs from each other and is comprised of two main parts: the basement membrane upon which endothelial cells are anchored and orientated, and the interstitial stroma which acts as a scaffolding or support structure (Haralson and Hassell, 1995). The basement membrane is further divided into the lamina lucida, lamina densa and lamina fibroreticularis (Mignatti and Rifkin, 1993; Adachi *et al.*, 1997) (Figure 1.1). The lamina lucida occurs directly beneath the cell layer and is supported by the lamina densa. All of these layers are supported by the fibroreticularis. The interstitial stroma lies beneath the basement membrane and contains cells such as fibroblasts, which continually synthesise and degrade ECM components (Haralson and Hassell, 1995).

The predominant ECM proteins are the members of the collagen family, particularly the fibrillar collagens [types I, II (in cartilage), III and V] and the 'mat-like' type IV collagen upon which cells are anchored (Adachi *et al.*, 1997). Other ECM constituents include glycoproteins (e.g. laminin, fibronectin, entactin, nidogen), proteoglycans, elastin (a non-glycosylated protein) and glycosaminoglycans (GAGs). Their relative distributions are shown in Figure 1.1. While the collagens are required for maintaining ECM tensile strength and provide a substratum upon which cells can grow, the glycoproteins play important roles in structural stabilisation of the ECM and are important ligands for cell-derived receptors. Maintenance of the integrity of glycoproteins and contact with the glycoproteins in the ECM via such receptors is necessary to give rise to signal transduction, allowing cell division and proliferation in attached cells. Elastin is responsible for maintaining elasticity and allowing transient deformation of the ECM during protein turnover. The proteoglycans consists of a protein core to which high molecular mass (M_r) GAGs are attached. These are responsible for filling in spaces in the ECM since they attract large hydration shells due to their nett anionic charge. The resultant 'swelling' provides mechanical strength while allowing solutes to diffuse easily through the ECM (Mignatti and Rifkin, 1993). The exact composition and relative amounts of ECM components are tissue specific and, therefore, this chapter will only consider the perivascular ECM as the focus of this study is PMNL invasive movement into the perivascular tissue.

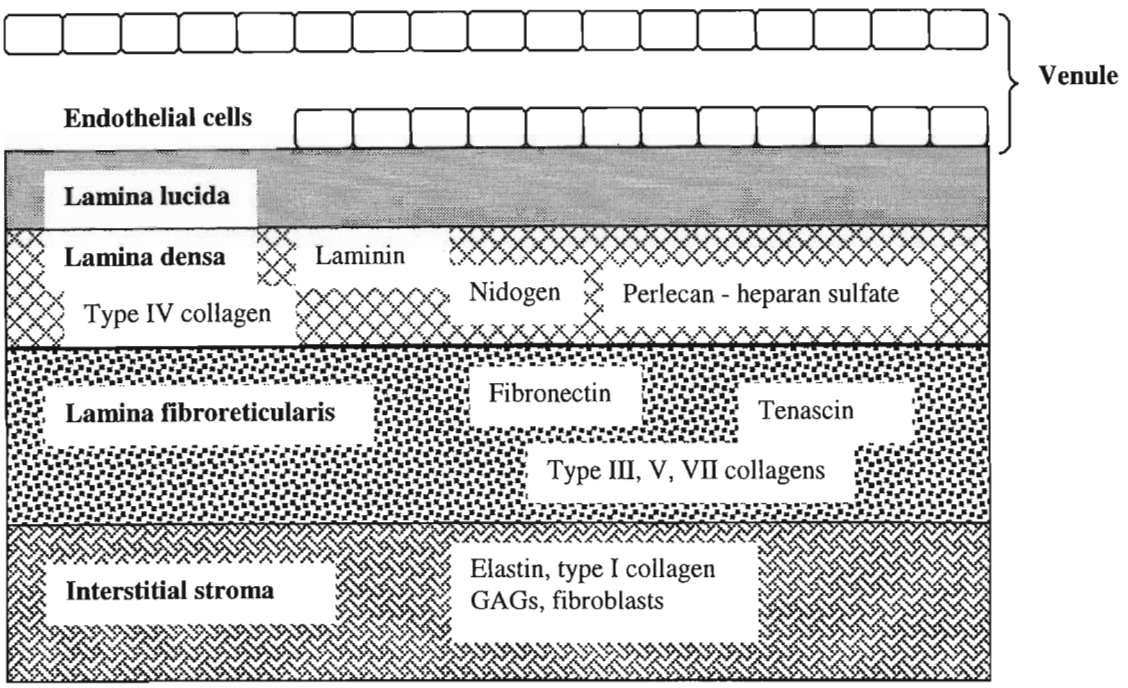

Figure 1.1 **A simplified representation of the spatial arrangement and components of the ECM.**

(from Mignatti and Rifkin, 1993; Adachi *et al.*, 1997).

As previously mentioned, cellular invasion of the ECM occurs in normal conditions (such as angiogenesis, blastocyst implantation, movement of fibroblasts and leukocytes). In such cases, protein degradation usually seems to be transient and balanced by increased synthesis and/or downregulation of proteinase activity by endogenous inhibitors. Pathological situations arise when ECM protein synthesis is defective (or downregulated) or when the local enzyme concentration exceeds that of endogenous inhibitors. This is evident in conditions such as rheumatoid arthritis, inflammation and possibly in invasive cancers (Weiss, 1989).

The proteinases responsible for ECM degradation may differ with respect to substrate specificity and the cell(s) of origin. Simple exclusion of potential candidate proteinases (serine, aspartate, cysteine, metallo-, threonine) on the basis of their pH optima and apparent lack of activity at physiological pH is inadvisable as favourable pH microenvironments may be formed in pockets between the cell surface and the target ECM molecules. These microenvironments possibly facilitate degradation and allow temporary protection of the enzyme from inhibitors present in the rest of the environment (Owen and Campbell, 1999). In addition, exclusion of candidate proteinases by virtue of their normal *in vivo* sites of action and occurrence (e.g.

intracellular/lysosomal) may be equally unsound since mistrafficking of enzymes to cell surfaces may occur naturally by default, and has been observed in transformed cells (Sloane *et al.*, 1994). For these reasons, any proteinase/glycosidase that shows activity towards an ECM component should be considered a candidate with potential for assisting cellular invasion, regardless of its accepted pH optimum and subcellular localisations. Furthermore, enzymes which do not cleave ECM components may exert their effects 'upstream' of the proteolytic/proteoglycolytic cascade by activating proteinase zymogens, which in turn, may cleave the ECM.

Tissue invasion by leukocytes and lymphocytes appears to occur during inflammation to allow PMNLs, monocytes, killer T-cells and antibody-producing B-cells to leave the bloodstream (extravasate) and travel to a site from which the inflammatory signals originate (Goetzl *et al.*, 1996). PMNL MMPs-8 (type I collagenase) and -9 (type IV/V collagenase; type I gelatinase), which are synthesised during specific periods of maturation of the PMNL and are stored in intracellular organelles known as 'granules', both display high proteolytic activity against ECM collagens and, hence, potentially play an important role in PMNL extravasation, tissue invasion and inflammation (Mainardi *et al.*, 1980; Murphy *et al.*, 1980; Bakowski and Tschesche, 1992; Edwards, 1994).

There is also considerable support for the possibility that only mechanical deformation of the ECM is used by the invading cell (Steadman *et al.*, 1997). This evidence has, however, been gained from *in vitro* methods (which may not reflect the *in vivo* situation) whereas *in vivo* methods support the role of MMPs in invasion (Nagai and Katori, 1988; Oda *et al.*, 1995; Kim *et al.*, 1998). For this reason, the compartmentalisation of the MMPs relative to their inhibitor (tissue inhibitor of matrix metalloproteinases/TIMP) and the regulation of the release of such granules may be important in strategies aimed at controlling inflammation.

1.3 PMNL granules and regulation of granule biosynthesis

All cells of the haematopoietic system are derived from bone marrow multipotent stem cells (Edwards, 1994) and are capable of mitotic division (clonal proliferation) or differentiation into myeloid or lymphoid stem cells. Upon differentiation, the cells become committed to producing myeloid-derived cells [platelets (blood clotting), erythrocytes (gaseous exchange), eosinophils (parasite killing, inflammation, chemotaxis), basophils (inflammation), PMNLs (inflammation and phagocytosis), monocytes (inflammation, phagocytosis and antigen presentation)] or

lymphoid cells [T-cells (killing of cells infected with viruses or intracellular pathogens) and B-cells (antibody production for pathogen opsonisation and killing via complement)], respectively (Roitt, 1994). The PMNLs are the first leukocyte population to reach the site of infection during inflammation and kill pathogens by releasing (or 'degranulating') reactive oxygen species, enzymes and bactericidal proteins from various populations of pre-synthesised cytoplasmic organelles ('granules') (Bainton, 1973; Weiss, 1989; Edwards, 1994; Roitt, 1994).

During PMNL maturation (myeloblast→promyelocyte→myelocyte→metamyelocyte→band cell→segmented cell), granules are synthesised in a maturation-dependent order and stored in the cytoplasm until their degranulation or release. The first type of granule synthesised in the myeloblast to promyelocyte stages of maturation, is histochemically positive for myeloperoxidase (MPO) and stains red/purple with azure dyes, indicating that it is marginally acidic. These granules were initially named primary granules as they are the first population to the synthesised and later they were named azurophil granules as they take up azure dyes (Damiano *et al.*, 1988). As the PMNL continues to progress through the myelocytic to the segmented stage, synthesis of azurophil granules decreases (since their synthesis is both maturation-dependent and transient) and other MPO-negative populations are synthesised. These were initially termed secondary granules, due to their time of synthesis, but this nomenclature later gave way to the term specific granules since they also stain positive for specific dyes. These granules are also found to contain the iron-binding protein, lactoferrin (Breton-Gorius *et al.*, 1980; Cramer *et al.*, 1985). Due to the limitations of the available techniques used during the early PMNL granule morphological studies, it was generally accepted that only two granule populations existed within the PMNL.

A third PMNL granule population containing neither MPO nor lactoferrin was subsequently discovered (Kjeldsen *et al.*, 1992; Sengeløv *et al.*, 1993). This granule population was enriched in type IV/V collagenase/gelatinase (proMMP-9), was termed the 'C-particle' or the 'gelatinase granule' and was found to be synthesised during the late segmented and band cell stages of PMNL maturation. This stage of expression is in contrast with the majority of lactoferrin (myelocyte/metamyelocyte stage) and MPO (myeloblast/promyelocyte stage) expression (Borregaard *et al.*, 1995). Subsequently, a fourth granule population was identified by high voltage free-flow electrophoresis and was termed the 'phosphasome' (due to the presence of alkaline phosphatase) or 'secretory vesicle' (Sengeløv, 1996). Due to the similarity in density of secretory vesicles and plasma membranes, it was found that efficient separation could only be

achieved by exploiting differences in membrane zeta (ζ) potentials in an electric field (Sengeløv and Borregaard, 1999).

The secretory vesicles are thought to be the last population synthesised during PMNL maturation, and are possibly formed by endocytosis (Borregaard and Cowland, 1997). They contain the majority of the receptors of ECM proteins and, due to their endocytic origin, they also contain some plasma proteins (Table 1.1).

The need for a reliable marker system that would allow accurate granule designation for various PMNL proteins that were discovered, prompted extensive research into the protein content of various granules. During the initial stages of such research, many incorrect and conflicting granule designations were made (Bainton *et al.*, 1971; Bainton, 1973; Absolom, 1986). Such ambiguity highlighted the need for more discriminating techniques for granule separation and characterisation.

Initially, electron microscopy (EM) made it possible to distinguish populations on the basis of morphology and electron density. Modern granule classifications, however, require additional information on protein content, size, shape and density of granules as well as granule marker content. There still remain conflicting opinions regarding granule population numbers and contents. At the time of the commencement of this study, the granule designation of some proteins (e.g. heparanase, and TIMP-1) and the identity and compartmentalisation of proMMP activators, relative to proMMPs, were unknown.

Table 1.1 shows the order of synthesis and protein content of the four main granule populations (azurophil, specific, gelatinase, secretory) accepted at the time of writing. The marker proteins used in classifying these granule populations are: MPO (azurophil), neutrophil gelatinase-associated lipocalin/NGAL (specific), lactoferrin (specific), proMMP-9 (specific and gelatinase) and alkaline phosphatase (secretory vesicles). From Table 1.1 it is evident that the PMNL contains a highly sophisticated and heterogeneous collection of proteins for a number of diverse cellular functions including pathogen destruction and extracellular ligand binding. Although only four main populations are commonly mentioned in communications, there are at least six granule species including:

- dense defensin-rich MPO-positive granules (azurophil type) (Pember and Kinkade, 1983; Oren and Taylor, 1995)
- light defensin-poor MPO-positive granules (azurophil type) (Pryzwansky and Breton-Gorius, 1985; Rice *et al.*, 1987)
- dense MPO-negative granules containing lactoferrin, NGAL and no gelatinase (specific type) (Kjeldsen *et al.*, 1994)
- intermediate MPO-negative granules containing lactoferrin, NGAL and gelatinase (specific type) (Kjeldsen *et al.*, 1992)
- light MPO-negative granules containing gelatinase but no lactoferrin (gelatinase type) (Sengeløv *et al.*, 1995)
- light MPO-negative granules containing alkaline phosphatase but no gelatinase (secretory type) (Sengeløv, 1996).

The secretory vesicles have been found to be enriched in receptors and to play an important role in allowing the PMNL to recognise and bind extracellular proteins during inflammation and diapedesis while the specific and gelatinase granules have been found to contain enzymes and proteins that generally exert their biological effect extracellularly [urokinase-type plasminogen activator (uPA), MMPs, histaminase etc.] (Borregaard and Cowland, 1997). The lactoferrin-positive specific granules and the azurophil granules contain proteins that are bactericidal and play a role in pathogen destruction [bactericidal permeability inducing protein (BPI), defensins, MPO etc.] during phagocytosis and/or extracellular degranulation (Edwards, 1994). The azurophil granules contain most of the digestive enzymes with broad pH optima. Since azurophil granules are rarely released, they are not equipped with many receptors (for ECM proteins or chemoattractants) as these are required to be released relatively early in PMNL activation, e.g. during diapedesis. Although the azurophil granules are considered to be marginally acidic (Anderson and Orci, 1988), the membrane-bound ATPase resident in azurophil granules probably functions to acidify the phagosomal compartment after ingesting a microorganism (Tapper, 1996). Reports have shown that the intraphagosomal pH initially rises [(due to the reduction of free protons to form hydrogen peroxide (H_2O_2)] and therefore, acidification via ATPases is required to allow full destruction of the ingested particle (Segal *et al.*, 1981).

It is not known how targeting of these maturation-dependent proteins to the correct granule occurs. Intuitively, it could be reasoned that the production and targeting of nascent proteins to

the four main granule populations would require highly sophisticated sorting mechanism(s) (e.g. signal retention motifs or complex glycosylation patterns) (Garwicz *et al.*, 1998). A complex series of post-Golgi vesicles and fusion machinery would also be required to ensure correct delivery to the appropriate granule type. Experiments have also shown that the mistargeting of certain proteins can result in their degradation by resident proteinases. Transfection of HL-60 PMNL-like cells with a vector containing the NGAL gene, for example, results in targeting of NGAL (a specific granule marker protein) to the azurophil granule where it is degraded (Le Cabec *et al.*, 1996). Since *active* human neutrophil elastase (HNE) and cathepsin G reside in the azurophil granule, they have the potential to destroy 'inappropriately included' proteins in the azurophil granule.

Gullberg *et al.* (1997) suggested that proteins destined for storage (i.e. granule proteins) are selected and packaged by aggregation while those destined for immediate secretion remain soluble. Although this hypothesis has not been proven, there is evidence to suggest aggregation of proteins with exceptionally high pI-values (>10) occurs by complexation with anionic GAGs (such as chondroitin sulfate) (Kostoulas *et al.*, 1997). This has been proposed to explain the high-density packing found in azurophil granules.

A more plausible hypothesis explaining the observed sorting of newly synthesised proteins, was put forward following *in situ* hybridisation studies on bone marrow cell mRNA transcripts (Fouret *et al.*, 1989). In this study, it was observed that gene transcription was transient and occurred at specific stages during PMNL maturation. This suggests that granule membrane and matrix compositions are determined by proteins cotranscribed and translated at a particular moment in time and suggests the existence of common transcriptional activators or the possibility of contiguous gene loci for protein cotranslation. The latter suggestion has been proven for the azurophil granule serine proteinases (Hanson *et al.*, 1990; Heusel *et al.*, 1991) but not for other proteins.

Selective targeting of proteins to a particular granule population, therefore, appears to be under control of developmentally regulated transcriptional factors. What is even more remarkable is that proteins that are coordinately transcribed and translated at the same stages appear to possess similar biological activities and/or functions (refer to Table 1.1). For example, most of the ECM receptors reside in secretory vesicles, both MMPs (proMMP-8 and -9) occur in the specific granules and all the serine proteinases and bactericidal peptides occur in the azurophil granules

(Borregaard *et al.*, 1993; Borregaard and Cowland, 1997). Therefore, the PMNL can perform separate *in vivo* functions (e.g. binding to ECM, pathogen killing) by releasing a single granule population.

An interesting link between the time of granule synthesis and order of release is shown in Table 1.2. The suggestion that the protein content of the different granule types is determined by the transient protein expression and simultaneous biosynthesis of various granule types has been termed the 'targeting by timing' hypothesis. Once all the proteins of the last PMNL granule population (i.e. the secretory vesicles) have been formed, there would apparently be no need for further gene transcription owing to the fact that blood PMNLs have a half life of ~6 h (Watson *et al.*, 1996). This may give rise to the apparent 'overlap' of granule marker proteins in population subtypes (as the synthesis of one marker protein diminishes as another commences). The transient expression system, therefore, seems to dispense with the need for a complex vesicular trafficking system from the Golgi stacks and ensures correct protein targeting.

Although it is widely assumed that mature PMNLs are transcriptionally inactive (due to the absence of a visible Golgi apparatus) and do not synthesise new proteins after full maturation has been reached, radioisotope uptake studies show that they do continue to express 'housekeeping' genes (e.g. glycolytic enzymes, cytoskeletal components) (Edwards, 1994). The changes in protein expression involved during the transition from a resting to an inflammatory PMNL have also not been extensively studied (partly due to the fact that inflammatory tissue PMNLs are difficult to isolate), but it is known that extensive glycogen accumulation occurs and that the PMNL half life extends to days (probably due to suppression of normal apoptotic signals) (Robinson *et al.*, 1982).

Unlike the closely related macrophage, the mature resting PMNL does not exhibit appreciable endocytic or fluid phase pinocytic activity. Upon stimulation, however, the rate of endocytosis increases and secretory vesicle-derived cell surface receptors are exposed onto the cell surface (Berger *et al.*, 1994). Endocytosis is thought to occur only during PMNL maturation, potentially explaining the presence of plasma proteins in the lumen of secretory vesicles and the use of human serum albumin (HSA) as a marker protein for such vesicles (see Table 1.1). Unlike conventional endocytosis, the membrane and contents of these vesicles are not recycled to the plasma membrane until the PMNL is activated (Kobayashi and Robinson, 1991; Borregaard *et al.*, 1993; Borregaard and Cowland, 1997).

In order to control the release of the various granule populations, the PMNL relies on cytoskeletal and fusion protein assembly. There is a distinct order of granule release during PMNL activation (Pryzwansky *et al.*, 1979; Dewald *et al.*, 1982; Lew *et al.*, 1986; Sengeløv *et al.*, 1993; Sengeløv *et al.*, 1995) and this is generally regulated by intracellular Ca^{2+} levels (Table 1.2). After an introduction to the role of PMNLs in fighting infection, a brief introduction of the PMNL cytoskeletal components and granule fusion proteins is presented to to give an overview of the events that occur during exocytosis/degranulation and how these are controlled. This is followed by a review of signal transduction in the PMNL and a review of the MMPs and their specific inhibitors, the TIMPs.

Table 1.1 **Established PMNL granule populations, their time of synthesis and membrane constituents and protein contents.**
(Dewald *et al.*, 1975; Mason *et al.*, 1991; Egesten *et al.*, 1994; Kjeldsen, 1995; Borregaard and Cowland, 1997; Mollinedo *et al.*, 1997).

	Azurophil granules	**Specific granules**	**Gelatinase granules**	**Secretory vesicles**
Time of synthesis	Myeloblast/Promyelocyte (First)	Myelocyte/Metamyelocyte (Second)	Band cell/segmented (Third)	Segmented (Fourth)
Membrane	CD63, CD68	CD11b, CD15, CD66, CD67	CD11b	Alkaline phosphatase*
	V-type H^+-ATPase	Cytochrome b_{558}	Cytochrome b_{558}	CR1, cytochrome b_{558}
		FMLP-R, fibronectin-R, laminin-R	FMLP-R, SCAMP	CD10, CD13, CD11b,
			uPA-R	CD14, CD16b, CD45
		G-protein$_\alpha$-subunit	VAMP-2	FMLP-R, SCAMP, uPA-R
		NB1 antigen	V-type H^+-ATPase	VAMP-2, C1q-R, DAF
		19 kDa protein, 155 kDa protein	DAG-deacylating enzyme	V-type H^+-ATPase
		Rap1, Rap2		
		SCAMP, VAMP-2		
		Thrombospondin-R, vitronectin-R		
		TNFα-R, uPA-R		
Lumen	Acid phosphatase, chondroitin sulfate, α1-proteinase inhibitor, MPO, sialidase, Proteinase-3 Ubiquitin protein, glycosidases, cathepsin G, defensins, HNE, lysozyme	β_2-microglobulin, proMMP-8, proMMP-9, NGAL, hCAP-18, histaminase, heparanase, lactoferrin, lysozyme, uPA, sialidase, SGP 28, vit B_{12}-binding protein	Acetyltransferase β_2-microglobulin, proMMP-9, lysozyme	HSA, tetranectin (and other plasma proteins)

* The underlined proteins represent currently accepted granule markers. -R = receptor

1.4 The role of PMNLs in fighting infection

The PMNL is responsible for engulfing and destroying opsonised pathogens (Rabinovitch, 1995). Compared to monocytes, PMNLs are the major leukocyte population (40-65%) in the bloodstream, while macrophages are responsible for pathogen destruction in the tissue (Edwards, 1994). PMNLs are not antigen presenting cells (APCs), but following phagocytosis and apoptosis, they release a large number of cytokines to attract other leukocyte APCs and facilitate the final removal of effete PMNLs (Savill *et al.*, 1989; Yamashita *et al.*, 1999).

The mature PMNL does not contain mitochondria and hence derives most of its energy (in the form of ATP) from glycolysis. Anaerobic respiration allows PMNLs to function under low oxygen conditions and frees up available oxygen for use in the respiratory burst rather than as a terminal electron acceptor in oxidative phosphorylation (hence the absence of mitochondria). In addition to the glycolytic pathway, PMNLs utilise the hexose monophosphate shunt to produce nicotinamide adenine dinucleotide phosphate (NADPH) - a key compound required in the respiratory burst by NADPH oxidase (Edwards, 1994; Hampton *et al.*, 1998; Babior, 1999). PMNLs destroy pathogens by oxidative and non-oxidative processes following degranulation and/or phagocytosis. Oxidative destruction processes, or respiratory burst, involves formation of free radicals from oxygen (e.g. O_2^-, H_2O_2, •OH) and conversion of H_2O_2 into hypohalous acids by MPO (Weiss, 1989; Hampton *et al.*, 1998; Babior, 1999). Free radicals may oxidise unsaturated lipids in the pathogen membrane and thereby exert a cytotoxic effect. In some cases, oxidative enzymes may be additionally responsible for activating or downregulating other PMNL proteins (Clark and Borregaard, 1985; Weiss, 1989). Non-oxidative processes of pathogen destruction include the use of cationic bactericidal peptides (defensins), proteinases, peptidoglycanases, lipases and glycosidases (Lehrer and Ganz, 1990; Edwards, 1994; Owen and Campbell, 1999).

Due to the short life span of a circulating PMNL (~5-6 h) (Watson *et al.*, 1996), the bone marrow may be required to synthesise up to $2x10^{10}$ cells per day in a healthy individual and even more during a bacterial, yeast or fungal infection. The life span of PMNLs can, however, be increased up to a few days if they extravasate and infiltrate into the perivascular tissue (Edwards, 1994).

Since the PMNLs are highly motile cells and are required to deform their shapes in order to phagocytose foreign substances, control granule mobilisation and migrate through tissue to sites of infection, regulation of their cytoskeletal network is complex. The PMNL cytoskeleton is composed of the microfilaments (actin, myosin), microtubules, intermediate filaments along with a wide range of anchorage and binding/crosslinking proteins that regulate the state of actin and tubulin polymerisation within the cytoplasm (Nabi, 1999). For migration, receptor recycling, phagocytosis or degranulation to occur, transient depolymerisation events followed by repolymerisation are required, and PMNLs are reliant on strict control of such processes. The polymerisation of certain cytoskeleton components is finely regulated by the intracellular $[Ca^{2+}]$ ($[Ca^{2+}_i]$). Such events will be considered in more detail in Section 1.5.

During chemotaxis and invasion, PMNLs respond in a number of sequential steps (Oda *et al.*, 1992) (see Figure 1.2). In the first instance, PMNLs are required to:

1. *identify and locate the source of the infection.* A wide (although, asymmetrical) distribution of receptors on the surface of PMNLs allows them to sense chemoattractant gradients, which are usually produced by endothelial, epithelial and stromal cells. In addition, bacteria release chemotactic formylated peptides and lipopolysaccharide (LPS), indirectly allowing activation of C5 to give rise to the anaphylatoxin and chemoattractant, C5a, via complement fixation (Foxman *et al.*, 1997). These compounds diffuse through the ECM, forming a chemotactic gradient. The PMNL is equipped with receptors capable of recognising and binding such common inflammatory mediators [e.g. *N*-formyl-L-methionyl-L-leucyl-L-phenylalanine (fMLP), interleukin-8 (IL-8), platelet activating factor (PAF), leukotriene B_4 (LTB_4), C5a, IgG]. Binding of ligand to receptor activates a signal transduction pathway and allows cell polarisation in the direction of the chemoattractant (Albrecht and Petty, 1998).

2. *expose receptors on their plasma membranes that will recognise and bind venular endothelial cells.* Upon recognition of the chemoattractant, the PMNL upregulates additional receptors onto its plasma membrane, including those which bind to ECM components (e.g. collagen, laminin, vitronectin, fibronectin) and endothelial ligands [e.g. intercellular adhesion molecule (ICAM)-1 and 2]. PMNLs attach to the surface of endothelial cells (a process known as 'rolling') via lectin-like proteins known as selectins. PMNLs bind to endothelial P-selectin, which is quickly shedded and replaced by E-selectin. To minimise hydrodynamic shear while attached to the endothelial cells, PMNLs upregulate L-selectin and a lectin-like protein called P-

selectin glycoprotein ligand-1 to form PMNL-PMNL interactions (Walcheck *et al.*, 1996). This assists the PMNLs to remain immobilised long enough to expose more receptors on the plasma membrane. Upon binding of PMNL $CD11_{(a/b/c)}$/CD18 (collectively known as the β_2-integrins) (Edwards, 1994) to endothelial ICAM-1, endothelial myosin light chain kinase is activated and results in cell contraction and transendothelial migration of PMNLs at tight- and adherence junctions (Feng *et al.*, 1998; Saito *et al.*, 1998).

3. *pass through adjacent endothelial cells and migrate into the tissue up a chemotactic gradient.* Recent studies by Foxman *et al.* (1997), on PMNL responses in competing chemotactic gradients, demonstrate that leukocyte migration is determined by the combination and sequence of chemotactic agonists encountered during extravasation and tissue infiltration. Since there may be more than one chemoattractant present in the tissue, the PMNL is capable of 'prioritising' the signals to which it responds. The simultaneous expression of multiple receptors (i.e. receptors for host- and pathogen-derived chemoattractants) is essential to allow PMNLs to 'home' onto a target cell.

4. *locate, phagocytose and kill the foreign organisms.* Microbe opsonisation is essential for recognition by PMNLs. This is accomplished by complement activation via the classical (IgG-mediated) and/or alternate pathway. Opsonisation of the microbe by either IgG or C3bi ensures phagocytosis and intracellular destruction. Intracellular as opposed to extracellular destruction is generally favoured since the products contained within the PMNL are not able to diffuse from the site of infection, thereby terminating stimulation of the PMNL and the humoral immune system. Intracellular destruction also ensures containment of reactive oxygen metabolites that may cause tissue damage if released extracellularly (Hampton *et al.*, 1998). Phagocytosis involves fusion of cytoplasmic granules with the nascent phagosomal membrane and gradual acidification to allow optimal activity of microbicidal proteins in the mature phagolysosome (Tapper, 1996). The NADPH oxidase complex is assembled in the phagosome during phagocytosis following fusion of the granule populations that contain the NADPH oxidase components. An increase in NADPH concentration, supplied by the hexose monophosphate shunt due to an increased glycolytic rate during phagocytosis, allows H_2O_2 formation ($NADPH + 2O_2 \rightarrow 2O_2^{\bullet-} + H^+ + NADP^+$). This is subsequently converted to hypochlorous acid (HOCl) by MPO and is responsible for pathogen destruction (Hampton *et al.*, 1998; Babior, 1999). Other reactive oxygen species (ROS) produced during phagocytosis include the hydroxyl radical ($\bullet OH$), singlet oxygen ($^1O_2$), chloramines, nitric oxide and peroxynitrite

(Edwards, 1994; Hampton *et al.*, 1998; Babior, 1999).

5. *produce secondary cytokines to recruit further inflammatory cells to the site of infection.* The PMNL produces the lipid inflammatory mediator, LTB_4, from arachidonic acid released either by the activity of phospholipase A_2 (PLA_2) or diacylglycerol lipase during signal transduction. This acts as a PMNL attractant and allows recruitment of more PMNLs to the site of infection. In some instances, PMNLs produce thromboxane B_2 and prostaglandin E_2 from arachidonic acid and these serve to promote further vasodilation and transport of PMNLs to the site of infection. Other cytokines produced include interleukins (IL-1, -6, -8) colony stimulatory factors (M-CSF, G-CSF), interferon-α and tumour necrosis factor-α (TNF-α) (Edwards, 1994).

6. *die via apoptosis after ingesting the foreign microorganism and become engulfed by tissue macrophages. The macrophages may subsequently process and display antigens to lymphoid cells and elicit further cell recruitment and/or IgG production.* The high concentration of reactive oxygen intermediates produced by the respiratory burst may cause cytotoxic effects to the PMNL (including DNA fragmentation, unsaturated lipid peroxidation and protein cross-linking) and, hence, induce apoptosis. Addition of antioxidants [dimethylsulfoxide (DMSO, reduced glutathione and *N*-acetyl cysteine] to PMNLs have been shown to suppress apoptosis (Watson *et al.*, 1996), thereby confirming the suicidal effect of the released ROS microbicidal compounds. Recent evidence by Yamashita *et al.* (1999) indicates the involvement of caspases in PMNL apoptosis. Therefore, the signal transduction pathway(s) involved in PMNL death add complexity to the process of PMNL turnover.

5. *if the organism is too large for phagocytosis, PMNL granules and their contents can also be released extracellularly.* This is known as 'frustrated phagocytosis' and involves extracellular release of enzymes within close proximity to the foreign particle to prevent diffusion and damage to the surrounding host tissue. All of the above events are summarised in Figure 1.2.

The process of tissue invasion described above requires fine regulation of both polymerisation status of the PMNL cytoskeleton (to allow both polarisation and deformation of the cell during extravasation) and differential granule release. The primary focus of this study is the localisation and release of MMPs relative to TIMP-1 in PMNLs and, therefore, a brief description of the PMNL cytoskeleton and the mechanisms controlling granule fusion and extracellular release is provided in Section 1.5.

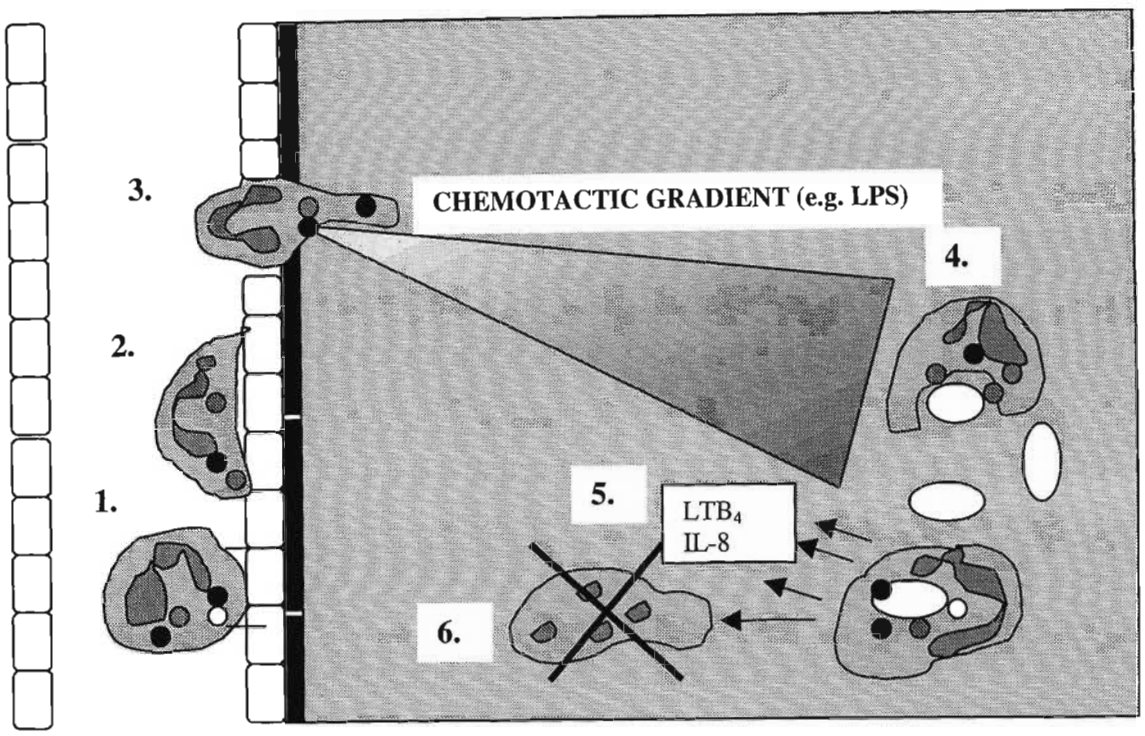

Figure 1.2 **Stages of PMNL chemotaxis and tissue infiltration.**

Upon detection of a chemoattractant, the PMNL rolls and adheres to the venular endothelium by means of receptors (1 and 2). Binding to the endothelial cells and signal transduction results in endothelial retraction and PMNL diapedesis can occur (3). The polarised cell migrates up the chemotactic gradient, where it finally encounters the foreign organism and phagocytoses it (4). This results in the production of inflammatory cytokines and lipid mediators (5) to attract other immune cells. Completion of phagocytosis and the presence of many reactive oxygen species may initiate PMNL apoptosis (6) and subsequent engulfment by larger tissue macrophages (Savill *et al.*, 1989).

1.5 PMNL cytoskeleton and regulated exocytosis

In addition to the ability to coordinately regulate the expression and packaging of granule protein into four distinct populations, the PMNL is capable of differential or selective granule release into a phagosome or into the extracellular space upon activation. Stimulation by *N*-formylated peptides (e.g. fMLP) and phorbol 12-myristate 13-acetate (PMA) result in the release of secretory granule components (identified by a decrease in alkaline phosphatase latency due to its exposure to the extracellular environment) followed by gelatinase and specific granule proteins, released in a concentration dependent manner, as the concentration of the

stimulatory agonist increases. Prolonged activation results only in marginal release of azurophil granule proteins (Schettler *et al.*, 1991). Therefore, during migration up a chemotactic gradient, the PMNL can release different granule populations as the concentration of the chemoattractant increases. The order of granule release relates well with the sequential ligands and/or barriers a PMNL encounters during chemotaxis. The many receptor molecules present in the secretory granules are exposed on the plasma membrane first in order to identify and bind ECM components, while collagenases (MMP-8 and MMP-9) and further ECM receptors are subsequently released when proteolysis through ECM components is required. Finally, the azurophil granules are released when the PMNL reaches the site of infection in the tissue (Weiss, 1989).

This hierarchy of release is tightly controlled by the level of free Ca^{2+}_i and the action of granule fusion proteins that allow fusion of phospholipid bilayers. The role of Ca^{2+}_i in regulating granule release was established using calcium ionophores such as A23187, altering the extracellular $[Ca^{2+}]$ ($[Ca^{2+}_{ex}]$) and assaying the supernatant fluid for exocytosed granule marker proteins (Edwards, 1994). However, some degranulated proteins (HNE, lactoferrin) were shown to remain associated with the plasma membrane post-release (Owen *et al.*, 1995; Borregaard and Cowland, 1997) while others were possibly degraded by proteinases that were usually partitioned intracellularly in different granule populations. Both scenarios result in protein underestimation and cast doubt on the accuracy of quantitative measurement of released proteins. More recently, a method known as patch clamp capacitance has been used to monitor granule fusion with the plasma membrane. This is achieved by monitoring the increase in plasma membrane capacitance that follows granule fusion during exocytosis (Jaconi *et al.*, 1990; Al-Mohanna *et al.*, 1997; Nüße *et al.*, 1998). This provides a more accurate view of the amount of fusion that has occurred, but does not identify the type of granule that has fused.

$[Ca^{2+}_i]$ may, however, be regulated by microperfusion and the exact order and $[Ca^{2+}_i]$ sensitivities of granules can thereby be established. Table 1.2 shows the interesting trend evident in PMNL granule release: the order of granule synthesis is the reverse of the order of release. In addition, the least dense granule population (i.e. the secretory vesicles) is the first to be released, while the most dense granule (both azurophil sub-populations) are the last. In establishing the order of granule release, most studies required complete depolymerisation of the actin microfilament network with cytochalasins - a non-physiological state, but necessary to ensure complete mobilization. Disruption of the microtubule system, however, results in

decreased granule exocytosis and, therefore, indicates the vital role of microtubule integrity for proper PMNL function (Hoffstein and Weissmann, 1978).

Table 1.2 The relationships of Ca^{2+} sensitivity and density on the order of granule release. (from Sengeløv *et al.*, 1993; Nüße *et al.*, 1998).

Granule population	Order of synthesis	Order of release	Density (g/ml)	$[Ca^{2+}_i]$ required for release of half of granule content (nM)	Granule Ca^{2+} affinity and binding cooperativity
Azurophil	First	(Last)	~1.12	680	Low
Specific	Second	Third	~1.07-1.10	550	Low
Gelatinase	Third	Second	~1.07-1.10	250	High
Secretory	Last	First	~1.05	140	High

The source, regulation and release of Ca^{2+}_i is indicated in Figure 1.4 (see Section 1.6). The increased $[Ca^{2+}_i]$ may allow granule fusion with the plasma membrane by two different (but not mutually exclusive) mechanisms. Firstly, *in vitro*, high $[Ca^{2+}_i]$ induces filamentous actin (F-actin) depolymerisation and hence allows passive fusion of granules with the plasma membrane (Hoffstein and Weissmann, 1978) whereas at low $[Ca^{2+}_i]$, a subplasmalemmal actin network would have formed a barrier to fusion with the plasma membrane. The high $[Ca^{2+}_i]$ also allows members of the annexin family to bind granule membranes and mediated fusion with the plasma membrane. Various annexins have been localised to different granule populations and are active in facilitating vesicle fusion (Rosales and Ernst, 1997). These will be discussed further in Chapter 6 where future investigations involving analysis of granule membrane phospholipid heterogeneity and, hence, annexin affinity are described.

In addition to the annexin proteins, there has been speculation regarding the possible involvement of members of the soluble NSF attachment protein (SNAP)/SNAP receptor (SNARE) families in mediating PMNL membrane fusion events. Although most of the research on the SNAP/SNARE proteins has been performed in neuronal cells, some members and their neuronal homologues have been identified in PMNLs (Brumell *et al.*, 1995). The SNAP/SNARE hypothesis proposes a mechanism whereby transport vesicles recognise themselves and the target membrane to which they are to fuse (Figure 1.3). Recognition is thought to occur by specific binding of proteins on the vesicle or granule (v-SNARE) to distinct

partner proteins on the target membrane (t-SNARE) (Bock and Scheller, 1997; Hackam *et al.*, 1998; Gerst, 1999). Association and binding of v-SNAREs to t-SNAREs is thought to be mediated by members of the Rab GTPase family. Upon formation of the heterodimeric complex (via Rab) a soluble ATPase, *N*-ethylmaleimide-sensitive factor (NSF) binds to the SNARE complex (assisted by α-SNAP) and hydrolyses ATP. ATP hydrolysis induces a conformational change in the complex and enables membrane fusion.

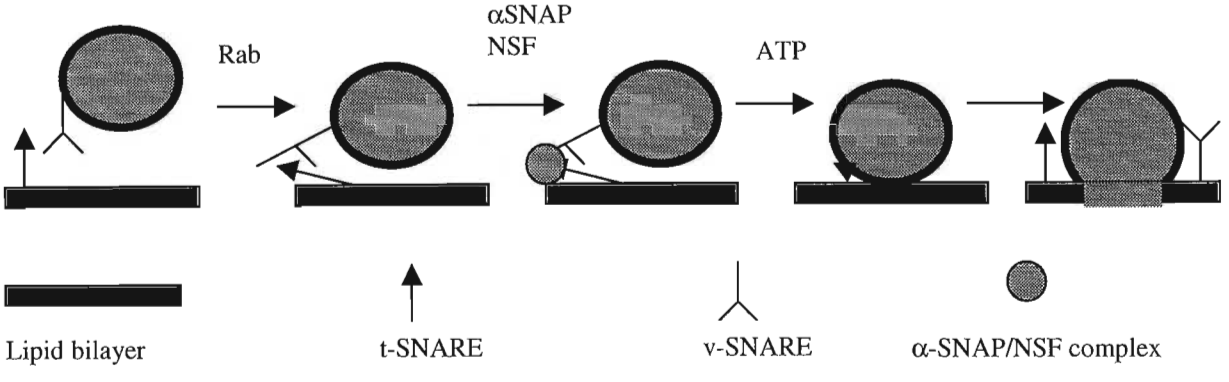

Figure 1.3 **Proposed mechanisms for vesicle fusion events by the SNAP/SNARE hypothesis.** Rab GTPases are involved in vesicle target recognition, followed by the action of α-SNAP and NSF (an ATPase) on the v- and t-SNARE complex. This leads to membrane fusion and disassembly of the SNARE complex (after Bock and Scheller, 1997).

Recently, the glycolytic enzyme glyceraldehyde 3-phosphate dehydrogenase (G3PDH) has also been identified as a potential candidate in Ca^{2+}-dependent vesicle fusion events in the PMNL (Hessler *et al.*, 1998). Experiments with artificial phospholipid liposomes show that G3PDH may have up to ten times greater fusion-promoting activity than annexin I on a mass basis. The role of G3PDH in vesicular fusion has been demonstrated in Chinese hamster ovary cells that show alterations in the endocytic pathway due to a G3PDH mutation (Robbins *et al.*, 1995).

Despite the convincing evidence that implicates fusogenic proteins and $[Ca^{2+}_i]$ transients in regulating selective granule release, little consideration has been given to other possible mechanisms of regulating the order of fusion. For instance, spatial differences between different granules and the plasma membrane may have an effect. If the granule populations were arranged in concentric 'bands' adjacent to the plasma membrane (with the secretory vesicles being closest and the azurophils remaining perinuclear), the observed order of

degranulation could possibly be explained. Electron microscopic studies, however, show a relatively random distribution of granules within the PMNL cytoplasm. Furthermore, it may be argued that the density differences between granules could also produce the release pattern observed, i.e. the azurophil granules, being the most dense, may arrive at the plasma membrane significantly later than the secretory and gelatinase granules assuming all granule populations were mobilised simultaneously. This physical parameter may not solely account for granule selectivity, but could play a significant part in any of the hypotheses put forward as, although biochemical interactions/associations are essential for initiating release, density differences have the potential to alter the *rate* of mobilisation.

Differences in associations with the cytoskeletal network (perhaps regulated by adaptor proteins) may also affect selective release at the initial stage of mobilisation. Schettler *et al.* (1991) have shown differential associations of granule populations with the cytoskeleton and immunoelectron microscopic analyses by Rothwell *et al.* (1989) revealed differential associations with tubulin. For this reason, in Chapter 5, an attempt was made to assess the possible granule interactions of known granules and the novel TIMP-1 vesicle (described in this thesis) with both actin and tubulin in order to gain insight into the cytoskeletal element that is potentially responsible for the release of the TIMP-1 vesicle.

The PMNL signal transduction pathways allow the cell to recognise and respond appropriately to a particular stimulus or stimuli. It provides a 'go between' for plasma membrane receptors and the target proteins or enzymes. For simplicity, the signal cascades for cytoskeletal dynamics will be described briefly, although signals are also transduced to the nucleus of cells to modulate gene transcription.

1.6 Signal transduction in the PMNL

The PMNL is equipped with highly complex signal transduction pathways. These sense changes in the extracellular environment that accompany inflammation and/or pathogen-induced complement fixation and initiate the appropriate response. Figure 1.4 is a simple representation of part of the highly complex sequence of events following recognition of various ligands by PMNL receptors on the plasma membrane. Common exogenous ligands which initiate a response in PMNLs include bacterial-derived formylated peptides (fMLP), LPS, PMNL-derived leukotrienes (LTB_4), anaphylatoxins, complement components, platelet activating factor, interleukins (especially IL-8), mast cell-derived histamine and ECM components (collagen,

laminin, vitronectin, thrombospondin, fibronectin) (Edwards, 1994).

The predominant intracellular signal transducing molecules are inositol phosphate derivatives [such as inositol phosphate (Ins P) and phosphatidylinositol (PI)], generated by phospholipase C (PLC) and the PLC product, diacylglycerol (DAG). Of the many derivatives, inositol 1,4,5 trisphosphate (Ins 1,4,5 P_3) has been studied most extensively due to its role in release of calreticulin-bound Ca^{2+} from intracellular storage organelles known as 'calciosomes' (Figure 1.4). Binding of Ins 1,4,5 P_3 to its receptor on the calciosome results in a transient rise in $[Ca^{2+}{}_i]$ (Volpe *et al.*, 1988). This affects a number of biological functions including F-actin depolymerisation [by activating gel actin (G-actin) capping proteins], regulated exocytosis, activation of the NADPH oxidase complex and cell migration. The $[Ca^{2+}{}_i]$ is decreased to resting rates by active pumping of Ca^{2+} into the calciosome by a membrane-bound Ca^{2+}-ATPase (Al-Mohanna *et al.*, 1997). This allows reformation and stabilisation of the cytoskeletal network and prevents any possible compressive damage to the cell (Edwards, 1994). Activation of PKC by DAG may lead to assembly of the NADPH oxidase complex and intiation of the respiratory burst, F-actin polymerisation, exocytosis and membrane fusion events (Figure 1.4).

Members of the Ras family of GTPases (Ras, Rac, Rho, Rap and Rab) are also involved in transducing signals from receptor tyrosine kinases (RTKs). The PMNL Ras homologues, Rap1 and Rap2 are responsible for initial transduction, while the phagocyte-specific Rac1 appears to function downstream (Katanaev and Wymann, 1998). In addition to exerting the regular end effects associated with the Rac family of Rho GTPases (membrane ruffling, activation of Rho etc.), Rac1 plays an important role in activation of the NADPH oxidase complex by complexing with two other cytosolic proteins, p47-*phox* and p66-*phox*, and assisting their membrane binding (Edwards, 1994; Babior, 1999). The Rho GTPase is also present in PMNLs and plays a role in formation of lamellipodia and actin bundles. Due to the fact that PMNLs do not possess a constitutive endocytic pathway and a Golgi complex, few Rabs (Rabs 1A, 2, 4, 6) are present (Borregaard and Cowland, 1997).

Upon activation, the PMNL is also capable of synthesising and releasing a number of biologically active compounds known as cytokines that can induce chemotaxis of more PMNLs (e.g. LTB_4, IL-8), induce PMNL maturation in circulating cells (G-CSF), acute phase protein release and T-cell activation (TNF-α) and stimulate B-cell maturation (IL-6) (Edwards, 1994) (Figure 1.2). More importantly, however, proteinases active against the ECM may be released

upon activation. This would involve selective granule mobilisation to the plasma membrane and release into the extracellular space following fusion events. During chemotaxis, the PMNL is required to traverse a number of barriers including the basement membrane, the ECM and the stromal tissue. The basement membrane is composed mainly of type IV collagen, while type I collagen predominates in the ECM and the stromal tissue (Mignatti and Rifkin, 1993). For this reason, enzymes active against collagen may assist PMNL invasion through the ECM and into the perivascular tissue. Unsurprisingly, the PMNL contains two collagen specific enzymes of the MMP family (MMP-8 and 9) that degrade types I and IV collagen at the neutral pH of the extracellular environment.

The MMP family has many members that differ with respect to substrate preference and cellular location. Together, the MMP members can degrade all known ECM components, ranging from elastin to proteoglycans and, therefore, are a very important group of proteinases as they have the greatest potential to disrupt the ECM to allow cell passage (Westermarck and Kähäri, 1999).

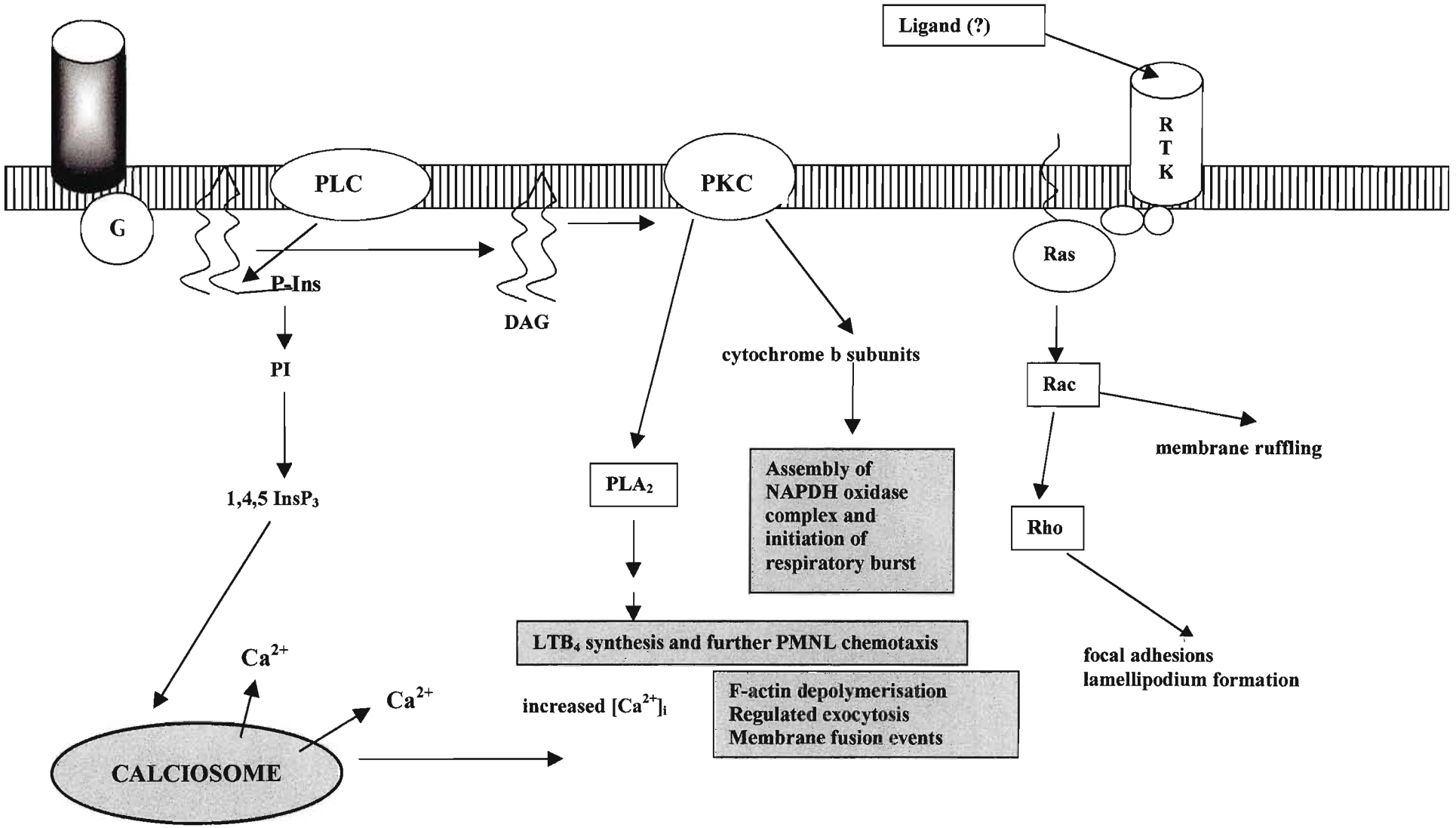

Figure 1.4 **Simple representation of a signal transduction cascade within the PMNL.**

1.7 The MMPs

Careful regulation of collagen synthesis and its breakdown is required in order to prevent two different but equally harmful conditions. Excess collagen may give rise to fibrotic disease, and, in conjunction with inefficient secretion from collagen-synthesising cells, keloids (Woessner, 1994). Insufficient collagen deposition or increased collagen degradation by collagenases will cause major defects in tissue strength and support of the ECM. Insufficient collagen may also allow invasive diseases to spread more rapidly through the body. The levels of MMPs are usually tightly controlled to maintain a fine balance between collagen synthesis and catabolism and have been implicated in many normal and pathological conditions (Table 1.3).

Table 1.3 MMP/matrixin involvement in tissue resorption and degradation.
(Woessner, 1991; 1994).

Normal processes	Pathological processes/conditions
Ovulation	Cancer invasion
Endometrial cycling	Tumour metastasis
Blastocyst implantation	Rheumatoid arthritis
Embryogenesis	Osteoarthritic cartilage formation
Salivary gland morphogenesis	Periodontal disease
Mammary development/involution	Wound/fracture healing
Cervical dilatation	Fibrotic lung disease
Foetal membrane rupture	Liver cirrhosis
Uterine involution	Corneal ulceration
Bone remodelling	Aortic aneurysm
Angiogenesis	Atherosclerosis
Tooth eruption	Gastric ulceration
Macrophage function	
PMNL function	

The MMP family currently contains 19 members that have been divided into four main classes [collagenases, gelatinases, stromelysins, membrane-type MMPs (MT-MMPs)] according to their substrate specificities and to some extent, heterogeneity in their domain numbers and structures (Westermarck and Kähäri, 1999). The classes, along with their members are shown in Table 1.4. The interstitial collagenases (MMPs-1, -8 and -13) cleave intact triple helical

collagen at a single Gly-Leu or Gly-Ile bond to produce ¾ [tropocollagen^{A} (TC^{A})] and ¼ (TC^{B}) fragments that are named according to their distance from the N-and C-termini respectively. The single site cleavage results in a decrease in melting temperature and hence collagen unwinding and gelatin formation. The gelatinases (MMPs-2 and -9) can cleave the gelatins in multiple positions, releasing small peptides that act either as chemoattractants, or are completely degraded by Pz-peptidases (Woessner, 1991). The stromelysins prefer proteoglycans as substrates rather than collagens and can also activate MMP zymogens (true for stromelysin-1/MMP-3). Although the protein core of proteoglycans are not exceptionally large, the attached GAGs attract water molecules and allow the proteoglycans to occupy a large volume relative to their size. Degradation of proteoglycans would therefore result in large unoccupied spaces within the ECM that would provide minimal resistance to movement of inflammatory cells and/or metastatic cells. The MT-MMPs differ from other MMP members since they are transmembrane proteins and do not cleave collagens. They have found to be responsible for activation of proMMP zymogens (Goetzl *et al.*, 1996). To date, MT1-MMP (MMP-14) has been positively identified as an extracellular activator of proMMP-2 although the substrates for many other MT-MMP members are currently unknown (Chambers and Matrisian, 1997). Apart from collagens, as Table 1.4 indicates, a number of unrelated substrates are also cleaved by MMP members.

Table 1.4 Classification and natural substrates of the MMPs.

(Adapted from Mallya *et al.*, 1990; Lennarz and Strittmatter, 1991; Woessner, 1991; Matrisian, 1992; Fosang *et al.*, 1993, 1994; Bu and Pourmotabbed, 1995; Cao *et al.*, 1995; Saito and Seiki, 1995; Shipley *et al.*, 1996; Yu *et al.*, 1996; Chambers and Matrisian, 1997; Pei, 1999a, 1999b; Westermarck and Kähäri, 1999; English *et al.*, 2000; Maquoi *et al.*, 2000; Park *et al.*, 2000).

Subclass	MMP	Major substrates
Interstitial collagenase	Fibroblast collagenase/MMP-1	Collagen type I-III, VII, X, aggrecan
	PMNL collagenase/MMP-8	Collagen type I-III, aggrecan, serpins
	Collagenase-3/MMP-13	Fibrillar collagens
Gelatinase/type IV/V collagenase	Gelatinase A/MMP-2	Gelatin type I, type IV collagen, aggrecan
	Gelatinase B/MMP-9	Gelatin type I & IV, type IV & V collagen, elastin, aggrecan
Stromelysin	Stromelysin-1/MMP-3	Proteoglycans, type IV collagen, gelatin types I, III, IV, V, proMMPs
	Stromelysin-2/MMP-10	
	Matrilysin/MMP-7	Gelatin type I, III-V, fibronectin, proteoglycan, elastin, aggrecan
Metalloelastase	MMP-12	Elastin, fibronectin
RXXR secreted-type	Stromelysin-3/MMP-11	Laminin, fibronectin, proMMP-9
RXXR membrane-type	MT1-MMP (MMP-14)	ProMMP-2, fibrillar collagen, proteoglycans, ECM glycoproteins, proMMP-2, TIMP-2, type I, II, III collagen, fibronectin, laminin, vitronectin, aggrecan
	MT2-MMP (MMP-15)	N/D
	MT3-MMP (MMP-16)	N/D
	MT4-MMP (MMP-17)	TNF-α
	MT5-MMP (MMP-24)	N/D
	MT6-MMP (MMP-25)	N/D
Unclassified	MMP-19	N/D
	Enamelysin (MMP-20)	Dental amelogenin
	Endometase (MMP-26)	Type I gelatin, α_1-proteinase inhibitor

The domain structures of the MMP members are highly conserved and consist of an N-terminal pro-peptide sequence (~10 kDa), a catalytic domain, a Zn^{2+}-binding region, a proline-rich variable region and a C-terminal domain that exhibits homology with hemopexin and vitronectin

(Woessner, 1991; Matrisian, 1992; Stetler-Stevenson, 1999; Westermarck and Kähäri, 1999). Both gelatinases (MMP-2, MMP-9) have extra fibronectin-like domains between the catalytic and Zn^{2+}-binding regions and MMP-9 has a unique α_2(V) collagen-like domain immediately N-terminal to the hemopexin/vitronectin domain (Figure 1.5). The MT-MMPs (MMP-14 to MMP-17) have C-terminal transmembrane regions that assist in anchoring to the plasma membrane and they have a furin-cleavage site (RXXR) immediately C-terminal to the pro-peptide sequence that permits intracellular activation by the Golgi-resident enzyme, furin (Yu *et al.*, 1996; Nakahara *et al.*, 1997).

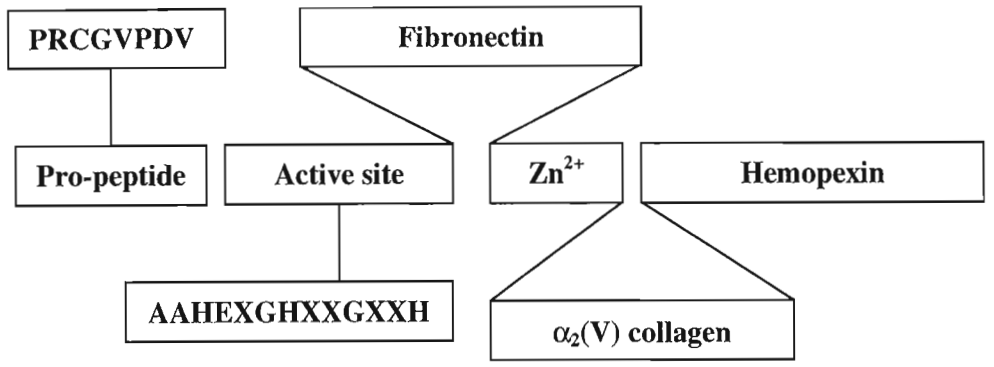

Figure 1.5 **Domain structure of MMPs.**

The pro-peptide, catalytic domain and the hemopexin domain are common throughout the MMP family (except for MMP-3 that lacks the hemopexin domain). The α_2(V) collagen like domain only occurs in proMMP-9. Further additions to this domain are described in the text (after Woessner, 1991).

The catalytic activity of the MMPs depend on the presence of histidine-coordinated Zn^{2+} in the conserved AAHEXGHXXGXXH (where X= a hydrophobic residue) active site and Ca^{2+} ions in the C-terminal domains to facilitate substrate binding. In addition to the three active site histidine residues, the Zn^{2+} atom also draws electrons away from the carbonyl group of the scissile bond and coordinates (and polarizes) a single water molecule that performs nucleophilic attack on the scissile bond (Bode *et al.*, 1999). MMP-7/matrilysin lacks the C-terminal domain and does not bind nor cleave collagens. All members (excluding the MT-MMPs) are secreted in inactive pro-forms, but recent evidence has shown possible intracellular activation routes (Lee *et al.*, 1997). Latency is maintained by pro-peptides with a highly conserved PRCGVPDV sequence where the cysteine residue associates with the active site Zn^{2+} and substitutes for the single water molecule.

The dissociation of the pro-sequence cysteine residue from the active site may be effected by use of organomercurial compounds to complex the cysteine sulfhydryl, or by oxidation of the cysteine sulfhydryl. Initial dissociation of the cysteine-Zn^{2+} semi-electrostatic/induced dipole interaction is followed by complete removal of the pro-peptide by autocatalysis and a drop in M_r of ~10 kDa. This mechanism is commonly referred to as the 'cysteine switch' (Springman *et al.*, 1990). Removal of the pro-sequence may also occur by non-MMP proteolysis. A number of proteinases cleave the pro-peptide domains *in vitro* [HNE, kallikrein, cathepsin G, trypsin, plasmin, mast cell chymase (Goetzl *et al.*, 1996)] but the *in vivo* activator molecules may also include members of the MT-MMPs. The MMPs appear to differ considerably with respect to their susceptibility to proteolytic activation and a number of contradicting reports have been published (e.g. Dewald *et al.*, 1982, Tschesche *et al.*, 1992; Mazzieri *et al.*, 1997). Therefore, it appears that more investigations into cell-specific activation pathways are required to avoid generalisation. So far, evidence for MT-MMP mediated MMP-2 activation has been reported, but activation pathways for other members may occur via a number of appropriate proteinases/biomolecules shown in Figure 1.6.

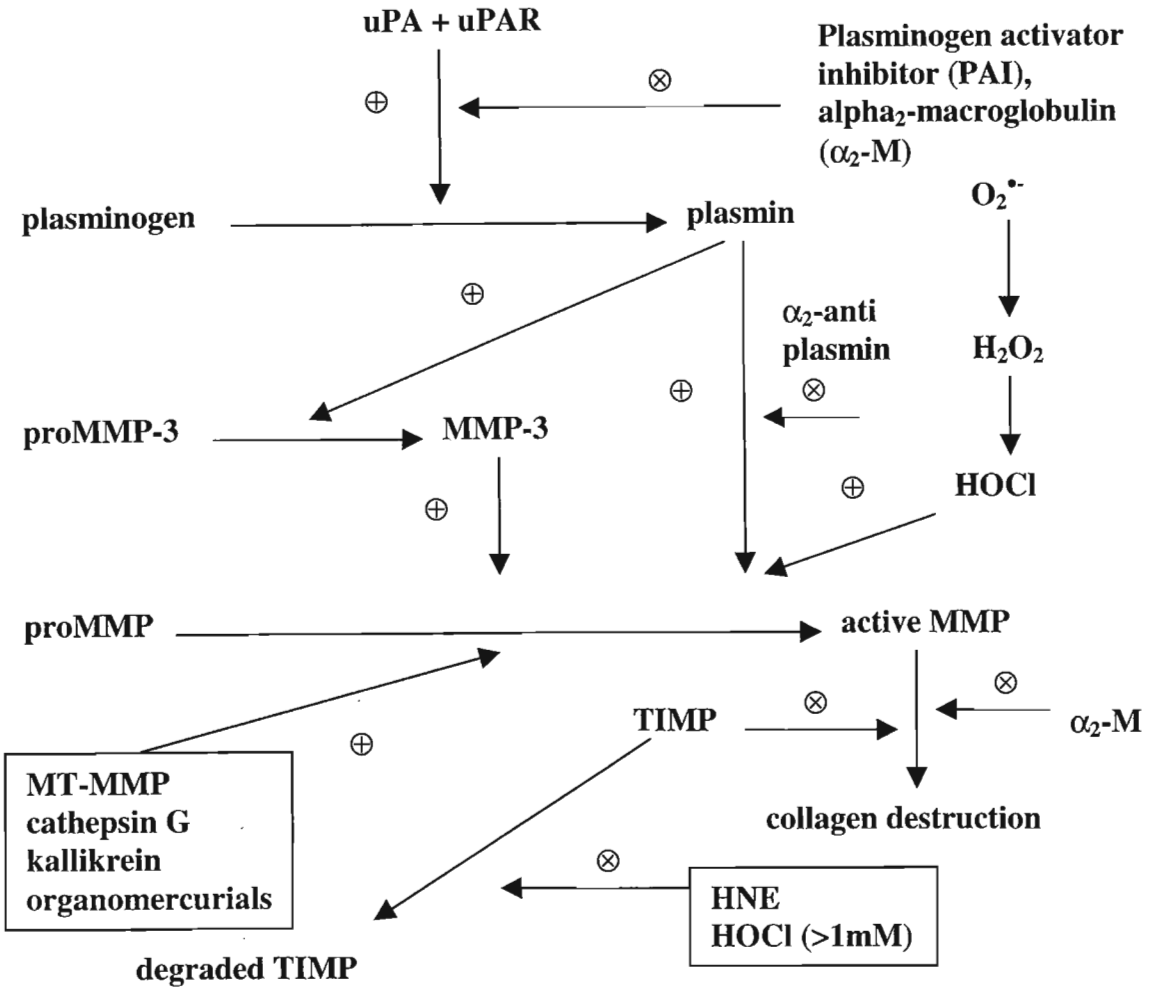

Figure 1.6 **A simplified cascade for MMP activation by various proteins and compounds.** (⊕) denotes activation and (⊗) denotes inhibition or protein destruction/degradation. (Adapted from Peppin and Weiss, 1986; Grant *et al.*, 1992; Michaelis *et al.*, 1992; Ogata *et al.*, 1992; Knäuper *et al.*, 1993; Itoh and Nagase, 1995; Murphy and Crabbe, 1995; Shapiro *et al.*, 1995; Mazzieri *et al.*, 1997; Okumura *et al.*, 1997).

Due to their neutral pH optima, substrate specificities and stability in the extracellular environment, MMPs have attracted considerable attention as potential proteinases involved in assisting cellular invasion including tumour metastasis and inflammation (Matrisian, 1992; Chambers and Matrisian, 1997; Stetler-Stevenson, 1999). Upregulation of MMP expression has been associated with increased invasiveness in numerous different cells lines (bladder carcinoma cell lines, A2058 melanoma cells, H-*ras* transformed rat embryo cells) and tumour biopsies (Chambers and Matrisian, 1997) (Table 1.5). In some cases, however, increased MMP secretion has resulted in decreased invasiveness of cells. This somewhat contradictory finding may be explained as excess collagenolysis may prevent cell attachment and movement by removing collagen substrata required for adhesion.

Table 1.5 Expression of MMPs in human tumour tissues (De Clerck *et al.*, 1994).

MMP	Cancer	Preferential expression
Collagenases	Colon, lung, head and neck, squamous cell carcinoma	Stroma and malignant epithelium
Gelatinases	Skin, breast, thyroid, prostate, colon, lung	Malignant epithelium
Stromelysins	Head and neck, breast, basal cell carcinoma, lung	Adjacent stroma
Matrilysin	Stomach, colon, lung, prostate	Malignant epithelium

A more long term and multifaceted role of MMPs in maintaining tumour homeostasis was presented by Chambers and Matrisian (1997) and implicates MMPs in primary tumour growth (and angiogenesis) up to initial and sustained growth of new metastases at distant sites. Although the exact functions of MMPs in new metastatic colonies are unknown, it has been suggested that they may be important in releasing growth factors from the ECM.

MMPs and TIMPs are secreted by all leukocyte cell types (Goetzl *et al.*, 1996) and their expression has been linked to various stages of cell differentiation of monocytes and macrophages and their expression of MMPs and TIMPs are sensitive to various stimuli (e.g. concanavalin A, PMA, growth factors) (Campbell *et al.*, 1991). Unlike other cell types that express MMPs, PMNLs do not constitutively secrete these proteins after they have been translated, but rather store them as proenzymes in granule populations as previously mentioned. Induction of mRNA expression at a particular stage of PMNL development is thought to be under control of transcriptional activators and enhancers common to all genes cotranslated and targeted to similar granule populations (Fouret *et al.*, 1989; Borregaard and Cowland, 1997). ProMMP-8 occurs in the PMNL specific granules, while proMMP-9 occurs in both the specific and the gelatinase granules (Ohlsson, 1980) (see Table 1.1).

MMP-8, like MMP-1 is referred to as a type I collagenase/interstitial collagenase but unlike MMP-1, prefers type I collagen over type III collagen (Mallya *et al.*, 1990). The large differences in collagenolytic activity (as revealed by k_{cat}/K_m values) are largely due to differing k_{cat} values, hence the two collagenases discriminate between different collagen types in the catalytic, rather than the binding step. While MMP-1 expression is common to many cells, MMP-8 was considered a PMNL-specific collagenase for many years (Hasty *et al.*, 1990; Devarajan *et al.*, 1991) until it was also identified in chondrocytes by Cole *et al.* (1996).

ProMMP-8 is extensively glycosylated and has a M_r of ~75-85 kDa, while the active species is 64 kDa. The M_r of the active species is variable depending on the mechanism of activation. MMP-9 cleaves both type IV and V collagens in addition to gelatins (Mainardi *et al.*, 1980; Hibbs *et al.*, 1985; Hibbs and Bainton, 1989; Borregaard *et al.*, 1987, 1995). Compared to MMP-2 (Opendakker *et al.*, 1991), MMP-9 cleaves type V collagen at a faster rate, but has historically been classified as a type IV collagenase. In PMNLs, proMMP-9 can be isolated as a 220 kDa homodimer although the reason for dimerisation is not fully understood. An unusual covalent 125 kDa heterodimeric complex between proMMP-9 and NGAL occurs in the specific granules (Kjeldsen *et al.*, 1993b, 1994; Xu *et al.*, 1994). The exact function of NGAL is uncertain although it may function to downregulate LTB_4 (or other prostaglandin derivatives) activation by sequestering LTB_4 or prostaglandins (or lipophilic hormones) in its core (Kjeldsen *et al.*, 1994; Flower, 1996). The reason for disulfide covalent attachment to proMMP-9 is even more enigmatic and no plausible theories regarding the possible *in vivo* function(s) of the heterodimer have been proposed to date. Recent *in vitro* evidence has, however, shown that NGAL can significantly increase the rate of $HgCl_2$-mediated proMMP-9 activation (Prof. H. Tschesche, Department of Biochemistry, University of Bielefeld, Germany, pers. comm.) and may be responsible for assisting proMMP activation after extracellular release.

The MMPs are regulated at multiple levels including transcription (mRNA stability), translation, secretion and activation (Gomez *et al.*, 1997). In the extracellular environment, MMP activity is downregulated by endogenous TIMPs and to a lesser extent, alpha$_2$-macroglobulin (α_2-M) (Nagase *et al.*, 1994). In cells that do not constitutively express MMPs, common inducers of MMP mRNA upregulation are PMA and TNF-α, whereas glucocorticoids such as dexamethasone are inhibitory. The converse, unsurprisingly, holds true for TIMP-1 mRNA synthesis (Ito *et al.*, 1990). However, these effects are largely cell-type specific as some biomolecules exert opposite effects in different cell types.

In order to regulate MMP activity after proMMP activation, members of the TIMP family are required. Unlike the larger broad spectrum proteinase inhibitor, α_2-M (720 kDa), TIMPs usually range in M_r from 21-30 kDa (Gomez *et al.*, 1997) and can, therefore, penetrate the ECM efficiently and inhibit active MMP in the tissue. In addition to the proMMPs, the PMNL synthesises and stores TIMP-1 (Triebel *et al.*, 1995). The members of the TIMP family, along with their interesting additional non-MMP inhibitory functions are described below and their mechanisms of MMP complexation and inhibition expanded in order to introduce TIMP-1, the

inhibitor found in PMNLs, that will be the focus of this study.

1.8 The TIMPs

The TIMP family contains four members to date, each sharing an overall low (30-51%) degree of amino acid homology but all containing an N-terminal $V^{18}IRAK^{22}$ consensus sequence (Table 1.6). Each TIMP molecule contains twelve cysteine residues that form six disulfide bridges and arrange the molecule into three knot-like structures (Denhardt *et al.*, 1993; Murphy and Willenbrock, 1995; Caterina *et al.*, 1997; Gomez *et al.*, 1997). Only TIMP-1 is glycosylated, but this is not essential for biological activity (Kleine *et al.*, 1993; Gomez *et al.*, 1997). The M_r's and major sites of expression are shown in Table 1.6 (Chambers and Matrisian, 1997). TIMPs inhibit all active MMPs by forming complexes of 1:1 stoichiometry but are inefficient at preventing proMMP autoactivation (Matrisian, 1992). The N-terminal domains of the TIMPs are responsible for MMP inhibition, while the C-terminal domains may have two different (but not mutually exclusive) functions. Some TIMPs bind to progelatinases (Murphy and Willenbrock, 1995), thereby deviating from the general view that TIMPs only bind and inhibit active MMPs. The N-terminal domains of proMMP-2 and proMMP-9 interact with the N-terminal domains of TIMP-2 and TIMP-1, respectively, and the fibronectin-like domain of the gelatinases may allow association with the C-terminal domains of the TIMP molecules. TIMP-1 binding to proMMP-9 is dependent on a disulfide (C^{468}-C^{674}) pair in the middle of the type V collagen-like domain of proMMP-9 (Goldberg *et al.*, 1992) (Figure 1.5). This may be responsible for the selectivity of TIMP-1 binding to proMMP-9 versus proMMP-2.

Research into the activation mechanism(s) of proMMP-2 by MT1-MMP (MMP-14) identified a role (though non-essential) for TIMP-2 in activation of the gelatinase by MT1-MMP (via formation of an MT1-MMP/proMMP-2/TIMP-2 heterotrimeric complex) and subsequent matrix degradation (Lichte *et al.*, 1996). This 'assistant' role of TIMP-2 in proMMP-2 activation, although counter-intuitive, may help to regulate the duration of MMP activity in a localised area by first ensuring that TIMP-2 is present before allowing proMMP-2 activation.

Table 1.6 Members of the TIMP family and their cellular locations.
(Chambers and Matrisian, 1997; Gomez *et al.*, 1997; Leco *et al.*, 1997).

	TIMP-1	TIMP-2	TIMP-3	TIMP-4
Molecular mass	28 kDa	21 kDa	24 kDa	22 kDa
Chromosomal location	Xp11.23-Xp11.4	17q23-17q25	22q12-22q13	?
Associated proteins	ProMMP-9	ProMMP-2	ECM	?
Major sites of expression	Ovary, bone	Placenta	Kidney, brain	Heart

In addition to functioning as MMP inhibitors, TIMPs are also involved in other non-MMP inhibitory biological processes (Table 1.7). Evidence from experiments involving truncated rTIMP-1 has shown that EPA (erythroid potentiating activity/growth factor activity) and MMP inhibition occur independently of each other (Chesler *et al.*, 1995). This is also true for the anti-apoptotic function of TIMP-1 since reduced and carboxymethylated (i.e. non-MMP inhibitory) TIMP-1 has been shown to prevent apoptosis (Guedez *et al.*, 1998).

Table 1.7 Pleiotropic functions of TIMP-1.

Function	Reference
Inhibition of apoptosis [induced by serum deprivation, X-rays, γ-rays, adriamycin, CD95, H_2O_2 and anoikis (loss of cell attachment)]	Guedez *et al.*, 1998; Li *et al.*, 1999
Inhibition of polyamine-induced angiogenesis	Takigawa *et al.*, 1990
Growth promoting activity	Avalos *et al.*, 1988; Hayakawa *et al.*, 1992; Denhardt *et al.*, 1993
DNA binding	Ritter *et al.*, 1999; Zhao *et al.*, 1998
Stimulation of gonadal steroidogenesis	Boujrad *et al.*, 1995
Induction of B-cell differentiation	Guedez *et al.*, 1998

The pleiotropic functions of TIMP-1 are not an unusual proteinase inhibitor characteristic. A dual role of proteinase inhibition and growth stimulation has also been identified in cystatin C and human pancreatic secretory trypsin inhibitor (Bertaux *et al.*, 1991). In addition, a number of other proteinase inhibitors have been shown to exhibit various biological activities unrelated to their role in proteinase inhibition. In particular, α_1-proteinase inhibitor exhibits bactericidal

activity and cysteine proteinase inhibitory activity upon *S*-nitrosylation with nitric oxide (Miyamoto *et al.*, 2000) and has been identified as a cell growth inhibitor (Yao *et al.*, 2000).

Regulation of TIMP expression differs between cell types and TIMP members. None of the pathways will be considered here since protein expression within the PMNL is transient and, to the best of our knowledge, terminal. TIMPs have, however, been shown to reduce the metastatic potentials of various malignant cells (e.g. M5076 sarcoma cells, B16-F10 melanoma cells, c-H-*ras* transformed rat embryo cells and HT-1080 fibrosarcoma cells) (Gomez *et al.*, 1997) and the invasive activity of PMNLs (Bakowski and Tschesche, 1992). Surprisingly, increased transcription and expression of TIMPs have also been associated with increased malignancy of non-Hodgkin's lymphomas, fibrous histiocytomas, human hepatocellular carcinomas and breast carcinomas (Grignon *et al.*, 1996; Chambers and Matrisian, 1997; Ree *et al.*, 1997). In these studies, the TIMP source occasionally appeared to be adjacent to non-neoplastic cells rather than the metastatic cells and this implies possible existence of intricate cellular cross-signalling networks. The *in vivo* interactions and roles of TIMPs and MMPs are, therefore, highly complex.

Despite the relatively unpredictable effect of TIMP expression on cellular invasiveness, there has been considerable success in the use of low M_r synthetic MMP inhibitors in reducing cellular metastases (Talbot and Brown, 1996). The most popular and effective MMP inhibitors have been the hydroxamate peptide derivatives containing various amino acid substitutions to improve specificities for the different MMP subclasses (Lelievre *et al.*, 1990). These peptides are termed 'right-side' inhibitors as their side chains interact with the active site S' pockets. The hydroxamate group interacts with the MMP active site Zn^{2+} atom (replacing the single water molecule) and prevents interaction with scissile bonds of collagen/proteoglycan substrates (Botos *et al.*, 1996; Bode *et al.*, 1999).

The hydroxamate peptide, batimastat (BB-94) has been shown to reduce metastasis in many cancer cell lines (Wang *et al.*, 1994). Problems with it's low water solubility have been overcome in the closely related compound, marimastat. Sulfhydryl-based MMP inhibitors with low IC_{50}'s (in the nanomolar range) have also become available and show promise in antagonising MMP-mediated cell/tumour metastasis (Schwartz *et al.*, 1992). Such low M_r inhibitors have the added advantage of gaining further access into tissues than TIMPs or α_2-M, as the size of synthetic MMP inhibitors may allow access to focal points of proteolytic activity

known to occur in tumour cells (Weaver *et al.*, 1996) and PMNLs (Campbell and Campbell, 1988). These proteolytic 'microenvironments' can be formed to delay or exclude inhibition by extracellular proteins. Although the hydroxamate-based MMP inhibitors show good inhibition kinetics *in vitro*, a recent investigation into the metabolism of the hydroxamate-based inhibitors, using a combination of mass spectrometry and gas chromatography, indicated that approximately 45-69% of the inhibitor is metabolised by human and rat liver microsomes in under an hour after administration (Peng *et al.*, 1999).

TIMP-1 mRNA was recently identified in PMNLs purified from contaminating platelets, eosinophils and basophils using Boyden chambers (Triebel *et al.*, 1995). Since the PCR amplicon was obtained in mature PMNLs, TIMP-1 synthesis may occur late in PMNL maturation. Previous western blotting investigations where PMNLs were probed with antibodies to TIMP-1 revealed no TIMP-1 and PMNLs were, therefore, thought to be incapable of TIMP synthesis (Cooper *et al.*, 1985; Okada *et al.*, 1988). Immunofluorescent labelling of PMNLs with TIMP-1 antibodies (raised against purified PMNL TIMP-1) subsequently also revealed high levels of TIMP-1 expression, although the exact subcellular location of TIMP-1 could not be established (Triebel *et al.*, 1995) and remained unknown until the current study was undertaken.

1.9 Objectives of the current study

At the commencement of this study, the complement of proteins in PMNL granules was still a matter of dispute and the mechanisms of activation, release and inhibition of PMNL MMPs was still poorly understood. No *in vivo* activators of PMNL proMMPs had been described and the subcellular localisation of TIMP-1, the endogenous inhibitor of MMPs, remained unknown. It was thought that localisation of TIMP-1 with respect to the proMMPs and the use of reliable marker proteins for different granule populations would assist in granule localisation. Similarly, it was thought that knowledge of the mechanism(s) involved in any potential differential extracellular release of proMMPs as compared with TIMP-1 would assist in the development of strategies for regulation of inflammatory conditions caused by the release of MMPs. Knowledge from this would, consequently, assist in the treatment of inflammatory disorders such as rheumatoid arthritis. Therefore, the primary aim of this study was initially to localise TIMP-1 with respect to other marker proteins for various granule populations and, subsequently, to assess the order of release of MMPs with respect to their inhibitor, TIMP-1.

In order to immunolocalise TIMP-1 with respect to the MMPs and other PMNL granule marker proteins, various antibodies were characterised and their specificities determined (Chapter 3). Identification of secretory vesicles using immunocytochemical labelling for HSA or via alkaline phosphatase histochemical means proved suboptimal and, therefore, secretory vesicle glycosylphosphatidylinositol (GPI)-anchored proteins were isolated and inoculated into chickens for antibody production to potentially provide a more reliable marker for secretory vesicles. Chickens were used for immunoglobulin production as the method for immunoglobulin collection from egg yolks is easier than drawing blood. A thorough investigation of the distribution of GPI-anchored proteins in human PMNLs by immunocytochemistry on ultrathin cryosections and subcellular density gradient fractions proved that GPI-anchored proteins occur solely in the secretory vesicles and are, therefore, suitable markers for this population.

Characterisation of anti-TIMP-1 antibodies led to the demonstration of a high M_r TIMP-1 species in all PMNL homogenates. Further experiments to confirm the identity of the immunologically demonstrated high M_r form of TIMP-1 and study the interesting high M_r form of PMNL TIMP-1, necessitated the designing of a novel western ligand blot system and a UV fluorescent reverse zymographic technique (Chapter 4). Results from the reverse zymogram support the notion that high M_r TIMP-1 retains the ability to bind proMMP-9 and inhibit active MMPs.

Following the confirmation of the specificity of the TIMP-1 antibodies, PMNLs were immunolabelled with markers for the azurophil, specific, gelatinase granules and the endocytic pathway and TIMP-1 localisation was established with respect to these markers. The results obtained show that TIMP-1 occurs in a unique, previously undescribed electron translucent vesicle separate from most granule marker proteins. Stereological analysis of the TIMP-1 vesicle showed that it occurs in two main populations of pleiomorphic shape, similar to secretory vesicles, and supports the notion that it is novel (Chapter 4).

Following identification of the unique TIMP-1 vesicle, the possible mode of regulation of release of the TIMP-1 vesicle was studied and the order of TIMP-1 vesicle release into the phagosome, relative to that of the proMMPs, was investigated by phagocytosis of IgG-opsonised latex beads followed by immunocytochemistry (Chapter 5). In order to establish whether differential interaction of various granule types with different elements of the

cytoskeleton could be responsible for the order and differential release of various granule populations, the interactions of the TIMP-1 vesicle and the gelatinase granules were studied using phalloidin-stabilised actin and paclitaxel-stabilised tubulin in conjunction with immunocytochemistry.

The results obtained from the latex bead studies showed that the TIMP-1 vesicle remained non-fusogenic with the phagosome and the cytoskeletal studies showed non-association of the TIMP-1 vesicle with elements identifiable as actin or tubulin. Therefore, the final objective of the study was to investigate the $[Ca^{2+}_i]$ sensitivity of the TIMP-1 vesicle relative to other granule populations to establish the order in which TIMP-1 is released as this may have important implications in MMP activation and inhibition (Chapter 5).

CHAPTER 2

General Materials and Methods

A variety of common biochemical techniques were employed throughout this study and are described here for convenience. Specialised techniques that were only used in specific chapters are outlined separately in the relevant chapter. All chemicals used throughout the study are, however, listed below.

2.1 Reagents

Most of the chemicals used in this study were from BDH (Poole, UK), Merck (Darmstadt, Germany), Sigma (St. Louis, USA) or Boehringer Mannheim (Mannheim, Germany) and were of the highest purity available. Protein molecular mass (M_r) standards for sodium dodecyl sulfate-polacrylamide gel electrophoresis (SDS-PAGE) were obtained from Pharmacia LKB Biotechnology (Lund, Sweden). *N*-[2-hydroxy-1,1-bis(hydroxymethyl)ethyl]glycine (Tricine), Triton X-114, cerium chloride, *N*-tris(hydroxymethyl)methyl-3-amino-propanesulfonic acid (TAPS), poloxyethylene (23) lauryl alcohol (Brij 35), DMSO, Coomassie Brilliant Blue G-250 and R-250, ethylene glycol-bis(β-aminoethyl ether)-*N,N,N',N'*-tetra acetic acid (EGTA), piperazine-*N,N'*-bis(2-ethanesulfonic acid) (PIPES), *N*-2-hydroxy-piperazine-*N'*-2-ethane sulfonic acid (HEPES), methylcellulose (25 centipoises), rabbit anti-mouse IgG, rabbit anti-lactoferrin IgG, alkaline phosphatase-conjugated goat anti-rabbit IgG, 5-bromo-4-chloro-3-indolylphosphate (BCIP), nitroblue tetrazolium (NBT), β-mercaptoethanol, 2,2'-azino-di-(3-ethyl)-benzthiozoline sulfonic acid (ABTS), L-arginine.HCl, silver nitrate, Tween 20, citrate-phosphate-dextrose blood anticoagulant, fish skin gelatin (FSG), poly-L-lysine, Freund's complete and incomplete adjuvants (FCA and FIA), 4-(2-aminoethyl)-benzenesulfonyl fluoride (AEBSF), dialysis membrane (12 kDa molecular exclusion limit), Na_2ATP, Percoll, RPMI-1640 cell culture medium, paclitaxel, 1 μm amine-modified latex beads, dithiothreitol (DTT), ionomycin, 7-amino-4-methylcoumarin (AMC), MeOSuc-Ala-Ala-Pro-Val-AMC, heparin-agarose and levamisole were from Sigma. Polyethylene glycol (PEG) 6 kDa and 20 kDa, porcine skin type I gelatin (300 bloom), glutaraldehyde, chlorauric acid and guanidine.HCl were from Merck. All acrylamide reagents, tertiary butanol (t-BuOH), Triton X-100, L-methionine, sodium deoxycholate (DOC), sodium cacodylate, ethylenediamine tetra acetic acid (EDTA), sodium azide, iodoacetic acid, trichloroacetic acid (TCA), paraformaldehyde (PFA),

formaldehyde, H_2O_2 and sucrose were from BDH. 2-amino-2-(hydroxymethyl)-1,3-propanol (Tris), phenylmethylsulfonylfluoride (PMSF), SDS and bovine serum albumin (BSA) fraction V were from Boehringer Mannheim. Dimethylformamide (DMF) and 2-methoxy-2,4-diphenyl-3(2*H*)-furanone (MDPF) were from Fluka (Buchs, Switzerland). Nitrocellulose membrane (0.45 μm) and enhanced chemiluminescence (ECL) reagents were from Amersham International (Buckinghamshire, UK). Nunc Immuno Maxisorp F96 multiwell plates were from Nunc Intermed (Roskilde, Denmark) and disposable sterile 0.45 μm and 0.22 μm filters were from Corning/Costar (Cambridge, USA). X-ray developing solutions were from Champion Photochemistry (Midrand, South Africa). Biotinylated phalloidin was a gift from Dr. Richard Kirsch (Liver Research Unit, University of Cape Town, South Africa) and was originally purchased from Molecular Probes (Eugene, USA). Rabbit anti-HSA IgG and rabbit anti-chicken IgY IgG were gifts from Dr. Rory Morty and Prof. Theresa Coetzer (both from the Department of Biochemistry, University of Natal, Pietermaritzburg, South Africa), respectively. Monoclonal antibodies against lysosome-associated membrane proteins (LAMPs)-1 and 2 were from the Developmental Studies Hybridoma Bank (University of Iowa, Iowa City, Iowa, USA). Distilled water (dist.H_2O) was obtained with a Milli-RO® 15 Water Purification System (Millipore, Marlboro, USA). Deionised water (dd.H_2O) was obtained with a Milli-Q Plus Ultra-Pure Water System (Millipore, Marlboro, USA) and had a minimum resistivity of 18 MΩ.cm.

2.2 Protein quantitation

Accurate protein quantification was necessary to standardise antigen and PMNL homogenate loading for SDS-PAGE, zymograms or western blots. Ideally, interference of lipids, reducing agents and buffer components should be minimal and the assay quick, reproducible and sensitive. The UV spectrophotometric protein assay and the Lowry assay lack sensitivity (Boyer, 1993), and, therefore, the Bradford (Bradford, 1976) and bicinchoninic acid (BCA) assays (Smith *et al.*, 1985) have gained popularity. The Lowry assay involves copper mediated oxidation of aromatic amino acid residues with the concomitant reduction of Folin-Ciocalteu (phosphomolybdic-phosphotungstate) to heteromolybdenum blue (Lowry *et al.*, 1951). The BCA assay, like the Lowry assay, relies on reduction but more specifically on the reduction of copper ($Cu^{2+} \rightarrow Cu^{+}$) that occurs upon interaction with protein peptide bonds (with the contribution from oxidisable Tyr, Cys, His residues) in alkaline conditions (Smith *et al.*, 1985). Upon reduction, bicinchoninic acid complexes with Cu^{+} in the ratio BCA:Cu^{+} = 2:1. This results in a colour shift and the stable complex can be quantified spectrophotometrically (λ_{max} = 562 nm). The sensitivity of the BCA assay is comparable to the conventional Bradford assay,

and although it is unaffected by the presence of chaotropes and detergents, it is substantially more expensive than the Bradford assay, quantification takes longer, heating steps are required (Smith *et al.*, 1985) and it is adversely affected by EDTA (the conventional MMP inhibitor) (Boyer, 1993). The Bradford assay (Bradford, 1976) with the linearisation modifications of Read and Northcote (1981) and Zor and Selinger (1996) were used in this study.

2.2.1 Bradford Dye-binding assay

The Bradford assay is a simple, cost-effective, stable, quick and reproducible assay for the quantification of proteins down to 50 ng (Zor and Selinger, 1996). It is unaffected by many chemicals (e.g. sucrose, urea, glycerol) but gives erroneously high absorbance readings when detergent [e.g. > 0.1% SDS and > 1% Triton series (Boyer, 1993)] or cellular-derived lipid is present in the sample. Reasons for this lie in the nature of the dye binding with amino acid residues exposed on the surface of the protein molecules undergoing quantification. The dye molecule contains six phenyl groups and two sulfonic acid groups and so interaction is mainly weak and non-covalent and occurs via hydrophobic (Y, F, W) and electrostatic (R, K) residues. Excess detergent may interact hydrophobically with the dye and cause a wavelength shift and an overestimation of protein content.

The Coomassie Brilliant Blue G-250 dye exists in three forms: red (λ_{max} = 470 nm), blue (λ_{max} = 590 nm) and green (λ_{max} = 650 nm). The original Bradford assay was based on the λ_{max} shift (465-595 nm) of dye molecules in the presence of protein, but recent investigations have shown non-linearity at 595 nm since there is an overlap of the red and blue dye species at this wavelength. To overcome this, Zor and Selinger (1996) suggested monitoring the decrease in $[\text{blue dye}]_{free}$ as well as the decrease in absorbance of the red dye form by establishing the A_{590}/A_{450} ratio. The A_{590}/A_{450} ratio exhibits linearity from 20 ng - 40 µg protein. This modification is reported to improve sensitivity ten-fold and allows quantification in the presence of up to 35-fold excess detergent (by weight) (Zor and Selinger, 1996).

2.2.1.1 Reagents

Bradford dye reagent. Serva Blue G dye (0.05g) was dissolved in phosphoric acid [50 ml of an 88% (v/v) solution] and absolute ethanol (23.5 ml). The solution was made up to 500 ml with dd.H_2O and stirred for 30 min at room temperature (RT) on a magnetic stirrer. The solution was filtered through Whatman No. 1 filter paper and stored in an amber bottle. Before use, the dye solution was checked for dye precipitation that would otherwise lead to erroneous protein

quantitation and refiltered and recalibrated if necessary.

Standard BSA solution (1 mg/ml). BSA (Fraction V) (0.1 g) was dissolved and made up to 100 ml with PBS.

2.2.1.2 Procedure

A standard curve was constructed using the standard BSA solution (1 μg/μl) for the range of 0-35 μg. Protein samples were made up to 50 μl with dd.H_2O in 1.5 ml Eppendorf microcentrifuge tubes and 950 μl of Bradford reagent was added. The tubes were sealed and gently vortexed to ensure even mixing of the dye reagent. The reaction was allowed to continue for 10 minutes before absorbances were read at 590 and 450 nm. Distilled water served as the blank for the determinations instead of dye reagent as in the conventional Bradford assay. This is necessary since more than one form of the Coomassie dye is monitored in the assay and absorbances are relative to dd.H_2O at each wavelength. Protein estimations for the modified Bradford assay were calculated from equations generated by linear regression analysis of standard curves for each batch of dye reagent made up.

2.3 Protein sample concentration

Protein samples that were in solution of an inconvenient volume were concentrated using various techniques suited to the intended future use of the protein sample. These techniques included concentrative dialysis against PEG 20 kDa using a dialysis membrane with an exclusion limit of approximately 10-12 kDa, lyophilisation, or organic solvent precipitation (described here).

2.3.1 Solvent precipitation

Where necessary, dilute solutions of proteins for SDS-PAGE analysis were concentrated by acetone precipitation (-80°C). Acetone has a low dielectric constant, which promotes aggregation of proteins as it disturbs the solvating water shells around proteins, and it is also useful in removing lipid contaminants that may affect protein migration in an SDS-PAGE run (Boyer, 1993).

For general protein precipitation, a modified acetone precipitation technique was used (Bollag and Edelstein, 1991). In this method, DOC [0.15% (w/v) in dd.H_2O] was added to a protein solution (100 μl 0.15% DOC/ml protein solution, 15 min, RT), followed by trichloroacetic acid [50 μl of a 100% (w/v) TCA solution/ml protein solution]. The precipitated protein was

centrifuged (10000 x g, 5 min, RT) and the pellet washed with acetone before air-drying. This method is reported to precipitate protein amounts as low as 1 μg.

2.4 SDS-PAGE

Polyacrylamide gel electrophoresis allows protein separation by differentiation migration to either the anode or cathode through a non-reactive matrix formed by acrylamide and *N,N'* methylene bisacrylamide comonomers that undergo free radical mediated polymerisation to form a meshwork of pores that sterically resist protein migration. Polymerisation is initiated by ammonium persulfate (radical source) and catalysed by TEMED (a free radical donor and acceptor). The M_r range of protein separation is determined by the total acrylamide concentration (acrylamide and bisacrylamide) and the acrylamide:bisacrylamide ratio (Boyer, 1993).

In the absence of SDS, the extent and direction of protein migration depends largely on the individual charge to mass ratios and this complicates M_r estimations. SDS partially denatures protein secondary structure and non-disulfide-linked oligomeric structures, conferring a nett negative charge on proteins due to the highly anionic sulfate group on the detergent. The SDS micelle may be either unilamellar or (possibly) bilamellar since it can interact in both a hydrophobic and electrostatic manner. Addition of a reducing agent (e.g. β-mercaptoethanol or dithiothreitol) and heating allows complete denaturation by breaking intra- and inter-disulfide bridges and by linearising the polypeptide chains by thermally overcoming folding kinetics. The resultant peptide can bind SDS with a stoichiometry usually ranging from 1.1 g SDS/g protein to 2.2 g SDS/g protein, but this may be even lower for very acidic proteins (e.g. 0.2 g SDS/g protein for glucose oxidase) (Bischoff *et al.*, 1998). Polypeptide linearisation and SDS binding allow migration to occur solely on the basis of M_r (*assuming* a constant SDS binding ratio) since all protein species carry nett negative charges and display an anodal migration. In gradient SDS-PAGE gels, a linear relationship exists between the relative migration of proteins and their respective M_r logarithms. This may then allow for M_r estimation but this should be done with caution since it does not take into account post-translational protein modifications (e.g. glycosylation, isoprenylation, GPI-anchoring) that may affect M_r estimation.

The three PAGE systems used in these studies were: Tris-glycine (Laemmli, 1970), Tris-tricine (Schägger and von Jagow, 1987) and native PAGE (Laemmli, 1970; Bollag and Edelstein, 1991) (described in Chapter 3).

2.4.1 Laemmli system

Electrophoretic stacking and separation of proteins by the Laemmli system relies on the different glycine ionisation states (pKa_1 = 2.45; pKa_2 = 9.6; pI = 6.025) that occur between the stacking and running gels. The stacking gel usually has a low total acrylamide concentration (%T) ranging from 3-5%, which does not sterically hinder most proteins and has an approximate pH of 6.8 at 4°C. Theoretical values obtained from the Henderson-Hasselbach equation estimate that 0.0015% of the glycine species are anionic and, hence, electrophoretically mobile. At pH 6.8, the rest predominate as glycine zwitterions that carry no charge. The running conditions for the Laemmli gels are constant current (i.e. constant charge per unit time) and in order to maintain this, the anionic protein species carry the charge in place of the zwitterions. This allows the proteins to stack in a thin band behind the highly mobile chloride ions. Entry into the resolving gel presents the protein band with both a pH increase and a pore size decrease (since %T can range from 5-20%). Deprotonation of the glycine zwitterions in the basic (pH 8.8) resolving gel allow an increase in [anionic glycinate] (from 0.0015% to 15.8%). This decreases the amount of charge the proteins are required to carry and allows them to separate with respect to M_r within the resolving gel.

2.4.1.1 Reagents

Acrylamide/bisacrylamide monomer stock solution (30% T, 2.67% C). Acrylamide monomer (58.4 g) and *N,N'*-methylenebisacrylamide (1.6 g) were dissolved and made up to 200 ml with dd.H_2O and degassed. The solution was filtered through Whatman No. 1 filter paper and stored at room temperature in an amber bottle.

4 x Running gel buffer (1.5 M Tris-HCl, pH 8.8). Tris (36.3 g) was dissolved in dd.H_2O (~180 ml), titrated to pH 8.8 with HCl and made up to 200 ml. The buffer was stored at 4°C.

4 x Stacking gel buffer (500 mM Tris-HCl, pH 6.8). Tris (12 g) was dissolved in dd.H_2O (~180 ml), titrated to pH 6.8 with HCl and made up to 200 ml. The buffer was stored at 4°C.

SDS stock solution [10% (w/v)]. SDS (10 g) was dissolved in dd.H_2O and made up to 100 ml. The solution was stored at room temperature.

Ammonium persulfate initiator solution [10% (w/v)]. Ammonium persulfate (0.05 g) was dissolved in dd.H_2O (500 µl) just before use. The solution was kept at 4°C for up to 1 week.

5 x Electrode (running) buffer [125 mM Tris-HCl, 960 mM glycine, 0.5% (w/v) SDS, pH 8.3]. Tris (30 g), glycine (144 g) and SDS (10 g) were dissolved in dist.H_2O and made up to 2 *l* without pH adjustment and stored at 4°C. When required, the 5 x stock solution (300 ml) was diluted with ice-cold dist.H_2O (1.2 *l*).

5 x Non-reducing treatment buffer [62.5 mM Tris-HCl, pH 6.8, 20% (v/v) glycerol, 2% (w/v) SDS]. Distilled H_2O (3.4 ml), 4 x stacking gel buffer (1 ml), glycerol (1.6 ml), SDS [1.6 ml of 10% (w/v) stock solution] and bromophenol blue [400 µl of a 0.5% (w/v) solution in dist.H_2O] were mixed together and stored at RT. When required, the sample buffer was diluted 1:4 with the protein samples and boiled for 5 min before flash cooling on ice and loading onto SDS-PAGE gels.

5 x Reducing treatment buffer [62.5 mM Tris-HCl, pH 6.8, 20% (v/v) glycerol, 2% (w/v) SDS, 5% (v/v) β-mercaptoethanol]. As for non-reducing buffer except that 400 µl β-mercaptoethanol was included.

M_r markers. Standards for M_r determination were: phosphorylase b (94 kDa), BSA (68 kDa), ovalbumin (45 kDa), carbonic anhydrase (30 kDa), soybean trypsin inhibitor (20.1 kDa) and α-lactalbumin (14.4 kDa). The lyophilised markers were reconstituted in reducing treatment buffer (100 ml) and boiled for 5 min. Aliquots were stored at 4°C.

2.4.1.2 Procedure

The SDS-PAGE electrophoresis unit (Hoefer® Mighty Small) was assembled according to manufacturers instructions. Glass plates, aluminium backings, plastic combs and 1.5 mm plastic spacers were cleaned with detergent and then with 70% (v/v) ethanol. The glass plates, spacers and aluminium backings were assembled in a gel caster, the bottoms sealed and tested for leakage.

Acrylamide monomer, dd.H_2O, gel buffer and SDS were mixed with fresh ammonium persulfate and TEMED as indicated for the running gel (Table 2.1), loaded into the sealed gel caster (overlaid with dd.H_2O to exclude oxygen) and allowed to polymerise. After polymerisation, the dd.H_2O was decanted and the stacking gel, made up as described in Table 2.1, was layered on top of the polymerised running gel. Plastic 10 well combs were

inserted into the stacking gel and polymerisation was allowed to occur (~30 min). The combs were removed, gels assembled into silicone-sealed electrophoresis units and pre-electrophoresed (30 min, 36 mA) before sample loading, to remove excess free radicals. During electrophoresis the gel was cooled using a circulating water bath (4°C) and protein samples were separated at 36 mA (unlimited voltage). The gel was subsequently either further processed (e.g. zymography or western blotting) or stained for protein.

Table 2.1 Reagent composition and proportions for two Tris-glycine gels.

	Resolving gel (%)			Stacking gel (%)	
Reagent	12.5%	7.5%	5%	4%	3%
Monomer (ml)	6.25	3.75	2.5	0.94	0.71
Resolving gel buffer (ml)	3.75	3.75	3.75		
Stacking gel buffer (ml)				1.75	1.75
10% SDS (µl)	150	150	150	70	70
Dd.H_2O (ml)	4.75	7.25	8.5	4.3	4.53
Persulfate (µl)	75	75	75	50	50
TEMED (µl)	7.5	7.5	7.5	15	15

2.4.2 Tricine system

The tricine gel system was originally designed with the purpose of resolving low M_r peptides (down to 1.45 kDa) (Schägger and von Jagow, 1987) by allowing them to be separated from pure SDS micelles of similar M_r that complicated peptide resolution in earlier Laemmli systems. The use of tricine (pKa = 8.15), high ionic strength running gel and conditions of constant voltage (i.e. constant force per unit charge) allow efficient separation of proteins in the range of 5-100 kDa in a resolving gel of constant porosity. Unlike Laemmli gels, no pH change is responsible for the superior resolution of tricine gels. The constant voltage conditions may allow the SDS-coated proteins to stack efficiently due to the fact that each species is experiencing a constant force. This would mimic the conditions in the Laemmli stacking gel. The tricine ion is predominately anionic at pH 8.25 (70.8% anionic) and can migrate faster than glycine in the stacking gel. Tricine shifts the upper stacking limit of the gels to below 30 kDa and this facilitates the separation of small peptides from SDS micelles. The order of increasing mobility would be: high M_r proteins (>30 kDa)>tricine>low M_r proteins (<30 kDa).

2.4.2.1 Reagents

Acrylamide/bis-acrylamide monomer stock solution (51% T, 5.88% C). Acrylamide monomer (48 g) and *N,N'*-methylenebisacrylamide (3 g) were dissolved in dd.H_2O (100 ml) and degassed. The solution was filtered through Whatman No. 1 filter paper and stored at room temperature in an amber bottle.

Gel buffer [3 M Tris-HCl, 0.3% (w/v) SDS, pH 8.45]. Tris (72.7 g) was dissolved in dd.H_2O (~180 ml) and SDS [6 ml of a 10% (w/v) stock solution] was added. The pH was adjusted to 8.45 with HCl and made up to 250 ml in a volumetric flask. The buffer was stored at 4°C.

Anode buffer (200 mM Tris-HCl, pH 8.9). Tris (24.22 g) was dissolved in dist.H_2O (~950 ml), adjusted to pH 8.9 with HCl, and made up to 1 *l*. The buffer was stored at 4°C.

Cathode buffer [100 mM Tris-HCl, 100 mM tricine, 0.1% (w/v) SDS, pH 8.25]. Tris (12.2 g) and tricine (17.9 g) were dissolved in dist.H_2O (~950 ml). SDS [10 ml of a 10% (w/v) stock solution] was added, the pH adjusted to 8.25 with HCl, and made up to 1 *l*. The buffer was stored at 4°C.

Ammonium persulfate initiator solution, reducing treatment buffer, non-reducing treatment buffer and M_r markers were prepared as described for the Laemmli system (Section 2.4.1.1).

2.4.2.2 Procedure

The gel was cast and polymerised as described (Section 2.4.1.2) using the proportions of reagents as shown in Table 2.2. Cathode buffer and anode buffer were added to the upper and lower chambers, respectively. Tricine gels were also pre-electrophoresed (70 V, 30 min) before sample loading. The voltage setting was set at 70 V (unlimiting current) until the bromophenol blue dye front had entered the running gel, whereupon it was increased to 100 V.

Table 2.2 Reagent composition and proportions for two Tris-tricine gels.

	Resolving gel (%)			Stacking gel (%)	
Reagent	10%	7.5%	5%	4%	3%
Monomer (ml)	3.6	2.66	1.77	0.5	0.375
Gel buffer (ml)	6	6	6	1.5	1.5
Dd.H_2O (ml)	8.4	9.34	10.23	4	4.12
Persulfate (µl)	60	60	60	50	50
TEMED (µl)	6	6	6	12	12

2.5 Staining of protein in SDS-PAGE gels

There are many techniques available for protein detection within polyacrylamide gels including fluorescent [terbium chloride (Copeland, 1994)], reversible [e.g. imidazole (Fernandez-Patron *et al.*, 1995), methyltrichloroacetate (Candiano *et al.*, 1996)] and permanently visible staining techniques (silver staining, Coomassie Blue) which each have their own particular application in protein visualisation.

Protein detection in PAGE gels was performed using either Coomassie Blue or silver, depending on the objective of the study. For zymography, all gels were stained with Coomassie since this method allows detection of enzyme activity down to the picogram range (Kleiner and Stetler-Stevenson, 1994; Bischoff *et al.*, 1998). This sensitivity is not due to direct protein detection, but absence of staining (e.g. of gelatin). Silver staining was carried out when it was necessary to assess purity of a protein fraction since Coomassie Blue may not detect contaminants present in very low concentrations (in the nanogram range). Both staining methods provide permanent records of the gel and can be stored for many months at low temperatures or vacuum dried.

2.5.1 Coomassie Blue

The method of protein binding is identical to that described for the Bradford dye (Section 2.2.1). The gel and the proteins take up the dye, but upon washing with a challenging solvent (methanol and acetic acid), the dye is leached from the areas of the gel devoid of protein. The dye-protein interaction is favoured over dye-solvent and this allows for destaining and band visualisation. Excessive destaining will result in dye removal from the protein known as "bleaching" (Kleiner and Stetler-Stevenson, 1994). The initial shrinkage of the gel caused by the alcohol and acid

destain is overcome by using a second destain containing less solvent and a greater water content to allow hydration.

2.5.1.1 Reagents

Coomassie Stain [0.5% (w/v) in 50% (v/v) methanol]. Coomassie Blue R-250 (0.5 g) and methanol (250 ml) were added to a 500 ml volumetric flask and made up to volume with dist.H_2O. The solution was stirred with a magnetic stirrer bar until the stain had completely dissolved (30 min-1 h, RT).

Destain solution I [50% (v/v) methanol]. Methanol (500 ml) and dist.H_2O (500 ml) were mixed together and stored at RT.

Destain solution II [5% (v/v) methanol]. Methanol (50 ml) and dist.H_2O (950 ml) were mixed together and stored at RT.

2.5.1.2 Procedure

After an electrophoresis run, the gel was placed in a clean glass container and covered with Coomassie stain. After ~4 h, the stain was decanted back into its original container (to be recycled) and the gel was submerged in destain solution I for ~4 h. After this time, the gel was placed in destain solution II until it had fully rehydrated. The gel was rinsed with distilled water and stored in zip-seal bags at 4°C until photographed.

2.5.2 Silver staining

There are three main silver staining methods available for the detection of proteins in the nanogram range: ammoniacal, non-ammoniacal and photoreduction (Desnoyers *et al.*, 1995). Of the three methods, the non-ammoniacal staining is safer and more sensitive.

Proteins in SDS-PAGE gels are fixed by precipitation (with methanol and acetic acid), chemical cross-linking (formaldehyde) and washed with ethanol to remove residual acid that can destroy sodium thiosulfate. Silver ions are supplied in the form of silver nitrate, as this is cheaper than silver lactate and has a higher dissociation constant (Dauscher, 1981). Thiosulfate is used by Blum *et al.* (1987) to complex insoluble silver ions and decrease background signals during silver reduction. Although thiosulfate is a weak reducing agent ($2S_2O_3^{2-} \leftrightarrow 2S_4O_6^{2-} + e^-$), it is not involved in reducing protein-associated silver ions (since it is also used as a fixer in photography). Blum *et al.* (1987) are vague regarding the precise mechanism of silver reduction

and amplification, stating only that a pH change (using Na_2CO_3) is necessary for development. No conventional reducing agents (e.g. hydroquinone, citrate, lactate) are included in the procedure. Formaldehyde functions primarily as a chemical fixative, but is also a known reducing agent [it is used in Bielschowsky's silver stain for axons (Bielschowsky, 1902)]. At concentrations below 2%, formaldehyde exists mainly as methylene glycol (Griffiths, 1993) which can be oxidised to formic acid and thereby reduce ionic silver to metallic silver. The reduced silver acts as a nucleus for further metal deposition and this amplification gives rise to visible bands within the gel.

2.5.2.1 Reagents

Fix solution [50% (v/v) methanol, 12% (v/v) acetic acid, 0.05% (v/v) formaldehyde]. Methanol (100 ml), acetic acid (24 ml) and formaldehyde [100 µl of a 37% (v/v) solution] were diluted to 200 ml with dd.H_2O.

Wash solution I [50% (v/v) ethanol]. Ethanol (100 ml) was diluted to 200 ml with dd.H_2O.

Pretreatment solution [0.02% (w/v) sodium thiosulfate]. Sodium thiosulfate ($Na_2S_2O_3.5H_2O$) (40 mg) was dissolved in dd.H_2O.

Impregnating solution [0.2% (w/v) silver nitrate, 0.075% (v/v) formaldehyde]. Silver nitrate ($AgNO_3$) (400 mg) was dissolved in dd.H_2O (199.85 ml) and formaldehyde [150 µl of a 37% (v/v) solution] was added just before use.

Develop solution [6% (w/v) sodium carbonate, 0.0004% (w/v) sodium thiosulfate, 0.05% (v/v) formaldehyde]. Sodium carbonate (Na_2CO_3) (12 g) and sodium thiosulfate ($Na_2S_2O_3.5H_2O$) (4 ml of pre-treatment solution) were mixed together in 199 ml dd.H_2O. Formaldehyde [100 µl of a 37% (v/v) solution] was added just before use.

Stop solution [50% (v/v) methanol, 12% (v/v) acetic acid]. Methanol (50 ml) and acetic acid (12 ml) were mixed together and made up to 100 ml with dd.H_2O.

Wash solution 2 [50% (v/v) methanol]. Methanol (50 ml) was diluted to 100 ml with dd.H_2O.

2.5.2.2 Procedure

The procedure for silver staining is outlined below. After staining, the gels were stored in stop solution in zip-seal bags at 4°C until photographed.

Table 2.3 Silver staining protocol for visualising proteins in polyacrylamide gels.

Step	Time
1. Fix	>1 h [or overnight (o/n)]
2. Wash 1	3 x 20 min
3. Pretreatment	1 min
4. Rinse	3 x 20 s
5. Impregnation	20 min
6. Water rinse	2 x 20 s
7. Develop	> 10 min
8. Water wash	2 x 2 min
9. Stop	10 min

2.6 Zymography

Like histochemical SDS-PAGE, zymography allows detection of enzyme activity after proteins have been electrophoresed (Gabriel and Gerston, 1992; Bischoff *et al.*, 1998). The resolving gel in zymography usually contains the proteinase substrate (e.g. casein, gelatin, fibrin) copolymerised within it or this may be added as an overlay after electrophoresis. The concentration of the substrate is important for optimal band formation, resolution and detection (Makowski and Ramsby, 1996). A non-reducing SDS-PAGE gel is used to ensure that enzyme activity is retained. Some enzymes, however, have been renatured and detected after reduction, boiling and incubation with chaotropes such as urea (Gabriel and Gersten, 1992). After electrophoresis, the gel is washed in unbuffered Triton X-100 that removes the SDS bound to the protein substrate and the samples that were electrophoresed. SDS is easily removed by this dilution since it has a significantly higher critical micelle concentration (CMC) than Triton X-100 [CMC_{SDS} = 8.27 mM; $CMC_{TX\text{-}100}$ = 0.24 mM (Sigma Handbook, 1998)]. Subsequent to the Triton X-100 wash, the gel is incubated at an optimal temperature in the appropriate buffer. The buffer should contain the relevant inhibitors for other proteinases that degrade the chosen substrate and it should contain the necessary cofactors if required. Enzyme

activity may subsequently be detected by staining the gels with either Coomassie Blue or Amido Black and appears as clear bands against a stained background containing the undigested substrate.

Zymography was used in this study for the detection of type I collagenase (MMP-8) and gelatinase (MMP-9) in crude PMNL homogenates that also contained TIMP-1. Due to the fact that SDS partially dissociates the pro-piece from the MMP active sites during electrophoresis, zymography may be used to identify both proMMPs and active MMPs since both exhibit activity as SDS results in the movement of the pro-piece of proMMPs away from the active site cleft, allowing them to exhibit apparent activity which resembles that of the mature enzyme (Murphy and Crabbe, 1995; Makowski and Ramsby, 1996). Gelatin is cleaved by a broad spectrum of proteinases from other classes (e.g. serine proteinases) in addition to MMP-9. For this reason, AEBSF was included to prevent degradation of the substrate by HNE and cathepsin G also present in the PMNL homogenates. MMP-8, however does not cleave gelatin, but can be detected by type I collagen zymography (Gogly *et al.*, 1998). Due to the cost of commercial type I collagen and the amounts required per gel (~2 mg), type I collagen was purified from rat skin (Section 5.4.1).

2.6.1 Reagents

Stock gelatin solution [1% (w/v) in dd.H_2O]. Porcine skin gelatin (300 bloom) (0.01 g) was added to 1 ml dd.H_2O. The solution was heated until the gelatin had dissolved. This solution was made up fresh each time.

Renaturation solution [2.5% (v/v) Triton X-100]. Triton X-100 (6.25 ml) was dissolved in dd.H_2O in a final volume of 250 ml.

Gelatinase zymography buffer [50 mM Tris-HCl, 200 mM NaCl, 5 mM $CaCl_2$, 0.02% (w/v) NaN_3, 0.02% (v/v) Brij 35, pH 7.5 at 37°C]. Tris (0.61 g), NaCl, (1.17 g), $CaCl_2.6H_2O$ (0.109 g), NaN_3 (0.02 g) and Brij 35 [67 µl of a 30% (v/v) solution] were dissolved in dd.H_2O (90 ml) and heated to 37°C. The pH was titrated to 7.5 with HCl and the volume made up to 100 ml. The solution was stored at 4°C.

Type I collagenase zymography buffer [100 mM Tris-HCl, 5 mM $CaCl_2$, 0.005% (v/v) Brij 35, 0.02% (w/v) NaN_3, pH 8.0 at 37°C]. Tris (1.211 g), $CaCl_2.6H_2O$ (0.109 g), Brij 35 [17 µl of a

30% (v/v) solution] and NaN_3 (0.02 g) were dissolved in dd.H_2O (90 ml) and heated to 37°C. The pH was titrated to 8.0 with HCl and the volume made up to 100 ml. The solution was stored at 4°C.

Zymogram staining solution [0.2% (w/v) Coomassie Brilliant Blue R-250]. Coomassie Brilliant Blue R-250 (0.5 g) was dissolved in 50% [(v/v) in dd.H_2O] methanol. For zymography, a second destaining solution was not required and the gel was simply submerged in dd.H_2O after staining was complete.

2.6.2 Procedure

The samples were run on a 7.5% Laemmli SDS-PAGE [containing either 1-1.5 mg/ml type I collagen (purified as described in Section 5.4.1) or gelatin]. Upon completion of SDS-PAGE, the gel was removed from the electrophoresis unit, rinsed briefly in dd.H_2O, placed in unbuffered renaturation solution (250 ml) and shaken on an orbital shaker (1 h, RT). This was repeated once more, after which the gel was placed in a clean plastic container, pre-warmed zymography buffer (250 ml) added and digestion was allowed to proceed for at least 12 h at 37°C. After this time, the gel was washed with dd.H_2O (3 x 1 min), stained (4 h), washed in dd.H_2O (1 h) and stored at 4°C until photographed.

2.7 Gradient separation of PMNLs

In order to isolate the PMNL fraction of leukocytes from whole human blood, it was necessary to separate these cells by isopycnic density centrifugation. Table 2.4 lists the density of each blood cell type and it is evident that a highly accurate and discriminating gradient is necessary to obtain a pure fraction of a particular cell population.

Table 2.4 Density values for human blood cell populations.
[290 milliosmols (mOsm), pH 7.4, 25°C] (Roos and de Boer, 1986).

Cell population	Density (g/ml)
Platelets	1.054-1.062
Monocytes	1.055-1.065
Lymphocytes	1.060-1.072
Basophils	1.065-1.075
PMNLs	1.080-1.084
Eosinophils	1.082-1.090
Erythrocytes	1.090-1.110

Percoll (polyvinylpyrrolidone-coated silica particles) is an isoosmotic, non-toxic density medium of low viscosity (Pertoft *et al.*, 1978; Roos and de Boer, 1986). This medium was, therefore, used in most of the PMNL gradient separations in the present study. All of the steps were conducted at low temperature to avoid endocytosis of the density medium by the monocytes and PMNLs, which would alter their true density. In this study, blood drawn for the isolation of PMNLs was prevented from clotting using EDTA in mildly acidic conditions and the cells were provided with glucose to ensure sustained glycolysis and, hence, cell viability. Anticoagulation by heparin was avoided since heparin tends to cause platelet aggregation and adhesion of platelets onto leukocytes (Roos and de Boer, 1986).

PMNLs can be isolated by isopycnic centrifugation using a single layer or two-layer gradient. The two-layer gradient is comprised of densities of 1.077 and 1.090 g/ml while the single layer has a density of 1.077 g/ml. The two-layer gradient allows purification of PMNLs free from erythrocytes, but the potential for causing monocyte contamination during aspiration is great. The single layer gradient was used since it efficiently separated PMNLs from monocytes and the Percoll density medium. Contaminating erythrocytes can subsequently be removed by hypotonic lysis using either dd.H_2O or ammonium chloride and bicarbonate. Lysis by dd.H_2O is non-specific and may damage PMNLs, affect viability and induce degranulation. Lysis by ammonium chloride/bicarbonate is selective for erythrocytes (at 4°C) since PMNLs do not contain carbonic anhydrase and the Band 3 chloride/bicarbonate anti-porter that are responsible for lysis. No detrimental effect on PMNL function has been reported using this lysis technique (Roos and de Boer, 1986).

Following density centrifugation, the PMNLs were stained with May-Grünewald/Giemsa (BDH, Poole, UK) to check purity and trypan blue to check viability. Trypan blue is excluded from being taken up by live/viable cells, but penetrates and stains dead cells. The May-Grünewald/Giemsa stain contains basic (e.g. azure B) and acidic (e.g. eosin Y) dyes to stain acidic (e.g. nucleic acids, PMNL azurophil granules) and basic (e.g. histones, eosinophil granules) cellular components respectively (Horobin, 1990). This allows both visualisation of the nuclear patterns (important for distinguishing leukocyte populations) and the cytoplasmic organelle composition.

2.7.1 Reagents

Phosphate buffered saline (PBS: 9.2 mM Na_2HPO_4, 1.3 mM NaH_2PO_4, 140 mM NaCl, pH 7.4). Na_2HPO_4 (0.13 g), NaH_2PO_4 (0.015 g) and NaCl (0.818 g) were dissolved in dd.H_2O in a final volume of 100 ml. No pH adjustment was necessary. The solution was autoclaved (121°C, 15 min) and kept at 4°C.

Percoll dilution buffer (100 mM NaH_2PO_4, 1.54 M NaCl). NaH_2PO_4 (1.19 g) and NaCl (8.99 g) were dissolved in dd.H_2O in a final volume of 100 ml. This solution was autoclaved and stored at 4°C.

Trisodium citrate (130 mM in dd.H_2O). Trisodium citrate.5½H_2O (11.60 g) was dissolved in dd.H_2O and made up to a final volume of 250 ml. The solution was autoclaved and stored at 4°C.

BSA [5% (w/v) in PBS]. BSA (5 g) was allowed to dissolve in PBS (80 ml) for 1 h. The solution was then made up to 100 ml, filter sterilised through 0.45 μm and 0.22 μm filters before storing at -20°C.

Percoll working solution. Stock Percoll (9.3 ml) was mixed with Percoll dilution buffer (700 μl) just before use.

Percoll density gradient (1.077 g/ml). PBS (5.69 ml), BSA [2.5 ml of the 5% (w/v) stock solution], trisodium citrate (2.5 ml of the 130 mM stock solution) and diluted Percoll (14.31 ml) were mixed together and kept on ice.

Erythrocyte lysis buffer (155 mM NH_4Cl, 10 mM K_2CO_3, 0.1 mM EDTA, pH 7.4 at 4°C). NH_4Cl (0.829 g), K_2CO_3 (0.138 g) and EDTA (0.003 g) were dissolved in dd.H_2O (80 ml) and cooled on ice. The pH was adjusted to 7.4 and the volume made up to 100 ml. The solution was filter sterilised and stored at 4°C.

PMNL resuspension and storage buffer [PBSG: 8 mM Na_2HPO_4, 1 mM KH_2PO_4, 140 mM NaCl, 3 mM KCl, 0.5 mM $MgCl_2$, 1 mM $CaCl_2$, 0.1% (w/v) glucose, pH 7.3]. Na_2HPO_4 (0.114 g), KH_2PO_4 (0.02 g), NaCl (0.818 g), KCl (0.02 g), $MgCl_2.6H_2O$ (0.01 g), $CaCl_2.6H_2O$ (0.013 g) and glucose (0.1 g) were dissolved in dd.H_2O (80 ml) and made up to 100 ml without pH adjustment. The solution was filter sterilised and stored at 4°C.

PMNL methanol fixative. Methanol (100%) was poured into a Coplin jar and kept at -20°C.

Trypan blue stock solution [0.4% (w/v) in 0.81% (w/v) NaCl and 0.06% (w/v) K_2HPO_4]. Trypan blue (0.04 g), NaCl (0.081 g) and K_2HPO_4 (0.006 g) were dissolved in dd.H_2O in a final volume of 10 ml. The solution was filter sterilised and stored at 4°C.

2.7.2 Procedure

Venous blood was drawn into a sterile centrifuge tube containing citrate-phosphate-dextrose anticoagulant (5 ml) to a final volume of 50 ml. The tube was centrifuged gently (200 x g, 20 min, RT) to form a buffy layer and separate leukocytes from the platelets which remained in the plasma supernatant. The majority of the platelet-rich plasma was removed and discarded. The buffy layer (including some of the erythrocytes) (10 ml) was carefully loaded onto a pre-cooled 1.077 g/ml Percoll gradient (5 ml) and centrifuged (600 x g, 30 min, 20°C). The inclusion of erythrocytes is necessary for generation of the gradient and effective separation and resolution. The gradient density was calculated using the following formula:

Desired density (g/ml) = X(0.0056) + 0.1(0.0227) + 0.1(0.0219) + (0.8-X)(0.1245) -1

Where X = ml PBS per ml final suspension

0.0056 = PBS density -1

0.1 = ml albumin and trisodium citrate per ml final suspension

0.0227 = density of 5% (w/v) albumin -1

0.0219 = density of 130 mM trisodium citrate -1

0.8-X = ml Percoll per ml suspension

0.1245 = density of Percoll -1 (Roos and de Boer, 1986)

After centrifugation and removal of the supernatant, the pelleted erythrocyte and PMNL/eosinophil layer was resuspended in lysis buffer (10 ml, 10 min, 0°C). Clearing of the red opaque suspension indicated erythrocyte lysis. The cells were quickly centrifuged (600 x g, 2 min, 20°C), washed once and resuspended in storage buffer (1 ml) and kept on ice.

For counting and viability tests, an aliquot of PMNL suspension (20 µl) was mixed with PBS (30 µl) and trypan blue stock solution (50 µl) in a 1.5 ml Eppendorf microfuge tube and incubated (10 min, RT). The cell numbers and the proportion of viable cells were then estimated using a haemocytometer. Typical PMNL yields were ~2-2.5x10^6/ml and cell viability >98%.

To assess purity, a small PMNL aliquot (20 µl) was dispensed onto a clean glass slide, air-dried and plunged into cold methanol (15 min, -20°C). The slide was transferred to May-Grünewald stain (15 min, RT) and to Giemsa stain (30 min, RT). The slide was rinsed briefly with dd.H_2O, dried and mounted.

PMNL preparations were either frozen for western blot characterisation of antibodies (Section 2.8) or fixed and processed for microscopy (Section 2.9.3).

2.8 Western Blotting

Enzyme-linked immunosorbent assays (ELISAs) are usually used to assess the primary antibody response on crude sera whereas western blotting provides information about antibody specificities and the target antigen, its M_r, activation status (i.e. enzyme pro-form vs. active species, unless specific antibodies against the pro piece are available), oligomeric arrangement

or post-translational modifications.

The SDS-PAGE gel thickness (0.5 mm to 1.5 mm) and %T affects protein transfer time and efficiency of transfer onto the nitrocellulose/nylon support. Generally a thinner gel (0.5-1 mm) allows good transfer but a thicker gel may be required to allow larger sample loading volumes and hence greater protein transfer. A high %T generally hinders protein transfer from the PAGE gel onto the solid support, but too low a %T impairs band separation and resolution. In addition, the inclusion of methanol in transfer buffers decreases the acrylamide pore size even further (Towbin *et al.*, 1979).

Transfer buffers such as the popular Gershoni buffer (Gershoni and Palade, 1982) contain methanol and SDS at a relatively high pH to ensure anodal migration of proteins. Methanol improves the binding capacity of proteins for the nitrocellulose membrane, but it decreases pore size, removes protein-bound SDS and may even precipitate proteins within the gel. Poor transfer can, therefore, be remedied by using methanol-free Gershoni buffer or 10 mM CAPS, pH 11 (De Maio, 1994; Dunbar, 1994).

The choice of support membranes for protein transfer is usually determined primarily by the subsequent investigation steps to be performed. For conventional probing with antibodies, nitrocellulose (binding capacity ~80-100 $\mu g/cm^2$) or nylon (binding capacity ~480 $\mu g/cm^2$) are suitable. Although nylon has an attractive binding capacity, blocking steps are usually performed at high temperatures. This may denature sensitive antigens and these membranes do not stain well with the anionic dyes required to check protein transfer efficiency. If protein sequencing is intended after transfer, then the use of polyvinyldifluoride (PVDF) (binding capacity ~130-400 $\mu g/cm^2$) is necessary since it can withstand the harsh chemicals used in the sequencing chamber. Protein association with membranes are either electrostatic (nylon, nitrocellulose, Immobilon® PVDF) or hydrophobic (PVDF) (Dunbar, 1994).

Blocking steps to prevent non-specific protein association with the membrane include protein [ovalbumin, BSA, haemoglobin, non-fat milk (not suitable for phosphorylation studies due to high levels of phosphoprotein)] or non-protein (polyvinylpyrrolidone) in the presence or absence of non-ionic detergent (such as Tween 20).

2.8.1 Chromogenic blots

Substrate products for chromogenic blots should ideally be light stable, insoluble and easily visible after photography and/or electronic scanning. The enzymes used most frequently in western blotting are alkaline phosphatase and horseradish peroxidase (HRPO), although glucose oxidase and β-galactosidase have found application. The substrate commonly used for HRPO detection is diaminobenzidine (DAB) in the presence of H_2O_2. Oxidation of DAB results in an insoluble osmiophilic indamine polymer that is dark brown in colour. Further enhancement of colour may be achieved using divalent metal ions such as nickel or cobalt (Harlow and Lane, 1988). Another HRPO substrate, 4-chloro-1-naphthol was found to produce less background and was preferred over DAB that also has the disadvantage of being carcinogenic. The common alkaline phosphatase substrate is BCIP. Cleavage of the phosphodiester bond produces an indoxyl that can undergo oxidation into an insoluble blue dimer called 5,5' dibromo 4,4' dichloro indigo. The colourless tetrazolium salt, NBT, is converted into an insoluble purple formazan upon reduction by the electrons liberated by the indoxyl. This product is more photostable than DAB or 4-chloro-1-naphthol and was the substrate of choice. Non-enzymatic detection of western blots such as silver amplified immunogold gave unacceptable background staining and was not performed (Moeremans *et al.*, 1984).

2.8.1.1 Reagents

Gershoni blotting buffer [25 mM Tris-HCl, 192 mM glycine, 20% (v/v) methanol, 0.01% (w/v) SDS, pH 8.3]. Tris (6.05 g), glycine (28.8 g) and SDS [2 ml of a 10% (w/v) solution] were dissolved in 1.6 *l* of dd.H_2O. Methanol (400 ml) was added and the solution was stored at -20°C without pH adjustment.

Ponceau S protein stain solution [0.1% (w/v) in 1% (v/v) acetic acid]. Ponceau S (0.1 g) and acetic acid (1 ml) were added to a 100 ml volumetric flask and made up to volume with dd.H_2O.

Tris-buffered saline (TBS: 20 mM Tris-HCl, 200 mM NaCl, pH 7.4). Tris (2.42 g) and NaCl (11.69 g) were dissolved in dd.H_2O (950 ml). The pH was adjusted to 7.4 with HCl and the volume was made up to 1 *l* with dd.H_2O.

Blocking solution [5% (w/v) non-fat milk powder in TBS]. Non fat milk powder (5 g) was dissolved in TBS (100 ml).

Endogenous phosphatase quenching solution. Levamisole (0.05 g) was dissolved in blocking solution (100 ml) just before use.

Peroxidase quenching solution. NaN_3 (0.1 g) was added to blocking solution (100 ml).

Alkaline phosphatase detection buffer (50 mM Tris-HCl, 5 mM $MgCl_2$, pH 9.5). Tris (0.61 g) and $MgCl_2.6H_2O$ (0.10 g) were dissolved in dd.H_2O (90 ml). The pH was adjusted to 9.5 with HCl and the volume was made up to 100 ml with dd.H_2O.

Alkaline phosphatase substrate solution [0.015% (w/v) BCIP, 0.03% (w/v) NBT in detection buffer]. BCIP (1.5 mg in 1 ml DMF) and NBT (3 mg) were dissolved in detection buffer (10 ml) just before use.

HRPO substrate solution [0.06% (w/v) 4-chloro-1-naphthol and 0.00014% (v/v) H_2O_2 in TBS]. 4-Chloro-1-naphthol [2 ml of a 0.3% (v/v) solution in methanol] was diluted in TBS (8 ml) and H_2O_2 [4 µl of a 35% (v/v) solution] was added just before use.

2.8.1.2 Procedure

Following SDS-PAGE (Section 2.4), the gel was dismantled from the electrophoresis unit, submerged briefly in ice cold transfer buffer together with Hybond™-C nitrocellulose hybridisation transfer membrane (0.45 µm) and Whatman filter paper. The transfer cassette (Hoefer® TE Series Transphor Electrophoresis Unit) was assembled and orientated in the electrophoresis chamber to ensure that the membrane was closest to the anode. The chamber was filled with ice-cold transfer buffer and stirred with a magnetic stirrer throughout the run. Transfer was performed at a constant current of 200 mA for 2 h. After this time, the gel and membrane were disassembled from the cassette and the outline of the gel was marked on the membrane. The membrane was rinsed with dd.H_2O and then stained with Ponceau S to visualise the M_r markers, the sample protein profiles and to assess the efficiency of the transfer. The positions of the lanes and the markers were marked by pricking the membrane gently with a needle point. The Ponceau S was decolourised with TBS and the membrane was air-dried before probing, or alternatively stored in a desiccator at 4°C.

Blocking solution containing either 2 mM levamisole or 0.01% (w/v) NaN_3 was added to the membrane (1 h, 20 ml) to prevent non-specific adsorption of antibodies and to quench

endogenous PMNL alkaline phosphatase and MPO, respectively. The membrane was washed in TBS (3 x 5 min, 10 ml/wash) and incubated with primary antibody diluted in 0.5% (w/v) BSA-TBS (2 h, 1 ml/lane). Following washing in TBS (3 x 5 min, 10 ml/wash), the membrane was incubated with the appropriate enzyme conjugated secondary antibody diluted in 0.5% (w/v) BSA-TBS (1 h, 1 ml/lane). The membrane was washed as before, immersed in the appropriate substrate and developed until distinct bands were observed against a lightly coloured background. The membrane was rinsed with dd.H_2O, dried and kept in the dark until photographed.

2.8.2 Enhanced chemiluminescence (ECL) blots

Chemiluminescence refers to the emission of blue light resulting from the HRPO/H_2O_2-mediated oxidation of cyclic diacylhydrazides (such as luminol). HRPO oxidises a peracid salt (in the presence of luminol) which leads to a raised oxidation state of the HPRO haem group. Upon returning to the ground state, a luminol radical is formed and emits light as it decays. In ECL, an enhancer molecule (such as phenol) is included in the reaction mixture to react with the HRPO haem group in place of the luminol. This leads to the formation of phenol radicals that in turn react to form luminol radicals and light is emitted in the manner as with unenhanced chemiluminescence. The ECL reaction is also considerably faster and is highly stable ($t_{1/2}$~60 min) (Durrant and Fowler, 1994). The light emission from the HRPO-linked secondary antibody is detected using blue-light sensitive X-ray film (λ_{max} = 428 nm). ECL is at least 10-fold more sensitive (<1 pg) than other radioactive and non-radioactive detection systems and signals can be obtained in less than a minute exposure. Multiple exposures can be taken due to the slow decay rate of light. Since no insoluble substrate products are produced in ECL, the membranes can be stripped and reprobed a number of times following thorough washing to remove substrate.

2.8.2.1 Reagents

Tris-EDTA-NaCl buffer (TEN: 25 mM Tris-HCl, 1 mM EDTA, 150 mM NaCl, pH 7.6). Tris (3.03 g), EDTA (0.29 g) and NaCl (8.77 g) were dissolved in dd.H_2O made up to 1 *l* without pH adjustment and autoclaved.

1 M $MgCl_2$ stock solution. $MgCl_2.6H_2O$ (50.83 g) was dissolved in dd.H_2O to a final volume of 250 ml and autoclaved.

5 M NaCl stock solution. NaCl (73.05 g) was dissolved in dd.H_2O to a final volume of 250 ml

and autoclaved.

Blocking solution [3 % (w/v) non-fat milk powder in TEN, pH 7.6]. Non-fat milk powder (3 g) was dissolved in TEN (100 ml) just before use.

Peroxidase quenching solution. NaN_3 (0.1 g) was added to blocking solution (100 ml).

ECL substrate solution. Equal volumes (500 µl) of detection solution 1 and 2 (containing H_2O_2 and luminol) were mixed before use.

2.8.2.2 Procedure

The ECL procedure is essentially the same as for the chromogenic blots, but Table 2.5 highlights some of the differences.

Table 2.5 Procedure for probing and detecting blotted proteins by ECL.

Step	Solution	Volume	Incubation time
1. Block and quench	3% milk-TEN + NaN_3	20 ml	30 min
2. Wash	3% milk-TEN	3 x 10 ml	3 x 15 min
3. Primary Antibody	3% milk-TEN	5 ml	2 h
4. Wash	3% milk-TEN	3 x 10 ml	3 x 15 min
5. Secondary Antibody	3% milk-TEN	10 ml	45 min
6. Wash	TEN	2 x 10 ml	2 x 15 min
7. Wash	TEN + 200 mM $MgCl_2$	2 x 12.5 ml	2 x 15 min
8. Wash	TEN + 1 M NaCl	10 ml	5 min
9. Wash	dd.H_2O	10 ml	1 min
10. Expose	ECL solution	125 µl/cm^2	30 s-10 min

After the final dd.H_2O wash, the nitrocellulose membrane was placed onto a clean glass support plate. All reagents and equipment were moved to a photography darkroom and all subsequent steps were performed in the dark (with safe lights). ECL substrate solution was prepared just before use and was dispensed onto the membrane with a micropipette, taking care to ensure even distribution. Excess solution was removed with filter paper and the membrane was sandwiched between two clear overhead projector transparency sheets, avoiding the inclusion of air bubbles and/or creases in the plastic. Hyperfilm™ ECL autoradiography film was cut to the

approximate size of the membrane and placed on top of the sandwiched membrane. The film and the membrane were transferred to an X-ray film cassette and film exposure was allowed to proceed for up to 10 min, depending on the signal strength. The cassette was opened and the film quickly transferred to developer (1 min), dd.H_2O (10 s) and then fixer (>10 min). The film was washed in dd.H_2O and allowed to dry. This process of film exposure could be repeated by varying the time of exposure until satisfactory results were obtained.

2.9 Cryoimmunocytochemistry and immunogold labelling

The main EM technique used in this study was transmission EM (TEM) on thawed cryoultramicrotomy sections and the immunocytochemistry method devised by Tokuyasu (Tokuyasu, 1978; 1980; 1986). Cryoultramicrotomy involves cutting thin (80-100 nm) sections of cell specimens at very low temperatures (less than -100°C). Unlike conventional resin embedding microscopy, the cells are fortified with concentrated (2.3 M) sucrose solutions in PBS that provide a sturdy glass-like medium for sectioning.

Sucrose serves as a cryoprotectant for the fixed specimen during freezing in liquid nitrogen (-199°C) by replacing the majority of cell-bound water. The freezing point of the remaining water is lowered considerably by the high sucrose concentration. With regular slow freezing, water forms large ice crystals known as hexagonal or cubic ice, the large structure of which would rupture cell membranes and destroy cell integrity. Addition of sucrose and rapid freezing rates (~10 000°C/s) allow water to form vitreous ice that does not undergo volume changes and has no crystalline structure (Dubochet *et al.*, 1982).

Cryoimmunocytochemistry avoids potential antigen destruction by allowing the use of relatively light fixation steps, by avoiding harsh fixation required for the use of resins. Membrane structure is, therefore, retained in cryoultramicrotomy and is not extracted by solvent dehydration. The whole tissue is preserved in a fully hydrated form, unlike resin embedding techniques. The low temperature also allows retention of antigenicity and the fully hydrated nature of the tissue provides a more 'life-like' view of the cell.

Sectioning of specimens requires the use of an ultramicrotome equipped with a cryoattachment suitable for ultrathin sectioning, a liquid nitrogen dispensing unit, tungsten-coated glass knives and formvar-coated, carbon-coated, glow-discharged nickel grids. Glass knives are produced by fracturing 1 inch glass strips into rectangles and then right-angled triangles to produce sharp

edges that can cut (or, rather, fracture) through hard resins and cryo specimens. Diamond knives may also be used, but these are very expensive. The glass knife-edge tends to blunt over time owing to the fluid nature of glass and, therefore, knives destined for resin sectioning have a finite lifespan. Cryo knives are, therefore, coated with a thin film of tungsten (Roberts, 1975) since this improves section delivery onto and along the knife surface, as the tungsten particles act like small 'ball bearings'. In addition, the tungsten film prevents fluid blunting of the knife-edge and so cryo knives effectively have an extended life span for sectioning.

The preparation of grids for cryo sectioning requires more effort than that required for conventional resin. The grid is first covered with formvar to provide a support for the section. This is followed by deposition of a thin layer of carbon onto the formvar. Finally, the grids are rendered hydrophilic by electron bombardment (glow-discharging). This is essential to ensure adherence of the section to the grid.

Immunolabelling involves incubation of thin cell sections with an antibody raised toward the antigen of interest (Sitte *et al.*, 1989). This is followed by incubation with another molecule that binds the antibody-antigen complex and allows detection in the electron microscope. A combination of protein A and rabbit primary antibodies are popular choices for labelling since protein A from *Staphylococcus aureus* recognises and binds the fragment crystallisable (Fc) region of the rabbit IgG (in a 1:1 stoichiometry) and does not interfere with the stability of the immune complex. Protein A is easily adsorbed to gold colloids and thus a particular antigen can be localised on a cell section. Protein A can bind Fc regions of other IgG species, but with lower affinity (Leunissen and de Mey, 1989; Griffiths, 1993). If the primary antibody has been raised in an animal species that exhibits low protein A binding (e.g. chicken IgY, the immunoglobulin present in egg yolks), a linker/bridging rabbit anti-IgY IgG may be used and this detected with protein A. Use of a linker also allows an increase in labelling density since more than one rabbit IgG binds per IgY molecule.

Control labelling reactions are essential for optimising protein A gold dilutions and identifying any potential non-specific high-affinity interactions of pre-immune sera with cell components. Controls include: 1), incubation of the section with preimmune IgG/IgY and detection with protein A gold; 2), incubation of the sections with protein A gold only and 3), adsorption of the primary antibody with soluble antigen followed by labelling the section. The former two controls are routinely employed; however, the latter control relies on the availability of pure

antigen and is not always possible. In all cases, the pre-immune antibodies and gold probes are used at the same level as used in the labelling with the specific antibodies.

2.9.1 Glass knife production and tungsten coating

The glass strip was cleaned with detergent and water, dried, positioned on a modified LKB 7800 glass knife maker with the ridged imperfect edge facing downwards and fractured to produce glass knives as described by Moorewood *et al.*, 1992. The knife-edges were examined and those with a barely visible counter-piece width (< 0.2 mm) were selected. The knives were coated with tungsten in an Edwards E306A high vacuum coater ($5x10^{-5}$ Torr, 5 min) (Roberts, 1975) and in a container with double sided tape along the bottom.

2.9.2 Preparation of grids for cryoultramicrotomy

Hexagonal 100 or 200 mesh nickel grids (ϕ = 3.05 mm) were immersed in 95% (v/v) ethanol, cleaned by sonication (5 min) and air-dried on filter paper. Formvar solution [0.25% (w/v) in chloroform] was poured into a Coplin jar to a level half of that taken up by a microscope slide. An ethanol-cleaned glass microscope slide was dipped into the solution and immediately withdrawn and the edge touched to a piece of filter paper. The thin film of formvar on the slide was visualised by condensation formed upon exhaling gently onto the slide. A scalpel blade was used to cut the formvar film along the sides of the slide. The slide was dipped into a container filled with distilled water at an angle of ~45° for 1 film or perpendicular if film from both sides of the slide were required. Nickel grids were placed shiny-side upwards onto the floating film with forceps. Once sufficient grids were applied to the film, another clean glass slide was positioned 45° to the film and brought down vertically to submerge the film (now adherent to the slide). The slide was positioned film-side up in the water and gently withdrawn. This method was used instead of the conventional scooping action since wrinkling and grid overlap is common with the scooping technique. The formvar-coated grids were allowed to air-dry overnight.

For carbon-coating, the grids were placed in an Edwards E306A high vacuum coater ($1x10^{-5}$ Torr, 5 s). Glow-discharging was performed in a modified Polaron E 15000 sputter coater (800 kV, 16 mA, 0.5 Torr, 10 s). The grids were stored in closed containers.

2.9.3 Labelling protocol

2.9.3.1 Reagents

Buffers and fixatives.

10 x PBS stock solution, pH 7.2. NaCl (8 g), KCl (0.2 g), Na_2HPO_4 (0.115 g), KH_2PO_4 (0.2 g) and NaN_3 (0.2 g) were dissolved in dd.H_2O (90 ml). The pH was titrated to 7.2 with NaOH and the volume made up to 100 ml. The solution was autoclaved and stored at 4°C.

1 x PBS working solution, pH 7.2. PBS stock solution (1 ml) was diluted with dd.H_2O (9 ml).

PFA stock solution [16% (w/v)]. PFA (16 g) was dissolved in dd.H_2O (80 ml), heated to 60°C (in a fumehood) and the solution was cleared with the dropwise addition of a NaOH solution. After cooling, the volume was made up to 100 ml and aliquots were stored at -20°C.

Glutaraldehyde fixative [1% (v/v)]. Glutaraldehyde [1 ml of a 25% (v/v) stock solution] was diluted to 25 ml with PBS.

Buffered fixative for cryoultramicrotomy [200 mM HEPES, 2% (w/v) PFA, 0.05% (v/v) glutaraldehyde, pH 7.2]. HEPES (4.77 g), PFA [12.5 ml of a 16% (w/v) stock solution] and glutaraldehyde [200 µl of a 25% (v/v) stock solution] were dissolved in dd.H_2O (90 ml). The pH was checked with indicator paper, adjusted to 7.2 with NaOH and made up to 100 ml.

Cryoprotectants.

2.1 M sucrose in PBS, pH 7.2. Sucrose (71.88 g) was dissolved in dd.H_2O to a final volume of 90 ml. The solution was microwaved until all the sucrose had dissolved. Once the solution had cooled, PBS (10 ml of a 10 x stock solution) was added and mixed thoroughly. The solution was stored at 4°C.

2.3 M sucrose in PBS, pH 7.2. Sucrose (78.73 g) was dissolved in dd.H_2O to a final volume of 90 ml. The solution was microwaved until all the sucrose had dissolved. Once the solution had cooled, PBS (10 ml of a 10 x stock solution) was added and mixed thoroughly. The solution was stored at 4°C.

Gelatin cell embedding solution [10% (w/v)]. Gelatin (1 g) was added to dd.H_2O (10 ml) and heated in a microwave until dissolved. This solution was always made fresh.

Sectioning, retrieval and staining solutions.

Aqueous uranyl acetate [2% (w/v)]. Uranyl acetate (2 g) was dissolved in dd.H_2O and made up to 100 ml and stored in the dark at 4°C.

Methylcellulose [2% (w/v)]. Methylcellulose (1 g) was dissolved in dd.H_2O (50 ml), left at 4°C for 2 days and centrifuged (20000 x g, 1 h, 4°C). The supernatant was stored at 4°C.

Cryosection pickup solution [1.15 M sucrose-PBS, 1% (w/v) methylcellulose]. Sucrose (500 µl of a 2.3 M sucrose-PBS solution) was mixed with methylcellulose [500 µl of a 2% (w/v) solution] (taking care to avoid air bubbles) and kept on ice.

Cryosection sealing solution [0.2% (w/v) uranyl acetate, 1.8% (w/v) methylcellulose]. Methylcellulose (900 µl) was mixed with uranyl acetate (100 µl) within 30 min of use and stored on ice.

Grid flotation gel [0.3% (w/v) agarose, 1% (w/v) gelatin in PBS]. Agarose (0.03 g) and gelatin (0.1 g) were dissolved in dd.H_2O (9 ml) and microwaved until dissolved. Upon cooling, PBS (1 ml of a 10 x stock solution) was added. The solution was poured into Petrie dishes and allowed to gel on ice.

Blocking and quenching solutions for immunolabelling.

All solutions were made up fresh as required.

BSA-PBS [1% (w/v) and 0.1% (w/v)]. BSA (10 mg or 1 mg) was dissolved in PBS (10 ml).

Glycine-PBS (20 mM). Glycine (0.15 g) was dissolved in PBS and made up to 100 ml.

FSG [1% (v/v)]. FSG (222 µl of a 45% [v/v] solution) was made up to 10 ml with PBS.

FSG-BSA [1% (v/v) FSG, 0.8% (w/v) BSA in 20 mM glycine-PBS]. FSG [1.11 ml of a 45% (v/v) solution] and BSA (0.4 g) were dissolved in glycine-PBS in a final volume of 50 ml. The

solution was centrifuged (10000 x g, 2 h, 4°C) to remove insoluble debris and the supernatant was aliquoted and stored at -20°C.

2.9.3.2 Procedure

For cryoultramicrotomy, PMNLs (1-2x10^6) were pelleted in a 1.5 ml Eppendorf microfuge tube (400 x g, 5 min, 4°C) and fixed with 2% (w/v) PFA, 0.05% glutaraldehyde in 200 mM HEPES, pH 7.4 (4°C, o/n). The cells were centrifuged gently (200 x g, 2 min, RT) and the fixative was removed. Residual aldehydes were quenched with 20 mM glycine-PBS (1 ml, 1 h, RT), whereafter warmed gelatin embedding solution (1 ml) was added to the cell pellet. The cell pellet was dispersed by gentle mixing and allowed to infiltrate the cells (1 h, 37°C). The cells were centrifuged (400 x g, 5 min, RT) and the gelatin solution was aspirated. The Eppendorf tube was placed in ice to allow the gelatin to solidify (20 min) and the pellet was infiltrated with 2.3 M sucrose-PBS (1 ml, 4°C, o/n). The pellet was carefully removed from the microfuge tube using a needle point, placed in successive droplets of 2.3 M sucrose-PBS until all the excess water had been removed and cut into small trapezoids (~0.125 mm^3), using a scalpel blade and a dissecting microscope. Each trapezoid was positioned on top of a small copper pin (2 mm ϕ x 12 mm), with the larger base resting on the pin surface. Excess sucrose was removed using a small piece of filter paper and the specimen was rapidly frozen in liquid nitrogen with continual shaking, to ensure quick heat dissipation and stored in liquid nitrogen.

Each specimen for sectioning was transferred to a pre-cooled cryoultramicrotome chamber (-100°C) of an RMC MT6000XL ultramicrotome, fitted with a CR2000 cryo attachment, and allowed to equilibrate (>5 min). Ultrathin sections (~80 nm) were cut with a tungsten-coated knife with a knife and specimen temperature of -100°C. Sections were maneuvered from the knife-edge using an eyelash attached to an orange stick. Sections were retrieved by quickly introducing a droplet of 1% methylcellulose/1.15 M sucrose-PBS in a 1 mm wire loop. Sections which 'jump' onto the droplet must be removed from the cryochamber before the droplet freezes (~2 s). The sections were transferred onto formvar-coated, carbon-coated, glow-discharged nickel grids that were placed, section side down, on a cooled gel of agarose and gelatin. This allows the sucrose to gently diffuse into the gel since floating of grids directly onto PBS can pull sections off during dissolution of the sucrose. When sufficient sections were cut and collected onto grids, the gel was placed in a 37°C incubator to melt the gel and allow grid retrieval.

Immunolabelling was performed by incubating the grids on small reagent droplets on Parafilm

at room temperature. The sequence of incubation is shown in Table 2.6. After incubation on the sealing solution (done on ice and in the dark), the grids were suspended in a wire loop (3.5 mm ϕ) and excess sealing solution was drawn off with filter paper, leaving the grid suspended in a thin film which is allowed to dry. The grids were removed from the loops by piercing the film with forceps and viewed in a Jeol 100CX or a Philips CW120 Biotwin TEM at 80-100 kV.

Table 2.6 Immunolabelling protocol for PMNL cryosections.

Step	Solution	Incubation time
1. Blocking[a]	2% gelatin, 1% BSA, 1% FSG all in PBS	10 min each
2. Aldehyde quenching	20 mM glycine-PBS	3 x 1 min
3. Blocking	0.1% BSA-PBS	1 min
4. Primary antibody (5 µl)	Diluted in 1% BSA-PBS	30 min
5. Wash[b]	0.1% BSA-PBS	4 x 1 min
6. Protein A gold (10 µl)	Diluted in 1% BSA-PBS	30 min
7. Wash	0.1% BSA-PBS	5 min
8. Wash[c]	PBS	4 x 5 min
9. Fixation	1% glutaraldehyde-PBS	5 min
10. Wash	PBS	5 min
11. Wash[d]	dd.H_2O	5 x 2 min
12. Membrane stabilisation	1% uranyl acetate/150 mM oxalate pH 7.0	5 min
13. Wash	dd.H_2O	2 x 5 min
14. Sealing	0.2% UA/1.8% MC	>10 min

[a] Towards the end of these studies, it was observed that FSG-BSA could substitute for all the other blocking solutions between steps 1 and 7. The FSG-BSA also greatly reduced background labelling.

[b] If a linker antibody is required, it is added here (30 min) and subsequently washed (with 0.1% BSA-PBS or FSG-BSA) (4 x 1 min).

[c] A high salt wash (1 M NaCl-PBS) was included here in double labelling experiments.

[d] In double labelling, the glycine quenching step (3 x 1 min) must follow to neutralise any residual glutaraldehyde before addition of the second primary antibody.

2.10 Production of 14 nm gold colloids by citrate and tannic acid-citrate

Gold colloid particles are produced by reduction of trivalent gold salts to gold metal ($Au^{3+} \rightarrow Au$). The size of the colloids are controlled by the concentration and strength of the reducing agent; under highly reducing conditions, many nuclei are formed that serve as growth centres for further reduction of Au^{3+} ions and many small colloidal gold particles are formed. Under less reducing conditions, fewer growth nuclei are formed and hence the average colloid diameter is greater. More accurately, the average particle diameter is inversely proportional to the cube root of the number of nuclei formed and hence colloid size is inversely proportional to the strength of the reducing agent (Griffiths, 1993). A number of reducing agents have been used in the production of gold colloids including white phosphorus, ethanol, ascorbic acid, and tannic acid-citrate. The tannic-acid citrate produces colloid sizes of low variance and is simple in practice. Tannic acid promotes a fast reduction (for nuclei formation) while citrate reduces at a slower rate and allows for growth of the colloid.

Gold colloids are lyophilic (i.e. they possess hydrophobic and anionic properties) and aggregate in solutions of high ionic strength. This tendency is important to bear in mind when adsorbing a protein of interest to a gold colloid (e.g. antibody, protein A, protein G, streptavidin, BSA). To prevent electrolyte-induced colloid aggregation, absorption is performed at a pH equal to pI + ½ of the protein (De Mey, 1986). This is to ensure that the nett charge on the protein is slightly negative (similar to the colloid) and electrostatic attraction is avoided and adsorption is predominantly by virtue of coulombic and van der Waals forces (Cuypers *et al.*, 1978). Upon completion of adsorption, a 'neutral' protein such as BSA (or in some cases PEG 20 kDa) is added to block any sites on the colloid unadsorbed to the protein of interest that may interact non-specifically on tissue sections.

An electrolyte challenge is used to establish the minimal amount of protein for adsorption and hence stabilisation of the colloid of a particular diameter. Chloride ions are used since they destabilise gold colloids to a greater extent than other halides ($Cl^- > Br^- > I^-$) (Handley, 1989). Colloid aggregation (instability) is indicated by a colour change from wine-red to a grey-blue. In this way, stabilising proteins may be serially diluted, a standard amount of gold added, allowed to adsorb and the greatest dilution of the protein stabilising the colloid (colloid remains pink) is established by the addition of chloride ions.

Labelling density, antibody penetration and steric hindrance effects are determined by the

colloid size. Generally, the smaller the colloid the better since high labelling densities, good penetration and minimal hindrances are possible. For multiple labellings, the probes should be as small as possible, but easily distinguished from each other. Gold colloids are stable for many months and may be directly applied to TEM studies.

In these studies, 14 nm BSA-gold colloids were prepared for use as fluid phase endocytic markers in cryoimmunocytochemistry. All other protein A gold particles (5, 10 and 15 nm) were purchased from the Department of Cell Biology, University of Utrecht, the Netherlands.

2.10.1 Reagents

All solutions were made up on the day required in clean glass containers from AR grade reagents.

Chlorauric acid [1% (w/v) in dd.H_2O]. $HAuCl_4$ (0.01 g) was weighed out just before use using a plastic spatula and dissolved in dd.H_2O (1 ml) in a clean glass test-tube wrapped with aluminium foil.

Trisodium citrate [1% (w/v) in dd.H_2O]. Trisodium citrate.$2H_2O$ (0.114 g) was dissolved in dd.H_2O and made up to 10 ml.

Tannic acid [1% (w/v) in dd.H_2O]. Tannic acid (0.1 g) was dissolved in dd.H_2O and made up to 10 ml.

2.10.2 Procedure

The $HAuCl_4$ solution (1 ml) and dd.H_2O (80 ml) were added to a clean glass beaker (designated A). Trisodium citrate (4 ml), dd.H_2O (16 ml) and tannic acid (25 µl) were added to a second glass beaker (designated B). The two separate solutions were heated to 60°C and then mixed together rapidly with stirring. Colloidal growth was allowed to continue until a red colour had developed (~25 min). The solution was heated to 95°C and cooled rapidly on ice.

2.10.3 Determination of the minimum amount of protein for colloid stabilisation

2.10.3.1 Reagents

Gold colloid stabilising solution [10% (w/v) BSA in dd.H_2O, pH 8.0]. BSA (1 g) was dissolved in dd.H_2O (8 ml). The pH was titrated to 8.0 with dilute NaOH and the volume made up to

10 ml.

Electrolyte challenge solution [10% (w/v) NaCl in dd.H_2O]. NaCl (1 g) was dissolved in dd.H_2O and made up to 10 ml.

2.10.3.2 Procedure

The determination of the minimal amount of BSA to stabilise the gold sol was performed according to Zsigmondy (1925). The gold sol was adjusted to pH 8.0 (½ pH unit above the pI of BSA) using NaOH and monitored with pH paper strips and dispensed into microtitre plate wells (100 µl/well). BSA [1-10 µl of the 10% (w/v) solution] was added to each well and the volume made up to 110 µl with dd.H_2O. The solutions were stirred gently and allowed to stand (10 min, RT). NaCl (10 µl) was added to each well, mixed, and allowed to stand for a further 5 min. The end point was identified as the well with the lowest [BSA] that did not turn blue (1 µl BSA/100 µl sol). The corresponding amount of BSA was quickly added to the entire volume of gold sol (1 ml/100 ml sol) with rapid mixing. The sol was pelleted (7000 x g, 30 min, 4°C) and resuspended in supernatant (1 ml). Size estimation and variance was determined by TEM by aliquoting and drying a droplet (10 µl) of the sol on a formvar coated nickel grid. A homodisperse sol of colloids of 14 nm diameter with a standard deviation of 8.8% was obtained and considered acceptable. No further purification through glycerol gradients was necessary and the sols were kept in aliquots of 50 µl at 4°C.

CHAPTER 3

PMNL GPI-anchored proteins as secretory vesicle marker proteins

3.1 Introduction

The primary aim of this thesis was to further investigate the intracellular localisation of TIMP-1 in PMNLs. Although Triebel *et al.* (1995) were able to detect the presence of TIMP-1 by immunofluorescence, the limited resolution of this method did not permit the authors to assign TIMP-1 to a specific intracellular location. For this reason, EM was employed in the current study. Unlike fluorescence microscopy, the high magnification and resolution of EM, when coupled with immunocytochemistry, allows the detection of proteins present in single organelles (rather than broad populations) and also permits identification of organelles and granules on the basis of morphology, electron density and size.

At the time of writing, the PMNL was known to contain at least five major granule populations, differing with respect to their size, protein composition and sensitivity to $Ca^{2+}{}_i$-induced degranulation (discussed in Sections 1.3 and 1.5). Localisation of TIMP-1 to any of the known granule populations was deemed important as it may provide important information regarding the possible order of TIMP-1 release during degranulation. In order to identify the various granule populations, a number of marker proteins have been identified that occur predominantly within a particular population (see Table 1.1). Although a considerable amount of overlap in protein expression occurs during PMNL maturation (and, therefore, may distribute a particular protein over more than one population), the following markers show the most discrete distribution: MPO (azurophil granules), lactoferrin (specific granules), proMMP-8 (specific granules), proMMP-9 (specific and gelatinase granules) and LAMPs-1 and -2 (multilaminar/multivesicular bodies) (Bainton, 1999).

At the time of writing, however, the only markers described for the secretory vesicles (one of the most recently discovered PMNL organelle populations) were HSA and alkaline phosphatase (Borregaard and Cowland, 1997). The secretory vesicle was originally described by Kobayashi and Robinson (1991) using alkaline phosphatase histochemistry and further characterised by Borregaard *et al.* (1992, 1993) and Sengeløv (1996). These vesicles are synthesised during the

band/segmented stage, just before full PMNL maturation. They are thought be derived from endosomes although, unlike true endosomes, they can be mobilised to the plasma membrane and release their contents. Unlike other PMNL populations, the non-membrane-bound lumenal proteins of secretory vesicles are all derived from endocytosed plasma (hence the use of HSA as a marker protein) and do not contain PMNL synthesised proteins. The primary function of the secretory vesicles is thought to be that of a major reservoir of endothelial adhesion proteins and receptors for ECM and complement components. They are highly sensitive to increases in $[Ca^{2+}_i]$ and are the most readily released organelle population during extravasation when the PMNL makes initial contact with the endothelium and ECM (Borregaard and Cowland, 1997).

The first part of this chapter describes the characterisation of PMNL granule marker protein antibodies, for subsequent use in the immunocytochemical localisation of TIMP-1 in PMNLs. In addition, a rabbit anti-HSA antibody was assessed for its suitability for the identification of secretory vesicles using immunocytochemistry. HSA and histochemistry for alkaline phosphatase were used as markers for the secretory vesicles. Unanticipated problems, however, necessitated an alternative approach and lead to the designing of a novel method for the detection of secretory vesicles (reported in the second part of this chapter).

As PMNL GPI-anchored proteins [all of which are hypothesised to reside in secretory vesicles (Cain *et al.*, 1995)] were potentially a marker for this organelle, they were purified by exploiting the temperature-dependent solubility characteristics of Triton X-114 (Brusca and Radolf, 1994), and partitioned from other Triton X-114 phase-partitioned proteins by deamination and cleavage of their anchors with nitrous acid. Antibodies towards the GPI-anchored proteins were raised in chickens and the reliability of such antibody preparations for the identification of secretory vesicles was verified using western blotting of PMNL granule fractions testing positive or negative for alkaline phosphatase. These antibodies were used to detect secretory vesicles in immunocytochemical studies in Chapter 4 to facilitate the assignment of TIMP-1 to a particular granule population.

3.2 Characterisation of antibodies against PMNL granule marker proteins

In order for an accurate immunolocalisation study to be performed on PMNLs, thorough assessment of antibody specificity using crude cell homogenates is required. Crude homogenates are used to allow the identification of any potential cross-reactivity of antibody preparations with unrelated proteins in the target tissue that may lead to incorrect localisation results. All of the rabbit and chicken primary antibodies used in this study were polyclonal and, therefore, have the potential to recognise and bind a number of epitopes. Rabbit antibodies are the most useful species for use in TEM immunocytochemistry (particularly immunogold labelling) as protein A from *S. aureus* binds the Fc region of rabbit IgG (Harlow and Lane, 1988). Protein A is, therefore, commonly adsorbed to gold colloids to provide an electron dense detection system for visualising antigen-bound antibodies on tissue sections. All of the antibodies used in this study were either purchased commercially [antibodies against the PMNL granule markers MPO (azurophil granules), lactoferrin (specific granules)] or supplied by other laboratories [antibodies against TIMP-1, proMMP-8 (specific granules), proMMP-9 (specific and gelatinase granules) and the PMNL secretory vesicle luminal marker, HSA]. Although the antibodies against proMMP-8, proMMP-9 and TIMP-1 had been characterised by western blotting of pure antigens (Bergmann *et al.*, 1989), no investigations on whole PMNL homogenates had been performed prior to this study. Since the MMPs share extensive sequence and domain homology (Section 1.7), the potential for cross-reactivity of antibodies with other members of the MMP family is great. Therefore, the first part of this chapter describes the specificity assessment of all supplied antibodies using western blotting.

3.2.1 Reagents

All western blotting reagents and buffers were prepared as described in Section 2.8.

3.2.2 Procedure

PMNLs were isolated (Section 2.7.2), resuspended in PBS (~$1x10^7$ cells/1 ml) and snap frozen in liquid nitrogen. When required, cells were thawed in the presence of 1 mM EDTA, 2 mM PMSF (or AEBSF) and 1% (w/v) NaN_3, centrifuged (10000 x g, 20 min, 4°C) and the supernatant (~80 µg/lane) was separated on a 10% reducing Tris-Tricine SDS-PAGE gel (Section 2.4.2) and blotted onto nitrocellulose (Section 2.8.1).

Membrane blocking and quenching of endogenous MPO and alkaline phosphatase activity was performed as described in Section 2.8.1. Primary antibodies used were: rabbit anti-lactoferrin (50 µg/ml), anti-MPO (25 µg/ml), anti-proMMP-8 (10 µg/ml), anti-proMMP-9 (10 µg/ml) and anti-HSA (20 ng/ml). Following washing in TBS (3 x 5 min, 10 ml/wash), the membrane was incubated with enzyme conjugated secondary antibody diluted in 0.5% (w/v) BSA-TBS [HRPO-conjugated sheep anti-rabbit IgG (1/10000) or alkaline phosphatase-conjugated goat anti-rabbit IgG (1/5000)]. The membrane was washed in TBS as before and developed with BCIP/NBT (Section 2.8.1) or ECL (Section 2.8.2).

3.2.3 Results and Discussion

The antibodies raised against MPO, lactoferrin and HSA only targeted proteins of the anticipated M_r on western blots of crude PMNL homogenates and were, therefore, judged specific (Figure 3.1). The western blots also confirmed the specificities of the proMMP-8 and proMMP-9 antibodies which had previously been characterised on only pure antigen (Osthues *et al.*, 1992) or semi-purified PMNL homogenates (Bergmann *et al.*, 1989) and not crude homogenates which contain all the antigens with which the antisera could potentially react. As bands were seen only at 82 and 92 kDa for proMMP-8 and -9, respectively, and control blots using pre-immune IgG gave no signals (results not shown), these antibodies, as in the case of all other antibodies against PMNL marker proteins, were judged specific and were shown not to cross-react with other PMNL granule proteins in crude homogenates.

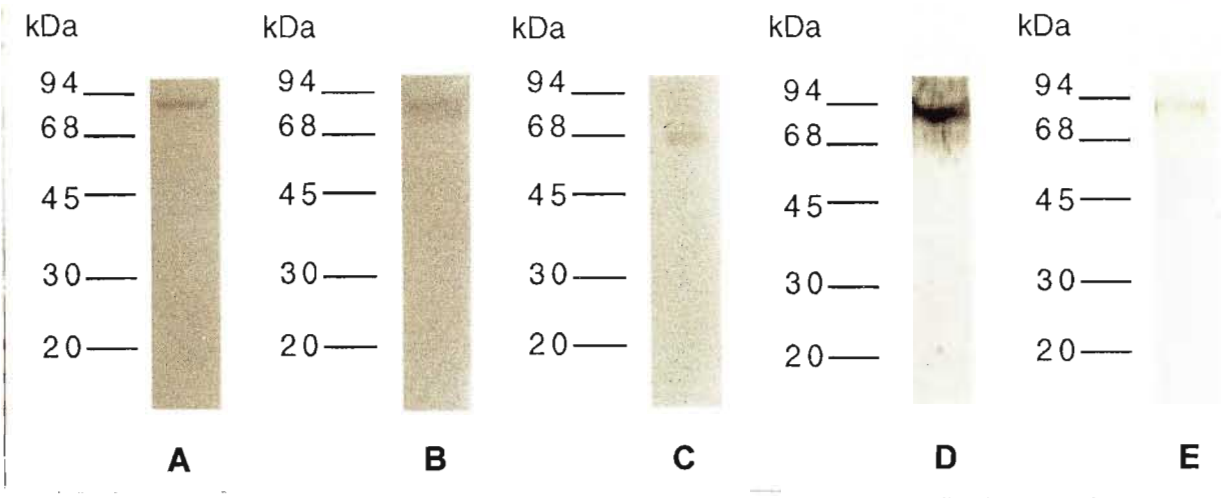

Figure 3.1 **Western blots of PMNL homogenates probed with antibodies against granule marker proteins.**

Homogenates (~80 µg/lane) were separated on a reducing 10% Tris-tricine SDS-PAGE gel and blotted onto nitrocellulose. The blots were probed with rabbit antibodies against: A), MPO (25 µg/ml); B), lactoferrin (50 µg/ml); C), HSA (20 ng/ml); D), proMMP-8 (10 µg/ml) and E), proMMP-9 (10 µg/ml). Primary antibody binding was detected with alkaline phosphatase-conjugated goat anti-rabbit IgG (1/5000) (A, B, D, E) or HRPO-conjugated sheep anti-rabbit IgG (1/10000) (C). Blots were developed with BCIP/NBT (A, B, D, E) or ECL (C).

3.3 Detection of PMNL secretory vesicles using immunocytochemistry and alkaline phosphatase histochemical techniques suitable for EM

Before the development of free-flow electrophoresis techniques for the separation of organelles of similar density on the basis of charge, alkaline phosphatase was considered a marker for the PMNL plasma membrane (Bainton, 1973; Bretz and Baggiolini, 1974). It is now appreciated that, in addition to HSA, alkaline phosphatase is also a marker for the secretory vesicles in the PMNL and only becomes associated with the PMNL plasma membrane when the PMNL is activated (Borregaard *et al.*, 1992; Borregaard and Cowland, 1997; Sengeløv and Borregaard, 1999). Unlike HSA which occurs as a soluble luminal protein, alkaline phosphatase is membrane bound and is attached via a GPI-anchor (Low *et al.*, 1987; Burroughs *et al.*, 1988; Englund, 1993; Cain *et al.*, 1995; Schneider and Ferguson, 1995). Unstimulated PMNLs are described to possess 'latent' alkaline phosphatase activity as alkaline phosphatase-containing vesicles are usually found inside PMNLs and activity can only be assayed in the presence of detergent (usually Triton X-100). Stimulated or 'primed' PMNLs lose their apparent latency as a result of integration of alkaline phosphatase into the plasma membrane, i.e. activity in PMNLs

may be demonstrated directly without the need for detergent (Borregaard *et al.*, 1992; Sengeløv, 1996; Sengeløv and Borregaard, 1999).

In this section of the study, HSA was assessed for suitability as a secretory vesicle marker for cryoimmunocytochemical labelling of secretory vesicles. Low density labelling with this antibody necessitated verification of labelling by another method. Alkaline phosphatase, an alternative secretory vesicle marker, was selected as successful histochemical localisation of alkaline phosphatase has previously been performed using cerium metal capture instead of conventional methods involving lead or aluminium (Kobayashi and Robinson, 1991; Takizawa and Robinson, 1993; Cain *et al.*, 1995; Takizawa *et al.*, 1998). The conventional capture methods are not ideal since the precipitated reaction products (e.g. aluminium phosphate) are coarse and highly damaging to glass and diamond knives used for sectioning. As cerium phosphate is reported to give a considerably finer electron-dense precipitate, is well retained in cellular compartments (Kobayashi and Robinson, 1991) and has been successfully used on both whole PMNLs and on ultrathin sections after cryoultramicrotomy and immunocytochemistry (Takizawa and Robinson, 1993; Takizawa *et al.*, 1998), this method was chosen for localising TIMP-1 in relation to secretory vesicles. The detection of alkaline phosphatase via the cerium phosphate method was, however, met with only limited success though the methods of Takizawa and Robinson (1993) and Kobayashi and Robinson (1991) were followed meticulously. This prompted method optimisation involving all aspects of the technique, including:

- *fixation.* Although alkaline phosphatase is reported to retain activity after fixation in 2% (v/v) glutaraldehyde (Kobayashi and Robinson, 1991), a milder fixative [2% (w/v) PFA, 0.05% (v/v) glutaraldehyde] was also used to ensure minimal enzyme denaturation prior to histochemistry.
- *buffer.* Sodium cacodylate (Kobayashi and Robinson, 1991), TAPS (Takizawa and Robinson, 1993) or HEPES were used to ensure that failure of the histochemistry was not due to nonspecific buffer effects.
- *detergent permeabilisation.* Whole cell histochemistry requires plasma membrane permeabilisation to allow access of substrate to membrane bound alkaline phosphatase. Both Triton X-100 and saponin were used for this purpose (at final concentrations of 0.006% and 0.004%, respectively, to gently delipidate the plasma membrane) and in some cases, both detergents were omitted.

- *substrate and capture metal.* Both *para*-nitrophenylphosphate (*p*NPP) and β-glycerophosphate were used as substrates and both cerium chloride and lead acetate were used as capture metals.
- *section staining.* Sections were stained with either phosphotungstate (Takizawa and Robinson, 1993), uranyl acetate or left unstained before sealing and viewing.
- *detection of the reaction product.* As cerium salts may produce a fine histochemical product indistinguishable from the electron dense staining components in PMNL organelles, such as specific granules, detection of the histochemical product using energy dispersive X-ray microanalysis (EDX) was also attempted on unstained sections.

The method reported by Takizawa and Robinson, (1993) for localisation of alkaline phosphatase was optimised in PMNLs for both pre- and post-labelling histochemistry. The post-labelling method was, however, preferred since detection of alkaline phosphatase via histochemical means (at pH levels as high as 9.5) was performed after immunocytochemistry and, therefore, should not compromise the antigenicity of target proteins.

3.3.1 Reagents

Alkaline phosphatase histochemical buffer (50 mM tricine, 100 mM TAPS, 2 mM $CeCl_3$, 2 mM $MgSO_4$, 2 mM *p*NPP, pH 9.3). Tricine (0.448 g), TAPS (1.216 g), $CeCl_3.7½H_2O$ (0.038 g), $MgSO_4$ (0.025 g) and *p*NPP (0.037 g) were dissolved in dd.H_2O (~30 ml) and the pH was titrated to 9.3. The solution was made up to 50 ml in a volumetric flask. The solution was made up fresh before use and kept at 4°C in the dark.

Negative control histochemical buffer. Prepared as described above, but including 2.5 mM levamisole (0.03 g/50 ml) as an alkaline phosphatase inhibitor.

Methylcellulose sealing solution [2% (w/v) methylcellulose in dd.H_2O]. Methylcellulose (1 g) was dissolved in ice-cold dd.H_2O (50 ml) and kept on ice.

Phosphotungstic acid/methylcellulose sealing and contrasting solution [0.1% (w/v) phosphotungstic acid/1.9% (w/v) methylcellulose]. Phosphotungstic acid [50 µl of a 2% (w/v) solution] was mixed thoroughly with methylcellulose [950 µl of a 2% (w/v) solution] and kept on ice (<30 min).

PMNL fixative and all cryoimmunocytochemistry buffers were prepared as described in Section 2.9.3.1 and the methylcellulose/uranyl acetate sealing solution was identical to the cryosection sealing solution described in Section 2.9.3.1.

3.3.2 Procedure

Immunocytochemical localisation of HSA. PMNLs were isolated from whole blood (100 ml) (Section 2.7.2) and prepared for cryoultramicrotomy and immunocytochemistry (Section 2.9.3.2). Ultrathin cryosections were immunolabelled for HSA (10 ng/5 µl) followed by 5 nm protein A gold (1/200, A_{520} = 0.036, 10 µl). FSG [1% (v/v)] was used for blocking (and antibody and gold probe dilution) instead of BSA to avoid potential non-specific binding of rabbit anti-HSA IgG to BSA. Control labellings contained either pre-immune rabbit IgG as the primary antibody or, alternatively, the primary antibody was omitted.

Alkaline phosphatase histochemistry. PMNLs were isolated from whole blood (100 ml) (Section 2.7.2) and fixed (1 h, RT). The cells were centrifuged (400 x g, 5 min, RT) and resuspended in histochemical buffer (1 ml, 1 h, 37°C). The cells were then processed for cryoultramicrotomy (Section 2.9.3.2). Alternatively, PMNLs were processed for cryoultramicrotomy without prior incubation in histochemistry buffer. In the latter case, ultrathin sections were retrieved on a droplet of 2.1 M sucrose-PBS and placed directly onto a nickel grid and transferred into histochemical detection buffer under various conditions (30 min-2 h, 22°C or 37°C). After the incubation, the sections were washed in dd.H_2O and sealed (methylcellulose, methylcellulose/uranyl acetate or the phosphotungstic acid solutions). Alternatively, the sections were transferred directly from the histochemical buffer to a sealing solution.

3.3.3 Results and Discussion

The labelling density (number of gold probes per secretory vesicle) obtained with the rabbit anti-HSA IgG on ultrathin cryosections was low (Figure 3.2 A) and the overall labelling density (total number of gold probes per cell) was considerably less than anticipated. As secretory vesicle HSA is thought to be derived from plasma via endocytosis during PMNL differentiation and maturation (Borregaard and Cowland, 1997) and due to the fact that that PMNLs may become activated or 'primed' during PMNL isolation (leading to endocytosis of HSA from the plasma and rendering secretory vesicles and endosomes morphologically and immunocytochemically indistinguishable), HSA was not pursued further as a secretory vesicle

marker protein.

A positive histochemical reaction product was only visible in unstained sections (i.e. lacking phosphotungstate or uranyl acetate counterstain). This product was just visible in the Philips CW120 Biotwin TEM at 100 kV (Figure 3.2 B). The reaction product is electron dense but, unfortunately, the cell morphology and membrane definition were poor. Detection of the reaction product proved similarly difficult using EDX, even when thicker sections (100-150 nm) were used. The detection of secretory vesicles via labelling for HSA or alkaline phosphatase histochemistry was, therefore, abandoned and an alternative method of labelling secretory vesicles was sought.

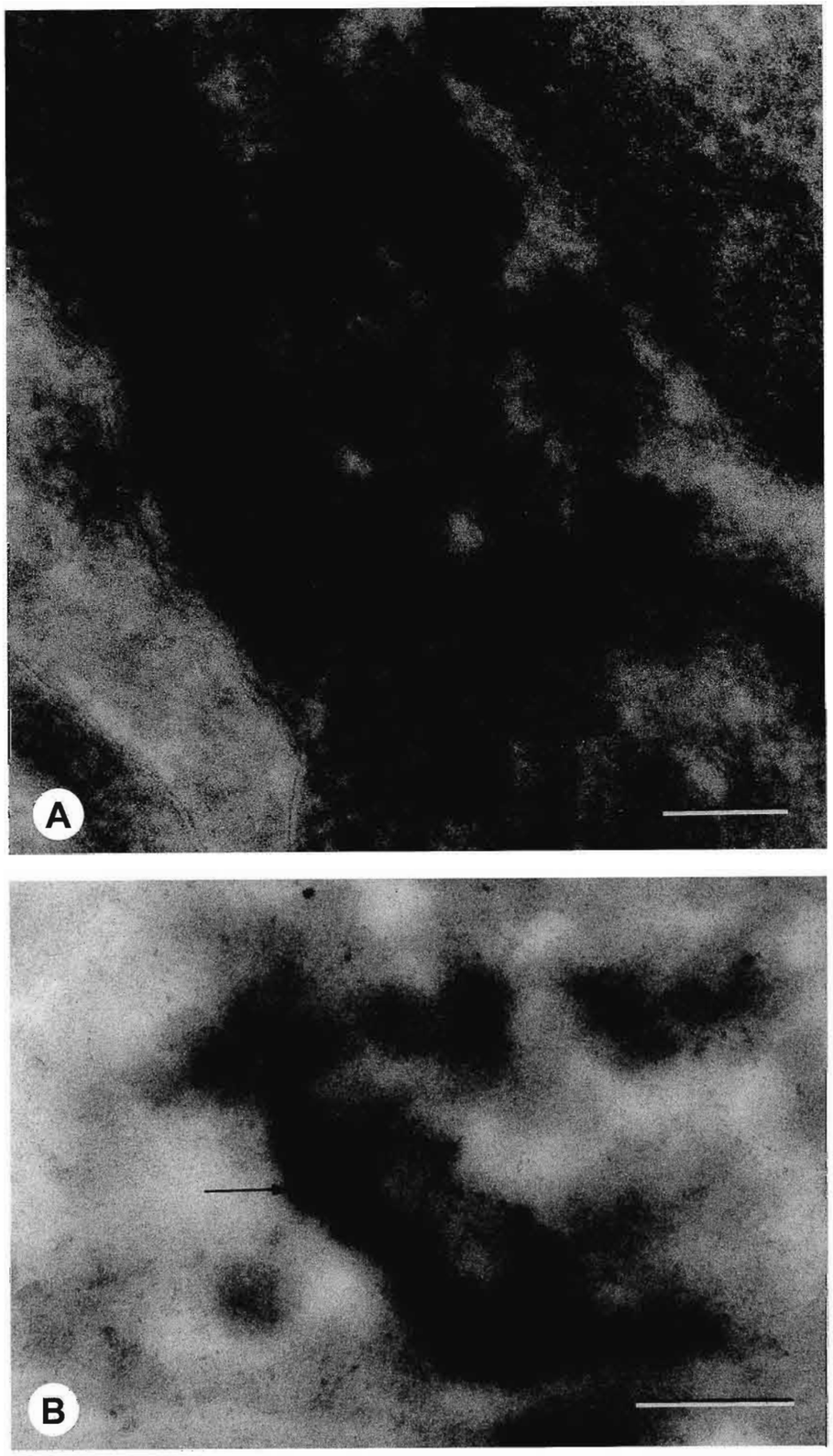

Figure 3.2 **Identification of PMNL secretory vesicles by immunocytochemistry and histochemistry.**

A), Immunocytochemistry of the secretory vesicle luminal marker protein, HSA (5 nm, arrow) on thawed ultrathin cryosections. The overall labelling density is too low in order for a correct localisation to be assigned. Bar = 100 nm. B), Histochemical detection of alkaline phosphatase by cerium phosphate metal capture. Note that a fine, electron dense reaction product is visible (arrow) and shows a roughly oval pattern due to the membrane anchoring of alkaline phosphatase via GPI. The high pH and absence of heavy metal staining of the section have resulted in poor preservation of cellular definition and make accurate identification of other PMNL granules impossible. Bar = 500 nm.

3.4 Purification of PMNL secretory vesicle GPI-anchored proteins and production of antibodies in chickens

As previously mentioned, alkaline phosphatase is a GPI-anchored protein and has been purified from the PMNL plasma membrane, following fMLP stimulation, using GPI-specific phospholipase C (PI-PLC) (Cain *et al.*, 1995). PMNLs contain at least eight GPI-anchored proteins, some of which have been localised to the secretory vesicles. These GPI-anchored proteins include: the low affinity IgG receptor (FcγIIIRB/CD16b) (Jost *et al.*, 1990; Kobayashi and Robinson, 1991; Takizawa *et al.*, 1998), endotoxin receptor (CD14) (Detmers *et al.*, 1995), complement decay-accelerating factor (DAF/CD55) (Berger and Medof, 1987), membrane attack complex inhibition factor (protectin/CD59), uPA receptor (CD87), CD67 (Jost *et al.*, 1991), GPI-80 (a protein that shares sequence homology with human biotinidase) (Suzuki *et al.*, 1999) and alkaline phosphatase. These proteins are absent in the secretory vesicles of individuals suffering from paroxysmal nocturnal hemoglobinuria (PNH) (Burroughs *et al.*, 1988), a condition resulting from defective GPI-anchor biosynthesis and attachment. GPI-anchored proteins are also known to reside in distinct membrane microdomains known as 'rafts' (Brown and Rose, 1992). Rafts are enriched with cholesterol, sphingolipids and glycolipids and are, therefore, relatively less fluid than other portions of cellular membranes. In most cell types, caveloe are formed in rafts. PMNLs lack the protein, caveolin, and therefore do not form caveolae (Sengeløv *et al.*, 1998). Rafts, however, may be used in PMNLs to package GPI-anchored proteins into a particular population of vesicles with a raft-like lipid composition, as this would allow efficient intercalation of the GPI-anchors. As it has been proposed that secretory vesicles might be the GPI-storage organelles of the PMNL (Cain *et al.*, 1995) it was, therefore, reasoned that antibodies to GPI-anchored proteins may potentially localise to the secretory vesicles and, hence, form good markers for the secretory vesicles. Methods for the isolation of GPI-anchored proteins were, therefore, explored and this approach was investigated.

All GPI-anchored proteins have the anchor addition site near the C-terminus (Udenfriend and Kodukula, 1995) (Figure 3.3). The protein is linked to phosphoethanolamine, which in turn is connected via phosphodiester linkage to a glycan. The glycan consists of a variable number of mannose residues linked to each other via $\alpha(1\rightarrow2)$, $\alpha(1\rightarrow4)$ or $\alpha(1\rightarrow6)$ bonds. Differential additions of either monosaccharides (mannose or glucose), acetylated monosaccharides (*N*-acetyl galactosamine) or further phosphoethanolamine residues gives rise to intra- and inter-species heterogeneity (Schneider and Ferguson, 1995). The glycan moiety terminates with a

glucosamine residue that is linked via an α(1→6) bond to *myo*-inositol. The *myo*-inositol is phosphorylated on its C1 atom and linked to a lipid (*sn*-1-alkyl-2-acylglycerol, *sn*-1,2-diacylglycerol, *sn*-1-acyl-2-*lyso*-glycerol, or ceramide (Englund, 1993).

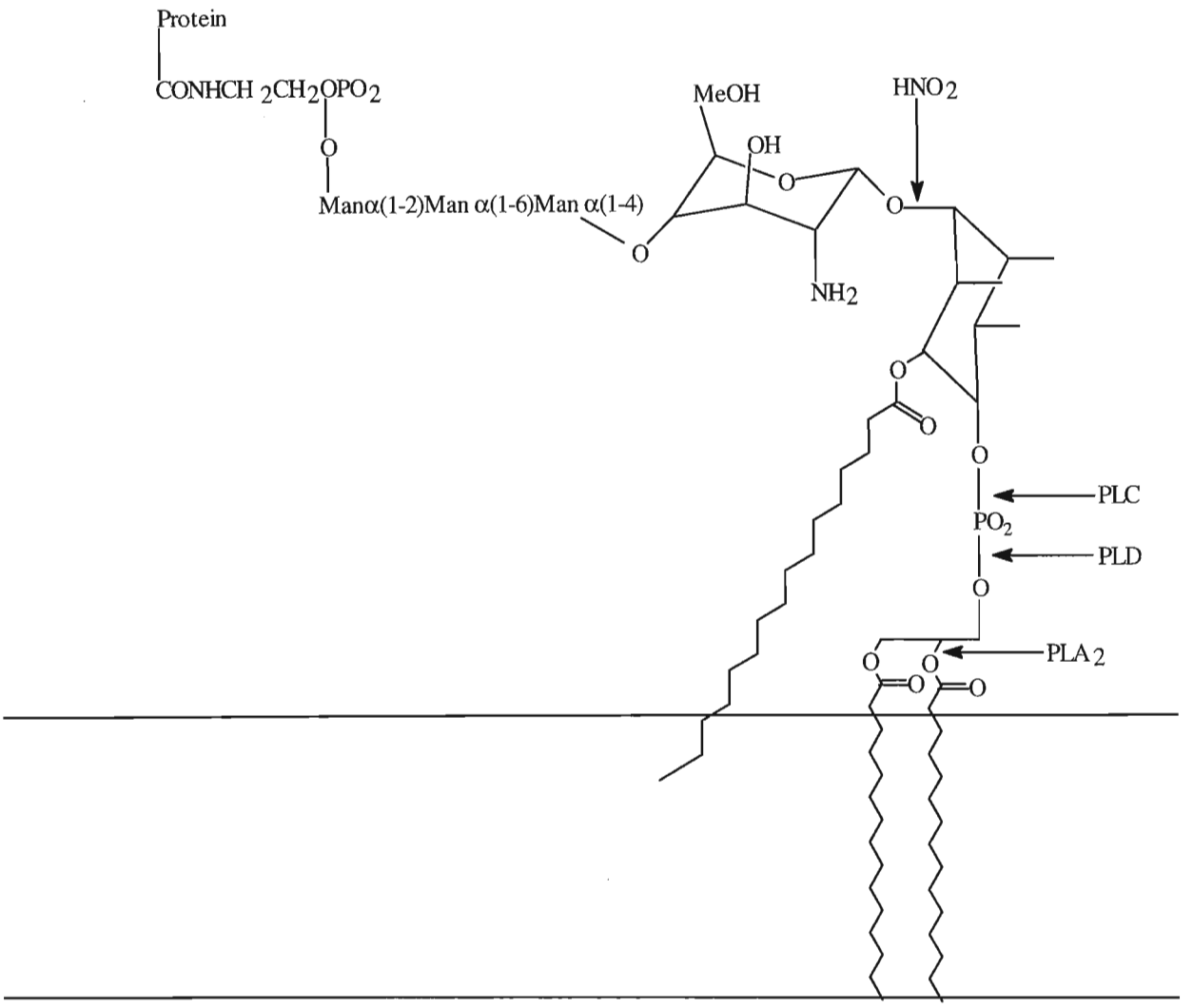

Figure 3.3 **Simplified structure of a eukaryotic GPI-anchored protein.**

The cleavage sites for PLA_2, PLD and PI-PLC are indicated. Acylation of *myo*-inositol with a fatty acid would render the protein 'resistant' to all three phospholipases, as the protein would remain anchored to the membrane via the *myo*-inositol-bound fatty acid even though the diacylglycerol moiety has been cleaved. Nitrous acid overcomes the limitations of phospholipases and allows release of the GPI-anchored protein from the membrane regardless of *myo*-inositol acylation. After Ferguson, 1989.

In order to isolate all GPI-anchored proteins for the production of anti-GPI-anchored protein antibodies, various isolation methods were considered. The simple method of GPI-anchored protein cleavage by phospholipase treatment, described by Cain *et al.* (1995) was not employed since:

- the phospholipases would contaminate the mixture of GPI-cleaved proteins and hence immunisations may produce both anti-GPI-anchored protein antibodies and anti-phospholipase antibodies. PMNLs contain endogenous phospholipases in azurophil granules and, therefore, antibody preparations recognising phospholipases and well as GPI-anchored proteins would be of little use.
- occasionally, the *myo*-inositol group of GPI-anchored proteins is acylated with a simple fatty acid residue [usually palmitate, e.g. human acetylcholinesterase, *Trypanosoma brucei* procyclic acidic repetitive protein] (Englund, 1993). This extra lipid portion can further stabilise intercalation of the GPI-anchored protein with the plasma membrane by inserting itself into the lipid bilayer, rendering the anchor resistant to PI-PLC and PLD. Such GPI-anchored proteins would not be released by phospholipase treatment and antibodies produced would, therefore, not identify all GPI-anchored proteins present in the cell.
- PMA or fMLP treatment of PMNLs is required to expose GPI-anchored proteins to the extracellular medium for phospholipase cleavage (Cain *et al.*, 1995). Along with phospholipase-cleaved GPI-anchored proteins, other luminal proteins (such as those in the secretory vesicles and other granule populations that are mobilised by PMA) may potentially be released into the extracellular medium and it would be impossible to distinguish which released proteins were originally GPI-anchored. In order to produce antibodies solely against GPI-anchored proteins, the soluble GPI-anchor-free proteins would need to be selectively fractionated from other soluble luminal granule proteins. This method was suitable for the isolation of alkaline phosphatase as the alkaline phosphatase protein band was separated from other proteins via electrophoresis and subsequently recognised by histochemistry and was excised and used for antibody production (Cain *et al.*, 1995). Such a method could not be used for the simultaneous purification of *all* GPI-anchored proteins, as these do not all have histochemical activity.

An alternative method for the purification of GPI-anchored proteins was described using the non-ionic detergent, Triton X-114 (Ko and Thompson, 1995). This method relies on the low cloud point (or phase separation temperature) of Triton X-114 to promote phase separation of hydrophilic proteins from hydrophobic membrane proteins (Brusca and Radolf, 1994). The high hydrophile:lipophile balance value of Triton X-114 (~12.4) indicates that the detergent is relatively non-denaturing while the cloud point (22°C in 150 mM NaCl) is at a temperature that is tolerated by all of the known PMNL GPI-anchored proteins. At temperatures greater than the cloud point, the detergent forms a turbid suspension that can be pelleted by centrifugation to

produce a dense, hydrophobic, detergent-rich pellet and a detergent-free aqueous phase (Brusca and Radolf, 1994).

The simple extraction method of Ko and Thompson (1995) may, however, be flawed due to the fact that it assumes that all the Triton X-114-partitioned hydrophobic proteins are GPI-anchored and overlooks the possibility of simultaneously extracting integral membrane- or isoprenylated proteins (e.g. Rab, Ras, Rac, Rho, nuclear lamins etc.), which would also be soluble in the detergent phase. Hence a method by which GPI-anchored proteins may be cleaved and separated from other Triton X-114-partitioned hydrophobic proteins was devised for the present study. It was decided to exploit the selectivity of nitrous acid (HNO_2) for cleaving GPI-anchors as nitrous acid cleaves the terminal glucosamine residue of the GPI-glycan moiety to produce 2,5 anhydromannose (Low *et al.*, 1987; Ferguson, 1989) (Figure 3.3). This method has the further advantage of freeing proteins from their GPI-anchors, regardless of whether or not the *myo*-inositol ring is acylated (Low *et al.*, 1987). Therefore, in this study, nitrous acid was used as a specific, non-enzymatic mechanism of release of GPI-anchored proteins from the detergent phase of Triton X-114-partitioned proteins. The cleavage of the GPI-anchors from the membrane fractions should render GPI-anchored proteins hydrophilic and these would, therefore, partition from the detergent phase into the aqueous phase and could be harvested after centrifugation. One possible disadvantage of nitrous acid deamination is the acidic condition (pH 3.5) under which cleavage is performed. The low pH could result in considerable protein denaturation and loss of biological activity. For the purposes of this study, however, maintenance of the biological activity of the GPI-anchored proteins was not a concern as long as the proteins maintained some resemblance to the original structure [although alkaline phosphatase is known to retain its activity after nitrous acid deamination (Low *et al.*, 1987)], since the proteins would be used primarily for immunisation and antibody production.

3.4.1 Isolation of GPI-anchored proteins by Triton X-114 phase partitioning and nitrous acid deamination

3.4.1.1 Reagents

50 x *para*-chloromercurophenylsulfonic acid (*p*CMPSA) stock solution (50 mM in DMSO). *p*CMPSA (0.021 g) was dissolved in anhydrous DMSO (1 ml) and kept at -20°C.

Lysis buffer [10 mM Tris-HCl, 150 mM NaCl, 1 mM *p*CMPSA, 2% (v/v) Triton X-114, pH 7.4 at 4°C]. Tris (0.0606 g), NaCl (0.438 g), *p*CMPSA (1 ml of a 50 mM stock solution) and

Triton X-114 (1 ml) were dissolved in dd.H_2O (~40 ml) and titrated to pH 7.4 with HCl. The volume was made up to 50 ml in a volumetric flask and stored at 4°C. The solution was made up fresh each time it was required.

Partitioning buffer [10 mM Tris-HCl, 150 mM NaCl, 1 mM *p*CMPSA, 0.06% (v/v) Triton X-114, pH 7.4]. Tris (0.0606 g), NaCl (0.438 g), *p*CMPSA (1 ml of a 50 mM stock solution) and Triton X-114 (30 µl) were dissolved in dd.H_2O (~40 ml) and titrated to pH 7.4 with HCl. The volume was made up to 50 ml in a volumetric flask and stored at 4°C. The solution was made up fresh each time it was required.

GPI-deamination buffer (250 mM Na-acetate, 200 mM $NaNO_2$, pH 3.5). Acetic acid (715 µl) and $NaNO_2$ (0.69 g) were placed in a 50 ml volumetric flask and made up to volume with dd.H_2O. No pH adjustment was necessary. The solution was made up just before use and kept in the dark.

TCA stock solution [50% (w/v) in dd.H_2O]. TCA (50 g) was dissolved dd.H_2O (~80 ml) and made up to 100 ml in a volumetric flask. The solution was stored at RT.

Acetone [100 % (v/v)]. Anhydrous acetone was kept at -80°C.

GPI-cleaved protein solubilisation buffer (50 mM tricine, 100 mM TAPS, 2 mM $MgCl_2$, pH 9.5). Tricine (0.896 g), TAPS (2.433 g) and $MgCl_2.6H_2O$ (0.04 g) were dissolved in dd.H_2O (~80 ml). The pH was titrated to 9.5 with HCl, the volume made up to 100 ml and stored at 4°C.

3.4.1.2 Procedure

PMNLs were isolated from whole blood (100 ml) (Section 2.7.2) and resuspended in PBSG (~$2x10^6$/ml). After 10 min, the PMNLs were centrifuged (400 x g, 5 min, 4°C) and resuspended in 10 ml lysis buffer. The PMNL suspension was stirred (1 h, 4°C) and centrifuged (8800 x g, 0°C, 10 min). The supernatant was removed and decanted into a sterile 15 ml centrifuge tube and frozen (3 days, -20°C). During this time, while most of the solution was frozen, a layer of thick debris accumulated at the bottom of the centrifuge tube. After thawing and mixing thoroughly, the suspension was used for Triton X-114 phase partitioning. It was first incubated at 32°C for 12 min and then centrifuged (3000 x g, 3 min, 32°C). The upper aqueous phase was

removed and stored at -80°C and the lower detergent phase was resuspended in ice-cold partitioning buffer (10 ml), briefly vortexed and placed on ice (10 min). Phase partitioning at 32°C was repeated and the detergent phase resuspended in partitioning buffer (10 ml), placed on ice for 10 min and then centrifuged (18000 x g, 10 min, 0°C). The supernatant was partitioned once again and the proteins in the final detergent phase were precipitated with cold acetone (10 volumes, 1 h, -80°C). The precipitated proteins were pelleted by centrifugation (13000 x g, 2 min, 0°C) and resuspended in deamination buffer (500 µl). The precipitated proteins were dissolved by sonication (20 min, 4°C) and deamination was allowed to continue in the dark (4 h, 37°C). Once the incubation was complete, TCA was added to the solution to a final concentration of 5% (w/v) and the protein solution was placed on ice to promote precipitation (1 h). The precipitated proteins were pelleted by centrifugation (13000 x g, 2 min, 4°C), resuspended in ice-cold lysis buffer (1 ml) and placed on ice for 1 h. During this time, integral membrane proteins, isoprenylated proteins, hydrophobic azurophil granule proteins (Sengeløv, 1996) and GPI-anchored proteins (that had not had their GPI-anchors cleaved by the nitrous acid), partition into the detergent phase, while those GPI proteins that had their anchors cleaved, partitioned to the aqueous phase (10 min, 32°C). The aqueous phase formed after centrifugation (3000 x g, 32°C, 3 min) was removed. TCA was added to the aqueous phase to final concentration of 5% (w/v) to precipitate the proteins (1 h, 0°C). The precipitated proteins were centrifuged (13000 x g, 2 min, 4°C) and resuspended in acetone containing 1% (w/v) TCA (12 h, -20°C). The proteins were pelleted by centrifugation (13000 x g, 10 min, 4°C), resuspended in GPI-cleaved protein solubilisation buffer (1 ml) and stored at -80°C.

3.4.2 Assessment of GPI-cleavage and phase partitioning using native PAGE

Native PAGE involves protein separation according to the protein charge to mass ratio and imposes minimal denaturation in order to retain oligomeric structure and preserve biological function. SDS is omitted from all buffers since it has the potential to denature sensitive proteins. To ensure optimal resolution in native PAGE, it is necessary to load small sample volumes (1-5 µl) or ensure that the ionic strength of the sample buffer is approximately 10-fold less than the gel buffer (Bollag and Edelstein, 1991) (as this would 'force' the proteins to carry the majority of the charge and migrate into the gel). Native PAGE was used to allow histochemical identification of alkaline phosphatase activity in samples using BCIP/NBT. Phosphatase activity generates insoluble purple/black bands that are light stable.

3.4.2.1 Reagents

Electrophoresis buffers and reagents were prepared as described in Section 2.4.1.

5 x Electrode (running) buffer. Prepared as described for the Laemmli system (Section 2.4.1.1) except that SDS was omitted.

Sample buffer [312.5 mM Tris-HCl, 50% (v/v) glycerol]. Tris [3.1 ml of a 1 M ([12.11 g/100 ml) stock solution], glycerol (5 ml) and dd.H_2O (1.9 ml) were mixed together. A few grains of bromophenol blue were added and the buffer was stored at RT.

Alkaline phosphatase detection buffer [50 mM tricine, 100 mM TAPS, 2 mM $MgCl_2$, 0.03% (w/v) NBT, 0.015% (w/v) BCIP, pH 9.5]. Tricine (0.896 g), TAPS (2.433 g) and $MgCl_2.6H_2O$ (0.041 g) were dissolved in dd.H_2O (~80 ml). The pH was adjusted to 9.5 and the solution was made up to 100 ml in a volumetric flask. Just before use, NBT (3 mg in 1 ml buffer) and BCIP (1.5 mg in 1 ml DMF) were added to 10 ml buffer.

3.4.2.2 Procedure

Aliquots (~20 μg) of Triton X-114 aqueous and detergent phases of PMNL homogenates at various stages of the GPI-anchored protein purification were mixed with an equal volume sample buffer and separated on a 7.5% continuous native PAGE gel under conditions described for the Laemmli system (Section 2.4.1). Upon completion of electrophoresis, the gel was rinsed briefly in alkaline phosphatase detection buffer (lacking BCIP/NBT) (20 min) and then submerged in alkaline phosphatase buffer containing BCIP/NBT in the dark (10 h). The gel was photographed and the bands scanned and analysed by densitometry with the AnalySIS® software imaging system.

3.4.2.3 Results and Discussion

The progress of GPI-anchored protein purification was established by detecting alkaline phosphatase activity by native histochemical PAGE. This confirmed the success of Triton X-114 in partitioning alkaline phosphatase activity from PMNL hydrophilic proteins, although trace activity was evident in the aqueous fraction. This may result from the action of endogenous PMNL phospholipases that are usually confined to the azurophil granules but possibly come into contact with their substrates during homogenisation in spite of the inclusion of *p*CMPSA [a PI-PLC inhibitor (Ko and Thompson, 1995)] in the lysis and partitioning buffers

(Figure 3.4 A, lane 1). The appearance of alkaline phosphatase in the aqueous phase after nitrous acid deamination indicates that GPI-anchor cleavage was successful. The apparent increase in total alkaline phosphatase activity obtained after nitrous acid deamination (lane 3) compared to that in the detergent phase (lane 2) may be due to the fact that Triton X-114 micelle formation may partially prevent substrate access to the active site of alkaline phosphatase molecules orientated to face the micellar lumen. Alternatively, the detergent may distort the enzyme conformation and, hence, decrease activity. Unlike lane 2, the samples in lanes 1 and 3 are detergent-free aqueous extracts and, therefore, the BCIP/NBT substrate is fully accessible to alkaline phosphatase, which should now be in an undisturbed conformation.

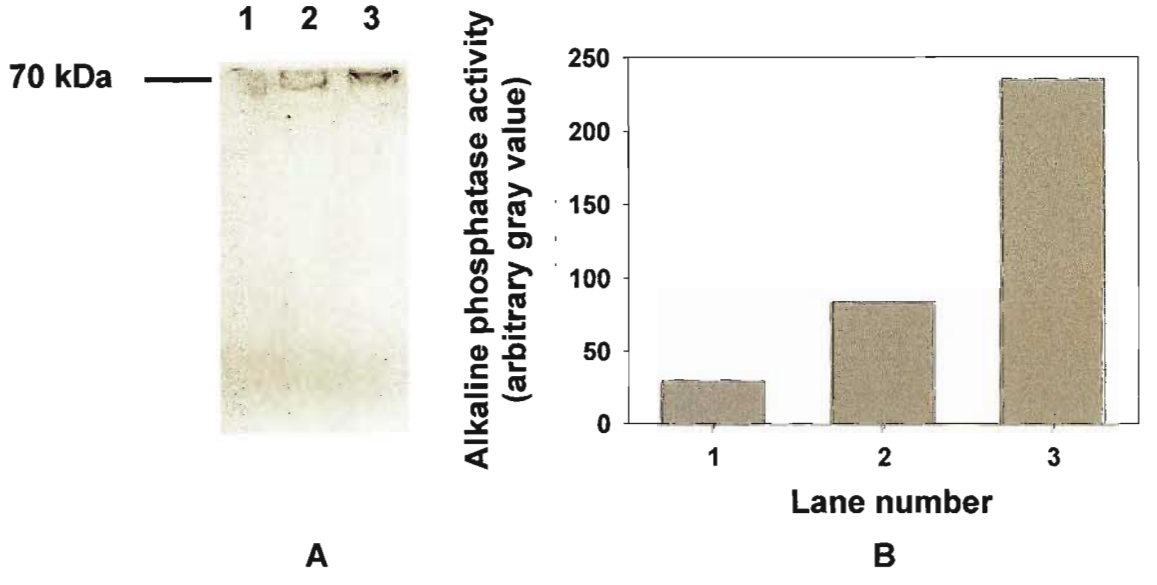

Figure 3.4 **Detection of PMNL alkaline phosphatase activity by native histochemical PAGE.** Aliquots (~20 μg) from various stages of the Triton X-114 purification were mixed with treatment buffer and separated on a 7.5% native PAGE gel and alkaline phosphatase activity detected with BCIP/NBT. A), Lane 1, Triton X-114 aqueous phase after initial PMNL lysis; Lane 2, detergent phase before deamination; Lane 3, aqueous phase after deamination. B), Densitometric comparison of alkaline phosphatase activity in (A). The alkaline phosphatase activity obtained in the final post-deamination aqueous phase (lane 3) is approximately 8-fold greater than that released by endogenous phospholipases (lane 1).

3.4.3 Production and isolation of antibodies against GPI-anchored proteins in chickens

Cost, practicality, species diversity and final antibody titre determine the choice of animal for antibody production. As mentioned in the introduction to this chapter, rabbits are especially popular in immunocytochemistry since protein A from *S. aureus* can be used in immunogold labelling as protein A coated onto gold probes retains its ability to bind the C_{H1} and C_{H2} domains of the Fc portion of rabbit IgG (Harlow and Lane, 1988). Unfortunately, blood collection from rabbits is difficult and final exsanguination is often necessary to ensure a good antibody yield. Laying hens produce antibodies (IgG) and target them to the yolks of eggs (IgY) to provide the chicken embryo with immunological protection until its immune system is developed. IgY yields from egg yolks are generally higher than IgG from other experimental animals (Losch *et al.*, 1986). Though protein A does not bind IgY, this disadvantage may be overcome using a rabbit anti-IgY linker antibody (Harlow and Lane, 1988; Griffiths, 1993). In this study, chickens were used for antibody production.

Antibodies were raised in chickens following inoculation of antigen emulsified with an adjuvant. Adjuvants are mineral oil-based [or suspensions such as $Al(OH)_3$ (Glenny *et al.*, 1926)] non-specific immune response stimulators which allow gradual release of antigen from the site of inoculation thus ensuring maximal exposure of the antigen to major histocompatibility complex (MHC) class II APCs. Efficient antigen uptake by APCs is required for optimal antibody response. This is strongly influenced by the site of inoculation and the size and form of antigen. The non-specific immune response is improved by the initial inclusion of molecules of pathogenic origin since they produce a 'depot' effect (where the antigen leaks slowly into the tissue, providing continual stimulation of the immune system and induces the infiltration of inflammatory APCs to the site), stimulate lymphokine production and subsequent B-cell proliferation. Heated killed *Mycobacterium tuberculosis*, *M. tuberculosis*-derived muramyl dipeptide (Ellouz *et al.*, 1974) or the lipid A portion of LPS (Johnson *et al.*, 1956) are ideal for producing a non-specific immune response. Adjuvant consisting of killed or attenuated *M. tuberculosis* and mineral oil is referred to as Freund's complete adjuvant (FCA) (Freund and McDermott, 1942; Freund, 1956) and is most commonly used for primary inoculations to stimulate the depot effect. Subsequent booster injections are comprised of emulsified antigen in Freund's incomplete adjuvant (FIA: FCA without *Mycobacterium*) to avoid formation of more granulomata in the chicken. Booster injections are necessary for continual stimulation of the

immune system and induction of the IgM →IgG class switch (Harlow and Lane, 1988). Further booster injections improve the titre and avidity of antibodies directed against the antigen (referred to as affinity maturation). A minimum of 2-3 weeks is recommended between boosts to avoid antigen clearing by high levels of circulating antibodies.

A number of methods exist for the isolation of antibodies. These include affinity chromatography [protein A/fixed *S. aureus* (Ey *et al.*, 1978); anti-IgG (Gurvich and Drizlikh, 1964)], ion exchange chromatography [diethylaminoethyl cellulose, hydroxyapatite (Bokovsky and Kennett, 1987)] and precipitation [ammonium sulfate, caprylic acid (Russ *et al.*, 1983) and PEG]. The method of PEG 6 kDa precipitation was used for isolation of IgG from human serum (Polson *et al.*, 1964) (Chapter 5) and IgY from chicken egg yolks (Polson *et al.*, 1985). PEG 6 kDa precipitates proteins by steric exclusion into the extrapolymer space as PEG removes hydration shells from protein molecules during dissolution (Ingham, 1990). As the concentration of PEG is increased, various proteins exceed their solubility limit and differentially precipitate out of solution, while PEG remains in the supernatant.

3.4.3.1 Reagents

Phosphate buffer [100 mM sodium phosphate, 0.02% (w/v) NaN_3, pH 7.6]. $NaH_2PO_4.H_2O$ (13.8 g) and NaN_3 (0.2 g) were dissolved in dd.H_2O (950 ml). The pH was adjusted to 7.6 with NaOH and the solution was made up to 1 *l* with dd.H_2O.

3.4.3.2 Procedure

For the production of antibodies towards the deaminated PMNL secretory vesicle GPI-anchored proteins, chickens were immunised with antigen as described below. Emulsification of antigen with adjuvant was accomplished by sonication (4°C, 20 min) and trituration through a 26-gauge needle. The suspensions were considered stable if they did not disperse when an aliquot was added to a droplet of saline (Harlow and Lane, 1988). All immunisations were administered into multiple sites in the breast muscle (both sides of the sternum) of laying hens and eggs were collected.

Table 3.1 **Immunisation protocol for the production of antibodies against PMNL GPI-anchored proteins in chickens.**

Week	Adjuvant	Antigen amount
0	FCA	~50 μg
3	FIA	~20 μg
6	FIA	~20 μg

Egg yolks were separated from the egg white using an egg separator and washed with dd.H_2O. The yolk sacs were punctured with a sterile Pasteur pipette and the yolk volume measured. Two volumes of phosphate buffer were added and mixed gently by inversion after sealing the cylinder with Parafilm. Crushed PEG 6 kDa was added to 3.5% (w/v) and dissolved by rotary inversion. The precipitated vitellin fraction (containing lipoproteins) was pelleted by centrifugation (4420 x g, 30 min, RT) and contaminating lipids were removed by filtering the supernatant fluid through cotton wool (moistened with dd.H_2O). PEG [8.5% (w/v)] was added to the clear filtrate to bring the final concentration to 12% (w/v). The solution was mixed, centrifuged (12000 x g, 10 min, RT) and the pellet dissolved in phosphate buffer, in a volume equal to that obtained after filtration through cotton wool. PEG was added to 12% (w/v), mixed and the solution was centrifuged (12000 x g, 10 min, RT). The supernatant fluid was discarded and the pellet washed briefly with phosphate buffer before dissolving the pellet in $1/6^{th}$ of the original egg yolk volume using phosphate buffer.

3.4.3.3 Results and Discussion

Assessment of the anti-GPI-anchored protein IgY titre was not performed due to the limited amounts of antigen available. Chickens were immunised once with antigen in FCA, and then boosted twice at three-weekly intervals again in FIA to ensure constant priming of the immune system. The eggs obtained one week after the second boost were used for IgY isolation in this study since these preparations should have the highest antibody titre.

Under conventional conditions, antibody specificity is established by western blotting of crude cell homogenates, assessing the number and M_r of bands obtained and comparing these against published data. The reported M_r's of some of the GPI-anchored proteins are: alkaline phosphatase (70-90 kDa) (Cain *et al.*, 1995), CD16b (45-75 kDa) (Jost *et al.*, 1990) DAF (65 and 73 kDa) (Cain *et al.*, 1995; Hatanaka *et al.*, 1996), CD14 (55 kDa) (Detmers *et al.*, 1995),

GPI-80 (58 kDa; deduced from the cDNA sequence) (Suzuki *et al.*, 1999) and CD67 (85-95 kDa) (Jost *et al.*, 1991). The ECL blots obtained on GPI-enriched Triton X-114 fractions showed a broad band ranging from 30-100 kDa (result not shown) and, therefore, did not assist in determining antibody specificity, but potentially indicated that GPI-anchored proteins in this M_r range were recognised. In addition, a western blot might detect bands of other (as yet uncharacterised) PMNL GPI-anchored proteins and, therefore, band analysis and antibody specificity assessment by western blotting was not seen to be very informative. It was, therefore, decided to assess the antibody specificity by examining the labelling pattern obtained by cryoimmunocytochemistry and subcellular granule fractionation. Since the GPI-anchored proteins are all membrane-bound and should be present on the inner membrane leaflets of electron translucent pleiomorphic organelles, it was reasoned that it would be relatively easy to assess the antibody specificity visually using immunocytochemistry. In addition, since the secretory vesicles are the least dense population of PMNL organelles, subcellular fractionation by density gradient centrifugation was performed to separate secretory vesicle from other PMNL granule populations and confirm the association of GPI-anchored proteins with the secretory vesicles. The location of the GPI-anchored proteins relative to other granule marker proteins was, therefore, established by both immunocytochemistry of ultrathin cryosections and western blotting of density gradient granule fractions.

3.5 Localisation of GPI-anchored proteins with respect to PMNL granule marker proteins by subcellular fractionation and immunocytochemistry

3.5.1 Subcellular fractionation

PMNL granules can be resolved into three distinct populations by density centrifugation on discontinuous Percoll gradients (reviewed by Kjeldsen *et al.*, 1999). This allows the granules to be resolved into α (azurophil granules), β (specific and gelatinase granules) and γ (secretory vesicles and plasma membrane) populations. Advances in free-flow electrophoresis (a method that separates vesicles by virtue of their ζ-potentials) have allowed resolution of plasma membrane from secretory vesicles. This allows intracellular (non-degranulated) secretory vesicles to be distinguished from those that have degranulated and fused with the plasma membrane. The chosen Percoll gradient used in this study is regarded as the most efficient in resolving the α, β and γ populations and has been reported to allow resolution of the β-band into a denser β_1-band (containing lactoferrin) and a lighter β_2-band (containing the bulk of proMMP-9) (Kjeldsen *et al.*, 1999).

3.5.1.1 Reagents

EGTA stock solution (100 mM, pH 7.4). $Na_2EGTA.4½H_2O$ (0.549 g) was dissolved in $dd.H_2O$ (9 ml), titrated to 7.4 with HCl and made up to 10 ml. The solution was aliquoted and stored at -20°C.

10 x Relaxation buffer (100 mM PIPES, 1 M KCl, 30 mM NaCl, 35 mM $MgCl_2$, 12.5 mM Na_2EGTA, pH 7.4 at 4°C). PIPES (3.02 g), KCl (7.45 g), NaCl (0.18 g), $MgCl_2.6H_2O$ (0.33 g) and $Na_2EGTA.4½H_2O$ (0.687 g) were dissolved in $dd.H_2O$ (80 ml), titrated to 7.4 with HCl and made up to 100 ml. The solution was autoclaved and kept at RT.

1 x Relaxation buffer (10 mM PIPES, 100 mM KCl, 3 mM NaCl, 3.5 mM $MgCl_2$, pH 7.2). PIPES (0.755 g), KCl (1.863 g), NaCl (0.045 g) and $MgCl_2.6H_2O$ (0.083 g) were dissolved in $dd.H_2O$ (200 ml), titrated to 7.2 with HCl and made up to 250 ml. The solution was filter sterilised through a 0.22 µm filter since autoclaving gave rise to precipitates in the buffer.

PMSF stock solution (200 mM). PMSF (0.0348 g) was dissolved in ethanol (1 ml), aliquoted into 200 µl fractions and kept at -20°C.

Stock AEBSF solution (100 mM in $dd.H_2O$). AEBSF (0.024 g) was dissolved in $dd.H_2O$ (1 ml) and kept at -20°C.

ATP stock solution (50 mM in 1 x relaxation buffer, pH 7.2). $Na_2ATP.4H_2O$ (0.312 g) was dissolved in 1 x relaxation buffer (9 ml), titrated to pH 7.2 with NaOH and made up to 10 ml. The solution was aliquoted into 1 ml fractions and kept at -20°C.

Stock Percoll solution (1.1245 g/ml) and 130 mM trisodium citrate were prepared as described in Section 2.7.1.

Percoll solution (1.05 g/ml). Relaxation buffer (4.546 ml), Na_3citrate (2 ml) and stock Percoll (3.454 ml) were mixed together just before use and kept at 4°C.

Percoll solution (1.07 g/ml). Relaxation buffer (2.864 ml), Na_3citrate (2 ml) and stock Percoll (5.135 ml) were mixed together just before use and kept at 4°C.

Percoll solution (1.12 g/ml). Relaxation buffer (20 µl) and stock Percoll (4.98 ml) were mixed together just before use and kept at 4°C.

10 x *p*NPP (45 mM). *p*NPP (0.417 g) was dissolved with dd.H_2O in a final volume of 25 ml. The solution was made up fresh and kept at 4°C.

10 x $MgCl_2$ (20 mM $MgCl_2$ in 1 x alkaline phosphatase buffer). $MgCl_2.6H_2O$ (0.041 g) was dissolved in 2 x alkaline phosphatase buffer (5 ml) and made up to 10 ml with dd.H_2O.

2 x alkaline phosphatase buffer [200 mM diethanolamine, 0.4% (v/v) Triton X-100, pH 9.75]. Diethanolamine (1.916 ml) and Triton X-100 (400 µl) were diluted with dd.H_2O, without pH adjustment, to a final volume of 100 ml and autoclaved. The buffer was kept at RT. To create a working solution, 2 x buffer (2.5 ml), dd.H_2O (1.5 ml), 10 x *p*NPP (500 µl) and 10 x $MgCl_2$ (500 µl) were mixed together just before use.

2 x MPO buffer (166 mM citric acid, 224 mM Na_2HPO_4, pH 5.6). Citric acid (3.189 g/100 ml) was added to an equal volume of $Na_2HPO_4.2H_2O$ (3.474 g/100 ml) solution and kept at 4°C.

50 x *p*CMPSA (50 mM in DMSO). Prepared as described in Section 3.4.1.1.

10 x cetyltrimethylammonium bromide (CTAB) [3% (w/v) in 1 x MPO buffer, pH 5.6]. CTAB (0.3 g) was dissolved in 1 x MPO buffer to a final volume of 10 ml. The solution was kept at 4°C.

All gelatinase zymography buffers and reagents were prepared as described in Section 2.6 and the PMNL resuspension buffer was prepared as described in Section 2.7.1. Western blotting reagents were prepared as described in Section 2.8.2.1.

3.5.1.2 Procedure

PMNL preparation and granule density centrifugation. PMNLs were isolated from whole blood (100 ml) (Section 2.7.2), counted (~$1x10^7$ cells), viability assessed (>98% trypan blue exclusion) and resuspended in EGTA-free relaxation buffer (5 ml) containing AEBSF at a final concentration of 2.5 mM (125 µl stock/5 ml). The cells were pelleted (400 x g, 5 min, 4°C), resuspended in EGTA-free relaxation buffer (5 ml) containing AEBSF at a final concentration

of 0.25 mM (12.5 µl stock/5 ml) and ATP at 1 mM (100 µl stock/5 ml). The cells were sheared by passage through a sterile 26-gauge needle (5 strokes) and then supplemented with EGTA to a final concentration of 1.5 mM (75 µl stock/5 ml). Unbroken cells and debris were pelleted (400 x g, 15 min, 4°C), the supernatant loaded onto a pre-cooled three layer (1.05/1.07/1.12 g/ml) Percoll gradient and centrifuged (37000 x g, 30 min, 4 °C). Fractions (500 µl each, 20 fractions in total) were collected by aspiration from the bottom of the centrifuge using a Pasteur pipette attached to a peristaltic pump. Each fraction was split into 8 aliquots of 50 µl each and kept at -80°C for future detection of marker proteins by immunochemical or enzymatic methods.

For the purposes of assigning GPI-anchored proteins to a particular granule population, the following markers were used to define various granules: MPO (azurophil), lactoferrin (specific), proMMP-9 (specific and gelatinase), proMMP-9/NGAL heterodimer (specific granules), alkaline phosphatase (secretory vesicles) (see Table 1.1).

Alkaline phosphatase colorimetry. For determination of latent alkaline phosphatase activity (secretory vesicle marker), each fraction (50 µl) was thawed and diluted with complete substrate (containing $MgCl_2$ and *p*NPP) (250 µl) before transfer to microtitre plates and incubation at 37°C (10-30 min). After sufficient colour had developed, the absorbances of the fractions were read at 405 nm in a spectrophotometer.

MPO ECL. Detection of MPO (azurophil granule marker) was performed by ECL as described by Dahlgren *et al.* (1993) as this method is considerably more sensitive than spectrophotometric detection with ABTS. Each fraction (50 µl) was thawed and diluted with relaxation buffer (200 µl) containing 0.3% CTAB (Rice *et al.*, 1987) (20 µl CTAB/200 µl) to solubilise the granules and allow substrate access to MPO. The tubes were incubated on ice (4°C, 30 min) before vacuum transfer onto nitrocellulose (pre-wetted with 1 x MPO buffer) using a Hoefer Slot Blot apparatus. This transfer allows protein binding to the membrane, while effectively removing the Percoll (since excess Percoll can inhibit MPO activity). Immediately after transfer, the membrane was washed briefly in 1 x MPO buffer and then submerged in ECL substrate (2 ml, 5 min) (Section 2.8.2.1). Excess substrate was removed, the membrane sandwiched in between two sheets of clear thin plastic and exposed to ECL X-ray film (5-10 min). After exposure, the film was developed and fixed before storage.

Lactoferrin western blot. For lactoferrin (specific granule marker) determination, each fraction (50 µl) was thawed and diluted in TEN (200 µl) containing 1 mM AEBSF (2 µl stock/200 µl), 1% (w/v) NaN_3 (0.002 g/200 µl) and 0.1% (v/v) Triton X-100. The mixture was kept on ice (4°C, 30 min) before vacuum transfer onto nitrocellulose using a Hoefer Slot Blot apparatus. After transfer, the membrane was dried (2 h, RT) and processed as described for western blotting and ECL (Section 2.8.2). The membrane was probed with rabbit anti-lactoferrin (1/1000) and detected with HRPO-sheep anti-rabbit IgG (1/5000).

GPI-anchored protein western blot. For detection of GPI-anchored proteins, fractions (50 µl each) were treated exactly as for detection of lactoferrin above. The membrane was probed with chicken anti-GPI IgY (10 µg/ml) and detected with HRPO-goat anti-chicken IgG (1/5000) and ECL (Section 2.8.2.1).

ProMMP-9 gelatin zymography. Finally, for detection of proMMP-9 (specific and gelatinase granule marker), each fraction (50 µl) was thawed and diluted with non-reducing treatment buffer (100 µl) (30 min, RT) to ensure complete solubilisation of proteins with SDS. A gelatinase standard was prepared by drawing blood from a fingertip prick (100 µl) and diluting it immediately with non-reducing treatment buffer (900 µl) (Makowski and Ramsby, 1996). A non-reducing 7.5% Laemmli SDS-PAGE gel was cast (Section 2.4.1), containing porcine type I gelatin (300 bloom) at a final concentration of 1.5 mg/ml in the running gel. After a 4% stacking gel was cast, the samples were loaded (10 µl/well) and electrophoresed. Upon completion of electrophoresis, the gel was disassembled, washed in 2.5% (v/v) Triton X-100 (2 x 200 ml, 2 x 1 h) and incubated in pre-warmed gelatinase buffer (18 h, 37°C) (Section 2.6.1). The gels were stained (Section 2.6.2) and then destained in dd.H_2O.

3.5.1.3 Results and Discussion

The latent alkaline phosphatase activity profile obtained (Figure 3.5 A, fractions 12-20, peaking at 15) matched that anticipated and indicated the presence of secretory vesicles. Since the detection limit of this colorimetric assay requires at least $5x10^6$ PMNLs (Sørensen and Borregaard, 1999), the development time of the assay varied according to PMNL yields.

The majority of MPO occurs in fractions 1-5, thereafter decreasing steadily and is absent from fractions 17-20 (Figure 3.5 B). A similar activity pattern was obtained by Dahlgren *et al.* (1993) (indicating that this pattern is reproducible), and is not due to inefficient granule fractionation or

granule lysis. Although the specific, gelatinase and secretory vesicles are thought to be MPO-negative, the low sensitivity of previous methods compared to ECL may have prevented the detection of small amounts of MPO throughout most PMNL granules as seen by us and Dahlgren *et al.* (1993). Alternatively, and more probably, the broad MPO activity profile may be due to density variance of MPO-positive subpopulations and may not imply colocalisation of MPO with other granule marker proteins. Indeed, immunocytochemistry of human PMNL sections supports this interpretation as, for example, MPO and lactoferrin do not colocalise (Cramer *et al.*, 1985) but these antigens may occur in granule fractions of similar buoyant density.

The distribution of lactoferrin is seen to occur between fractions 2-5, increasing steadily between fractions 5-12, peaking at fraction 9 (Figure 3.5 C). Therefore, fractions 6-10 were designated to correspond to the main population of lactoferrin-positive specific granules. As in the case of MPO, the relatively broad distribution of lactoferrin may reflect the varying densities of specific granule subpopulations due to the transient expression of PMNL granule proteins during maturation.

The detection of proMMP-9 was accomplished by gelatin zymography instead of western blot or ELISA due to the higher degree of sensitivity afforded by zymography (picogram level detection versus nanogram) (Kleiner and Stetler-Stevenson, 1994; Sørensen and Borregaard, 1999) (Figure 3.5 E). Unlike ELISA, gelatin zymography allows simultaneous visualization of all three proMMP-9 forms (92 kDa proMMP-9, 125 kDa proMMP-9/NGAL heterodimer, 220 kDa proMMP-9 homodimer) present in PMNL specific and gelatinase granules (Makowski and Ramsby, 1996) and, due to the high sensitivity of zymography, may produce less distinct (clear cut) proMMP-9-positive fractions than those obtained by ELISA. The absence of appreciable proMMP-9 in fractions 1-5 reaffirms the validity of the decision to define lactoferrin-positive specific granules from fraction 6 (as specific granules contain both lactoferrin and proMMP-9). Therefore, fractions 6-10 contain both lactoferrin and proMMP-9 and may represent the major population of specific granules (Figure 3.5 C and E). The majority of proMMP-9 occurs in fractions 9-13, as these fractions contain the broadest bands of gelatinolytic activity (Figure 3.5 E, solid line). Since fractions 9-13 do not appear to contain appreciable lactoferrin, they may be classified as the major population of gelatinase granules. Although NGAL has been considered as a specific granule marker (Kjeldsen *et al.*, 1994), the presence of the 125 kDa proMMP-9/NGAL heterodimer in fractions from 5-20 (Figure 3.5 E)

suggest its distribution is more widespread and occurs in granules of varying density that lack lactoferrin (since lactoferrin is not present in fractions 14-20) (Figure 3.5 C). The level of homodimeric proMMP-9 (220 kDa) and monomeric proMMP-9 (92 kDa) both peak at fractions 9 and 10, therefore fractions 9-20 were designated to represent gelatinase granules (Figure 3.5 E). Although proMMP-9 activity is seen in fractions 12-20 and this overlaps the distribution of alkaline phosphatase (Figure 3.5 A), these fractions may represent subpopulations of gelatinase granules that differ in density (and, therefore, cosediment with secretory vesicles) but do not contain alkaline phosphatase and/or other GPI-anchored proteins.

The GPI-anchored proteins appeared to occur between fractions 10 and 20, peaking in fractions 13 and 14 (Figure 3.5 D). This distribution mirrors that of alkaline phosphatase (Figure 3.5 A) since alkaline phosphatase is, itself, a GPI-anchored protein. There also appears to be a subpopulation of GPI-anchored proteins in fractions 8 to 12 (Figure 3.5 D, thin line). This subpopulation has previously been identified as alkaline phosphatase-positive (Borregaard *et al.*, 1993). Direct immunolocalisation of GPI-anchored proteins with respect to established granule marker proteins in whole PMNL sections was used to confirm that GPI-anchored proteins occur solely in secretory vesicles, separate from other granule markers. Immunocytochemistry, together with TEM, has an advantage over subcellular fractionation in that it can distinguish different granule populations of similar density, thereby avoiding the possible false-positive colocalisation designations that may occur by studying markers in subcellular fraction homogenates obtained by density centrifugation.

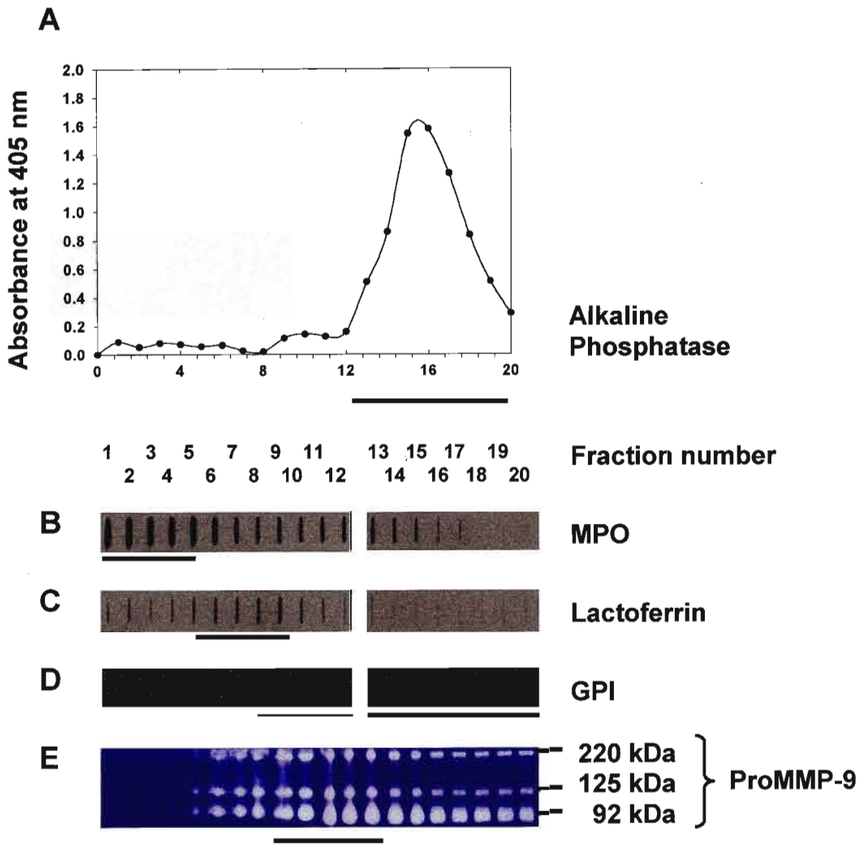

Figure 3.5 **Subcellular fractionation of PMNL granules by density gradient centrifugation and immunolabelling of fractions to assess the distribution of GPI-anchored proteins with respect to granule markers.**

PMNLs were disrupted by passage through a 26-gauge needle and the postnuclear supernatant applied on top of a discontinuous 3 layer Percoll gradient and centrifuged. A), Detection of latent alkaline phosphatase (secretory vesicles) using *p*NPP. B), Slot blot of granule fractions for MPO detection by ECL. C), Slot blot of fractions probed with rabbit anti-lactoferrin (1/1000) and detected with HPRO-conjugated sheep anti-rabbit IgG (1/5000) and ECL. D), Slot blot of fractions probed with chicken anti-GPI-anchored protein IgY (10 μg/ml) and detected with HRPO-conjugated goat anti-chicken IgG (1/5000) and ECL. E), Detection of proMMP-9 by gelatin zymography. Three forms of proMMP-9 occur in PMNLs: 92 kDa (proMMP-9 monomer), 125 kDa (proMMP-9/NGAL heterodimer), 220 kDa (proMMP-9 homodimer). The thick lines represent the fractions corresponding to maximal distribution of a particular protein. The thinner line in (D) possibly represents a subpopulation of GPI-anchored proteins.

3.5.2 Immunocytochemistry

Immunocytochemistry was performed on whole PMNL ultra-thin cryosections to verify the observed localised distribution of GPI-anchored proteins to secretory vesicles, i.e. to alkaline phosphatase-positive fractions obtained by density centrifugation. Due to the limited resolving power of density fractionation with organelles of similar density, it was deemed necessary to ensure that GPI-anchored proteins occurred in compartments separate from all other granule marker proteins, besides alkaline phosphatase, if GPI-anchored proteins were expected to serve as markers for secretory vesicles.

3.5.2.1 Reagents

All reagents and buffers were prepared as described in Section 2.9.3.2.

3.5.2.2 Procedure

PMNLs were isolated from whole blood (100 ml) (Section 2.7.2), counted (~$2x10^6$ cells), viability assessed (>98% trypan blue exclusion) and processed for cryoultramicrotomy and immunocytochemistry (Section 2.9.3.2). Ultrathin cryosections were labelled for GPI-anchored proteins (125 ng/5 µl), followed by rabbit anti-IgY linker antibody (20 µg/ml) and 5 nm protein A gold (1/300, $A_{520} = 0.024$, 10 µl, 30 min, RT). Sections were also labelled for a second antigen with either rabbit anti-MPO (25 ng/5 µl) (azurophil granules), rabbit anti-lactoferrin (125 ng/5 µl) (specific granules), rabbit anti-proMMP-9 (100 ng/5 µl) (specific and gelatinase granules), monoclonal anti-LAMP-1 (1/100) or monoclonal anti-LAMP-2 (1/100) IgG (multilaminar/multivesicular bodies). The monoclonal antibodies required a rabbit anti-mouse IgG linker antibody (1/500), and all of the second antigens labelled were detected with 10 nm protein A gold (1/300, $A_{520} = 0.037$, 10 µl, 30 min, RT).

3.5.2.3 Results and Discussion

Labelling for GPI-anchored proteins occurred predominantly on the membranes of electron translucent vesicles of pleiomorphic shape, resembling the morphology of secretory vesicles (Figure 3.6 A-F). Membrane labelling of organelles usually tends to be low due to the fact that proteins may be asymmetrically distributed, thus reducing the chance of detection during random sectioning. The relatively high labelling density for the GPI-anchored proteins (5-10 gold particles per organelle, in comparison to most other membrane proteins) is possibly due to the fact that the antibody preparation recognises a number of epitopes (theoretically, peptides

derived from at least 8 known PMNL GPI-anchored proteins) (Figure 3.6 A-F).

No colocalisation of GPI-anchored proteins with the major granule marker proteins, MPO, lactoferrin and proMMP-9 was observed in double labellings (Figure 3.6 A, B-D). Occasionally, labelling for GPI-anchored proteins was detected in multilaminar vesicles [Figure 3.6 F (inset)] that are known to contain LAMPs (Cieutat *et al.*, 1998; Bainton, 1999). Of the two marker proteins for the multivesicular/multilaminar bodies, LAMPs-1 and -2 (Cieutat e*t al.*, 1998), only LAMP-2 colocalised with GPI-anchored proteins to any appreciable extent in this study (Figure 3.6 F). This result is in disagreement with a previous investigation that provided evidence (using granule fractionation) for localisation of both LAMPs to the secretory vesicles (Dahlgren *et al.*, 1995). Any discrepancy between our results and those obtained previously may reflect the limitations of the granule fractionation technique for resolving different vesicle fractions of similar density. It is, therefore, essential that all granule fractionation studies be corroborated with immunocytochemical data obtained from whole PMNL sections.

Sparse labelling for GPI-anchored proteins was detected on the plasma membrane (Figure 3.6 F). Since PMNLs are easily primed and the secretory vesicles are readily exocytosed, the presence of GPI-anchored proteins in the plasma membrane as reported before (Detmers *et al.*, 1995) may be due to inadvertent priming of PMNLs during PMNL purification and subsequent handling. To reduce the risk of priming, we routinely use ammonium chloride for erythrocyte lysis instead of distilled water, as the latter is known to damage and potentially activate PMNLs (Roos and de Boer, 1986). Therefore, the low plasma membrane labelling for GPI-anchored proteins seen in this study may be attributed to negligible secretory vesicle release induced by ammonium chloride lysis relative to that potentially induced by distilled water treatment.

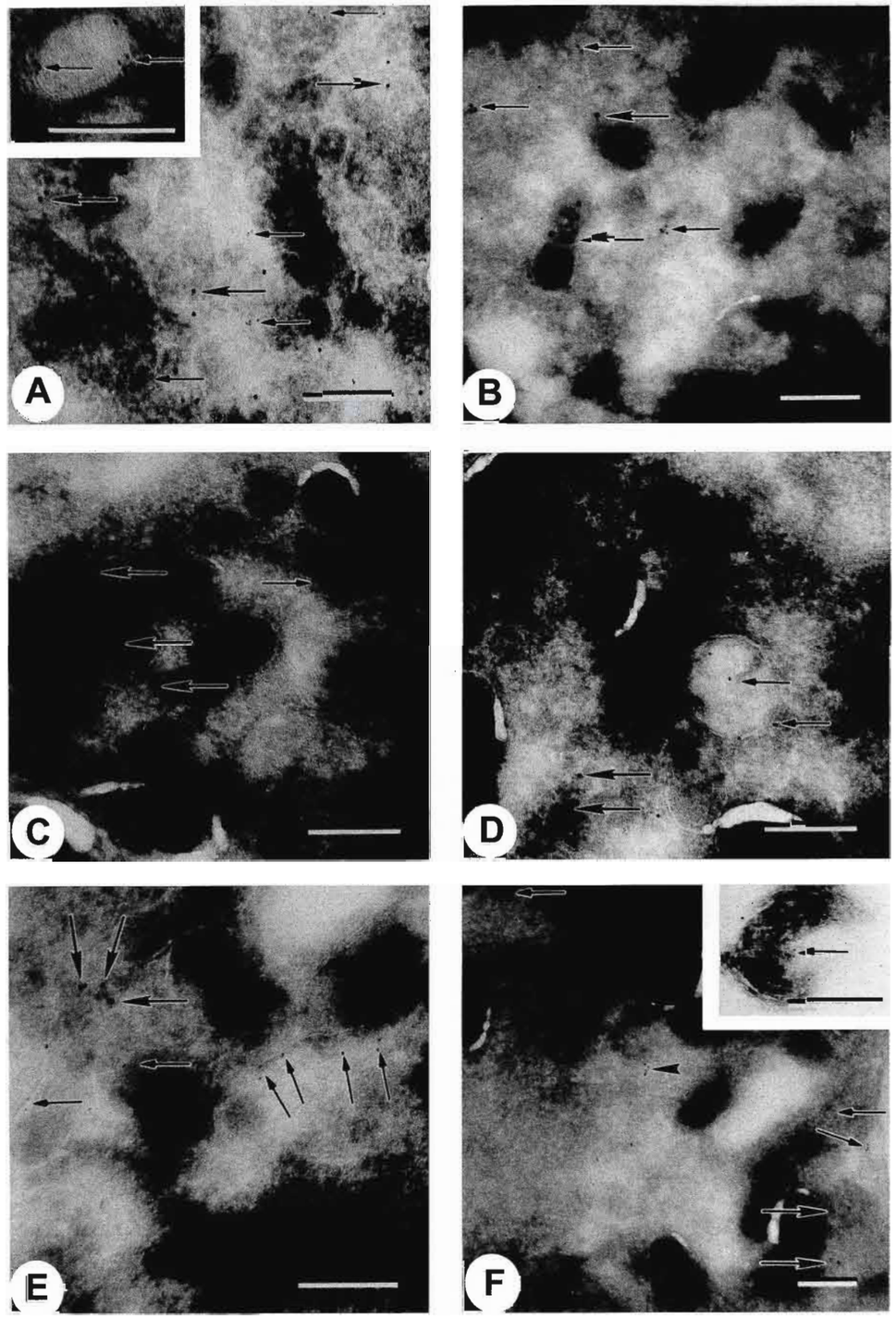

Figure 3.6 **Immunolocalisation of GPI-anchored proteins with respect to PMNL granule protein markers on thawed ultrathin cryosections.**

A), GPI-anchored proteins (5 nm; small arrows) and the azurophil granule marker, MPO (10 nm; large arrows). Inset: Single labelling for GPI-anchored proteins. Note that gold probes only occur on the inner leaflet of the membrane and appear polarised (arrows). Also note that the vesicle appears to be enveloped by more than one lipid bilayer. B), GPI-anchored proteins (5 nm; small arrows) and the specific granule marker, lactoferrin (10 nm; large arrows). The majority of lactoferrin occurs in a typical dumbbell shaped organelle while the GPI-anchored proteins are found in small, round vesicles. C) and D), GPI-anchored proteins (5 nm; small arrows) and the specific and gelatinase granule marker, proMMP-9 (10 nm; large arrows). GPI-anchored proteins appear polarised (C; small arrows) and separate from proMMP-9. Note that GPI-labelled vesicles appear both oblong and electron dense (C) and round and electron translucent (D). E), GPI-anchored proteins (5 nm; small arrows) and the multilaminar/multivesicular body marker, LAMP-1 (10 nm; large arrows). The single 5 nm gold probe present in the LAMP-1 labelling body possibly represents background labelling as all other 5 nm probes occur separate from LAMP-1. F), GPI-anchored proteins (5 nm; small arrows) and the multilaminar/multivesicular body marker, LAMP-2 (10 nm; large arrows). The majority of GPI-anchored proteins occur separately from LAMP-2-positive bodies, although some colocalisation is evident (arrowhead). Inset: A multilaminar organelle labelling for GPI-anchored proteins (5 nm). Bars = 200 nm.

No colocalisation of GPI-anchored proteins with lactoferrin-positive specific granules was found (Figure 3.6 B), whereas previous authors have reported localisation of GPI-anchored CD67 on the limiting membrane of specific granules (Jost *et al.*, 1991). This may be due to false-positive labelling for CD67, however, as labelling for CD67 on MPO-positive azurophil granules also occurred in the study by Jost *et al.*, 1991b, indicating some non-specific labelling for CD67. To avoid non-specific membrane labelling, stringency washes (1 M NaCl in PBS) were routinely employed in this study to ensure that all labellings observed are true and representative. It is, therefore, felt that the lack of specific granule labelling for the GPI-anchored proteins reflects the true *in vivo* distribution of these proteins.

Secretory vesicles have been described as tubular (Kobayashi and Robinson, 1991) and electron translucent (Jost *et al.*, 1991), but the results presented here show that they also occur as vesicles that are electron dense (Figure 3.6 C), circular (Figure 3.6 A and B), oblong (Figure 3.6 E), dumbbell-shaped (Figure 3.6 C and E) or multilaminar [Figure 3.6 F (inset)]. Although the immunocytochemistry results prove that GPI-anchored proteins reside in vesicles separate from other granule proteins (with the exception of some LAMP-2), they also highlight the potential dangers associated with classifying granule populations on the basis of morphology. In particular, the GPI-anchored protein-rich dumbbell-shaped, electron dense organelles (Figure 3.6 C and E) are a case in point as these would conventionally be classified as a specific (lactoferrin-positive) granule judged solely on morphological grounds. This would, however, be incorrect since GPI-anchored proteins and lactoferrin do not colocalise (Figure 3.6 B).

The morphological heterogeneity of GPI-anchored protein-rich secretory vesicles may provide further support for their proposed origin. Secretory vesicles are thought to represent endosomes formed late during PMNL development that subsequently 'evolve' into $Ca^{2+}{}_i$-sensitive regulated secretory vesicles (Borregaard and Cowland, 1997). Recent cryoimmunocytochemistry studies on B-cells have described six types of endosomal compartments that exhibit maturation-dependent morphological differences (Kleijmeer *et al.*, 1997). This study shows that early endosomes are simple in structure (circular and oval) and generally electron-translucent. As they mature into late endosomes, they become multivesicular and, finally, multilaminar in appearance. Therefore, the simple GPI-anchored protein-positive vesicle in Figure 3.6 A (inset) may represent an early endosome that 'evolved' into a secretory vesicle and the GPI-anchored protein-rich multilaminar body [Figure 3.6 F (inset)] may, therefore, represent a late endosome

(formed during PMNL maturation) that subsequently 'evolved' into a secretory vesicle. The multilaminar/multivesicular bodies present in PMNLs have been reported to be LAMP-positive. In addition, Bainton (1999) reports that the PMNL multilaminar body, unlike the PMNL multivesicular body, does not contain the cation-independent mannose-6-phosphate receptor. Since organelles that are LAMP-positive *and* cation-independent mannose-6-phosphate receptor-negative are designated late endosomes (Clague, 1998; Bainton, 1999), this fact provides an explanation for the observed low level of colocalisation of GPI-anchored proteins and LAMP-2 and the high level of GPI-anchored protein labelling in the multilaminar body [Figure 3.6 F (inset)]. GPI-anchored proteins may occur in secretory vesicles that are derived from early endosomes [Figure 3.6 A (inset)] and these may subsequently mature into LAMP-positive late endosomes upon acquiring the LAMP-antigens and the multilaminar conformation (Figure 3.6 F).

3.6 Discussion

Our understanding of the role and significance of GPI-anchor addition to proteins has been predominantly gained from studies on polarized epithelial cells. Epithelial cells contain distinct apical and basolateral surfaces that allow them to perform various vectorial functions *viz.*, secretion, absorption and ion transport (Lisanti and Rodriguez-Boulan, 1990). The apical and basolateral surfaces differ with respect to protein and lipid composition, which has allowed these cells to evolve a mechanism by which certain proteins may be selectively targeted and delivered to the apical surface, i.e. GPI-anchor addition. Although GPI-anchor addition to epithelial cell proteins is essential for correct apical surface targeting, GPI-anchored proteins are also found in a number of non-polarised cells [e.g. *T. brucei* variant surface glycoprotein, erythrocyte acetylcholinesterase (Ferguson, 1989; Schneider and Ferguson, 1995; Udenfriend and Kodukula, 1995) and PMNLs (although PMNLs *do* polarise into anterior and posterior regions during locomotion and phagocytosis, they do not contain distinct apical and basolateral surfaces)]. In the case of non-polarised cells, addition of GPI-anchors to certain proteins may be preferable rather than adding transmembrane spanning domains for at least two reasons. Firstly, the lipid anchor permits greater lateral diffusion in the plasma membrane [in fact, the diffusion coefficients of lipids (e.g. the lipid portion of GPI anchors) is ~10^{-8} cm^2/s versus ~10^{-10} cm^2/s for membrane proteins] (Field and Menon, 1993). This may be important if GPI-anchored proteins are required to migrate to a particular area on the cell surface, such as during IgG-mediated phagocytosis (via GPI-anchored FcγIIIRB/CD16b). Secondly, most GPI-anchored proteins may be easily shed from the plasma membrane by phospholipases, thereby circumventing the need

for endocytosis and intracellular proteolytic degradation to downregulate their activity. This ability to quickly shed GPI-anchored proteins is of particular use to trypanosomes as this allows them to continually evade the immune response by continually presenting and shedding variant surface glycoprotein to avoid opsonisation.

Unlike other non-polarised cells, PMNLs do not constitutively transport and display GPI-anchored proteins on the plasma membrane, but rather target and store them in intracellular secretory vesicles (Kobayashi and Robinson, 1991; Edwards, 1994; Borregaard and Cowland, 1997). This is probably possible due to maturation-dependent protein expression that occurs during PMNL development, i.e. all GPI-proteins are synthesised at the same final stage of PMNL development and are, therefore possibly, packaged into the secretory vesicles which are synthesised last (Borregaard and Cowland, 1997). In order to permit effective intercalation and stabilisation of GPI-anchors in the secretory vesicle membranes, it is possible that these organelles are rich in glycosphingolipids (e.g. sphingomyelin, glucosyl ceramide).

In addition to selectively expressing GPI-anchored proteins at the band/segmented stage of PMNL development, the PMNL has evolved to selectively attach GPI-anchors to the proteins required to be released first, i.e. proteins involved in early PMNL adhesion and phagocytosis, *and* ensure that they are simultaneously expressed and targeted to the highly $Ca^{2+}{}_i$-sensitive secretory vesicles for rapid mobilisation.

The biological functions of most PMNL GPI-anchored proteins (with the exception of alkaline phosphatase) are well known and most of our understanding of their importance has come from individuals suffering from PNH. PNH usually involves a defect in either GPI-anchor biosynthesis and/or attachment and, therefore, most PMNL GPI-anchored proteins are either absent or present in reduced numbers (Field and Menon, 1993). A decrease in uPAR expression, in conditions such as PNH, leads to impaired PMNL migration, possibly due to reduced uPA binding and activation of proteinases required for PMNL migration (Pedersen *et al.*, 1996). Loss of GPI-anchored proteins involved in complement degradation, e.g. CD55/DAF (which inhibits assembly of, or accelerates the dissociation of, C3/C5 convertases thereby regulating the complement cascade at the C3 hydrolysis step) and CD59 (inhibits the final step of the complement cascade by preventing the formation of the membrane attack complex) (Hatanaka *et al.*, 1996), is accompanied by apoptosis (Dransfield *et al.*, 1994; Jones and Morgan, 1995). A decrease in CD16b expression has been implicated in apoptosis and early-

onset periodontitis (Dransfield *et al.*, 1994; Nemoto *et al.*, 1997). Such an early onset may result as PMNLs would not recognise and bind IgG-opsonised organisms. Unfortunately, it is not presently known how the loss of GPI-anchored proteins results in PMNL apoptosis.

Conversely, a reduction of CD55 and CD59 expression has been identified in a number of human leukemia cell lines and may be the result of the limited maturation of these cells (Hatanaka *et al.*, 1996). In addition, PNH patients are known to occasionally develop acute myelocytic leukemia, presumably due to a pleiotropic effect resulting from the reduction in the number of GPI-anchored proteins. Reduced GPI-anchored protein expression may, therefore, potentially serve as early prognostic markers of malignant transformation. The identification of further PMNL GPI-anchored proteins may, therefore, help to expand our knowledge of PMNL function in the context of inflammation [e.g. the recent discovery of GPI-80 may improve our knowledge of PMNL adherence and migration (Suzuki *et al.*, 1999)] and, possibly, cancer.

The primary aim of this chapter was to assess the specificities of supplied antibodies raised against PMNL granule marker proteins for use in immunocytochemical localisation studies. Problems associated with both immunocytochemical and histochemical methods for the detection of secretory vesicle HSA and alkaline phosphatase, respectively, led to the designing of the simple and highly selective method for the purification of GPI-anchored proteins reported here. This method successfully dispenses with the need for phospholipases and/or preparative purification by SDS-PAGE, while uniquely allowing purification of any *myo*-inositol-acylated GPI-anchored proteins.

In addition to describing a new method for GPI-anchored protein isolation, the results from this study, for the first time, prove the hypothesis that GPI-anchored proteins solely reside in secretory vesicles. This was confirmed both by subcellular fractionation and immunocytochemistry using the antibodies raised against the GPI-anchored protein antigens isolated using the newly developed procedure. Our results from the immunocytochemical studies also describe the morphological heterogeneity of secretory vesicles and the finding that some GPI-anchored proteins colocalise with LAMP-2 and reside in multilaminar compartments lends further support to the endocytic origin of these organelles.

Although the primary aim of the chapter was to identify a specific secretory vesicle marker for use in further immunocytochemical localisation studies of TIMP-1 (Chapter 4), the method

described for GPI-anchored protein purification could routinely be used for the identification of novel PMNL GPI-anchored proteins. As reduced GPI-protein expression may have the potential to serve as an early prognostic marker for leukemias, the anti-GPI-anchored protein antibodies raised in this chapter may be useful in ELISA and western blotting methods for the diagnostic detection of reduced levels of GPI-anchored proteins.

The characterization of a high M_r form of TIMP-1 formed the prior focus of the following chapter when, during the characterisation of anti-TIMP-1 antibodies to be used in the subsequent immunolocalisation of TIMP-1, the antibodies targeted an unanticipatedly high M_r form of TIMP-1 in PMNL homogenates. Though the specificity of the anti-TIMP-1 antibody used in the immunolocalisation of TIMP-1 was verified when a monoclonal anti-TIMP-1 antibody from a commercial source gave similar results, further studies were carried out to ensure that the labeling seen was due to the targeting of TIMP-1 (i.e. an inhibitor with the ability to bind and inhibit an MMP), and not due to recognition of similar epitopes. The discovery that such forms also occur in plasma, lead to further investigation into the possible functional (inhibitory) capacity of such forms.

CHAPTER 4

Characterisation of high M_r TIMP-1 forms and subcellular localisation of TIMP-1

4.1 Introduction

By the time PMNLs have entered the bloodstream from the bone marrow, granule synthesis and protein targeting (by an as yet unknown mechanism) have usually ceased and, therefore, granule protein gene transcription has usually already terminated (Edwards, 1994; Borregaard and Cowland, 1997). However, Triebel *et al.* (1995) were successful in detecting transcripts of TIMP-1 mRNA in chemotactically activated "mature" PMNLs using the reverse transcriptase polymerase chain reaction (RT-PCR). Constitutive expression of TIMP-1 does occur in other cell types (e.g. fibroblasts), but it is usually regulated either developmentally [e.g. in monocytes (Campbell *et al.*, 1991)] or by paracrine signalling (TIMP-1 is upregulated by cytokines IL-1β, transforming growth factor-β1, oncostatin M and TNFα or downregulated by concanavalin A or dexamethasone) (Gomez *et al.*, 1997). At the commencement of this study, the translation of TIMP-1 mRNA, previously demonstrated in mature PMNLs, could be speculated to occur via one of at least two processes, either of which, by analogy with the expression of other PMNL proteins, would give rise to a specific pattern of TIMP-1 distribution. In the first possible process, like other cytosolic PMNL proteins, TIMP-1 mRNA may be constitutively translated and not transiently translated like most PMNL granule proteins (Fouret *et al.*, 1989), and might similarly also be cytosolically translated and become localised in the cytoplasm. Alternatively, in the second case, transcription and translation of TIMP-1 might occur late in PMNL maturation when the secretory vesicles are formed. In this case, the protein might be packaged as a luminal component of secretory vesicles (since secretory vesicles are synthesised late in mature PMNLs).

The data indicating the presence of TIMP-1 mRNA in chemotactically activated "mature" PMNLs (Triebel *et al.*, 1995) would have been more informative if the maturation status of the PMNLs expressing TIMP-1 had been confirmed, e.g. by assaying for alkaline phosphatase activity [a secretory vesicle marker (Borregaard *et al.*, 1992)]. The presence of alkaline phosphatase would have indicated that the PMNLs were mature and all the granule populations

had been synthesised. A way in which the question of when TIMP-1 is expressed could have been addressed, would have been to use the HL-60 promyelocytic cell line. DMSO-treated HL-60 cells partially differentiate to resemble PMNLs but do not fully mature or synthesise specific granules as they remain MMP-8-negative, lactoferrin-negative and vitamin B_{12}-binding protein-negative (Collins *et al.*, 1977; Devarajan *et al.*, 1991; Borregaard and Cowland, 1997). Performance of RT-PCR on the DMSO-treated HL60 promyelocytic 'PMNL-like' leukemia cells and mature, normal blood PMNLs and demonstration of TIMP-1 mRNA in both cell types would further support the hypothesis that the expression of TIMP-1 is constitutive and not just expressed terminally during biogenesis of the secretory vesicles.

Besides demonstrating the presence of alkaline phosphatase-containing vesicles, PMNLs may also be designated mature if both Golgi stacks and mitochondria are absent, as the presence of Golgi signifies incomplete granule protein biosynthesis and, hence, PMNL immaturity (Edwards, 1994). Despite this, scientific papers still continue to present protein localisation results using PMNL electron micrographs with distinct Golgi stacks and mitochondria (e.g. Segal *et al.*, 1980; Jost *et al.*, 1990; Berger *et al.*, 1994). Apart from the fact that these structures indicate that the PMNLs are not yet fully mature, such cells are almost indistinguishable from monocytes and the identity of the cell cannot be unequivocally established without further verification e.g. staining with the lipophilic dye, Sudan Black (Absolom, 1986). In the current study, therefore, localisations were performed only on mature PMNLs (lacking Golgi and mitochondria) to ensure that all of the granule populations had been synthesised.

The first part of this chapter describes the identification and preliminary characterisation of an unexpectedly high M_r form of TIMP-1 revealed by western blotting of PMNL homogenates during TIMP-1 antibody characterisation for use in immunolabelling. In order to further characterise this high M_r TIMP-1 species, an MMP-9 fraction was prepared from sputum using three-phase partitioning (TPP) and a western ligand blot of PMNL homogenates was designed to prove the identity of the high M_r TIMP-1 form by virtue of its ability to preferentially bind proMMP-9. As previously mentioned (Section 1.8), TIMP-1 and TIMP-2 are capable of inhibiting all *active* MMPs, but also exhibit specific binding to the C-terminal domains of proMMP-9 and -2 *zymogens*, respectively. This specific binding of TIMP-1 to proMMP-9 was exploited in the western ligand blot used in this study and the TIMP-1/proMMP-9 complex formed by treatment of high M_r TIMP-1 with proMMP-9 was subsequently detected by probing

with antibodies against proMMP-9. A number of methods were attempted to dissociate the high M_r form of TIMP-1, but with no apparent success. These included the addition of antioxidants to PMNL homogenates to reduce the risk of protein crosslinking by PMNL ROS (assuming the high M_r TIMP-1 form was an oxidation artefact), and reduction and carboxymethylation of PMNL proteins (in 6 M guanidine-HCl) prior to electrophoresis and western blotting, to ensure that TIMP-1 was sufficiently denatured. Drawing on the knowledge that TIMP-1 is exceptionally heat stable and displays specific binding to heparin, PMNL homogenates were diluted, boiled and the supernatant passed through a heparin-agarose column. TIMP-1 was step-eluted with salt and this resulted in a M_r reduction from 66 kDa to approximately 28-30 kDa. Therefore, the 66 kDa form of TIMP-1 in PMNLs is non-covalent and may possibly be dissociated by the synergistic effects of heat and dilution or by the competitive dissociation of the complex by the preferential binding of the TIMP-1 monomer to heparin-agarose.

In addition, the designing and optimisation of a new UV fluorescent reverse zymography method for the detection of TIMPs in crude samples is described, and was used to confirm that high M_r TIMP-1 species retain the ability to inhibit active MMP-9. The UV fluorescent zymogram overcomes problems associated with conventional reverse zymograms of crude protein samples. Unlike regular Coomassie Blue-stained reverse zymograms, the UV fluorescent zymogram allows continuous monitoring of gelatin digestion and allows the specific visualisation of the proteinase substrate (i.e. fluorescent gelatin) without interference from sample proteins or the proteinase itself.

Antigen localisation using ultramicrotomy and immunogold labelling may potentially provide valuable high-resolution information on the subcellular localisation and, hence, role(s) and regulation of antigens of interest - information that is not provided by techniques employing cell-free assays or immunofluorescence. In this chapter, the primary aim was to establish the localisation of TIMP-1 in PMNLs. Prior to this, the intracellular location of TIMP-1 was unknown, although at one time it was thought to be cytosolic (Murphy *et al.*, 1980). This reasoning probably originated from the belief that, in other cell types, some of the cathepsin inhibitors (the stefins) are cytosolically located (Green *et al.*, 1984) and such a localisation would ensure that accidental spillage of enzymes into the cytoplasm (however remote the possibility) would be quickly inhibited.

In the second part of this chapter, therefore, the immunolocalisation of TIMP-1 with respect to currently recognised granule marker proteins, the proMMPs and markers for the endocytic pathway on ultrathin cryosections is described. Due to the novel localisation of TIMP-1 to a distinct compartment, separate from most other granule marker proteins, the stereology and density of this new 'vesicle' were also investigated in an attempt to estimate its possible maturation-dependent time of synthesis. Should TIMP-1 be present in a vesicle subset distinct from other populations, as judged by stereology, buoyant density and separate localisation with respect to most known marker proteins, such a separate localisation of TIMP-1 may have important consequences for controlling MMP activity during inflammation and basement membrane traversal, since the PMNL may differentially regulate the release of MMPs and TIMP-1.

4.1.1 Characterisation of anti-TIMP-1 antibodies and a high M_r form of TIMP-1

In keeping with the practise of antibody characterisation using crude cell homogenates, the rabbit anti-TIMP-1 antibody was assessed for specificity against crude, variously treated, PMNL homogenates. Initial western blots revealed antibody reactivity with only a high M_r band at 66 kDa, assumed to be TIMP-1. To prevent the generation of homogenisation-induced species of TIMP-1, azide was included to inhibit MPO activity, and DMSO and L-methionine were added to serve as hydroxyl radical and HOCl scavengers, respectively (Peppin and Weiss, 1986).

4.1.1.1 Reagents

PMNL lysing buffer [PBS containing 1 M NaCl and 10% (v/v) DMSO]. NaCl (5.84 g) and DMSO (10 ml) were added to 70 ml PBS (Section 2.7.1), made up to 100 ml in a volumetric flask and stored at 4°C.

Denaturation buffer (6 M guanidine-HCl, 500 mM Tris-HCl, 2 mM EDTA, pH 8.1). Guanidine (14.33 g), Tris (1.51 g) and Na_2EDTA (0.018 g) were dissolved in dd.H_2O (20 ml) and titrated to pH 8.1 with NaOH. The volume was made up to 25 ml and kept at RT in the dark.

10 x DTT stock solution (714 µmoles in denaturation buffer). DTT (0.11 g) was dissolved in denaturation buffer (1 ml) just before use.

10 x Iodoacetic acid stock solution (1.43 mmoles in denaturation buffer). Iodoacetic acid (0.265 g) was weighed out in a fume hood and dissolved in denaturation buffer (1 ml) just

before use.

Wash buffer [50 mM Tris-HCl, 5 mM $CaCl_2$, 0.05% (v/v) Brij 35, 0.02% (w/v) NaN_3, pH 7.4]. Tris (0.606 g) and $CaCl_2.2H_2O$ (0.074 g) were dissolved in 90 ml dd.H_2O. Brij 35 [167 µl of a 30% (v/v) solution] was added and the pH was titrated to 7.4 with HCl. The volume was made up to 100 ml and stored at 4°C.

Elution buffer [50 mM Tris-HCl, 5 mM $CaCl_2$, 0.05% (v/v) Brij 35, 0.02% (w/v) NaN_3, and either 180 mM, 250 mM or 2 M NaCl, pH 7.4]. Prepared as above, but including 1.051 g, 1.461 g or 11.69 g NaCl/100 ml before pH adjustment.

All SDS-PAGE and western blotting reagents were prepared as described in Sections 2.4 and 2.8, respectively.

4.1.1.2 Procedure

Antibody characterisation by electrophoresis and western blotting. PMNLs were isolated as described (Section 2.7.2) and ~$1x10^7$ cells/ml were resuspended in PBS containing 1 M NaCl and 10% (v/v) DMSO (Hibbs *et al.*, 1985) and snap frozen in liquid nitrogen. When required, cells were thawed in the presence of 1 mM EDTA, 2 mM L-methionine, 2 mM PMSF (or AEBSF) and 1% (w/v) NaN_3, centrifuged (10000 x g, 20 min, 4°C) to remove insoluble debris and the supernatant aspirated. Homogenates were separated on a 10% reducing Tris-Tricine SDS-PAGE gel (~80 µg/lane) (Section 2.4.2) and blotted onto nitrocellulose (Section 2.8.1.2).

PMNL homogenate reduction and carboxymethylation. PMNLs were isolated as described above and the supernatants from homogenised PMNLs (300 µl) were lyophilised in a 1.5 ml Eppendorf microfuge tube. The lyophilised protein was weighed (6.8 mg) and dissolved in denaturation buffer (340 µl) to make a 20 mg/ml solution. The solution was placed in a water bath (30 min, 80°C) to allow protein denaturation and DTT (71.4 µmoles/6.8 mg protein) was added to reduce protein disulfide bonds (Cleland, 1964). The mixture was incubated (30 min, 80°C) before iodoacetic acid was added (143 µmoles). The solution was titrated to pH 8.0 with 25% (v/v) ammonia (Geisow and Aitken, 1989). Carboxymethylation was allowed to continue in the dark (25 min, RT) and the solution was dialysed against dd.H_2O (12 h, 4°C) before lyophilisation. The lyophilised, carboxymethylated proteins were dissolved in reducing treatment buffer (100 µl), boiled (5 min), separated on a 10% reducing Tris-tricine SDS-PAGE

gel (20 µl/lane) and blotted onto nitrocellulose. To ensure that the rabbit anti-TIMP-1 antibody was specific, blots were also probed with a commercial monoclonal anti-TIMP-1 antibody (17.5 µg/ml) (Calbiochem, clone produced by Fuji Chemicals, Japan) and detected with alkaline phosphatase-conjugated goat anti-mouse IgG (1/4000).

Heat treatment and affinity chromatography. A heparin-agarose chromatography matrix (10 ml) was packed into a glass chromatography column (ϕ = 1.5 cm; h = 5.66 cm), equilibrated with 1 column volume of elution buffer and washed with 2 column volumes of wash buffer.

PMNLs were isolated from 100 ml whole blood (Section 2.7.2), resuspended in wash buffer (~$1x10^7$ cells in 1 ml) and snap frozen in liquid nitrogen. When required, the cells were thawed briefly and frozen again in liquid nitrogen. This was repeated twice more and the final thawed homogenate was added to pre-heated wash buffer (45 ml, 60 °C) in a sterile 50 ml centrifuge tube. The tube was placed in a boiling water bath (20 min) during which the temperature of the buffer increased to 85°C. After this time, the tube was removed from the water bath and placed in crushed ice until the temperature had dropped to 4°C (30 min-1 h). The tube was centrifuged (1000 x g, 10 min, RT) to remove aggregated proteins and the supernatant was loaded onto the heparin-agarose column at a flow rate of 20 ml/h (5.66 cm/h). Once the unbound material had eluted, the column was washed with 2 column volumes of wash buffer and step eluted with elution buffer containing 180 mM, 250 mM and 2 M NaCl (2 column volumes each). The eluted fractions were concentrated by dialysis against PEG 20 kDa and precipitated with acetone (Section 2.3.1). The pellets (6-8 µg) were resuspended in reducing treatment buffer (30 µl), boiled (5 min), separated on a reducing 10% Tris-tricine SDS-PAGE gel and blotted onto nitrocellulose. The membrane was probed with rabbit anti-TIMP-1 IgG (20 µg/ml), followed by HRPO-conjugated sheep anti-rabbit IgG (1/5000) and detected by ECL (Section 2.8.2.2).

4.1.1.3 Results and Discussion

Preliminary results on routinely homogenized TIMP-1 samples revealed that the rabbit anti-TIMP-1 IgG antibody (to be used in subsequent labeling studies) detected a single high M_r band at 66 kDa (Figure 4.1 A). This M_r is much higher than that expected for the TIMP-1 monomer (28-30 kDa) (Denhardt *et al.*, 1993; Murphy and Willenbrock, 1995; Gomez *et al.*, 1997). The possibility that the 66 kDa TIMP-1 form arose due to covalent cross-linking of TIMP-1 (to another TIMP-1 molecule or randomly to any PMNL protein) by ROS, released from the PMNLs during homogenisation, (Stricklin and Hoidal, 1992) was considered. A predominant

PMNL ROS species capable of protein cross-linking is HOCl, produced by the activity of MPO on H_2O_2 (Weiss, 1989; Anderson *et al.*, 1999). It is, therefore, not surprising that the antioxidants DMSO and L-methionine, included during preparation of the homogenate, also apparently did not prevent the formation of the high M_r TIMP-1 form. Therefore, it was hypothesised that the 66 kDa form of TIMP-1 is not an oxidative artefact, but may represent a TIMP-1 homodimer (or heterodimer with another PMNL protein) that is exceptionally resistant to reduction and heat. TIMP-1 has been reported to be exceptionally resistant to reduction (Stricklin and Welgus, 1983), and therefore, in an attempt to improve TIMP-1 denaturation, PMNL homogenates were reduced and carboxymethylated in 6 M guanidine-HCl to promote protein denaturation prior to reducing SDS-PAGE and western blotting. These treatments also did not result in a M_r reduction to the expected 28-30 kDa of monomeric TIMP-1 (Figure 4.1 B). The commercial monoclonal anti-TIMP-1 antibody used also only detected a single band at 66 kDa (Figure 4.1 C), thereby supporting the presence and possible identity of the high M_r form of TIMP-1, previously revealed by the polyclonal antibodies (obtained from the University of Bielefeld), and the TIMP-1 content of the 66 kDa band.

A final attempt to reduce the TIMP-1 M_r by a combination of heat and dilution following by affinity chromatography (Drouin *et al.*, 1988) proved successful and apparently yielded only monomeric TIMP-1 as western blotting and immunolabelling revealed only one band at ~28-30 kDa (Figure 4.1 D). No TIMP-1 was detected in the unbound fraction or the 180 mM NaCl fraction (results not shown). The 66 kDa form of TIMP-1 in PMNLs, therefore, appears to be non-covalent as it can be disrupted under specific conditions. Whether the 66 kDa form exists *in vivo* or if it represents artefactual dimerisation caused by homogenisation and/or release of PMNL granule components is not known, however.

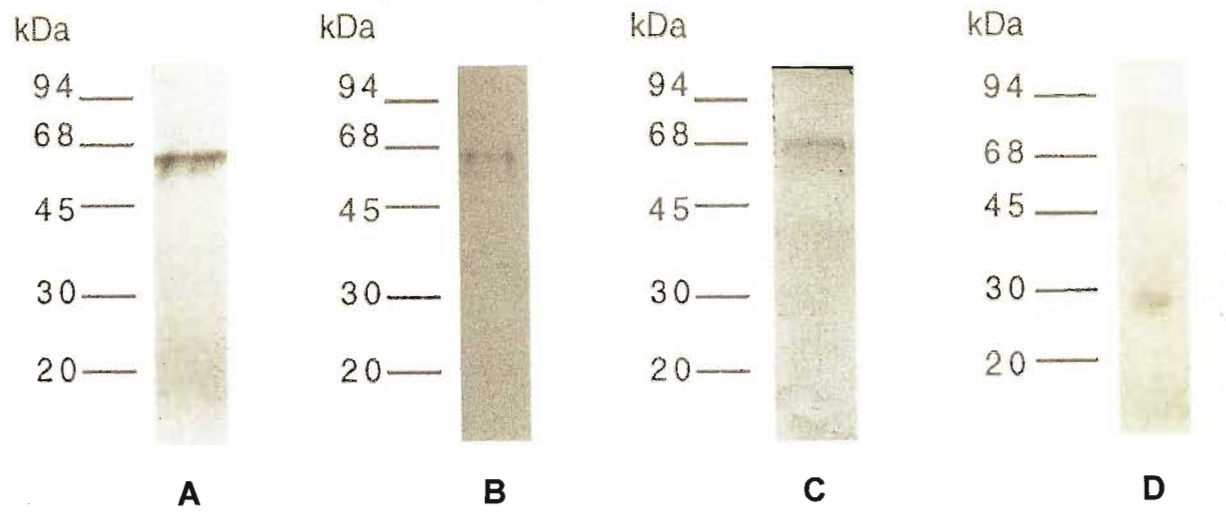

Figure 4.1 **Western blots of PMNL homogenates probed with antibodies against TIMP-1.** PMNL homogenates (~80 μg/lane) were separated on reducing 10% Tris-tricine SDS-PAGE gels, blotted onto nitrocellulose and probed with rabbit anti-TIMP-1 IgG (20 μg/ml) (A, B, D) or monoclonal anti-TIMP-1 IgG (17.5 μg/ml) (C). A), PMNL homogenate treated with oxidant scavengers and azide prior to electrophoresis. B), PMNL homogenate reduced, carboxymethylated and denatured in 6 M guanidine-HCl prior to electrophoresis. C), PMNL prepared as for (B). D), PMNL homogenate, diluted and boiled prior to affinity chromatography on heparin-agarose. The eluted fraction was concentrated by acetone precipitation before SDS-PAGE. Antibody binding was detected with either alkaline phosphatase-conjugated goat anti-rabbit IgG (1/5000) (A, B), HPRO-conjugated sheep anti-rabbit IgG (1/5000) (D) or alkaline phosphatase-conjugated goat anti-mouse IgG (1/4000) (C). Blots were developed with BCIP/NBT (A, B, C) or ECL (D).

The literature available on TIMP-1 reveals very little information regarding high M_r forms as it is generally accepted that TIMP-1 occurs solely as a monomer. High M_r TIMP-1 "contaminants" have, however, been reported in a number of purification procedures. These have, however, been dismissed as artefacts and were not pursued further. A 66 kDa form has previously been identified during TIMP-1 purification from mouse bone calvaria (Nagayama *et al.*, 1984) and polymeric forms of TIMP-1, resistant to reduction, have been identified by western blotting in sputum samples (Sorsa *et al.*, 1994). Additionally, brief mention has been made of the tendency of pure TIMP-1 to "auto-polymerise" into complexes upon storage (Cawston *et al.*, 1986a; 1986b). These observations, however, allow no further speculation as to the biological significance of these polymers or the mechanism(s) by which they are formed.

A brief investigation by Stricklin and Hoidal, (1992) into the effects of ROS, secreted by PMNLs, on TIMP-1 provided evidence that low concentrations of HOCl (<1 mM) cause TIMP-1 aggregation, whereas higher concentrations have been reported to completely destroy TIMP-1 function (Shabani *et al.*, 1998). Reports on analysis of TIMP-1 isolates from tissue extracts by western blotting, reveal the possible presence of high M_r TIMP-1 forms (i.e. possible polymeric forms) ranging between 66 and 120 kDa (Mercer *et al.*, 1985; Cawston *et al.*, 1990; Fujimoto *et al.*, 1994; Salo *et al.*, 1994; Uitto *et al.*, 1994). These forms are not mentioned in TIMP reviews (Denhardt *et al.*, 1993; Murphy and Willenbrock, 1995; Gomez *et al.*, 1997).

In this study, dissociation of the 'complex' may have occurred due to the effect of dilution but is more likely to have occurred due to the preferential binding of the TIMP-1 monomer to the highly negatively charged heparin-agarose chromatography groups. TIMP-1 has been previously described as possessing a fairly unique five member β-barrel structure and two loop regions, which are responsible for oligosaccharide/oligonucleotide-binding ability (Murzin, 1993; Gomez *et al.*, 1997). Formation of the high M_r TIMP-1 may, therefore, be a result of such activity, i.e. it may be due to intermolecular binding to N-linked carbohydrate residues present on the TIMP-1 monomers (as TIMP-1 is glycosylated), or may be due to the binding of two TIMP-1 monomers to negatively charged oligonucleotides/oligosaccharides (e.g. DNA, GAGs) released form the PMNL during homogenisation. In this study, the 66 kDa immunoreactive band initially obtained in western blots was tentatively identified as TIMP-1 using two different sources of antibody, and confirmed after the high M_r form was reduced in M_r to that of the monomer. Since the high M_r TIMP-1 form does not appear to be a covalent association, it may either represent a homogenisation artefact or the true *in vivo* form of TIMP-1. Since such high Mr forms of TIMP-1 may occur and have relevance *in vivo*, it was considered important to determine whether the high M_r TIMP-1 form can both *bind* and *inhibit* MMPs. To this end, a western ligand blot was devised to investigate the proMMP-9 binding capacity of the 66 kDa TIMP-1 form and a UV fluorescent reverse zymogram was designed to determine whether high M_r TIMP-1 retains MMP inhibitory function. Though it was reasonably certain by this stage that the antibodies to be used in the subsequent labeling were targeting TIMP-1 and were specific, such studies would also serve to verify the presence of TIMP-1 in a non-immunological fashion.

4.2 Strategies employed to elucidate the nature and functionality of the 66 kDa TIMP-1 species

To determine if high M_r TIMP-1 retains the ability to bind MMP, a western ligand blot was designed whereby PMNL homogenates are reduced, separated by reducing SDS-PAGE and blotted onto nitrocellulose (i.e. the 'western blot'). This would serve to both immobilise TIMP-1 and allow separation of TIMP-1 from other homogenate proteins. After immobilisation onto nitrocellulose, the membrane may be incubated with proMMP-9 (i.e. the 'ligand') as TIMP-1 binds specifically to it via the proMMP-9 C-terminal domain (Murphy and Willenbrock, 1995). The formation of a TIMP-1/proMMP-9 complex may subsequently be detected by probing with an antibody against proMMP-9.

To determine whether the high M_r form of TIMP-1 could inhibit active MMPs, the use of a reverse zymography system was considered necessary. Here, the PMNL homogenate proteins are separated by electrophoresis though an SDS-PAGE gel containing both an MMP source and an MMP substrate (e.g. gelatin) (Murphy and Willenbrock, 1995). Upon completion of electrophoresis, the MMP (activated by SDS present in the gel and running buffers) digests the gelatin substrate throughout the gel, except in areas that contain active TIMP-1 (Oliver *et al.*, 1997). As MMP inhibition would result in a band of undigested gelatin in the gel, the inhibitory capability of the high M_r TIMP-1 form could easily be established.

Three of the main problems associated with reverse zymography, however, are associated with the optimisation of: 1), the amount of proteinase used and 2), the length of time for which digestion is allowed to proceed and 3), the inability to continuously monitor gelatin degradation. If insufficient gelatin is degraded, no bands of inhibition will be visible in the gel. Conversely, if excess digestion occurs, the concentration of proteinases in the gel will exceed that of the inhibitor, resulting in complete gelatin digestion and no visible bands of inhibition (Oliver *et al.*, 1997). The ability to continuously monitor the progress of gelatin digestion would solve both these problems. Therefore, a novel reverse zymogram, using UV fluorescent gelatin, was designed to allow continuous monitoring of digestion. Due to the fact that proMMP-9 would be required for the western ligand blot and that it is a popular proteinase source in both regular and reverse zymograms, it was considered ideal for the analysis of high M_r TIMP-1 inhibitory function.

Since pure proMMP-9 was not available, the method of proMMP-9 isolation from sputum (Davis, 1991) was adopted and modified using a TPP fractionation procedure (Dennison and Lovrien, 1997). This procedure allowed the selective fractionation of proMMP-9 from active MMP-9 species in sputum and provided a low cost, high yield source of proMMP-9 for use in western ligand blotting and reverse zymography.

4.2.1 Isolation and characterisation of proMMP-9 using TPP, gelatin zymography and western blotting

TPP involves the precipitation of proteins by exploiting their differential requirements for a minimal level of hydration in order to achieve solubility and uses partitioning between an organic solvent (t-BuOH) and an aqueous phase containing increasing concentrations of a dehydrating, highly soluble polyvalent salt [$(NH_4)_2SO_4$]. Initially, protein solutions are resuspended in buffer and mixed with t-BuOH to a final concentration of 30% (v/v). Tertiary BuOH is miscible in aqueous solutions of low ionic strength, but partitions to form an organic phase upon salt addition and, initially, proteins are dissolved in both the t-BuOH and aqueous phase. Addition of $(NH_4)_2SO_4$ causes a decrease in the effective concentration of hydration shells around the proteins and t-BuOH since the sulfate ion tetrahedron (SO_4^{2-}) requires ~13 water molecules for complete charge sequestration (versus ~6 for monovalent anions such as F^-, Cl^-) (Dennison and Lovrien, 1997). The polyvalent nature of $(NH_4)_2SO_4$ causes a sharp increase in ionic strength and this results in protein dehydration and, initially, an accompanying increase in t-BuOH-protein association. The presence of increasing levels of t-BuOH induces an increased alpha-helical structure in the protein as the level of $(NH_4)_2SO_4$ increases. Dehydration occurs and proteins are brought to their solubility limit (Pike and Dennison, 1989). At this point, the low dielectric constant of t-BuOH allows protein molecules to associate and finally precipitate out of solution. The butanolated, precipitated protein has a density greater than t-BuOH but less than the aqueous phase and, therefore, forms an interface that can be easily harvested after low speed centrifugation. The advantages of TPP over conventional salting out methods include the removal of lipid and other hydrophobic contaminants (e.g. pigments), the selective destruction of some proteins [mainly oligomeric proteins such as haemoglobin (Pike and Dennison, 1989; Dennison and Lovrien, 1997)] and the production of an essentially dehydrated, salt-free precipitate that does not require dialysis or desalting by passage through Sephadex G-25 prior to use in subsequent analytical steps or further purification. This method was successfully used to fractionate sputum proteins that were subsequently analysed by gelatin zymography and silver staining to assess which precipitate contained the highest concentration of crude proMMP-9.

4.2.1.1 Reagents

Electrophoresis, gelatinase zymography and western blotting reagents were prepared as described in Sections 2.4.2.1, 2.6.1 and 2.8, respectively.

4.2.1.2 Procedure

Warmed (≥ 24°C but < 30°C) t-BuOH was added to a protein solution to a final concentration to 30% (v/v) using the ratio:

T = X/0.7 where T = total volume (protein + t-BuOH)

X = original volume of protein solution

Hence, the volume of t-BuOH to add to make the final volume 30% (v/v) with respect to t-BuOH is T-X.

After a 12 h fast, sputum (20 ml) was collected from a healthy human donor into a sterile 50 ml centrifuge tube and clarified by centrifugation (10000 x g, 10 min, 4°C). Tertiary BuOH (8.571 ml) was added to the clarified sputum to produce a final t-BuOH concentration of 30% (v/v). Crushed $(NH_4)_2SO_4$ (3.68 g) was added slowly to the mixture to change the salt concentration from 0-20% (w/v). After complete dissolution, the mixture was centrifuged (6000 x g, 10 min, RT) and the solution decanted. The precipitated protein layer remained on the side of the tube and was kept at 4°C. The rest of the decanted solution was placed in a sterile 50 ml centrifuge tube and crushed $(NH_4)_2SO_4$ was added to 40% $(NH_4)_2SO_4$ and the process repeated to obtain precipitates for the concentrations: 20-40, 40-60 and 60-80% (w/v) $(NH_4)_2SO_4$. When required, the pellets were dissolved in MMP buffer. The gelatinolytic activities of each TPP fraction (~15 µg/lane) was determined by zymography on a non-reducing 10% Tris-tricine SDS-PAGE gel containing 1 mg/ml gelatin (Section 2.6.2). The fractions were also separated on reducing SDS-PAGE gels (Section 2.4.2.2) and silver stained (Section 2.5.2.2). The fraction containing the purest form of proMMP-9 (judged by zymography and silver staining) was also blotted onto nitrocellulose (Section 2.8) and probed with anti-proMMP-9 IgG (4 µg/ml) to verify that the fraction contains the precursor form of MMP-9.

4.2.1.3 Results and Discussion

TPP provided a quick, convenient method of fractionating proMMP-9 (Figure 4.2 A and B). The 60-80% TPP fraction showing a single gelatinolytic band at a M_r similar to proMMP-9

(~92 kDa) (Figure 4.2 A; lane 5) with the fewest other contaminating proteins (Figure 4.2 B; lane 5). This fraction was successfully used to confirm all previous anti-MMP-9 antibody specificities. Western blot analysis of this fraction using the anti-MMP-9 antibody confirmed the presence of a 92 kDa proMMP-9 (Figure 4.2 C), while gelatin zymography of 0-20, 20-40, 40-60% fractions showed the presence of various lower M_r active forms of MMP-9 (Figure 4.2 A; lanes 2-4) previously observed in sputum (Davis, 1991).

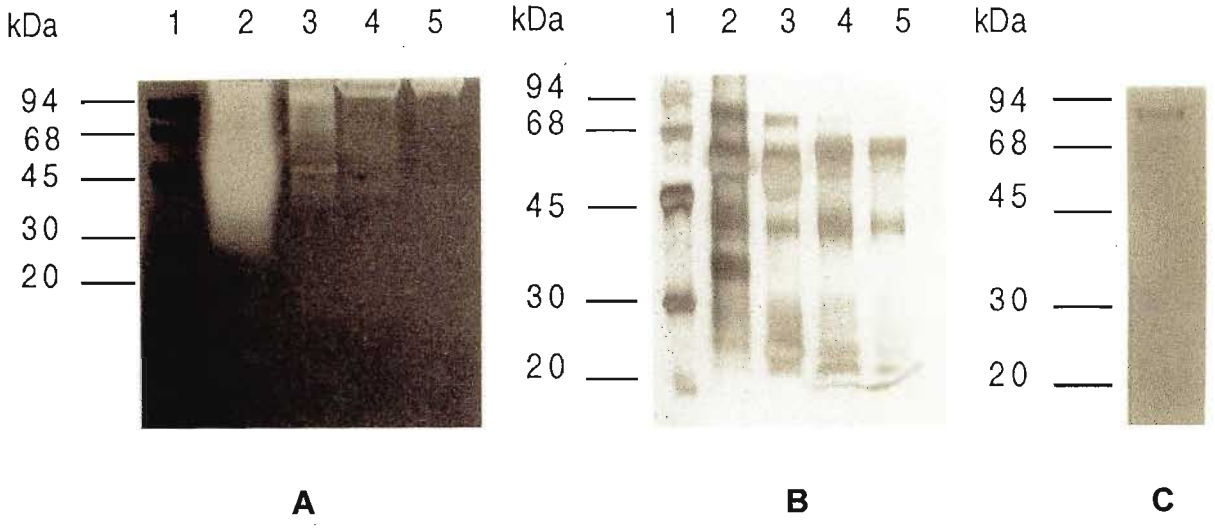

Figure 4.2 **Gelatin zymography, silver staining and western blotting analysis of TPP sputum fractions.**

Aliquots of TPP fractionated sputum (15 µg/lane) were separated under non-reducing conditions on a 10% Tris-tricine SDS-PAGE gel containing 1 mg/ml gelatin (A) and under reducing conditions without gelatin (B). Lane 1, M_r markers; Lane 2, 0-20% $(NH_4)_2SO_4$; Lane 3, 20-40% $(NH_4)_2SO_4$; Lane 4, 40-60% $(NH_4)_2SO_4$; Lane 5, 60-80% $(NH_4)_2SO_4$. Gels were stained with Coomassie Blue (A) or silver (B). C), A TPP fraction (60-80%) (~15 µg) was separated by reducing 10% Tris-tricine SDS-PAGE and blotted. The membrane was probed with rabbit anti-MMP-9 IgG (4 µg/ml) and detected by alkaline phosphatase-conjugated goat anti-rabbit IgG (1/5000) and BCIP/NBT.

4.2.2 Western ligand blot with TPP-enriched sputum proMMP-9

Western ligand blotting or western blot overlaying involves incubation of a blotted protein (e.g. a receptor, nucleotide binding protein etc.) with a solution containing the appropriate ligand, followed by detection of the bound ligand. Detection may either be direct (e.g. use of a radiolabelled ligand) or indirect (e.g. probing the blot with an antibody against the ligand) (De Maio, 1994). The ligand blot is quicker than a conventional gel overlay where both species

(e.g. receptor and ligand) are retained in a matrix and allowed to slowly interact by diffusion. One of the limitations of the western ligand blot is that it is unsuitable for investigating protein interactions that are SDS-stable as protein dissociation will not occur and ligand binding sites may remain occupied after electrophoresis (De Maio, 1994). In addition, western ligand blots are reliant on successful renaturation of binding sites after electrophoresis and blotting. Previous experiments by Osthues *et al.* (1992) using pure TIMP-1 showed that TIMP-1 retains the ability to bind MMP even after it has been subjected to non-reducing SDS-PAGE and western blotting onto nitrocellulose. However, as *some* proMMP-9/TIMP-1 complexes are resistant to dissociation by SDS (Sorsa *et al.*, 1994), reducing SDS-PAGE had to be used in the study on crude PMNL homogenates (as possible endogenous proMMP-9/TIMP-1 complexes may not be fully dissociated by non-reducing conditions). The reduction of protein disulfide bridges that is necessary for efficient protein separation during SDS-PAGE, can theoretically be reversed by simple reoxidation by dissolved atmospheric oxygen present in the incubation buffers or with oxidised glutathione (De Maio, 1994). During the designing of the western ligand blot for the investigation of the 66 kDa high M_r TIMP-1 'complex', it was appreciated that TIMP-1 contains 6 disulfide bridges that might all be broken during reduction and electrophoresis. For this reason, correct disulfide bond reformation may be a problem during the renaturation of TIMP-1 after blotting. Although the probability that all twelve cysteine residues would reform the *correct* 6 disulfide bridges was considered low, the western ligand blot was nevertheless attempted and compared with blots of the reduced and boiled PMNL homogenates that were either probed directly with anti-TIMP-1 (as described in Section 4.1.1), or first incubated with the crude proMMP-9-containing TPP fractions prepared from sputum and probed with anti-proMMP-9 IgG, i.e. treated as a western ligand blot.

4.2.2.1 Procedure

PMNL homogenates (~150 µg/lane) were separated on a reducing 10% Tris-tricine SDS-PAGE gel and blotted. The blots were air-dried (2 h, RT) and then stored in a desiccator at 4°C. TPP was performed on sputum (20 ml) and the precipitated 60-80% fraction (containing proMMP-9) was kept at 4°C. The nitrocellulose membranes with blotted PMNL homogenates were blocked (Section 2.8.1.2) and the 60-80% TPP fraction containing proMMP-9 was dissolved in 5% (w/v) non-fat milk-TBS (2 mg in 10 ml) and added to the membrane (2 h, RT). The membrane was probed with rabbit anti-MMP-9 IgG (10 µg/ml, 1 ml, 2 h, RT) and detected with alkaline phosphatase-conjugated goat-anti rabbit IgG (1/5000) and BCIP/NBT (Section 2.8.2).

4.2.2.2 Results and Discussion

Although reducing SDS-PAGE was used in this study [as opposed to non-reducing SDS-PAGE and western blotting by Osthues *et al.* (1992)], it was anticipated that the disulfide bridges of TIMP-1 might reform after blotting and TIMP-1 would regain its native tertiary structure and allow proMMP-9 binding via the C-terminal domain of TIMP-1.

The above hypothesis proved true. After treatment of the blot of crude PMNL homogenate with the partially purified sputum proMMP-9 TPP fraction, four bands of approximately 92 kDa, 66 kDa, 30 kDa and 20 kDa (Figure 4.3) were visible, instead of the single 92 kDa proMMP-9 band observed when probing the untreated homogenate (Figure 3.1 E). From available M_r data in the literature, the 92 kDa band was deduced to represent the proMMP-9 already present in the PMNL homogenate, while the 66 kDa band was hypothesised to represent the TIMP-1/proMMP-9 complex formed by the binding of the blotted 66 kDa high M_r TIMP-1 form to the overlaid proMMP-9. The 30 kDa band which bound the overlaid proMMP-9 was hypothesised to correspond to low amounts of monomeric TIMP-1, possibly visualised by this technique (compared to regular western blotting) due to a signal amplification effect achieved after proMMP-9 binding to TIMP-1. Lastly, the 20 kDa band possibly represents a proMMP-9/NGAL heterodimer (formed between the overlaid proMMP-9 and NGAL present in the blotted PMNL homogenate) similar to that which usually exists as a disulfide-linked form in PMNL specific granules (Kjeldsen *et al.*, 1993b; Xu *et al.*, 1994).

The results obtained with the western ligand blot indicated that the 66 kDa form of TIMP-1 is the major species present in PMNL homogenates, but that there was also a low concentration of monomeric TIMP-1. The monomeric TIMP-1 form was possibly detected via binding of proMMP-9 (and this, in turn, bound to rabbit anti-proMMP-9 IgG) whereas it was largely undetected with the anti-TIMP-1 antibodies. This may be explained by differences in avidity of the mouse/rabbit anti-TIMP-1 IgG and rabbit anti-proMMP-9 IgG for the two blotted antigens, the lower recognition of blotted proteins possibly resulting from some distortion of epitopes due to blotting of TIMP-1. The use of the western ligand blot may have allowed detection of low levels of TIMP-1 via binding of proMMP-9 (which, in turn, binds to anti-proMMP-9 IgG) as it relies on the recognition and labelling of a non-blotted protein, i.e. proMMP-9. The use of the western ligand blot may, therefore, offer a relatively simple system for potentially improving the detection limits of blotted antigens where recognition by antibodies is weak.

The initial discovery of TIMP-1 in PMNLs occurred when a non-covalent TIMP-1/proMMP-9 heterodimeric complex was identified during MMP-9 isolation procedures in which approximately 10% of the isolated proMMP-9 was found complexed with TIMP-1 (Triebel *et al.*, 1995). Dissociation of the complex was shown to produce monomeric TIMP-1, free from proMMP-9. The monomeric TIMP-1 identified on the western ligand blot of PMNL homogenates in this investigation may exist *in vivo* or may have similarly originated by partial dissociation of a heterodimeric complex of proMMP-9 and TIMP-1 during reduction and boiling.

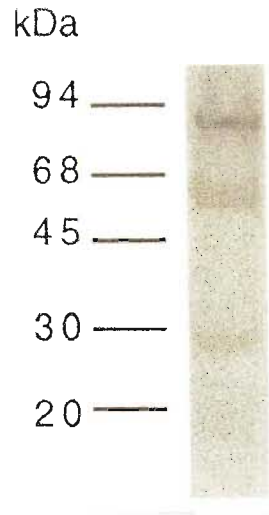

Figure 4.3 **Western ligand blot of PMNL homogenates probed with TPP-fractionated sputum proMMP-9 and rabbit anti-proMMP-9 IgG.**

PMNL homogenate (~150 µg) was separated on a reducing 10% Tris-tricine SDS-PAGE gel and blotted. The membrane was incubated with a 60-80% $(NH_4)_2SO_4$ proMMP-9 TPP fraction (2 mg/10 ml), probed with rabbit anti-proMMP-9 IgG (10 µg/ml) and detected with alkaline phosphatase-conjugated goat anti-rabbit IgG (1/5000) and BCIP/NBT.

Our findings that the high M_r form of TIMP-1 is capable of binding proMMP-9 after blotting, even under reducing conditions, suggests that at least the C-terminal domain of TIMP-1 renatures after blotting since only the C-terminal domain of TIMP-1 can interact with the C-terminal domain of proMMP-9 (Murphy and Willenbrock, 1995). The N-terminal domains of TIMP-1 and proMMP-9 cannot interact due to the occlusion of the MMP-9 active site by the pro-piece (Gomez *et al.*, 1997, Huang *et al.*, 1997). Hence, the 66 kDa form of TIMP-1 retains some MMP binding activity.

4.2.3 A novel UV fluorescent reverse zymographic technique for the investigation of the MMP inhibitory activity of high M_r TIMP-1 forms

The interaction of TIMP-1 with active MMPs occurs at both the N- and C-terminal domain regions of the MMP molecule to bring about full inhibition (Murphy and Willenbrock, 1995; Huang *et al.*, 1997). Interaction of the active sites in the MMP N-terminal domains with the N-terminal region of TIMP-1, however, only occurs when the pro-piece of an MMP zymogen has been removed (e.g. by proteolysis or, in the case of zymography, distorted by SDS) and the active site is exposed (Gomez *et al.*, 1997). This subsequently gives rise to enzyme inhibition.

Although the western ligand blot showed that the 66 kDa TIMP form binds proMMP-9, such a system cannot supply any information on inhibitory activity, mediated via association of the N-terminal region, of this high M_r form of TIMP-1. This question required the use of a TIMP activity (or functional) assay. A common assay for TIMPs involves the incubation of a putative TIMP-containing sample with a known amount of pure, active MMP (any active MMP since all TIMPs inhibit these with equal efficiencies, though MMP-3/stromelysin-1 is preferred) (Murphy and Willenbrock, 1995). This assay subsequently monitors the decrease in MMP activity against a particular substrate (usually a fluorescent peptide derivative) (Knight *et al.*, 1992). The presence of endogenous MMPs in the PMNL homogenate would not pose a problem in such an assay as these can be selectively denatured by heat (100°C) or low pH (pH 2-3) - conditions that do not denature TIMPs (Lefebvre and Vaes, 1989; 1992; Murphy, 1992; Murphy and Willenbrock, 1995). In this study, the problem with this assay lay in the cost of pure MMP-3 for the activity assay. In addition, the activity assay does not provide information on the M_r of the TIMP species inhibiting the active MMP. Another, although less popular, technique for assessing TIMP-1 activity is reverse zymography. This technique, however, does not require a very pure source of MMP (hence, a crude preparation of proMMP-9 from sputum was used in this study) and allows M_r estimation of inhibitor species (Murphy and Willenbrock, 1995).

Reverse zymography allows detection of proteinase inhibitors in samples that have been separated by SDS-PAGE. The running gel contains a homogeneously dispersed proteinase substrate (e.g. gelatin, plasmin) and its corresponding proteinase. The gel is placed in an appropriate buffer and the proteinase allowed to partially digest the incorporated substrate. Inhibitor molecules in the electrophoresed sample prevent substrate degradation at the position

in the gel where they have migrated during the electrophoretic run. The result, after staining the gel, is a light background of partially digested substrate and darkly stained bands where the inhibitors are present (Murphy and Willenbrock, 1995; Oliver *et al.*, 1997).

Reverse zymography requires a proteinase source in order digest the substrate in the gel and has been used to successfully identify and determine the biological activity of purified TIMPs using pure gelatinases (proMMP-2 and proMMP-9) incorporated into the gel (Oliver *et al.*, 1997). Fortunately, the proteinase does not necessarily need to be pure and can be obtained from crude sources such as PMA-stimulated fibroblast culture medium (Murphy and Willenbrock, 1995). In such a system, any contaminant proteins in the sample for analysis may, however, result in stained protein bands which resemble bands of proteolytic inhibition, as Coomassie Blue staining cannot distinguish sample proteins from undigested substrate. This may give rise to results which incorrectly indicate the presence of inhibitors. Furthermore, dilution of the crude preparation may not alleviate the problem as it may simultaneously decrease the concentration of TIMP in the sample to below the detection limits of the reverse zymography system.

These facts prompted the designing of a novel reverse zymography method that would allow selective visualisation of undigested gelatin, while proteins present in the applied sample or those proteinases dispersed in the gel would not be visible. The reported inconsistency of fibroblast-derived gelatinase-containing media (Oliver *et al.*, 1997) and lack of available pure gelatinase also prompted an investigation into an improved MMP source that would provide greater yield, ease of purification and lowered concentrations of contaminating proteinases. The sputum proMMP-9, prepared using TPP as previously described (Section 4.2.1), was used as the required proteinase source.

A method was sought to visualise and distinguish undigested gelatin from proteins present in crude samples, as this is not possible if the gel is stained with Coomassie Blue. Modification of gelatin with fluorescein isothiocyanate (FITC), tetramethylrhodamine isothiocyanate (TRITC) or 4-phenylspiro[furan-2(3H),1'-phthalan]-3,3'-dione (fluorescamine) was considered as such labels, once the substrate is cleaved, would allow detection of only the undigested gelatin fragments (indicative of TIMP presence) without detecting other non-TIMP protein species present in crude samples. It was thought that this detection system would provide a selective alternative to the regular Coomassie Blue stain that stains all proteins. Two major drawbacks with dyes such as FITC and TRITC is the tendency of these dyes to rapidly photobleach and the

fact that no apparatus was available for irradiation of an entire gel, at the correct wavelength, to incite fluorescence.

A furanone derivative, 2-methoxy-2,4-diphenyl-3(2*H*)-furanone (MDPF), used as a fluorogenic collagenase fibril assay by O'Grady *et al.* (1984) showed great promise for such a purpose. Unlike other fluorogenic compounds, MDPF fluorescence is reported to be photostable and pH stable (pH 2-12). In addition, the coupling reaction to proteins is simple and only requires dialysis to remove unlinked MDPF from the target substrate protein. MDPF reacts with primary amines to form highly UV fluorescent, stable fluorophores. Free, uncoupled MDPF is hydrolysed to a non-fluorescent hydroxyfuranone derivative. Detection and recording of UV fluorescence of inhibition bands is theoretically possible since the wavelength emitted from a UV transilluminator (~310 nm used for visualisation of ethidium bromide stained DNA agarose gels) is sufficiently close to the λ_{ex} of MDPF (385 nm) (O'Grady *et al.*, 1984). Therefore, a new UV fluorescent reverse zymogram technique was designed and optimised using such a fluorophore. This was used to discern whether the 66 kDa high M_r TIMP-1 form in crude PMNL homogenates is capable of inhibiting active MMPs. In addition, this technique was applied to plasma samples to investigate the presence of various TIMP species and ensure that the new technique will find application in the identification of TIMPs in other crude sample sources.

4.2.3.1 Reagents

Coupling buffer (50 mM Na-borate, 100 mM NaCl, pH 9.0). Boric acid (0.309 g) and NaCl (0.584 g) were dissolved in dd.H_2O (~80 ml) and titrated to pH 9.0 with NaOH. The volume was made up to 100 ml in a volumetric flask and the solution was stored at 4°C.

Dialysis buffer [0.2% (v/v) acetic acid, pH 4.0]. Acetic acid (10 ml) was added to dd.H_2O (~4.9 *l*) and titrated to pH 4.0 with NaOH. The volume was made up to 5 *l* in a volumetric flask and the solution was stored at 4°C.

Anhydrous acetone. Sodium sulfate was added to acetone in an Erlenmeyer flask with gentle shaking. Water-bound sodium sulfate remained at the bottom of the flask, firmly stuck to the base.

TPP fractionated sputum (60-80% fraction). Prepared from 20 ml sputum as described in Section 4.2.1.

Gelatinase zymography buffer [50 mM Tris-HCl, 200 mM NaCl, 5 mM $CaCl_2$, 0.02% (v/v) Brij 35, 0.02% (w/v) NaN_3, pH 7.5 at 37°C]. As described in Section 2.6.1.

Reverse zymogram fixative [12.5% (w/v) TCA in dist.H_2O]. TCA (12.5 g) was added slowly to dist.H_2O (~80 ml) and made up to 100 ml in a volumetric flask.

4.2.3.2 Procedure

All the steps were performed in the dark, as MDPF is light sensitive. Type I (300 bloom) gelatin (0.1 g) was dissolved in coupling buffer (10 ml) using a magnetic stirrer bar (1 h, 4°C). MDPF (0.005 g in 1 ml anhydrous acetone) was added dropwise (1 h, 4°C) with constant stirring. After all the MDPF had been added, the solution was centrifuged (5000 x g, 10 min, 4°C) and the pellet resuspended in dialysis buffer (10 ml) and dialysed against this solution (5 *l*, 12 h, 4°C). The resultant volume of the gelatin solution obtained after dialysis was measured and the solution was stored in 1 ml aliquots, wrapped with aluminium foil at -20°C.

PMNLs were isolated from whole blood (100 ml) (Section 2.7.2), resuspended in PBSG (1 ml) and flash frozen in liquid nitrogen. Plasma obtained during PMNL isolation was frozen undiluted in liquid nitrogen. Standard Tris-tricine 10% SDS-PAGE gels were cast (Section 2.4.2) and included MDPF-gelatin (0.0025 g in 1 ml), TPP-fractionated sputum (~0.5 g) and AEBSF (0.007 g) prior to polymerisation of the running gel. Frozen PMNL homogenates were thawed in the presence of 2 mM AEBSF and 10% (v/v) DMSO to reduce ROS released during PMNL lysis. The cells were sonicated in ice cold water (4 x 30 s) and centrifuged (1000 x g, 5 min, 4°C) and the supernatant was aspirated. Aliquots of PMNL supernatant were assayed for protein using the modified Bradford procedure (~3.48 mg/ml). Frozen plasma samples were allowed to thaw in the absence of AEBSF and DMSO (10 min, RT). PMNL homogenates (7 µg to 70 µg) or plasma samples (20 µl) were mixed with an equal volume of non-reducing treatment buffer (30 min, RT or boiled for 2 min), or half their volume of reducing treatment buffer and boiled before loading. The gels were pre-electrophoresed for 30 min and then run with the electrophoresis unit covered with aluminium foil. Upon completion of electrophoresis, the gel was washed in unbuffered 2.5% (v/v) Triton X-100 (2 x 100 ml, 1 h, RT) and placed in preheated gelatinase buffer (100 ml, 24-60 h, 37°C). Gelatin

degradation was monitored by periodically removing the gel from the buffer and irradiating it (300-310 nm) on a UV transilluminator (Fotodyne, New Berlin, USA). Bands of MMP inhibition (i.e. undigested MDPF-gelatin) fluoresced intensely against a pale background of digested gelatin fragments after a period of optimal digestion. The gel was photographed using a camera equipped with a UV filter and Polaroid type 667 film while being irradiated on the transilluminator. The gel was fixed (2 h, RT) and stored in 0.2% (v/v) acetic acid, pH 4.0 in the dark (4°C).

The reverse zymogram of the plasma samples were photographed after 36 h and then immersed in ice-cold Gershoni blotting buffer (Section 2.8.1.1) and prepared for western blotting (Section 2.8.1). The membrane was probed with rabbit anti-TIMP-1 IgG (20 μg/ml) and detected with alkaline phosphatase-conjugated goat anti-rabbit IgG (1/5000) and BCIP/NBT.

4.2.3.3 Results and Discussion

PMNL homogenates. In the novel reverse zymogram system, bands of inhibition were usually evident after 24 h, although the optimal digestion time was found to be 36 h. Bands of inhibition of between 68 kDa and 100 kDa were evident in samples that had been boiled in non-reducing buffer (Figure 4.4 A). No bands of inhibition were observed for PMNL samples that had either: 1), been boiled in reducing treatment buffer or 2), incubated in non-reducing treatment buffer and left unboiled (results not shown). The use of non-reducing treatment buffers may be necessary to maintain disulfide bridge-related structure of TIMP-1 while the requirement for SDS and boiling may be necessary to dissociate preformed proMMP-9/TIMP-1 heterodimers in PMNL homogenates which may prevent TIMP-1 binding and inhibition of the SDS-activated proMMP-9 included in the polyacrylamide gels. The proMMP-9/TIMP-1 heterodimeric complex is sensitive to both SDS and boiling (Cawston *et al.*, 1990; Murphy, 1992; Murphy and Willenbrock, 1995) and, therefore, would have been dissociated during this treatment. As TIMP-1 is resistant to boiling for up to 10 minutes (Murphy and Willenbrock, 1995), it would retain its native conformation after boiling in non-reducing treatment buffer and, hence, may survive such treatment and give rise to the positive results in the reverse zymogram. This interpretation is supported by western blotting and probing of PMNL homogenates (boiled in non-reducing treatment buffer) with rabbit anti-TIMP-1 IgG, which confirmed that the multiple high M_r bands represent TIMP-1 (Figure 4.4 B). The results presented here show that the MMP inhibitory function of high M_r TIMP-1 forms are sensitive to reduction, i.e. they require intact disulfide bridges, but also suggest that heat treatment of the homogenate (in the

presence of SDS) is required before inhibition of MMPs in the substrate gel can occur. The observed sensitivity of TIMP-1 to reduction appears to contradict the results of the western ligand blot (Section 4.2.2). However, it is necessary to bear in mind that the western ligand blot and the reverse zymogram were used to assess two different functions of TIMP-1. The western ligand blot assessed whether blotted, reoxidised TIMP-1 could *bind* proMMP-9 (via interaction of the C-terminal domains of both TIMP-1 and proMMP-9) and the reverse zymogram assessed whether high M_r TIMP-1 forms could *inhibit* MMP-9 (via interaction of the N-terminal domains of both TIMP-1 and MMP-9). Therefore, although blotted TIMP-1 used in the western ligand blot was reduced, it was subsequently exposed to atmospheric oxygen during drying and this may have allowed partial reoxidation of the reduced TIMP-1 cysteine residues in the C-terminal region to allow proMMP-9 binding. Although this blotted 66 kDa TIMP-1 form may refold sufficiently to bind proMMP-9, it may however, not retain inhibitory activity. This could have only been identified via reverse zymography. Overall, the PMNL reverse zymograms prove that high M_r TIMP-1 forms are capable of MMP inhibition. The exact structure and *in vivo* function(s) of these forms, however, remain unknown.

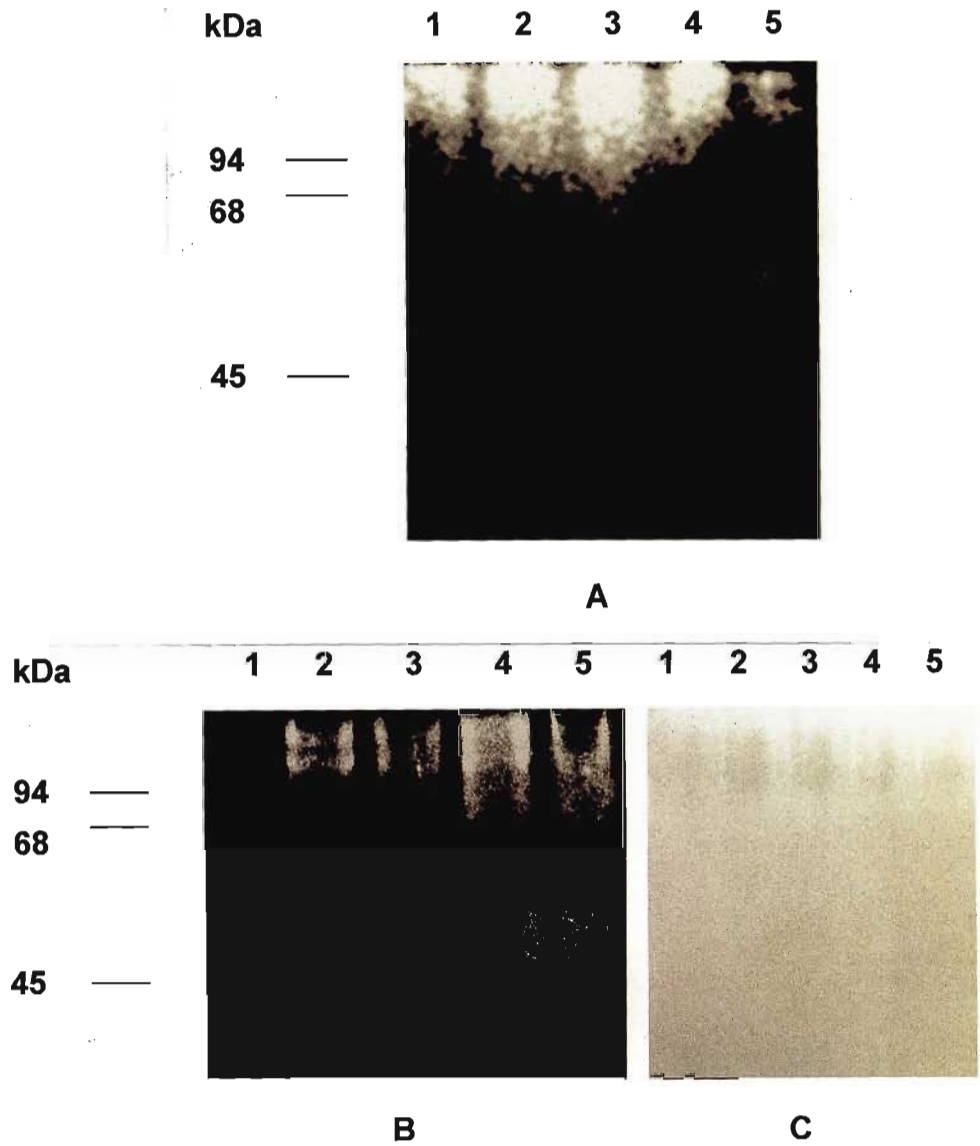

Figure 4.4 **Detection of high M_r TIMP species by UV fluorescent reverse zymography of PMNL homogenates and plasma, and confirmation by western blotting.**

MDPF-labelled gelatin (2.5 mg/gel) and TPP-fractionated sputum (60-80%) were copolymerised into the running gel of a 10% Tris-tricine SDS-PAGE gel. A), Lanes 1-5, PMNL homogenates (70, 55, 45, 35, 28 μg) were diluted in an equal volume of non-reducing treatment buffer and boiled for 2 min before electrophoresis. B), Plasma samples (20 μl) were diluted with an equal volume of non-reducing treatment buffer and either incubated at RT for 30 min before electrophoresis or boiled (1-5 min). Lane 1, RT; Lane 2, boil 1 min; Lane 3, boil 2 min; Lane 4, boil 3 min; Lane 5, boil 4 min; Lane 6, boil 5 min. The gels were irradiated at 310 nm with a UV transilluminator to visualise bands of undigested MDPF-gelatin. C), The reverse zymogram (B) was blotted after 36 h incubation and probed with rabbit anti-TIMP-1 IgG (20 μg/ml). The blot was detected with alkaline phosphatase-conjugated goat anti-rabbit IgG (1/5000) and BCIP/NBT.

Plasma samples. Analysis of the reverse zymograms of plasma samples showed two predominant bands of inhibition (Figure 4.4 C, lane 2). One was approximately 100 kDa while the other was greater than 100 kDa, although exact M_r estimations by zymography cannot be made (Hummel *et al.*, 1996). The 100 kDa high M_r form possibly represents a proMMP-9/TIMP-1 complex since it has been observed that the majority of human plasma proMMP-9 exists complexed to TIMP-1 (Fujimoto *et al.*, 1994). Alternatively, it could represent similar stable TIMP-1 'polymers', i.e. forms similar to those that have previously been identified in salivary samples (Salo *et al.*, 1994), since the bands remained after boiling plasma samples in non-reducing treatment buffer for up to 5 min; conditions known to dissociate proMMP-9/TIMP-1 complexes (Cawston *et al.*, 1990). The protein species causing the band of inhibition was confirmed as containing TIMP-1 as blotted reverse zymograms revealed a faint band after probing with rabbit antibodies against TIMP-1 (Figure 4.4 C). The faint signal obtained is possibly due to diffusion of TIMP-1 during the reverse zymogram incubation period, prior to blotting.

General methodology and technique optimisation. The major advantage of the use of MDPF in reverse zymograms is the ability to periodically monitor the progress of gelatin degradation using a UV transilluminator. This allows the optimal signal:noise ratio to be continually assessed and the optimal time of digestion to be determined. Although the UV fluorescence of MDPF-gelatin is intense to the naked eye, it is, however, difficult to capture using Polaroid film, and, therefore, digital scanning and contrast enhancement was required. Digital scanning has been used in the presentation of regular reverse zymography results (Oliver *et al.*, 1997) and is the preferred method of reverse zymogram presentation in scientific journals. The optimal time of gelatin digestion (36 h) was longer than originally anticipated. This may be due to the high fluorescence of the MDPF-gelatin and the substantial degradation of gelatin by MMP-9 required before a clear contrast between bands of inhibition and the rest of the gel could be appreciated. The most impressive feature of this reverse zymogram procedure is the exceptional photostability of MDPF to UV radiation. No appreciable decrease in fluorescence was observed when test gels (containing only MPDF-gelatin) were irradiated continually up to 30 min. This feature makes MDPF an attractive candidate for other techniques requiring stable fluorophores at low wavelengths.

After the verification of the presence of TIMP-1 using both western ligand blotting and this

reverse zymogram technique, confidence in the specificity of the anti-TIMP-1 antibody to be used in the immunolocalisation of TIMP-1 was also established and these studies were commenced.

4.3 Localisation of TIMP-1 with respect to the proMMPs and granule marker proteins using cryoimmunocytochemistry on ultrathin PMNL sections

As mentioned previously in the introduction to this chapter, no absolute assignment of any particular antigen to a single granule type may be possible due to the transient and often overlapping synthesis of granule proteins. Hence, when a protein is considered a 'marker' it should be interpreted to mean merely that the protein expression may peak in the particular granule population (Figure 4.5). This overlap of synthesis may occur due to the overlapping expression of mRNA as was demonstrated by Fouret *et al.* (1989) using *in situ* hybridisation for HNE mRNA. Colocalisation of simultaneously expressed proteins may, however, not occur if the mechanism for protein targeting was complex and relies on specific motifs or phosphomannosyl 'signatures' such as in the case with lysosomal enzymes, where mannose 6-phosphate targeting occurs (Cieutat *et al.*, 1998). Such sorting signals, however, seem to be lacking in PMNLs.

The granule localisation of TIMP-1 was unknown at the commencement of this study but could potentially provide information regarding the probable stage of development at which TIMP-1 is synthesised and the probable order of release of TIMP-1 versus other luminal granule proteins during degranulation (the order of release being approximately related to the reverse of the order of synthesis - see Table 1.2). For example, if TIMP-1 resides in the gelatinase granules, it would be released simultaneously with proMMP-9, but before proMMP-8 in the specific granule, and after secretory vesicle proteins. As TIMP-1 is responsible for the inhibition of active MMPs, knowledge of the granule localisation and regulation of TIMP-1 release may have major implications in designing strategies to control MMP-mediated PMNL invasion and inflammation.

The location of TIMP-1 with respect to the proMMPs would be equally interesting as, during the purification of PMNL MMP-9, 10% of isolated proMMP-9 is found complexed with TIMP-1 (Triebel *et al.*, 1995). This observation gives rise to the question of whether the isolated proMMP-9/TIMP-1 heterodimer is simply an artefact generated by granule destruction during purification or if it occurs *in vivo* and what its role would be. The immunolocalisation studies presented here were, therefore, designed to assign TIMP-1 to one or more of the

granules and organelles present in unstimulated PMNLs and to check whether TIMP-1 colocalises with proMMP-9, as such a colocalisation may indicate that the proMMP-9/TIMP-1 complex occurs *in vivo*.

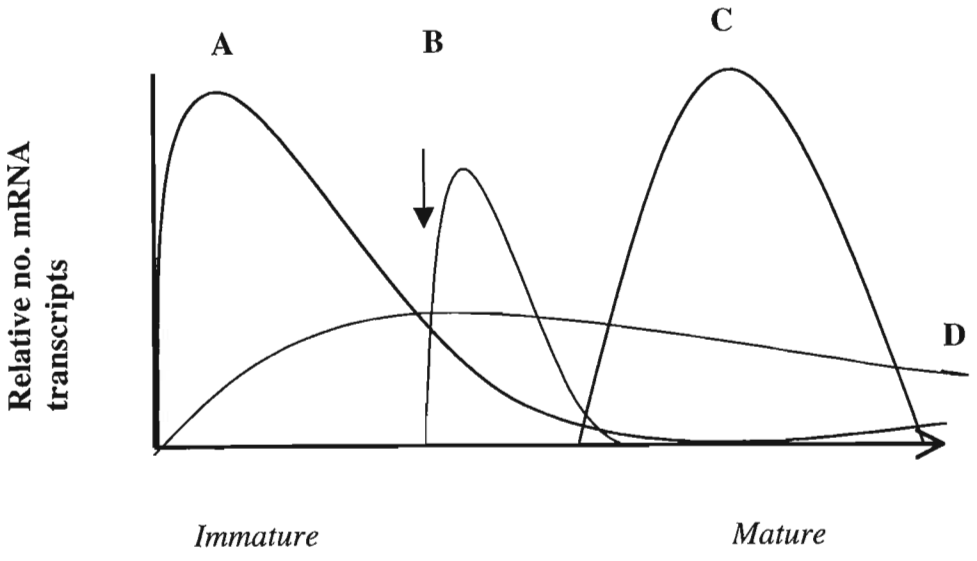

Figure 4.5 **Representation of transient granule protein/mRNA expression and overlap during PMNL differentiation.**

Hypothetically, mRNA transcripts from proteins A, B, C are translated at distinct stages during maturation, while translation of D remains relatively constant, assuming that transcripts are translated immediately. At some stages, there is overlap of mRNA transcription (arrow), although this occurs infrequently and usually involves a small number of transcripts relative to the total transcribed. In the PMNL context, (A) could represent MPO; (B), lactoferrin; (C), proMMP-9 and (D), lysozyme (Edwards, 1994). Adapted from Fouret *et al.* (1989).

The granule markers selected for assignment of TIMP-1 to a particular granule type were chosen after extensive review of the literature and are summarised in Table 4.1. The study was commenced after extensive characterisation of antibodies to be used in TIMP-1 localisation.

Table 4.1 **PMNL granule marker proteins used in the immunocytochemical localisation of TIMP-1.**

Granule population	Marker protein(s)
Azurophil	MPO
Specific	Lactoferrin
Specific	ProMMP-8
Specific and gelatinase	ProMMP-9
Secretory vesicles	GPI-anchored proteins
Multivesicular/multilaminar bodies	LAMP-1 and LAMP-2
Late endosomes/Lysosomes	14 nm BSA-gold

4.3.1 Reagents

Labelling reagents, buffers and fixatives were prepared as described in Section 2.9.3.1 and 14 nm BSA-gold colloids were prepared as described in Section 2.10.2.

4.3.2 Procedure

Visualisation of the endocytic pathway by pulse-chase with 14 nm BSA-gold particles. PMNLs (~$2x10^6$/ml) in serum-free RPMI-1640 medium were pulsed with BSA-coated 14 nm gold particles (1:50 dilution; A_{520} = 0.552) for 1 hour, washed thoroughly in fresh medium, and chased for a further 3 hours (all at 37°C) in order to label the late endosomal compartment (Berger *et al.*, 1994). Cells were washed and fixed for processing for cryoultramicrotomy and immunolabelling.

Cryoultramicrotomy and immunocytochemistry. PMNLs were fixed [2% (w/v) PFA, 0.05% (v/v) glutaraldehyde in 200 mM HEPES. pH 7.2] overnight at 4°C, residual aldehyde groups quenched (20 mM glycine in PBS, pH 7.2) and cells pelleted (400 x *g* for 2 minutes), embedded with 10% (w/v) gelatin, and processed for cryoultramicrotomy as previously described (Section 2.9.3.1). Ultrathin cryosections (60-80 nm) cut on an RMC MT6000XL ultramicrotome at -100°C were retrieved on 1.15 M sucrose/1% (w/v) methylcellulose droplets (Liou *et al.*, 1996), placed on carbon coated, glow-discharged nickel grids and labelled for TIMP-1 (150 ng/5 µl) and either MPO (76 ng/5 µl) (azurophil granules), lactoferrin (125 ng/5 µl) (specific granules), proMMP-8 (50 ng/5 µl) (specific granules), proMMP-9 (100 ng/5 µl) (specific and gelatinase granules), GPI-anchored proteins (50 ng/5 µl) (secretory vesicles) or LAMP-1 (1/120) and

LAMP-2 (1/200) (multivesicular/multilaminar bodies) (Table 4.1). Sections were fixed with 2% (v/v) glutaraldehyde in PBS and quenched with 20 mM glycine in PBS after labelling with the primary antibody and a 5 nm protein A gold probe (1:200; A_{520} = 0.036; 10 µl; 30 min, RT). Binding of the second antibody was visualised using a 10 nm protein A gold probe (1:250; A_{520} = 0.044; 10 µl; 30 min, RT). The sections were stained and sealed as described in Section 2.9.3.2. For labelling with LAMPs, a rabbit anti-mouse IgG linker antibody was used at a 1/500 dilution before incubation with protein A gold.

Stereological and statistical analysis. Diameters of the various PMNL granule populations were statistically measured on random sections of whole cells. This was done by measuring the mean diameter of multiple random sections of each population, using at least three micrographs with primary magnifications of 27 500 and 33 000, on a minimum of 11 granules, each granule type being defined by its content of a particular marker protein. If granules were not exactly spherical, the mean of two different diameters through the centre was used. The diameters of dumbbell-shaped granules were not included in diameter estimations, and significant differences in diameter between the TIMP-1 vesicle and other granule types were established using one-sided Student's *t*-tests (since the null hypothesis was that the mean diameter of the TIMP-1 vesicle was greater than other granules). Diameter estimations were compared with those previously published (Kjeldsen *et al.*, 1993b). Approximate mean profile areas were calculated for spherical organelles using the measured diameters. Labelling density for a particular antigen was assessed by counting the number of specific gold particles per granule/organelle/vesicle on a minimum of seven or more such organelles and expressed as gold particles/μm^2 (Weibel, 1979). Non-specific (background) particles (on cytosol or nucleus) were counted and similarly expressed.

The degree of colocalisation of a particular granule antigen with TIMP-1 was established by counting the number of gold particles colocalising with TIMP-1, relative to the total number of gold particles for that particular antigen on each micrograph (in a minimum of 15 granules containing the marker of interest), and expressing this as a percentage.

4.3.3 Results and Discussion

Immunolocalisation of TIMP-1 with respect to granule marker proteins. TIMP-1 was mainly localised to an organelle that has a surface density approximately half that of the azurophil granule population (Table 4.2). These organelles are distinctive from other granules (except the

secretory vesicles) in electron translucency and their roughly ellipsoidal shape. TIMP-1 showed no colocalisation with the azurophil granule marker protein, MPO, on thawed cryosections (Figure 4.6 A). In some cases, sparse colocalisation of TIMP-1 with HNE, another azurophil granule marker protein was seen (results not shown). There is some slight uncertainty of this result, however, since translocation of azurophil granule proteins does occur occasionally upon sectioning (Elliott *et al.*, 1995). In addition, colocalisation of TIMP-1 and HNE is unlikely to occur since HNE degrades TIMP-1 *in vitro* (Okada *et al.*, 1988; Itoh and Nagase, 1995) and the proteins would, possibly be incompatible in the same organelle. Such a hypothesis seems to be supported by stereological and quantitative data (Table 4.2).

Specific granules, identified by labelling for lactoferrin and proMMP-8 (Murphy *et al.*, 1977; Breton-Gorius *et al.*, 1980; Cramer *et al.*, 1985), showed very little colocalisation with TIMP-1. Lactoferrin was found predominantly in round, electron dense granules (Figure 4.6 B). Similar results were found for double labellings for TIMP-1 and proMMP-8 and -9. ProMMP-8 labelled granules were electron-dense and dumbbell shaped (Figure 4.6 C) whilst those containing only proMMP-9 [i.e. gelatinase granules (Dewald *et al.*, 1982; Borregaard *et al.*, 1992; Kjeldsen *et al.*, 1993a)] were smaller, circular and electron-dense (Figure 4.6 D). The majority of proMMP-8 and proMMP-9 did not colocalise with TIMP-1 (Figures 4.6 C and D, respectively). The predominantly separate labelling of proMMP-9 and TIMP-1 (Figure 4.6 D) suggests that only a small portion of proMMP-9 (~22.6%, Table 4.2) occurs in a proMMP-9/TIMP-1 heterodimeric complex *in vivo*, while most of TIMP-1 remains separate from all other granule marker proteins.

No colocalisation of TIMP-1 with secretory vesicle marker, GPI-anchored proteins, was observed (Figure 4.7 A). On the basis of their lack of multilaminar or multivesicular shape and lack of labelling for LAMPs-1 and -2 (Figure 4.7 B) or BSA-gold (Figure 4.7 C), the TIMP-1 vesicles do not appear to be components of the endocytic pathway. The absence of TIMP-1 in the late endosomal compartment proves that labelling seen for TIMP-1 is not due to TIMP-1 that has been endocytosed from plasma. The organelle containing TIMP-1, therefore, does not seem to be part of the endocytic pathway and thus the TIMP-1 present in PMNLs is most likely to represent that synthesised by the PMNL.

Stereology and quantitation. Results are presented in Table 4.2. This table reflects qualitative- and relative quantitative results only, as many variables that may alter the pattern and density of

immunolabelling cannot be taken into account in the labelling system used. A truly quantitative approach would require the calculation of labelling efficiencies for this system (Horisberger, 1989; Slot *et al.*, 1989). Only positive colocalisations and relative comparisons across different granules are, therefore, reliable. Negative colocalisation may only suggest that the antigens present are below the detection limits under the fixation and labelling conditions used. In this study, the diameters measured for established granule populations compared favourably with those previously reported (Rice *et al.*, 1987; Kjeldsen *et al.*, 1993b). Labelling of PMNL sections showed that TIMP-1 was mainly located in electron translucent organelles, on average slighter larger than azurophil granules, significantly larger than other granule or vesicle populations, but significantly smaller than BSA-gold containing late endosomes/lysosomes (Table 4.2). From these results, it is clear that the TIMP-1 vesicle represents a unique organelle (we propose that it be named the 'TIMP-1 vesicle') that requires further investigation to establish its regulation and other resident protein components. The term 'vesicle' is chosen since, like the secretory vesicles, the TIMP-1 vesicles are mostly electron translucent and exhibit some pleiomorphism (ranging from predominantly large and oval to smaller and more oblong), although not as great as the secretory vesicles (Kobayashi and Robinson, 1991).

Our estimation of proMMP-9 colocalisation with TIMP-1 (~22.6%) is higher than that of 10% estimated by Triebel *et al.* (1995). It is, therefore, possible that of the total 22.6% colocalisation, 10% represents proMMP-9 associated with TIMP-1 as a heterodimer while the remaining 12.6% represents proMMP-9 unassociated with TIMP-1 (i.e. proMMP-9 monomers or homodimers) in the TIMP-1 vesicle. This is, however, speculative since immunocytochemistry cannot discriminate between complexed and uncomplexed forms of proMMP-9 in the TIMP-1 vesicle.

In summary, colocalisation with TIMP-1 only occurred in distinct translucent, ellipsoidal granules distinct from other PMNL granule populations and the endocytic pathway. The density of this vesicle was the focus of the next study into the characteristics and localisation of TIMP-1.

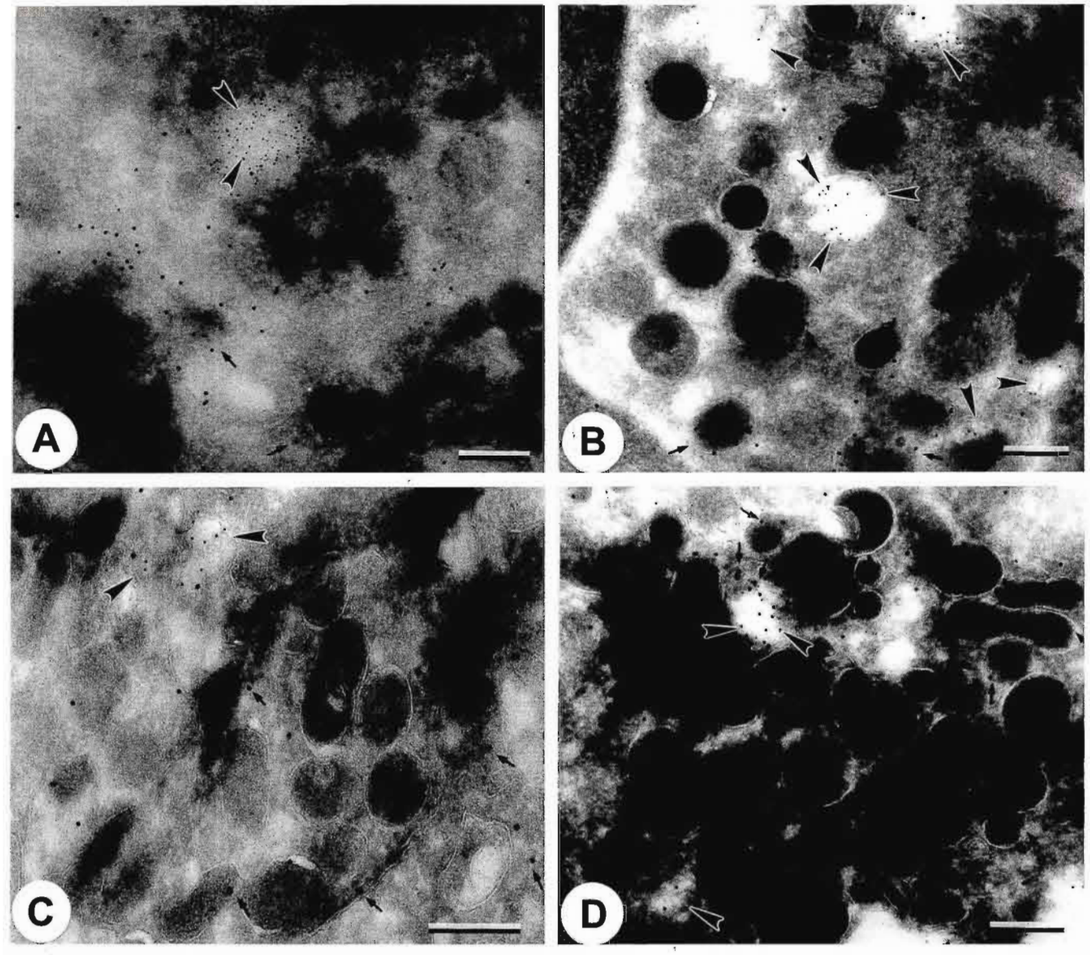

Figure 4.6 **Immunolocalisation of TIMP-1 with respect to markers for the azurophil (MPO), specific (lactoferrin, proMMP-8, and proMMP-9) and gelatinase (proMMP-9) granules on thawed ultrathin cryosections.**

A), TIMP-1 (5 nm gold; arrowheads) and MPO (10 nm; small arrows). B), TIMP-1 (5 nm gold; arrowheads) and lactoferrin (10 nm gold; small arrows). C), TIMP-1 (5 nm gold; arrowheads) and proMMP-8 (10 nm gold; small arrows). D), TIMP-1 (5 nm gold; arrowheads) and proMMP-9 (10 nm gold; small arrows). Bars = 200 nm.

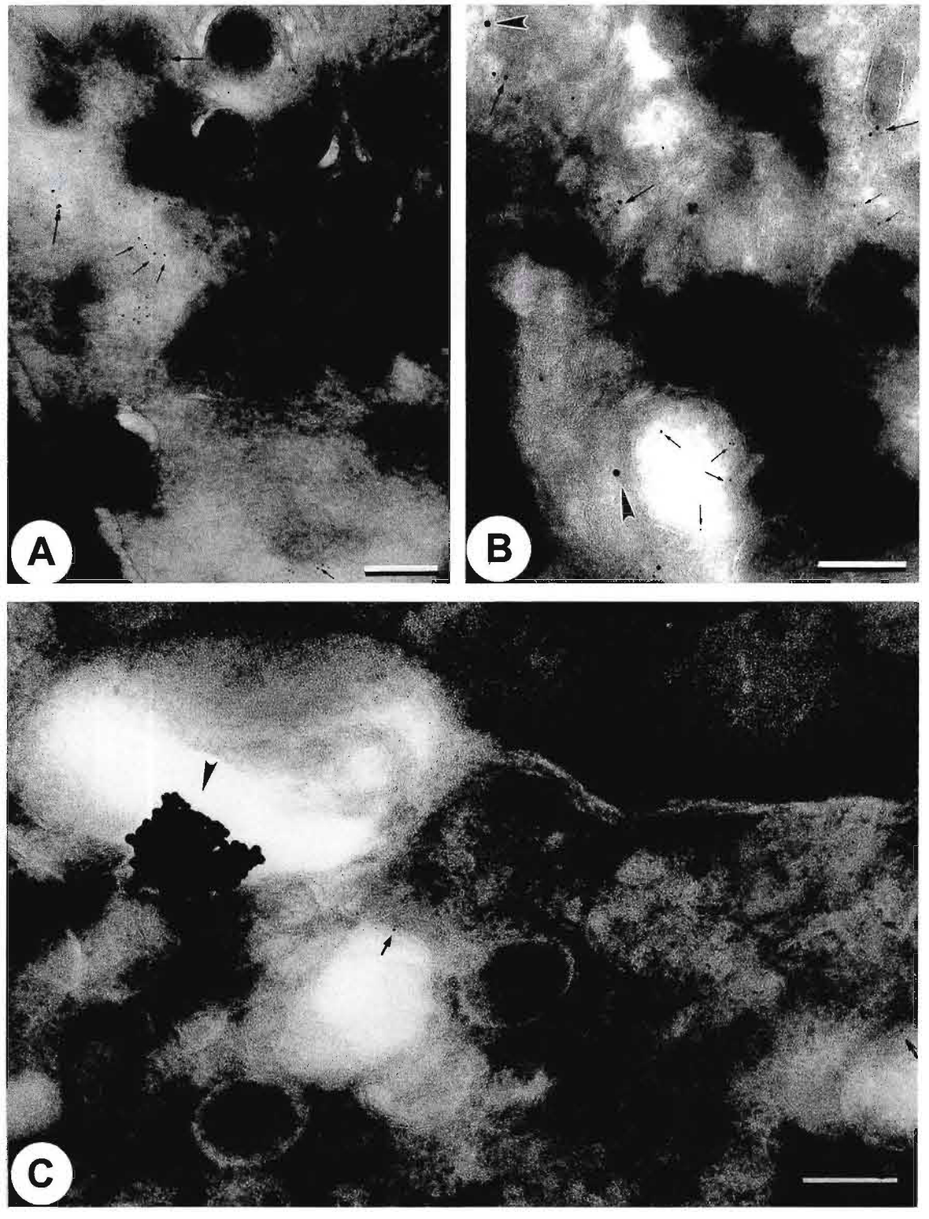

Figure 4.7 **Immunolocalisation of TIMP-1 with respect to markers for secretory vesicles (GPI-anchored proteins), multivesicular/multilaminar bodies (LAMPS-1 and -2) and late endosomes/lysosomes (14 nm BSA-gold) on thawed ultrathin cryosections.**

A), GPI-anchored proteins (5 nm; small arrows) and TIMP-1 (10 nm gold; larger arrows). B), TIMP-1 (5 nm gold; small arrows), LAMP-1 (10 nm; larger arrows) and LAMP-2 (15 nm; arrowhead). C), TIMP-1 (5 nm gold; arrows) and BSA-gold (14 nm; arrowhead). Bars = 200 nm.

Table 4.2 Stereological analysis of immunocytochemical results

Marker protein	Granule population	Diameter (nm)[a]	Student's *t*-value	Mean profile area (μm^2)	Gold particles/ μm^2	Background particles/μm^2 background	Gold particles/ organelle[a]	Colocalisation with TIMP-1 (%)[b]
TIMP-1	TIMP-1[c]	266±84 (15)		0.056±0.005	334±233	0	19±13 (15)	100
MPO	Azurophil	237±74 (17)	1.01[NS(e)] (30 *df*)	0.045±0.004	205±176	8	9±8 (20)	0.9 (3/322)
Lactoferrin	Specific	161±41 (11)	3.79** (24 *df*)	0.021±0.008	650±415	6	13±9 (15)	3.5 (6/169)
ProMMP-8	Specific	168±35 (11)	3.61** (24 *df*)	0.022±0.005	127±60	49	3±1 (15)	14.5 (20/138)
ProMMP-9	Specific/ Gelatinase	133±36 (11)	4.89** (24 *df*)	0.014±0.004	214±111	1	3±2 (15)	22.6 (26/115)
GPI proteins	Secretory	ND[d]	ND[d]	ND[d]	ND[d]	0	6±3 (7)	1.4 (2/139)
LAMP-1	Multi-vesicular or	ND[d]	ND[d]	ND[d]	ND[d]	1	3±1 (11)	0 (0/127)
LAMP-2	Multi-laminar bodies	ND[d]	ND[d]	ND[d]	ND[d]	0	1±0.5 (10)	0 (0/96)
BSA-gold	Lysosome	406±200 (7)	2.35* (20 *df*)	0.13±0.03	303±142	2	39±18 (10)	0 (0/406)

[a] Number in parentheses indicates the number of granules/vesicles/organelles over which estimations were made.

[b] Colocalisation was determined by expressing the number of gold particles counted for the labelling for a particular antigen colocalising with TIMP-1 (y) as a percentage of the total number of gold particles counted for that antigen (x + y) and expressed as y/(x + y) x 100% e.g., for MPO, out of a total of 322 gold particles representing labelling for MPO (x + y), only 3 of these (y) colocalised with TIMP-1.

[c] We propose that this organelle be named the TIMP-1 vesicle

[d] ND, not determined. Diameter and mean profile area estimations for the secretory vesicle and LAMP-positive structures were not possible due to the highly pleiomorphic nature of these vesicles/organelles.

[e] NS, *, ** Indicates that from one-sided Student's *t*-tests, diameter differences of a particular granule with respect to TIMP-1 are either non-significant (NS), or significant at the 5% (*) or the 1% (**) level for the relevant degrees of freedom (*df*)

4.4 Analysis of the TIMP-1 vesicle by subcellular density fractionation

PMNL granule populations differ with respect to their density, which may be partly due to the differential protein content in each population and their relative size. The correlation between granule density and time of synthesis during PMNL maturation has been highlighted previously (Section 1.4) (i.e. the density of granules decrease during PMNL maturation), and this chapter describes the use of granule fractionation on a modified discontinuous Percoll gradient to gain insight into the stage of maturation of PMNLs during TIMP-1 expression. The information obtained from the density of the TIMP-1 vesicle was seen to also provide an idea of the hypothetical order of its release relative to the MMP-containing granules.

4.4.1 Reagents

MPO assay buffer (83 mM citric acid, 112 mM Na_2HPO_4, 910 µM ABTS, 0.125 µl/ml H_2O_2, pH 5.6). Citric acid (1.594 g) and $Na_2HPO_4.2H_2O$ (1.737 g) were dissolved in dd.H_2O (~80 ml), titrated to pH 5.6 with NaOH and the volume made up to 100 ml in a volumetric flask. Before use, ABTS.$(NH_3)_2$ (0.05 g) and H_2O_2 (12.5 µl) were added to the solution.

MPO stop solution [10% (w/v) SDS]. SDS (1 g) was dissolved in dd.H_2O (10 ml) and kept at RT.

All other reagents were prepared as described in Section 3.5.1.

4.4.2 Procedure

Subcellular fractionation was performed as described in Section 3.5.1 and 29 fractions of 1 ml each were collected. Alkaline phosphatase activity was detected by *p*NP release while MPO was assayed with ABTS, as the sensitivity required was not as crucial as that required in Chapter 3 (Section 3.5.1).

Aliquots (10 µl) of each granule fraction were placed in a microtitre plate well and made up to 150 µl with substrate. The reactions were stopped with MPO stop solution (15 µl) after 20 to 30 minutes (Schettler *et al.*, 1991) and of alkaline phosphatase stop solution (1 ml) after 20 minutes (Andrews and Krinsky, 1986), respectively. Both assays were performed at 25°C and activity monitored by recording absorbances at 405 nm. Fractions giving similar activities were pooled and processed for cryoultramicrotomy and immunolabelling for MPO and TIMP-1 as

described in Section 2.9.3.2.

4.4.3 Results and Discussion

Figure 4.8 shows the successful resolution of the PMNL granule populations into the conventional α, β and γ fractions. The activity profile for MPO shows two distinct peaks that may represent the dense, defensin-rich and light, defensin-free azurophil granules. Unfortunately, the specific and gelatinase granules cannot be completely resolved from each other using the current density gradient techniques and it is expected that free flow electrophoresis might assist in this regard in a similar manner in resolving the secretory vesicles from the plasma membrane. The TIMP-1 vesicle partitioned to the lightest fraction (alkaline phosphatase-positive) (Figure 4.8) although the immunocytochemistry results (Figure 4.5 A) clearly show that these two proteins reside in separate compartments. The information regarding the TIMP-1 vesicle buoyant density serves to shed some light on the possible time of synthesis during maturation. The density similarity to that of the secretory vesicles suggests that the synthesis of TIMP-1 and the other protein components of this granule occur late in PMNL development, thereby lending some support to the hypothesis raised earlier regarding the occurrence of TIMP-1 mRNA transcripts in mature PMNLs (Triebel *et al.*, 1995).

The possibility that TIMP-1 is synthesised after the secretory vesicles (and the GPI-anchored proteins) exists. The late synthesis of TIMP-1 would account for its presence in mature PMNLs, its low density and electron translucency, but the time of its synthesis could only be accurately confirmed by performing *in situ* hybridisation on bone marrow PMNLs of differing maturation status, by a method similar to that used to establish gelatinase as a marker of terminal differentiation (Borregaard *et al.*, 1995). Although it is tempting to suggest that late synthesis and low density indicate that TIMP-1 degranulation occurs early during PMNL activation, the exact mechanism of regulation of the TIMP-1 vesicle requires investigation and forms the focus of the following chapter. The results of this density gradient study, however, confirm the localisation of TIMP-1 to a light organelle fraction resembling the secretory vesicles.

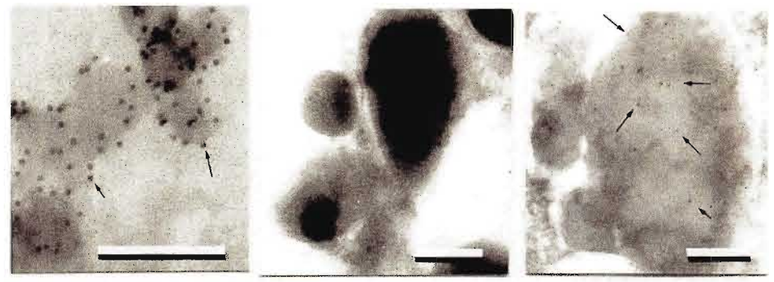

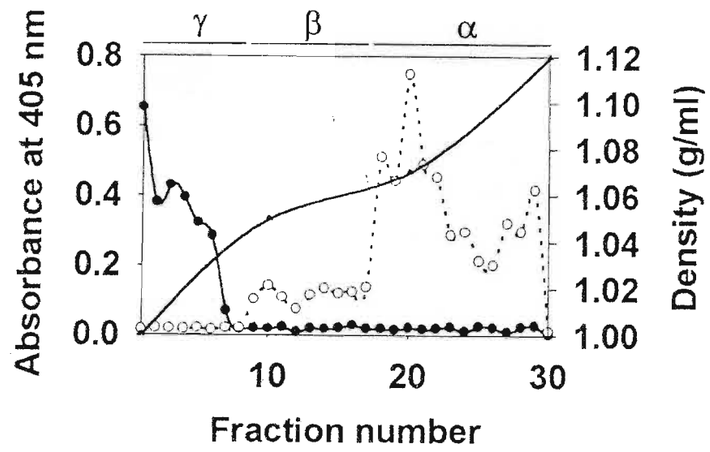

Figure 4.8 **Subcellular fractionation of PMNL granules by density gradient centrifugation and immunolabelling of fractions to assess the density of the TIMP-1 vesicle.**

PMNLs were disrupted by sonication and the postnuclear supernatant was applied on top of a discontinuous Percoll gradient and centrifuged. Granule fractions were pooled on the basis of the presence of alkaline phosphatase activity (γ fraction; secretory vesicles/plasma membrane) and MPO (α fraction; azurophil granule fraction), or absence of both enzymes (β fraction; specific and gelatinase granules). Latent alkaline phosphatase activity (solid circles) was detected with *p*NPP and MPO activity (open circles) with ABTS, both at 405 nm. A plot of the relative density is given by the solid line (no circles). Pooled granule fractions were processed for cryoultramicrotomy and labelled for TIMP-1 and MPO. TIMP-1 was found only in the γ fraction (left micrograph; 10 nm gold; small arrow), and MPO in the α fraction (right micrograph; 5 nm gold; small arrows).

4.5 Discussion

This section of the study describes for the first time the localisation of TIMP-1, previously thought to be cytosolic, to a novel vesicle in human PMNLs. This study also revealed some interesting results and raises many questions, one of which is whether the high M_r form of TIMP-1 that is resistant to heat, SDS, chemical reduction and carboxymethylation and 6 M guanidine hydrochloride, but sensitive to the synergistic effects of heat and dilution, is an isolation artefact or whether it exists *in vivo*.

The initial characterisation of TIMPs by Stricklin and Welgus (1983) showed that, in some cases, TIMPs required reduction and carboxymethylation in 6 M urea before full denaturation could be achieved. The *number* of disulfide bridges present in TIMPs might not confer the impressive structural resistance to denaturing conditions [e.g. cathepsin B, a lysosomal proteinase, also contains six disulfide bridges (Musil *et al.*, 1991) but is sensitive to reduction and carboxymethylation], but rather the *relative positioning* of the disulfides with respect to each other may be of greatest importance. If located close together in the tertiary structure, the disulfide bonds of TIMP-1 might synergistically stabilise the inhibitor. Therefore, if a few disulfide bridges were reduced, the remaining intact bridges could retain the overall conformation until reoxidation occurred. Under conditions where excess reducing agents are present, the possible synergistic cooperativity of disulfide bridges may no longer apply. However, if reducing conditions were removed and the molecule allowed to reoxidise, the oxidation of two cysteine residues into a single disulfide bridge may potentially allow or promote the reformation of the other bridges - a process similar to the 'zippering' found in gene transcription factors (e.g. leucine zippers) (Branden and Tooze, 1991). Therefore, the positioning of the disulfide bridges and the number of bridges could be responsible for maintaining the structural stability of TIMP and might explain the difficulties experienced in this study in the attempts to reduce TIMP-1. The above is merely speculation and does not, however, provide an explanation for the origin or reason for the occurrence of the 66 kDa form of TIMP-1. It may, however, assist in explaining why reduced and blotted TIMP-1 was able to bind proMMP-9 in the western ligand blot.

Another possible reason for existence and predisposition of TIMP-1 to assume the high M_r form may relate to protein aggregation. Protein aggregation has been recognised as one possible

mechanism responsible for selectively removing proteins destined for storage in regulated secretory organelles, from the constitutive secretory pathway (e.g. insulin aggregation in pancreatic B-cells). Aggregation is usually induced by altering the ionic composition of the lumen (usually via acidification or the presence of certain cations) and accompanied by dehydration, until the proteins are rendered insoluble (Arvan and Castle, 1998). Proteins destined for regulated secretion usually carry particular motifs to either retain them in a post-Golgi compartment or direct them to an immature granule. The topic of signal motifs in PMNL granule targeting has been mentioned briefly (Section 1.4). It is generally accepted that protein targeting to a particular granule occurs simply due to cotranslation of proteins at a particular time during PMNL maturation and that motifs are not required (Garwicz *et al.*, 1998). Therefore, a motif-independent mechanism of protein sorting such as aggregation, could allow compartmentalisation of TIMP-1 to the TIMP-1 vesicle. The presence of proMMP-9 in the TIMP-1 vesicle (as shown by the immunocytochemistry study in this chapter) is probably due to the fact that proMMP-9 retains the ability to bind high M_r TIMP-1 (a feature demonstrated by the western ligand blot presented here) and may coaggregate with TIMP-1 during PMNL maturation after the majority of proMMP-9 has been packaged in the specific and gelatinase granules.

If TIMP-1 exists as a complex *in vivo*, this might allow for selective sorting and storage in a particular granule type. If TIMP-1 occurred as an insoluble complex, this might allow for higher density packing of the inhibitor and possibly increased resistance to proteolytic degradation by sequestering susceptible regions from enzymes or ROS. The question then arises as to how the high M_r form of TIMP-1 in the PMNL resists reduction during reducing SDS treatments, while other granule proteins appear to solubilise and produce expected M_r bands during SDS-PAGE analysis and western blotting. Interestingly, TIMP-1 is the only TIMP member known to produce high M_r forms and is the only member that is glycosylated. Glycosylation does not play a role in enzyme inhibition [as deglycosylated TIMP-1 retains full inhibitory activity (Gomez *et al.*, 1997)], therefore its exact function is not known. In addition, proMMP-9 is glycosylated and known to form homodimers (220 kDa) that exhibit full biological activity. The closely related and non-glycosylated proMMP-2 does not form homodimers (Makowsky and Ramsby, 1996). This raises a further question of whether glycosylation plays a similar role in TIMP-1 dimerisation/aggregation or whether dimerisation occurs via hydrophobic interactions. It would be interesting to inhibit TIMP-1 glycosylation in PMNLs [e.g. using tunicamycin since the oligosaccharides present on TIMP-1 are N-linked

(Docherty *et al.*, 1985)] and observe whether the 66 kDa form still occurs. Alternatively, the N-linked oligosaccharides could be enzymatically removed by N-glycosidase F and observed for any reduction in TIMP-1 M_r following treatment. Although TIMP-1 and proMMP-9 both form homodimers, proMMP-9 homodimers are not stable to reduction and boiling. It is plausible that TIMP-1 homodimerisation, in conjunction with dehydration-induced aggregation (during packaging into granules) and the inherent physical stability of TIMP-1, gives rise to high M_r TIMP-1 species, similar to that described in this present study.

Irrespective of the mechanism(s) involved in generating the TIMP-1 66 kDa form, it is interesting that it retains full biological activity against active MMP-9. Further studies involving the effect of TIMP-1 'aggregation' on its EPA/growth factor, anti-apoptotic or anti-angiogenic activity could be assessed on the appropriate cell type. It is possible that aggregation might improve EPA function by rendering the TIMP-1 molecule bivalent and allowing EPA-receptor cross-linking upon binding. Alternatively, the aggregation of TIMP-1 might function as a 'slow release' mechanism to ensure that TIMP-1 regulation of extracellular MMP activity is controlled and constant. This might allow for the persistent release of small amounts of TIMP-1, thereby avoiding the risk of exposing all the TIMP-1 (in soluble form) to potential proteolytic degradation by HNE or oxidative degradation by MPO.

The compartmentalization of most of the TIMP-1 to a distinct vesicle, largely separate from ProMMP-8 and -9, may allow the PMNL to selectively degranulate TIMP-1, without releasing the proMMPs. Such a pool of free TIMP-1 could be released prior to proMMP degranulation, to provide sufficient extracellular TIMP-1 to control the extent of MMP activity. Alternatively, it could be released after proMMP degranulation and activation, allowing initial proteolysis and invasion to occur, but subsequently terminating proteolysis and limiting tissue damage.

The colocalisation of TIMP-1 with varying amounts of proMMP-9 in a minor vesicle subpopulation may assist in a finer regulation of PMNL-derived MMP proteolytic activity. Colocalisation suggests that these proteins may be released as a heterodimer. As TIMP-1 binds to proMMP-9 at a site distant from its inhibitory binding site, proMMP-9 may be able, in effect, to carry TIMP-1 'piggy-back' to its site of action. Here, after proMMP-9 activation, the TIMP-1 could be responsible for the local inhibition of MMP-9 and, hence, its limited action. ProMMP-8, released together with TIMP-1 (but uncomplexed to TIMP-1) may have a similar limited action. To assist the passage of PMNL through the ECM, it is proposed that PMNLs

allow limited release of both proMMP-8 and -9 to effect proteolysis and that the subsequent timely release of TIMP-1 may play an important role in rapidly inhibiting and, hence, localising and controlling the extent of MMP activity. The location of TIMP-1, separate from its target enzymes, in a vesicle that may be differentially mobilised, would facilitate the required fine regulation of such a proteolytic process.

Assuming that any colocalisation of TIMP-1 with other granule markers indicates time of granule biosynthesis, the colocalisation of TIMP-1 with proMMP-9 in minor TIMP-1 subpopulations suggests that TIMP-1 synthesis may occur between metamyelocytic and terminal differentiation, but before secretory vesicle biogenesis, as GPI-anchored proteins were not found in TIMP-1-labelled vesicles.

The existence of a discrete localisation for TIMP-1 in the TIMP-1 vesicle raises questions regarding its differential regulation of release relative to other granule populations. Does it associate with components of the cytoskeleton to allow release into the extracellular environment and/or into the phagosome? The order of TIMP-1 release relative to other granule populations was, therefore, assessed by latex bead phagocytosis combined with cryoimmunocytochemistry in Chapter 5. In addition, the interaction of the TIMP-1 vesicle with cytoskeletal components was investigated using stabilised actin and tubulin and, finally, the Ca^{2+} dependency for TIMP-1 vesicle exocytosis, compared to other PMNL granule populations, was assessed with ionomycin.

CHAPTER 5

Investigations into the differential mobilisation of the MMPs and TIMP-1 with respect to other PMNL granules

5.1 Introduction

The PMNLs are the first leukocyte population to arrive at the site of infection during inflammation. In order to extravasate and traverse the ECM to gain access to surrounding perivascular tissue, the PMNL is thought to release MMPs to degrade types IV and I collagen present in the basement membrane and stromal tissue, respectively. All known PMNL granules are under the control of regulated exocytosis. This allows discrete granule populations to be selectively mobilised as required (Edwards, 1994; Sengeløv, 1996; Tapper, 1996; Borregaard and Cowland, 1997). The newly identified TIMP-1 vesicle may allow the PMNL to either selectively retain or release TIMP-1, as required, to regulate MMP activity. The ultimate aim of PMNL invasion into the tissue is to phagocytose and kill invading organisms.

Phagocytosis is the mechanism by which leukocytes ingest foreign particles (e.g. bacteria, fungi) that have been coated or opsonised with either IgG or complement (Rabinovitch, 1995; Allen and Aderem, 1996; Tapper, 1996). Following ingestion, the foreign particle is sealed off into a separate intracellular membrane-bound compartment termed a 'phagosome' (Absolom, 1986; van Oss, 1986; Allen and Aderem, 1996). The phagosome is gradually acidified (by means of H^+-ATPase pumps) while fusion with vesicles containing lysosomal proteinases (in the case of macrophages) or granule populations (in PMNLs) occurs in a process termed 'phagosomal maturation' (Tapper, 1996). This generally observed order is possibly established since the pH optima of the various granule population proteins differ considerably. The order of fusion allows proteins with neutral to slightly basic pH optima to fuse with the phagosome relatively early, before acidification of the phagosome inhibits their biological activities and promotes those with an optimum in the acid range, e.g. MPO (Bentwood and Henson, 1980; Segal *et al.*, 1981). This allows the phagosome to acquire new luminal and membrane proteins over time while phospholipids are recycled to the plasma membrane to maintain overall surface area and membrane characteristics of the cell and also to assemble the NAPDH oxidase complex for the respiratory burst (Desjardins *et al.*, 1997).

Killing of the foreign ingested particle may, therefore, occur enzymatically (via proteinases, glycosidases, lipases) and/or non-enzymatically (via cationic peptides, ROS, HOCl). If the phagocyte is an APC (e.g. a macrophage), the peptide fragments of the digested pathogen are displayed, together with MHC class II molecules, on the cell surface and an immune response is elicited. However, if the phagocyte is not an APC, as is the case with the PMNL, then an immune response may still be elicited by production and release of cytokines and chemotactic factors, which attract other immune cells to the site of infection (Edwards, 1994).

The role of microfilaments and microtubules in the processes of phagocytosis and extracellular release have been confirmed using drugs that can selectively depolymerise actin (the cytochalasins) or tubulin (colchicine) (Dustin, 1978; Edwards, 1994). From these studies, it is known that pseudopod formation and particle capture in PMNLs are actin-dependent processes while phagosome formation and degranulation into the extracellular medium are mainly reliant on intact microtubules. During phagocytosis, it is thought that the actin scaffolding, directly beneath the plasma membrane, is disassembled and repolymerisation occurs at distinct sites giving rise to filopodia (small membrane projections) and subsequently, to pseudopodia (larger, flat membrane projections). Once the entire particle is enveloped, the surrounding membrane pinches off from the cell surface (although sometimes granule release can occur before sealing occurs and their contents are spilt into the extracellular medium) and the phagosome is transported to the centre of the cell (Blocker *et al.*, 1997; 1998). This centripetal movement suggests movement along a microtubule track towards the microtubule organising centres that are positioned in the middle of the cell. Since microtubule depolymerisation prevents granule transportation to the phagosome, phagosome maturation and extracellular release (Dustin, 1978), granule transport to the phagosome may occur via such tracks, perhaps with the aid of a motor protein such as kinesin or dynein (depending on the direction of granule movement) (Schettler *et al.*, 1991; Blocker *et al.*, 1997). In macrophages, however, it seems that phagosomal movement is microtubule-dependent (Blocker *et al.*, 1997, 1998; Harada *et al.*, 1998), while vesicle membrane fusion events are dependent on actin (Diakonova *et al.*, 1997).

Once PMNL granules have been transported to the phagosome, membrane fusion events between the phagosome and the granules are thought to require members of the SNAP/SNARE family (and their respective adaptor proteins) and the annexin family of Ca^{2+}-dependent phospholipid-binding proteins. Although predominantly confined to synaptic cells, various t- and v-SNAREs as well as the other proteins important for fusion (NSF, Rabs etc.) have been

identified in PMNLs (Brummell *et al.*, 1995). If the SNAREs are responsible for correct targeting and fusion of heterogeneous membrane compartments, then the role and purpose of PMNL annexins seems unclear. Furthermore, PMNLs also possess an 'orphan' fusogen in the form of G3PDH (Hessler *et al.*, 1998). This raises the question of why three distinct membrane fusogenic protein families (or, rather, four if one includes the Rab GTP-dependent fusogens) are required for membrane fusion processes.

The specific annexin members involved in phagocytosis and phagosome fusion events have been studied extensively in the macrophage (Diakonova *et al.*, 1997; Hackam *et al.*, 1998) and in the PMNL (Ernst, 1991; Maridonneau-Parini and de Gunzburg, 1992; Le Cabec and Maridonneau-Parini, 1994; Sjölin *et al.*, 1994; Kaufman *et al.*, 1996; Sjölin and Dahlgren, 1996; Rosales and Ernst, 1997). Each member differs in its affinity for the various phospholipids and their derivatives present on vesicle or granule membranes. In PMNLs, different annexins have been identified on different granule populations (Table 6.1) and it has been proposed that the order of granule fusion into the phagosome might, therefore, be established by annexins. Here, the increase in $[Ca^{2+}_i]$ during phagocytosis would bind to annexins thereby allowing the annexins to associate with granule membrane phospholipids and mediate fusion with the nascent phagosome. As different granule populations fuse with the phagosome, the overall phospholipid composition of the phagosome may alter due to the action of endogenous phospholipases (i.e. phosphatidylcholine and phosphatidylethanolamine may be converted into phosphatidic acid), allowing different annexins to bind the phagosome and mediate homotypic fusion with another phosphatidic acid-rich granule population. Unfortunately, no *detailed* investigations into the possible heterogeneity in membrane phospholipid composition and distribution between PMNL granules have been conducted [although it is known that the plasma membrane and secretory vesicles are low in phosphatidylethanolamine and high in phosphatidylcholine relative to other granule populations (Bjerrum *et al.*, 1989; Borregaard *et al.*, 1993)], and thus the mechanism of maintaining selectivity of granule population fusion during phagocytosis and exocytosis remains unsolved.

During granule fusion into the phagosome and phagocytic killing, it is not uncommon for the PMNL to degranulate proteinases and other enzymes into the extracellular medium (Absolom, 1986; van Oss, 1986; Schettler *et al.*, 1991; Edwards, 1994; Tapper, 1996). In addition to proteinases, some MPO activity is often detected in supernatants of phagocytosing PMNLs. This may help in destroying pathogens surrounding the PMNL that have not yet been

phagocytosed (Bainton, 1973; van Oss, 1986; Watson *et al.*, 1996). After phagocytosis, the PMNL either regurgitates the killed organism or retains it within the phagosome. If the organism is retained, the PMNL will undergo programmed cell death or apoptosis. Regurgitation may allow other immune cells (that are APCs) to take up the now innocuous pathogen debris, display the antigens on their surface and signal a concerted immune response. Although PMNLs contain a battery of microbicidal proteins/compounds and are the fastest migrating leukocyte population, they are short-lived and serve only a limited role - the rapid killing of pathogens and production of cytokines in order to recruit additional leukocytes and stimulate lymphocyte proliferation. PMNLs undergo apoptosis via a caspase-dependent mechanism upon completion of phagocytosis, giving rise to high concentrations of ROS. They can however, if necessary, scavenge their own ROS with ascorbic acid to prevent toxic oxidative damage to the host (Wang *et al.*, 1997). A common feature of apoptosis in PMNLs is DNA fragmentation (DNA laddering) and the display of phosphatidylserine (PS) on the outer leaflet of the plasma membrane (Fadeel *et al.*, 1998). PS is a ligand for annexin V (commonly expressed by macrophages) and serves as a signal for phagocytosis of the PMNL by larger tissue macrophages (Watson *et al.*, 1996; Fadeel *et al.*, 1998; Yamashita *et al.*, 1999). Despite their short life, PMNLs serve an important role in fighting infection and in inflammation.

Both encapsulated (hydrophilic) and non-encapsulated (hydrophobic) bacteria become opsonised via recognition and binding to antibodies and complement. In order to identify and bind opsonised foreign particles *in vivo*, PMNLs possess receptors for complement fragments (C3b and C3bi), and IgG in the secretory vesicles (Borregaard and Cowland, 1997). Vesicles containing these receptors are rapidly mobilised to the plasma membrane, before other granule populations. Interaction of the phagocyte and the particle to be phagocytosed is then influenced by hydrophilic and hydrophobic (van der Waals) forces on the particle and the phagocyte. Considering that, like erythrocytes, both phagocytes and encapsulated bacteria possess nett negative ζ-potentials, it may seem unlikely that initial contact could be established between the two cell types due to electrostatic repulsion (Absolom, 1986; van Oss, 1986). Fortunately, bacteria have relatively small radii (with respect to the phagocyte) and phagocytes have the ability to extend pseudopodia around them. Van der Waals forces, strengthened by decreasing the separation distance, can thereafter overcome the repulsive ionic forces and phagocytosis can occur (van Oss, 1986).

Although hydrophobic interactions are vital for initial contact between the phagocyte and the

particle, interactions mediated only by these forces may severely compromise the ability of the phagocyte to destroy the ingested particle. A recent study by de Chastellier and Thilo (1997) highlighted the importance of both particle size and surface chemistry in determining the ultimate fate of phagocytosed particles. From TEM studies of latex bead uptake by J774 mouse macrophages, it was shown that a wide size range of latex beads can be ingested, although the number of latex beads found in each phagosome decreased as the bead size increased. In addition, phagocytosis of hydrophobic latex beads (>0.5 μm) prevents maturation of the phagosomes into phagolysosomes, though the phagosomes remain capable of fusing with early endocytic vesicles (de Chastellier and Thilo, 1997). This was established by observing that compartments labelled with hydrophobic beads did not fuse with 'lysosomes'/late endosomes that were labelled with pulsed-chased gold particles. In biological circumstances, this would be of great significance since phagocytic killing (by means of acidification and concomitant proteolytic degradation) would be inhibited. It was suggested that the hydrophobic nature of the beads resulted in tight association of the bead with the inner leaflet of the phagosomal membrane, thereby potentially preventing membrane recycling, acquisition of enzymes and 'maturation' (reliant on the acquisition and subsequent loss of membrane proteins). Similar experiments performed with hydrophilic latex beads (0.9 μm) and protein coated hydrophobic beads (0.1-1 μm) showed complete phagosomal maturation as gold particles (that were pulse-chased to label late endosomes) were identified in the same compartment as the latex beads (de Chastellier and Thilo, 1997). It was, therefore, postulated that hydrophobic *M. tuberculosis* organisms may inhibit phagosomal maturation in a similar manner to ensure intracellular growth and survival. If true, this may explain why *Toxoplasma gondii* and *Chlamydia trachomati* may similarly survive and multiply within phagocytes (Rabinowitz *et al.*, 1992). In the current study, the size and surface properties of the latex beads used for phagocytosis studies was carefully considered as full maturation of the phagosome was required in order to study the complete sequential release of marker proteins and TIMP-1 into the phagosome.

MMPs are stored in PMNLs in a precursor, inactive form and, hence, would not be relevant in invasion and inflammatory conditions unless they were activated. The MMPs do not possess any known anti-microbial function, but inclusion of MMPs into the phagosome may result in their activation by enzymes/compounds cosecreted into the phagosome. The order of TIMP-1 release into the phagosome relative to the proMMPs and the other PMNL granule marker proteins may be important in such an activation process. In most circumstances, the order of granule fusion into the phagosome is the same as that during degranulation (i.e. secretory

vesicles fuse first, azurophil last) (Bainton, 1973; Bentwood and Henson, 1980; Joiner *et al.*, 1989; Jaconi *et al.*, 1990; Rosales and Ernst, 1997). During phagocytosis, the MMPs and TIMP-1 may either be degranulated into the extracellular medium or released into the phagosome, or both. In either case, if TIMP-1 is released *after* the MMPs, then it may regulate MMP activity against collagens or other substrates (e.g. ECM components) by inhibiting MMPs after they have had a brief period in which to degrade these substrates. In this case, the MMPs may be activated by either PMNL-secreted enzymes/compounds or by those secreted by surrounding cells. However, if it is released extracellularly or into the phagosome *before* the proMMPs, then TIMP-1 may regulate MMP activity or activate the proMMP in a manner similar to that described for MMP-2 and TIMP-2 (Yu *et al.*, 1996). Here, TIMP-2 is involved in the initial activation of proMMP-2 via an MT-MMP as MT-MMP-mediated proMMP-activation requires the formation of an MT-MMP/proMMP/TIMP heterotrimeric complex. Once activated, the MMP is able to degrade the ECM to a limited extent before being inhibited by TIMP [if TIMP escapes being degraded by degranulated HNE (Okada *et al.*, 1988; Itoh and Nagase, 1995) and/or ROS (Stricklin and Hoidal, 1992; Shabani *et al.*, 1998)]. In this way, the cell may ensure that MMP-mediated proteolysis is limited by making TIMP an essential component of both MMP activation and inhibition.

Instead of investigating the order of release of TIMP-1 and the proMMPs into the supernatant, therefore, the initial investigation focussed on the order of release of these proteins into the phagosome as the phagosome provides a central 'depot' for the fusing granules and thus time-dependent inclusion of various proteins can be and monitored by immunocytochemistry (using antibodies against the various granule marker proteins) and TEM.

In the final part of this study, differential association of granules with the cytoskeleton elements, F-actin and tubulin, was studied and the Ca^{2+}_{i}-induced mobilisation of the TIMP-1 vesicle relative to other granule populations was studied using the ionophore, ionomycin, in conjunction with buffers containing increasing levels of free Ca^{2+}_{ex}. As release (extracellular and intracellular) of all known PMNL granules is known to be differentially regulated by $[Ca^{2+}_{i}]$ (Lew *et al.*, 1984; 1986; Jaconi *et al.*, 1990; Lollike *et al.*, 1995; Borregaard and Cowland, 1997; Nüße *et al.*, 1998), it was hypothesised that the TIMP-1 vesicle was similarly regulated.

5.2 Phagocytosis of IgG-opsonised latex bead and immunocytochemical analysis of PMNL granule fusion

The process of phagocytosis is sensitive to various factors including temperature, pH, osmolarity and the presence or absence of various cations (Absolom, 1986). In addition, the PMNL itself is highly sensitive to environmental factors and great care should be taken to avoid non-specific activation or 'priming' of PMNLs during the purification protocols employed. Thereafter, the optimal temperature (37°C) and pH (7.2) for phagocytosis are relatively simple parameters to provide and maintain. The maintenance of optimal osmolarity (~290 mOsm) (overall concentration of salts and sugars) is essential for phagocytosis as hyperosmotic conditions (>400 mOsm) in particular reduce the efficiency of phagocytosis and cause cell shrinkage. This parameter is difficult to ensure unless commercial culture medium of known osmolarity is used. The divalent Mg^{2+} and Ca^{2+} cations are also essential for phagocytosis. These are generally required to be at a concentration of 1-2 mM, or less if the particle to be ingested is opsonised (Absolom, 1986). The mechanisms by which the cations assist phagocytosis are unknown, but it has been suggested that they may assist with receptor-ligand binding. In addition, $[Ca^{2+}_{ex}]$ might play a role in the regulation of assembly of cytoskeletal elements required for pseudopodium formation and phagocytic ingestion.

For the study on IgG-mediated latex bead uptake and phagocytosis, RPMI-1640 medium was chosen since it is well suited for the culturing of leukocytes (292 mOsm/kg H_2O, containing Ca^{2+} and Mg^{2+}) particularly in the absence of serum (Absolom, 1986). Serum was omitted in this study since it contains MMP and TIMP species (Welgus and Stricklin, 1983; Cawston *et al.*, 1986b; Fujimoto *et al.*, 1994) that may be simultaneously included into the phagosome from the fluid medium during phagocytosis and hence may complicate the interpretation of the intended immunolocalisation studies. In addition to MMPs and TIMPs, serum also contains complement proteins that may adsorb or coat the phagocytic beads. This could result in latex beads being taken up via complement receptors rather than IgG receptors and may alter the order and extent of granule fusion with the phagosome (Edwards, 1994; Joiner *et al.*, 1989). Phagocytosis via an IgG receptor-mediated mechanism was chosen as this is known to result in full maturation of the phagosome, i.e. fusion of granules in the 'conventional' order (secretory first, azurophil last), unlike the limited fusion found, for example, following phagocytosis of C3b-opsonised particles (Edwards, 1994). Furthermore, IgG opsonisation was chosen since the low affinity receptor for IgG (FcγIIIRB/CD16b) is known to reside as a GPI-anchored protein in the secretory vesicles,

the first granule population to fuse with the plasma membrane and phagosomal compartment (Detmers *et al.*, 1995; Borregaard and Cowland, 1997).

5.2.1 Reagents

Borate-buffered saline, pH 8.6. Boric acid (H_3BO_3) (2.16 g), NaCl (2.19 g), NaOH (0.7 g) and HCl [620 µl of a 37% (v/v) solution] were dissolved in dd.H_2O (~950 ml). The pH was titrated to 8.6 with NaOH and the solution was made up to 1 *l* with dd.H_2O.

Phosphate buffer [100 mM sodium phosphate, 0.02% (w/v) NaN_3, pH 7.6]. NaH_2PO_4 (1.38 g) and NaN_3 (0.02 g) were dissolved in dd.H_2O (80 ml), titrated to pH 7.6 with NaOH, made up to volume and stored at 4°C.

Amine-modified 1 µm latex beads. These were purchased from Sigma as a 10% (w/v) solution in sterile water. The beads were sonicated (3 x 30 s) before use to ensure even dispersal.

Poly-L-lysine cell adhesion solution [0.1% (w/v) in dd.H_2O]. Poly-L-lysine hydrobromide (150-300 kDa) (0.01 g) was dissolved in dd.H_2O (10 ml) and stored at -20°C.

Immunolabelling, cryoultramicrotomy and fixative solutions were prepared as described in Section 2.9.3.1.

5.2.2 Procedure

Human IgG isolation by PEG precipitation. Blood (50 ml) was drawn into a sterile centrifuge tube containing no anticoagulant, and allowed to clot (4°C, o/n). The clotted blood was centrifuged (400 x g, 10 min, RT) and the serum aspirated. One volume of human serum was mixed with two volumes of borate-buffered saline. Crushed PEG 6 kDa was added to the diluted serum to 14% (w/v), gently dissolved by inversion, and the mixture centrifuged (12000 x g, 10 min, RT). The pellet was redissolved in the original serum volume, using phosphate buffer. PEG was added to 14% (w/v), dissolved, and the solution centrifuged (12000 x g, 10 min, RT). The pellet containing the human IgG was redissolved in half the original serum volume, using phosphate buffer containing 60% (v/v) glycerol, and stored in aliquots at -20°C.

Phagocytosis. PMNLs were isolated from whole blood (100 ml) (Section 2.7.2) and

resuspended in ice-cold sterile PBS. The PMNLs were then centrifuged (400 x g, 5 min, 4°C) and resuspended in RPMI-1640 medium (2.5 ml) containing 200 mM L-glutamine, pH 7.2. PMNLs (400 µl, $1.09x10^6$ cells) were dispensed into sterile 1 ml Eppendorf tubes and kept on ice. Latex beads (32 µl) were mixed with human IgG (32 µl, ~100 µg) and allowed to adsorb (20 min, RT). The IgG-opsonised beads were added to the PMNLs (8 µl/Eppendorf) and phagocytosis was allowed to proceed for various time intervals (30 s, 1, 3, 5, 10, 20, 30, 60 min) at 37°C. Phagocytosis was terminated by addition of fixative (400 µl). Fixation was allowed to continue for 1 h on ice, the cells were pelleted (400 x g, 1 min), fresh fixative added (400 µl) and the pellets fixed for a further 12 h at 4°C. After this time, the pellets were processed for cryoultramicrotomy and labelled as described in Section 2.9.3.2. Before interpretation of the labellings was performed, it was necessary to ensure that the phagosome was maturing and that the protein A-gold used to detect the antibody-labelled antigens would not non-specifically recognise and bind to the Fc region of human IgG adsorbed to the latex bead. This would result in false positive labelling for granule marker proteins as it would not be possible to distinguish protein A-gold bound to human IgG from protein A-gold bound to an antibody against a granule marker protein that has fused with the phagosome. IgG-coated latex beads were, therefore, fixed as described above and labelled with protein A gold. In choosing the latex bead for this particular experiment, the suggestions of de Chastellier and Thilo (1997) were implemented and 1 µm beads that were amine-modified to improve the surface hydrophilic characteristics were used.

Scanning electron microscopy. To obtain an indication of when phagocytosis commenced, PMNLs were allowed to adhere to poly-L-lysine coated coverslips and phagocytosis was allowed to progress as described above. The cells were fixed (1 h, RT) and processed for SEM (Section 5.4.2).

5.2.3 Results and Discussion

For the purpose of this study, we were particularly interested in the fusion kinetics of the TIMP-1 vesicle with respect to that of its *in vivo* target molecules [the MMPs, which conveniently are granule markers themselves (proMMP-8, specific granules; proMMP-9, specific and gelatinase granules)] and other granule markers (lactoferrin for the specific granules and MPO for the azurophil granules). The following pattern of incorporation of various proteins into the phagosome was hypothesised prior to labelling (Table 5.1).

Table 5.1 **Anticipated order of granule release into the phagosome containing IgG-opsonised 1 μm amine-modified latex beads engulfed by unprimed/resting PMNLs.**

Order into phagosome	Granule type	Protein components
First	Secretory	GPI-proteins (including IgG receptor)
Second	Gelatinase	ProMMP-9
Third	Specific	Lactoferrin, proMMP-8, pro-MMP-9
Fourth	Azurophil	MPO
?	TIMP-1	TIMP-1

The labelling seen in this study was shown to be specific as human IgG-adsorbed latex beads incubated with protein A gold (Figure 5.1 B) showed no non-specific affinity for protein A. Therefore, none of the gold labelling present in latex bead phagosomes in cell sections is due to non-specific interactions of protein A-gold with the adsorbed human IgG. This is not unexpected, as the immunoreactivity of the adsorbed human IgG would, theoretically, have been blocked during fixation of the PMNLs (i.e. prior to cryoultramicrotomy and immunocytochemistry) and, hence, rendered unable to bind protein A (Slot and Geuze, 1984; 1985). Nonetheless, it was considered necessary to confirm that this was the case. Figure 5.1 C shows a high magnification view of the phagosome and shows that the surface of the bead and the bilayer membrane surrounding it, are not closely apposed to each other, as is the case with non-maturing phagosomes. Furthermore, Figure 5.3 B shows some membrane recycling from the phagosome (possibly to redisplay receptors on the plasma membrane surface) which further substantiates a phagosome maturation process.

Initial contact of the PMNLs with the latex beads and the onset of phagocytosis occurred after approximately 5 minutes (Figure 5.1 A). During this time, the beads become surrounded by the pseudopodia (mediated by actin filaments) and the separated phagosomal compartment are sealed off and released from the plasma membrane and into the cytoplasm. In comparison to previous investigations (Bainton, 1973; Segal *et al.*, 1980), the PMNL phagocytic kinetics described here are considerably slower. This is possibly due to the fact that the PMNLs in this study were not primed before phagocytosis. The elegant TEM histochemical study of phagocytosis kinetics and order of fusion by Dorothy Bainton (Bainton, 1973) involved PMNLs that were primed with *S. typhosa* LPS β and phagocytosis was reported to occur 30 seconds after incubation of the PMNLs with *E. coli*. The latex bead study of Segal *et al.* (1980) did not involve priming, but PMNLs and the latex beads were "...rapidly stirred in a chamber - a

process that results in the rapid uptake of the particles". Both priming (Bainton, 1973) and vigorous collision-induced phagocytosis (Segal *et al.*, 1980) would have been unsuitable for this particular study, since cell damage and/or degranulation may be induced using these methods. Such damage and degranulation, prior to phagocytosis, could complicate studies on the order of granule release into the phagosome due to the possible inclusion of such externally released proteins from damaged cells into the phagosome of non-damaged cells. Although the kinetics of uptake of latex beads in this study is slower than previously reported, the lag in phagocytosis also implies that no 'activation' or priming occurred during PMNL isolation and this was considered highly desirable.

The inclusion of the secretory vesicle components did not require confirmation by means of immunocytochemical labelling since binding and uptake of the latex beads by the PMNLs should have been dependent on binding of the GPI-anchored IgG receptor (FcγIIIRB/CD16b). There appeared to be no fusion of the gelatinase granule with the phagosome since no proMMP-9 labelling (10 nm gold) was evident in the phagosome throughout the entire phagocytic period (1 h). The granule appeared to remain within the cytoplasm and some extracellular release and association of proMMP-9 with the plasma membrane was evident (results not shown). Previous studies have shown that proMMP-9, like both HNE and lactoferrin, may remain electrostatically associated with the plasma membrane after degranulation (Gaudin *et al.*, 1997). In contrast, lactoferrin became incorporated into the phagosome within 10-20 min and this was evident by the appearance of 10 nm gold particles within the phagocytic vesicle (Figure 5.2 A). From the results obtained with the labelling for lactoferrin, it was presumed that a similar pattern would emerge upon labelling for proMMP-8, which also resides in the specific granule. This was found to be untrue; the majority of proMMP-8 appeared to remain non-fusogenic with the phagosome (Figure 5.2 B). A relatively low density of proMMP-8 labelling was found in the phagocytic compartment, but this never exceeded more than ~5 gold particles per bead (Figure 5.2 B) (compared to >15 particles/bead obtained with lactoferrin). Although it is not correct to compare labelling densities for two different antibodies (with different titres and avidities) and two different antigens (of possibly unequal amounts within a cell), comparison of the relative concentration of the same antigen in *different* organelles, labelled at the same time may be validly made by comparing their relative labelling densities. On the basis of this (i.e. comparing the labelling obtained in the phagosome with that seen in specific granules), the relative amount of proMMP-8 released into the phagosome was very low.

The appearance of MPO within the phagosome after 1 h (Figure 5.3 A) indicated that phagocytosis was complete and that the organelle had fully matured. Throughout the entire course of phagocytosis, the TIMP-1 vesicle (like the gelatinase granule and the majority of proMMP-8-positive specific granules) remained non-fusogenic with the phagosome (Figure 5.3 A, large arrow). These results are interesting since they imply that the PMNL may possess a mechanism for the selective inclusion of relevant granules into the phagosome. Simply put, the PMNL may recruit only granules containing useful receptors and luminal proteins for phagocytic destruction. This would explain the failure of proMMP-8- and proMMP-9-containing granules and TIMP-1 vesicles to fuse with the phagosome, as these proteins would not be anticipated to have bactericidal properties These results suggest that the other (as yet unidentified) proteins in the TIMP-1 vesicle and gelatinase granules may not be involved in the destruction of IgG-opsonised, phagocytosed microorganisms.

The results from the phagocytosis study raised one main question, that of how the PMNL maintain selective granule fusion during phagocytosis, i.e. how the PMNL excludes the TIMP-1 vesicle, gelatinase granules and proMMP-8-positive specific granules from the phagosome, while permitting fusion of secretory vesicles, lactoferrin-positive specific granules and azurophil granules. The TIMP-1 vesicle and proMMP-9 positive granules may not associate with the simple microtubules that have been shown to bind azurophil granules and lactoferrin-positive specific granules (Rothwell *et al.*, 1989). Association with different cytoskeletal components or non-association may be responsible for preventing the fusion of proMMP-9 and TIMP-1 with the phagosome, as Schettler *et al.* (1991) found that the majority of proMMP-8 and -9 are not associated with the cytoskeleton (see Table 5.2). This potential differential association of granules with cytoskeletal elements was studied using the method of Rothwell *et al.*, (1989).

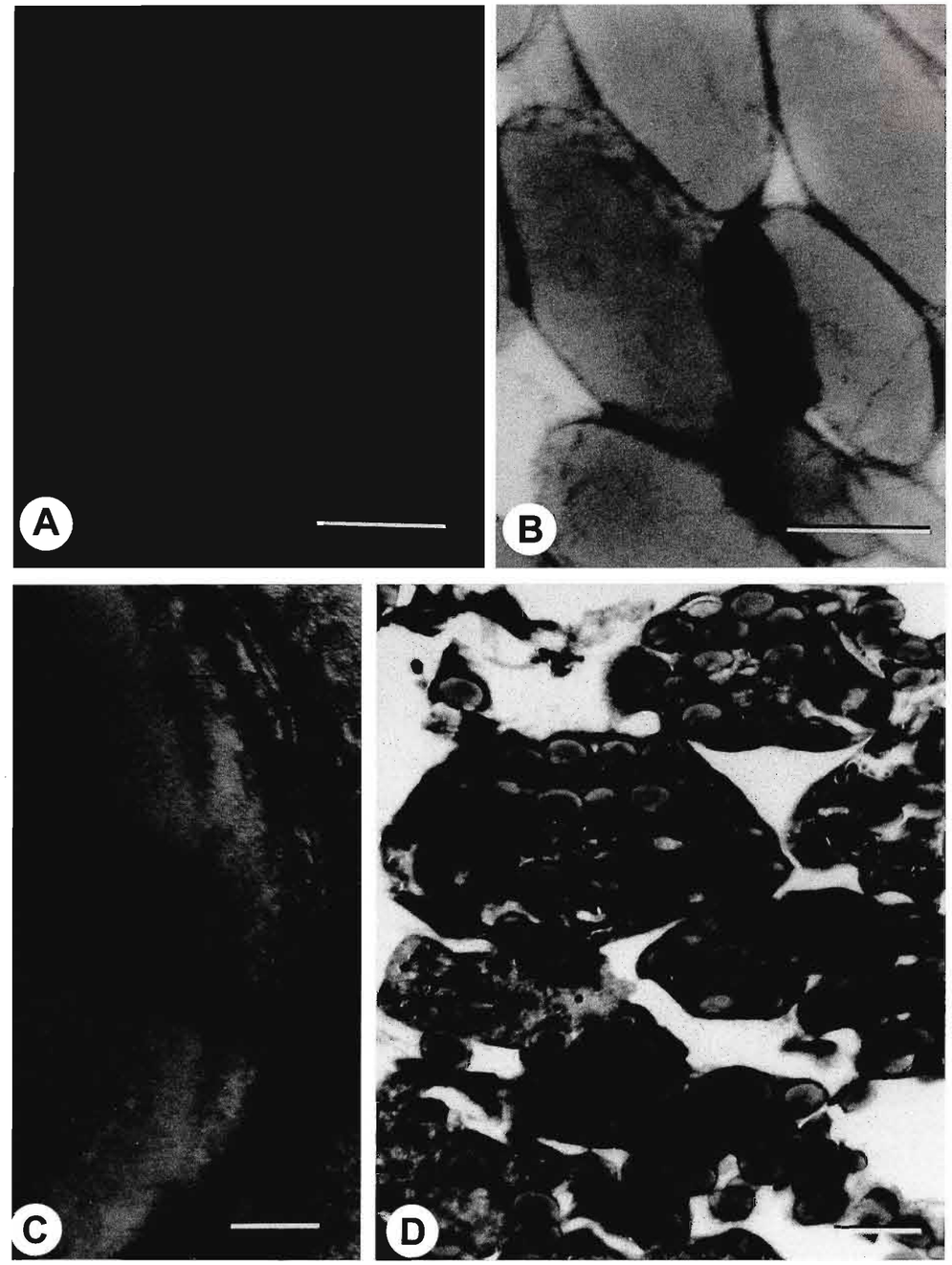

Figure 5.1 **Phagocytosis of human IgG opsonised amine modified 1 μm latex beads by PMNLs.** A), SEM image showing ingestion of latex beads by purified PMNLs. Two beads appear associated with the plasma membrane (presumably via FcγIIIRB receptors), while the PMNL extends filopodia to engulf other beads within close proximity. Bar = 2 μm. B), Latex bead control. Latex beads were opsonised with human IgG, fixed and incubated with protein A gold (10 nm) to assess whether protein A exhibits affinity towards human IgG species purified by PEG precipitation and to ensure that subsequent immunolabelling of the phagosome are not due to binding of human IgG on the IgG-opsonised bead. No binding of protein A is visible. Bar = 500 nm. C), High magnification of a phagocytosed latex bead, showing the lipid bilayer of the phagosomal membrane (arrow). Note that the membrane is not closely apposed to the surface of the latex bead and this indicates that the surface characteristics (i.e. amine-modification and IgG opsonisation) permit maturation of the phagosome. Bar = 50 nm. D), Overview of PMNLs that have ingested latex beads (1 h). A number of PMNLs have ingested multiple beads that are easily visible in the cytoplasm. The ability of PMNLs to phagocytose opsonised particles is retained throughout the duration of the experiment. Bar = 200 nm.

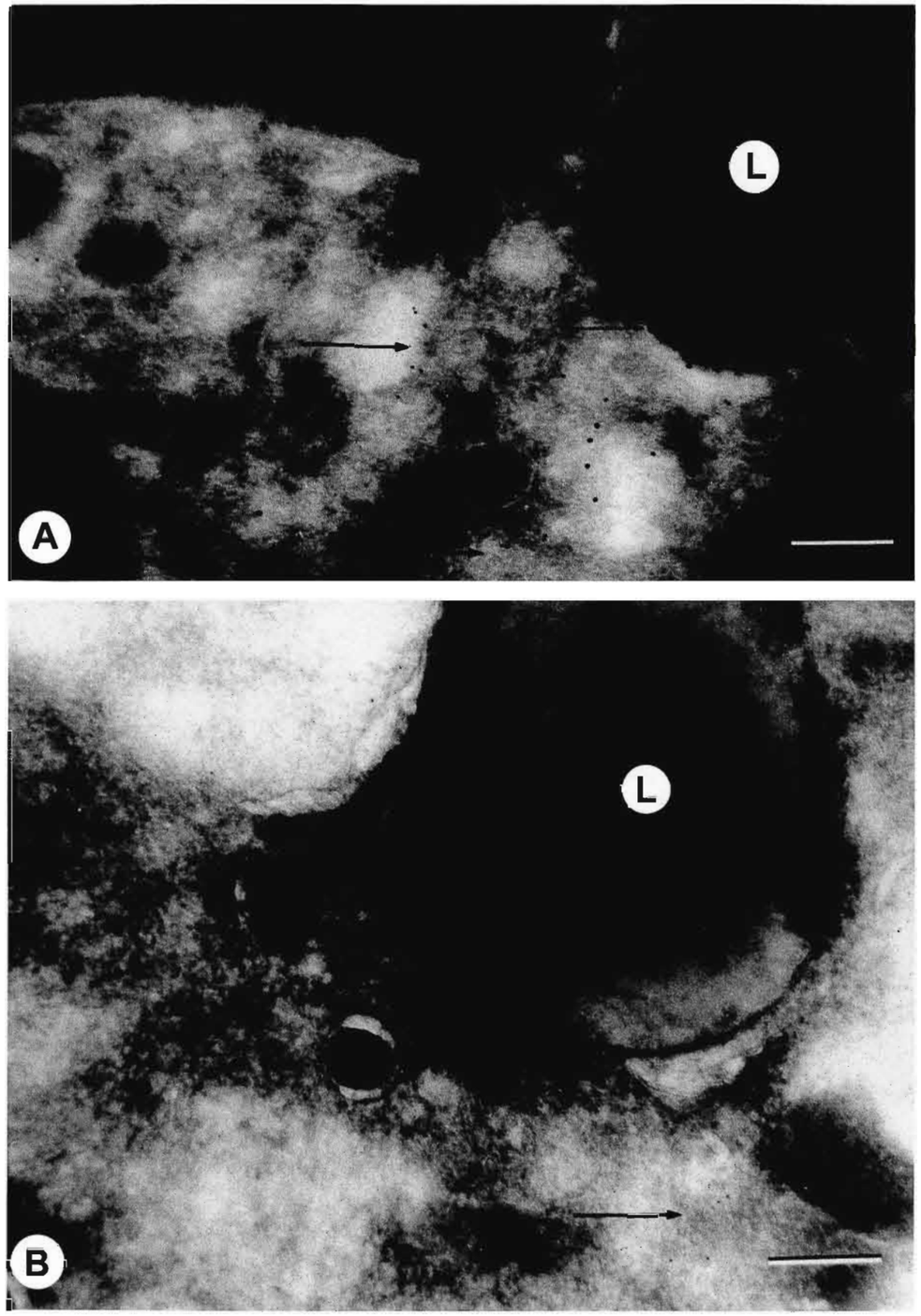

Figure 5.2 **Immunolocalisation of TIMP-1 with respect to the specific granule marker proteins, lactoferrin and proMMP-8, on thawed PMNL cryosections after 20 min phagocytosis of IgG-opsonised 1 μm latex beads.**

A), TIMP-1 (5 nm) and lactoferrin (10 nm). Lactoferrin has entered a number of phagosomes (right-hand side; small, thin arrow) while the electron translucent organelle containing TIMP-1 remains separate (large, thick arrow). Bar = 200 nm. B), TIMP-1 (5 nm) and proMMP-8 (10 nm). TIMP-1 (large, thick arrow) remains non-fusogenic with the phagosome (L), but some proMMP-8 entered (small, thin arrow). Bar = 200 nm.

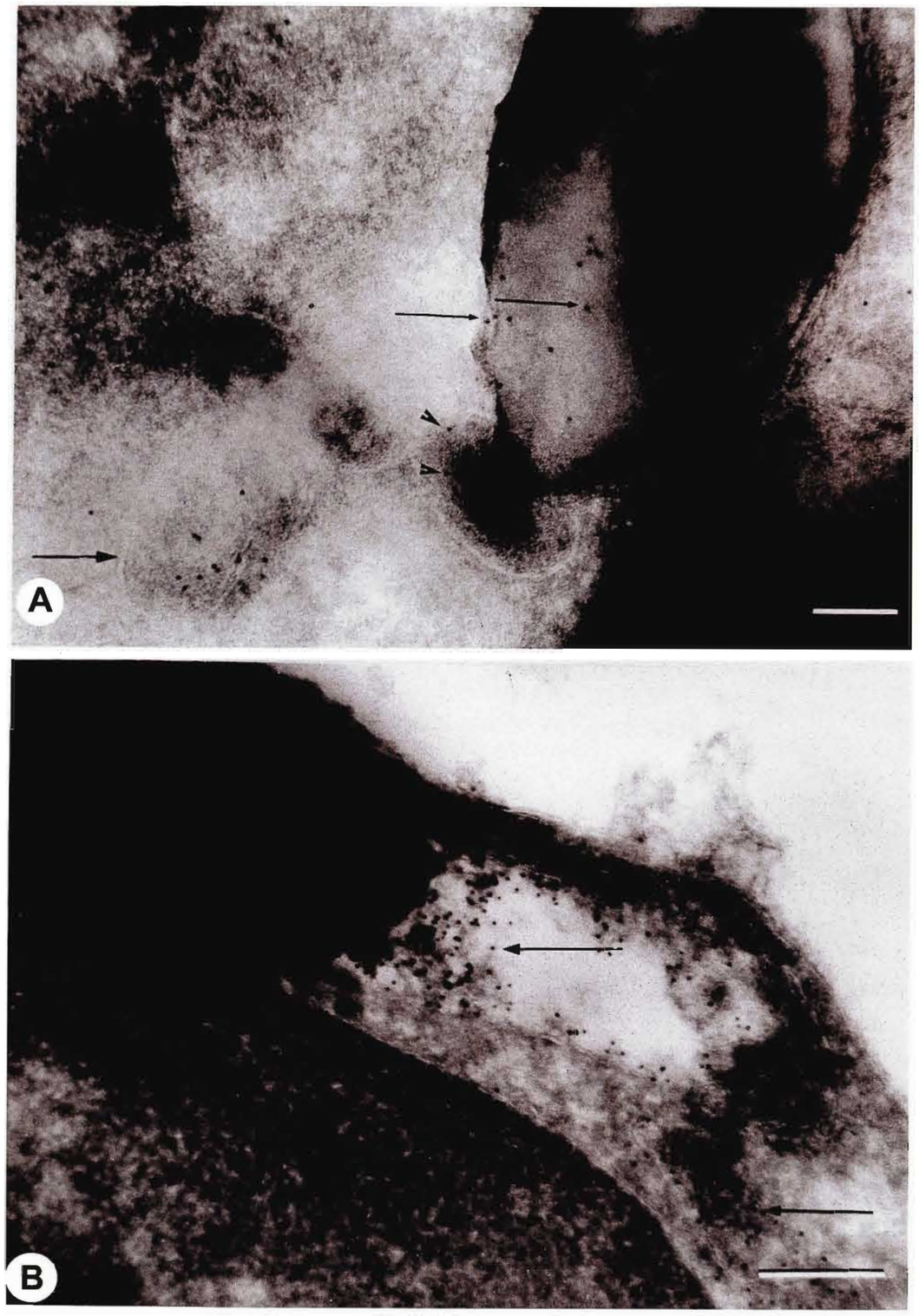

Figure 5.3 **Immunolocalisation of TIMP-1 with respect to the azurophil granule marker protein, MPO and the specific granule marker protein, lactoferrin, on thawed PMNL cryosections after 1 hour phagocytosis of IgG-opsonised 1 μm latex beads.**

A), TIMP-1 (5 nm) and MPO (10 nm). The phagosomes are filled with MPO (small, thin arrows), indicating that the phagosome has fully matured. Some MPO-positive azurophil granules have yet to fuse with the phagosome (large, thick arrow). No TIMP-1 has fused with the phagosome after 1 h ingestion (arrowhead). Bar = 100 nm. B), TIMP-1 (5 nm) and lactoferrin (10 nm). The phagosome has begun to recycle its contents by pinching off into small pleiomorphic electron translucent vesicles (arrow indicates lactoferrin). TIMP-1 is not visible in the section. The exact destination of the vesicles is not known, but is presumed to be the plasma membrane, perhaps to assemble the NADPH oxidase and expose it to the extracellular fluid to destroy uningested pathogens. Bar = 200 nm.

5.3 Preparations of PMNL actin and tubulin and visualisation of granule interactions

A study performed by Rothwell *et al.* (1989), demonstrating differential association of PMNL granules with tubulin (microtubules) achieved by lysing PMNLs, spreading the lysate onto nickel grids (with or without purified tubulin) and examining these grids, under the TEM after immunocytochemical labelling was seen to provide good visualisation of granule-tubulin interactions. Using this technique, it was established that MPO-positive (azurophil granules) and lactoferrin-positive (specific granules) associated with tubulin (microtubules). The number of these granules binding to tubulin increased following fMLP stimulation (prior to cell lysis) or following addition of the ATPase inhibitor, sodium orthovanadate (Na_3VO_4), while granule associations decreased in the presence of *N*-ethylmaleimide. From these observations, it was suggested that attachment of granules to tubulin is via a kinesin-like system.

The studies of Schettler *et al.* (1991), provided evidence that MMP-8-positive granules (perhaps a subset of the specific granules) and gelatinase granules, unlike azurophil and lactoferrin-positive specific granules, do not appear to associate with the cytoskeleton (Table 5.2). Experiments involving incubations in colcemid (to depolymerise microtubules) and cytochalasin B (to depolymerise F-actin), followed by centrifugation and analysis of the granule pellets or supernatants, demonstrated that MMPs were released by degranulation when microfilaments were depolymerised. This release is, however, not due to these granules associating with or binding microfilaments. Resting PMNLs possess polymerised actin networks immediately beneath the plasma membrane that are thought to prevent the accidental release of granule contents into the extracellular fluid (Hoffstein and Weissmann, 1978). Depolymerisation of this network allowed granules that do not associate with tubulin (i.e. lactoferrin-negative, proMMP-8-positive specific granules and proMMP-9-positive specific and gelatinase granules) to fuse with the plasma membrane and release their contents. Azurophil granules and lactoferrin-positive-specific granules were not released by this treatment as, although the subplasmalemmal actin network is disassembled by cytochalasin to allow fusion with the plasma membrane, these granules still remain associated with the intact microtubules. Depolymerisation of microtubules, on the other hand, prevented the release of all granule populations examined since the subplasmalemmal actin network acts as a barrier, preventing all granules from fusing with the plasma membrane.

Table 5.2 **Differential partitioning of PMNL granule proteins following lysis, differential centrifugation and assay by ELISA (Schettler *et al.*, 1991).**

	Supernatant fluid	Pellet
HNE	22%	78%
MPO	36%	64%
Lactoferrin	14%	86%
MMP-8	90%	10%
MMP-9	95%	5%

The focus of this section of the study was to establish how the mobilisation of the TIMP-1 vesicle is regulated and as a first step to this end, the method of Rothwell *et al.* (1989) was used to visually assess whether the TIMP-1 vesicle associates with either F-actin (microfilaments) or tubulin (microtubules).

Cytoskeletal components, unlike other intracellular structures (e.g. membranes, nucleus and organelles), are difficult to visualise by conventional TEM and immunocytochemistry in whole cell sections due to the difficulty in obtaining sections, that expose the entire longitudinal aspect of microfilaments or microtubules (Langanger and de Mey, 1989). In addition, the dynamic nature of the cytoskeletal system - cycling between polymerisation and depolymerisation occurs at a rapid rate - is highly sensitive to various chemical (pH, nucleotide binding, ionic strength), physical (temperature) and biochemical regulators (capping proteins, severing proteins). In order to ensure that the cytoskeleton is preserved during fixation, these factors need to be considered when choosing a fixation regime.

In designing the current experiment, care was taken to maximise the recovery of polymeric actin and tubulin after cell lysis. This involved ensuring the correct biochemical and physical conditions as summarised below (Table 5.3). Polymeric tubulin is sensitive to the same conditions as those displayed in Table 5.3, except that polymeric tubulin preferentially binds GTP rather than ATP (although ATP will still bind polymeric tubulin and preserve integrity) (Dustin, 1978; Langanger and de Mey, 1989). The calcium specific chelator, EGTA, was used to promote polymerisation of both G-actin and tubulin. Therefore, in order to promote the stabilisation of F-actin, a buffer of low pH and high ionic strength, containing a calcium chelator, is required. Thereafter, to irreversibly 'lock' the polymeric F-actin and tubulin and thereby prevent dilution-mediated depolymerisation (Langanger and de Mey, 1989), phalloidin (from *Amanita phalloides* mushroom) and paclitaxel/taxol (from *Taxus yannanensis* tree bark)

were used (Thomas, 1982). Na_3VO_4 was included to improve the yield of bound granules by decreasing the rate of ATP hydrolysis by ATPases (Rothwell *et al.*, 1989). ATP was included to bind the ATPase, thereby possibly ensuring correct conformation and efficient binding of granules (possibly via adaptor proteins) to the cytoskeletal components.

Table 5.3 Factors influencing actin polymerisation status.
After Langanger and De Mey, 1989.

	F-actin (polymer)	G-actin (monomer)
pH	5-6	8-9
Ionic strength	100 mM NaCl	Low ionic strength (<<100 mM NaCl)
Nucleotide preference	ATP	ADP
Cation preference	Mg^{2+}	Ca^{2+}
Temperature	37°C	4°C

5.3.1 Reagents

100 x ATP stock solution (100 mM). Na_2ATP (0.05 g) was dissolved in actin/microtubule stabilising buffer (1 ml) just before use.

100 x AEBSF stock solution (100 mM). AEBSF (0.03 g) was dissolved in actin/microtubule stabilising buffer (1 ml) just before use.

100 x EGTA stock solution (100 mM). EGTA (0.05 g) was dissolved in actin/microtubule stabilising buffer (1 ml) just before use.

100 x Na_3VO_4 stock solution (1.5 mM). Na_3VO_4 (0.03 g) was dissolved in microtubule buffer (1 ml) just before use.

Paclitaxel stock solution (1 mM). Paclitaxel (1 mg) was dissolved in DMSO (1 ml) and kept at -20°C.

Biotinylated phalloidin stock solution (1 mM). Biotinylated phalloidin (1 mg) was dissolved in DMSO (1.26 ml) and kept at -20°C.

Actin buffer [20 mM imidazole, 100 mM KCl, 2 mM $MgCl_2$, 0.02% (w/v) NaN_3, pH 7.5 at 37°C]. Imidazole (0.068 g), KCl (0.373 g), $MgCl_2.6H_2O$ (0.02 g) and NaN_3 (0.01 g) were dissolved in dd.H_2O (~30 ml) and heated to 37°C. The pH was titrated to 7.5 with HCl, made up to 50 ml in a volumetric flask and stored at 4°C.

Actin stabilising buffer [20 mM imidazole, 100 mM KCl, 2 mM $MgCl_2$, 1 mM EGTA, 1 mM ATP, 1 mM AEBSF, 5 µM phalloidin, 0.02% (w/v) NaN_3, pH 7.5 at 37°C]. EGTA (10 µl of stock solution), Na_2ATP (10 µl of stock solution), AEBSF (10 µl of stock solution) and phalloidin (5 µl) were added to 965 µl actin buffer just before use.

Microtubule buffer [10 mM PIPES, 2 mM $MgCl_2$, 5% (v/v) glycerol, 0.02% (w/v) NaN_3, pH 6.9 at 37°C]. PIPES (0.162 g), $MgCl_2.6H_2O$ (0.02 g), glycerol (2.5 ml) and NaN_3 (0.01 g) were dissolved in dd.H_2O (~30 ml) and heated to 37°C. The pH was titrated to 6.9 with HCl, made up to 50 ml in a volumetric flask and stored at 4°C.

Microtubule stabilising buffer [10 mM PIPES, 2 mM $MgCl_2$, 1 mM EGTA, 1 mM ATP, 15 µM Na_3VO_4, 1 mM AEBSF, 5% (v/v) glycerol, 2 µM paclitaxel, 0.02% (w/v) NaN_3, pH 6.9 at 37°C]. EGTA (10 µl of a stock solution), Na_2ATP (10 µl of stock solution), Na_3VO_4 (10 µl of stock solution), AEBSF (10 µl of stock solution) and paclitaxel (2 µl) were added to 968 µl microtubule buffer just before use.

Fixative solution [2% (v/v) glutaraldehyde in actin/microtubule buffer]. Glutaraldehyde (80 µl) was added to 920 µl of either actin or microtubule buffer just before use.

Negative stain solution [2% (w/v) uranyl acetate in dd.H_2O]. Prepared as per Section 2.9.3.1.

5.3.2 Procedure

PMNLs were isolated from whole blood (100 ml) (Section 2.7.2), resuspended in PBSG (2 x 1 ml) and allowed to incubate for 10 min on ice. PMNLs were spun down gently and re-suspended in either actin stabilising buffer (containing phalloidin, AEBSF and ATP) or microtubule stabilising buffer (containing paclitaxel, AEBSF and ATP) (100 µl, 30 min, 37°C). PMNLs were lysed by sonication (4 x 30 s) and passage through a 22-gauge needle (5 strokes). The lysed cells were spun (100 x g, 5 min, 37°C) and the supernatant fluid was split into

aliquots (4 x 25 µl). Each aliquot was treated with either the addition or omission of EGTA and Na_3VO_4 as outlined below (Table 5.4). The solutions were incubated (30 min, 37°C) before a 10 µl aliquot was taken from each Eppendorf tube and dispensed onto Parafilm. Formvar coated nickel grids were placed face down on the droplets and the cytoskeletal preparations (containing attached granules and vesicles) allowed to adsorb (10 min, RT). The grids were transferred to fixative [2% (v/v) glutaraldehyde in stabilising buffer] (10 min), washed thoroughly in PBS and immunolabelled for either proMMP-8, proMMP-9 or TIMP-1 and detected with 10 nm protein A gold as described in Section 4.3.2. The grids were washed in dd.H_2O (5 x 2 min) and negatively stained with 2% (w/v) aqueous uranyl acetate (10 min). The grids were dried by touching on filter paper, air-dried and stored on double-sided adhesive tape.

Table 5.4 **Protocol outlining the selective inclusion or omission of Na_3VO_4 and EGTA in PMNL cytoskeletal preparations to optimise granule binding to F-actin or polymeric tubulin.**

Actin	+ EGTA?	+ Na_3VO_4?	Tubulin	+ EGTA?	+ Na_3VO_4?
1	✔	✔	1	✔	✔
2	✔	✘	2	✔	✘
3	✘	✔	3	✘	✔
4	✘	✘	4	✘	✘

5.3.3 Results and Discussion

Despite its use in cellular structure measurement, a disadvantage of negative staining lies in its tendency to obscure cell morphology and, therefore, some detail is lost. Nonetheless, the results shown in Figure 5.4 indicate that the experimental protocols were successful in promoting and stabilising the cytoskeletal filaments, but the number of granules binding to the filaments were low and time consuming to locate. In general, the majority of the granules were found to be unassociated, but Figure 5.4 A-C show that a small number of granules were associated with the cytoskeleton. This low level of binding was also reported by Rothwell *et al.* (1989) who found that the average number of granules bound per microtubule polymer (average length = 2 µm) was between 0.125 and 0.14 for MPO-positive granules and between 0.28 and 0.3 for lactoferrin-positive specific granules. Both F-actin and polymeric tubulin strands have distinct diameters ($\phi_{F\text{-}actin}$= 5-7 nm; $\phi_{tubulin}$= 25 nm) that were measured and used in identification of the cytoskeletal elements. Granules binding to cytoskeletal elements resembling tubulin, did not label for either TIMP-1, proMMP-8 or -9. Tubulin-bound granules might, therefore, represent

azurophil granules.

Granules labelling for proMMP-9 (Figure 5.5 A) and TIMP-1 (Figure 5.5 B) were, however, found to be associated with two relatively complex cytoskeletal structures, the three-dimensional nature of which is apparent with the negative stain. This structure may possibly represent actin networks since F-actin does form interstrand complexes (Langanger and De Mey, 1989; Edwards, 1994). In addition, myosin interacts with actin and is responsible for movement of F-actin strands relative to each other (Edwards, 1994). Simple morphological scrutiny and measurement, therefore, did not assist in the identification of the cytoskeletal complex as the known measurements for tubulin and actin ($\phi_{F\text{-}actin}$= 5-7 nm; $\phi_{tubulin}$= 25 nm) did not correspond to the thickness of either of these structures. The identity of this complex would, however, be relatively straightforward to solve if streptavidin-gold was used to bind the biotinylated phalloidin used to stabilise the F-actin structures (Harlow and Lane, 1988; Griffiths, 1993).

The current study demonstrated that TIMP-1 and proMMP-9 are associated with cytoskeletal structures, morphologically dissimilar to the easily identifiable tubulin or F-actin to which other granules were associated. The majority of the labelled granules were found free on the formvar grids and it is unknown whether the low level of cytoskeletal association is reflective of the true *in vivo* biochemical environment or if this is the result of the sonication technique employed to lyse the PMNLs. The results suggest minimal association of proMMP-9 containing granules (as described by Schettler *et al.*, 1989) and TIMP-1 vesicles with a cytoskeletal structure different to that bound by other granules. These results seem to offer a potential explanation for the observed non-release of TIMP-1 and proMMP-9 into the phagosome while all other granules appeared to fuse during phagocytosis of IgG-opsonised latex beads.

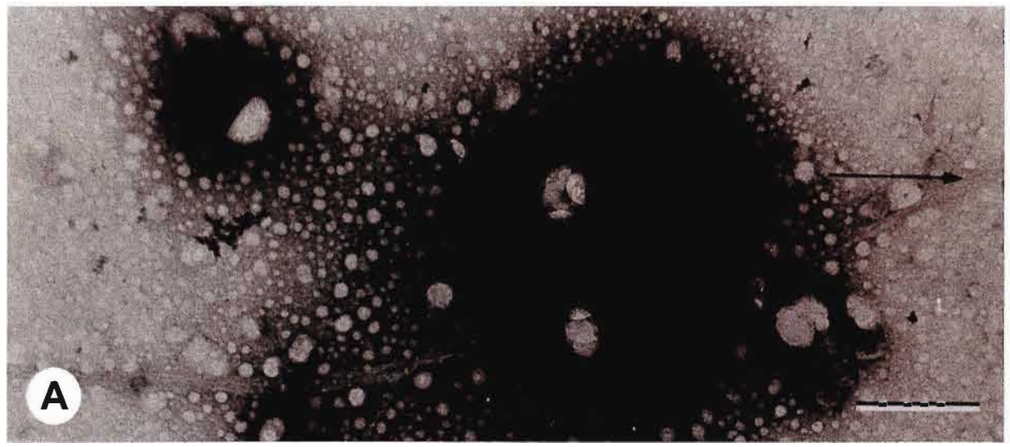

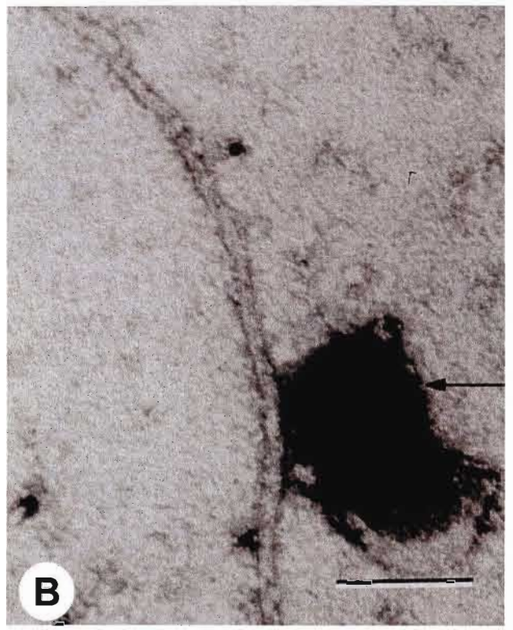

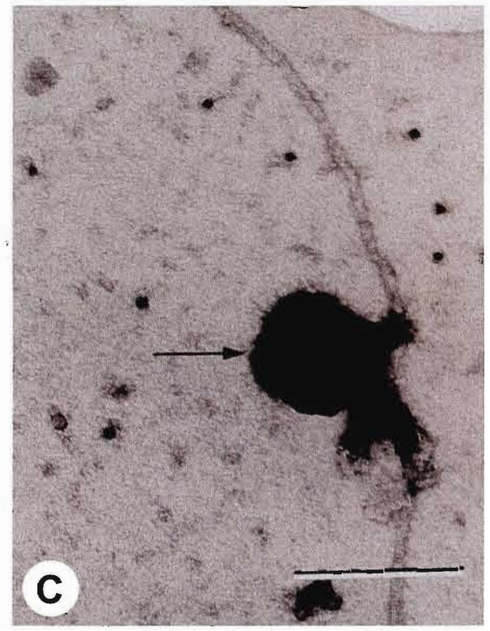

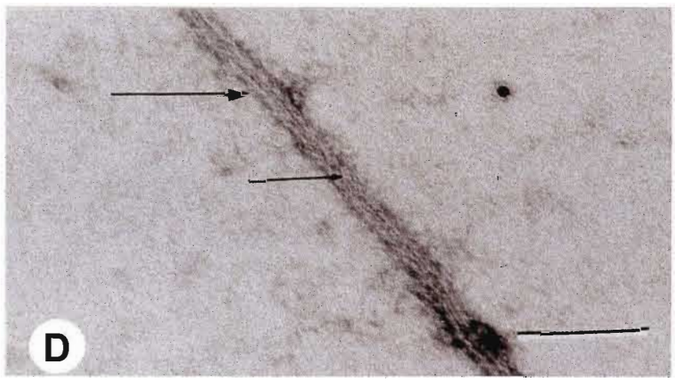

Figure 5.4 **Stabilised microfilaments and microtubules bound to PMNL granules.**

A), F-actin stabilised with phalloidin. The microfilament has a rope like appearance due to interfilament associations (arrow) and appears to have bound many PMNL granules, none of which labelled for TIMP-1, proMMP-8 or -9. Bar = 400 nm. B and C), Polymeric tubulin stabilised with paclitaxel/taxol. Granules (arrows) bound to tubulin and immunolabelled for proMMP-8, do not label and, therefore, represent granules from a population deficient in proMMP-8, possibly an azurophil granule. Bars = B), 100 nm; C), 200 nm. D), High magnification micrograph of stabilised polymeric tubulin, showing the distinctive inner (small, thin arrow) and outer diameters (large, thick arrow), collectively measuring ~25 nm. Bar = 100 nm.

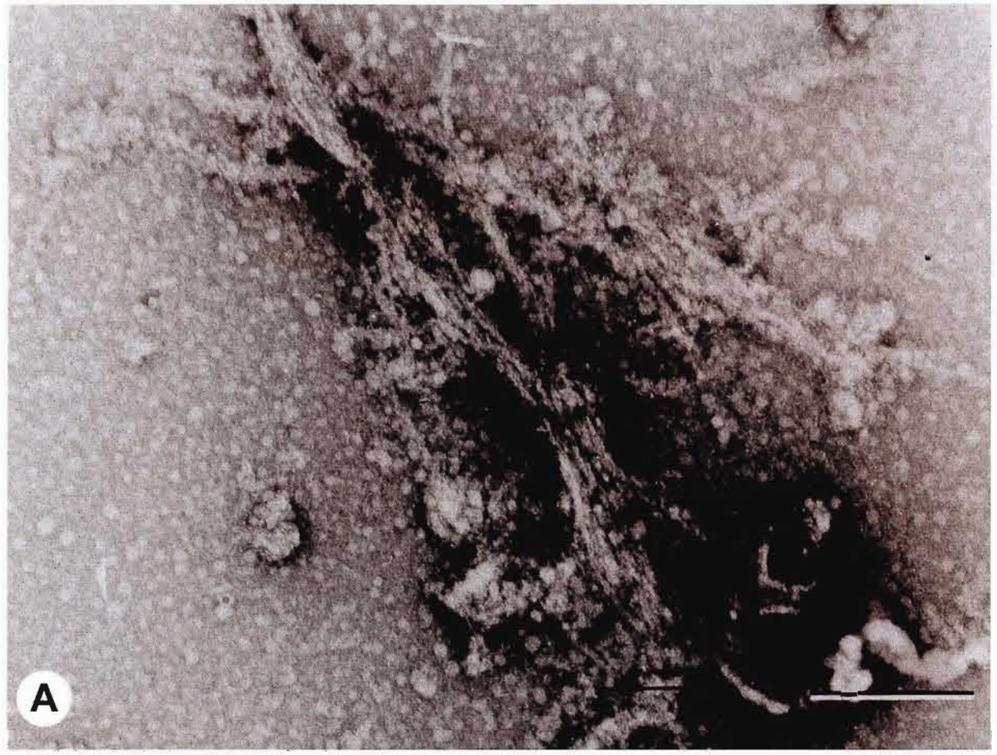

Figure 5.5 **Immunolabelling of PMNL granules bound to stabilised cytoskeletal components for proMMP-9 and TIMP-1.**

A), Immunolabelling for TIMP-1. TIMP-1 localises to a vesicle (arrow) associated with cytoskeletal components unlike those identified in Figure 5.4. Identification by morphology is impossible, and the complex might, therefore, represent complexes between different cytoskeletal components. Bar = 200 nm. B), Immunolabelling for proMMP-9. A proMMP-9 granule (arrow) is bound to a cytoskeletal structure unlike those identified in Figure 5.4. Bar = 200 nm.

In order to understand how the PMNL mobilises granules that do not associate with the cytoskeleton, it was necessary to confirm that the TIMP-1 vesicles, gelatinase granules and proMMP-8-positive specific granules, like all other known PMNL granules, are exocytosed in response to increases in $[Ca^{2+}_i]$. Fusion of granules with the phagosome is generally regulated by both membrane fusion proteins (annexins, SNAREs etc.) and increases in $[Ca^{2+}_i]$. Fusion may, therefore, occur independently of increases in $[Ca^{2+}_i]$ (such as occurs with the SNAP/SNARE proteins) or in concert with increases in $[Ca^{2+}_i]$ (as occurs when the annexins are involved). To understand the lack of fusion of proMMP-8, proMMP-9 and TIMP-1 with the phagosome, it was necessary to assess whether fusion of these organelles is induced by increases in $[Ca^{2+}_i]$. If not, then their lack of fusion with the phagosome may be due to the lack of other conditions appropriate for fusion to be induced by the binding of the relevant membrane fusion proteins.

To assess the Ca^{2+}_i-regulated mobilisation of the TIMP-1 vesicle, proMMP-8-positive specific granule and the gelatinase granule, PMNLs were permeabilised with the liposoluble ionophore, ionomycin, and the $[Ca^{2+}_i]$ was increased using a buffer system containing increasing levels of Ca^{2+}. Detection of the release of the various granule populations, induced using ionomycin and Ca^{2+}-containing buffers, was, therefore, achieved by assaying for HNE (by fluorimetry), lactoferrin (by ELISA) and proMMP-8 and -9 (by collagen and gelatin zymography, respectively), while TIMP-1 was detected by western blotting. In order to perform novel zymographic assays to detect proMMP-8 release, rat skin type I collagen was isolated and the purity and structural integrity of the collagen isolates were assessed by SDS-PAGE and scanning EM (SEM), respectively.

5.4 Isolation and characterisation of type I collagen for the detection of MMP-8 release

Despite their lack of tertiary collagen-like structure, once thought to be crucial for recognition and binding of MMPs, the different peptide substrates available for the various subclasses of the MMP family show good specificity [though some investigations involving the synthesis of covalently linked tripeptide derivatives have been carried out to improve substrate specificity by mimicking the trimeric structure of collagen (Goli *et al.*, 1992)]. The development of these 7-methoxycoumarin fluorogenic peptide substrates (using dinitrophenyl groups as internal quenchers) allows rapid, sensitive detection of collagenolytic activity (nanomolar to picomolar range depending on the MMP) (Netzel-Arnett *et al.*, 1991; Knight *et al.*, 1992).

At the commencement of the current investigation it was, however, reasoned that detection of MMP-8 or MMP-9 activity in crude PMNL homogenates using fluorogenic substrates would be unsuccessful given the fact that PMNL homogenates contain the endogenous inhibitor, TIMP-1.

Type I collagen is the preferred substrate for the PMNL interstitial collagenase, MMP-8 (Birkedal-Hansen, 1987; Cawston and Barrett, 1979; Harris and Vater, 1980; Murphy *et al.*, 1980; Cawston and Murphy, 1981; Murphy *et al.*, 1982; Hasty *et al.*, 1990). The MMP cleaves the heterotrimeric collagen complex at a single site (Gly^{775}-Leu^{776} and Gly^{775}-Ile^{776}), thus generating the so-called ¾ (TC^A) and ¼ (TC^B) fragments. These fragments have lower melting temperatures (T_m TC^A = 32°C, T_m TC^B = 28°C) than the original trimer (TC T_m = 40-41°C) (Harris and Vater, 1980) and are, therefore, more susceptible to further degradation by the relatively non-specific gelatinases at physiological temperature.

Although the detection of interstitial collagenase (such as MMP-8 and MMP-1) activity by identifying the fragment patterns produced is highly specific, the assays require long incubation times (16-24 h) and enzyme detection is further delayed by the need to separate the generated fragments by SDS-PAGE and subsequently to stain and destain the gel. To improve the sensitivity and decrease the amount of time (4 h-16 h) required to assay fractions of potential collagenolytic activity, Cawston and Barrett (1979) introduced a simple method for the purification of type I collagen from rat skin and radioactive labelling using [1-^{14}C] acetic anhydride. Detection of type I collagen degradation is made possible by precipitating the ¾ fragment and intact, undigested collagen using dioxane or by centrifugation, leaving the ¼ fragment in the supernatant and allowing detection by scintillation counting.

Methods for the detection of gelatinolytic activity by zymography have been extensively published, however, and are suitable for crude samples containing both MMPs and TIMPs. Unfortunately, at the commencement of this study, no zymographic method for the detection of type I collagenase (e.g. MMP-8) activity had been reported. In order to develop such a method, type I collagen was purified from rat skin according to the method suggested by Cawston and Barrett (1979).

5.4.1 Purification of rat skin type I collagen

The type I collagen isolation procedure of Cawston and Barrett, 1979 provides large amounts of pure type I collagen in quantities that would otherwise be prohibitively expensive if purchased commercially. This collagen was used to develop and optimise a type I collagenase zymography method for the detection of MMP-8 instead of using the less convenient radioactivity method used by Cawston and Barrett, 1979. Zymography allows detection of both latent and active MMP species since both are active after electrophoresis (since the SDS allows dissociation of the pro-peptide cysteine switch and allows enzyme activity without autocatalytic cleavage of the pro-peptide and M_r reduction) - an advantage over both the fibril degradation/fragmentation assay and any fluorogenic peptide assay.

5.4.1.1 Reagents

All stock solutions were autoclaved and stored at 4°C.

NaCl stock solution [20% (w/v) in dd.H_2O]. NaCl (2 kg) was dissolved in dd.H_2O (~8 *l*) and made up to 10 *l*.

Acetic acid stock solution (5 M). Acetic acid (286 ml, ρ = 1.05 g/ml) was added to dd.H_2O (~700 ml) and made up to 1 *l* in a volumetric flask.

Sodium phosphate stock solution (1 M Na_2HPO_4). Na_2HPO_4 (70.98 g) was dissolved in dd.H_2O (400 ml) and made up to 500 ml in a volumetric flask.

All solutions below contained 0.03% (v/v) toluene as a preservative and were not autoclaved. They were stored at 4°C.

NaCl working solution 1 [0.9% (w/v) NaCl in dd.H_2O with 0.03% (v/v) toluene]. NaCl stock solution (450 ml) was diluted to 1 *l* with dd.H_2O and toluene (300 µl) was added.

NaCl dialysis solution 2 [5% (w/v) NaCl in 100 mM acetic acid with 0.03% (v/v) toluene]. NaCl stock solution (6 *l*), acetic acid stock solution (480 ml) were added to distilled water (16 *l*) and made up to 24 *l* and toluene (7.2 ml) was added.

Acetic acid working solutions [500 mM, 200 mM, 100 mM with 0.03% (v/v) toluene]. Acetic acid stock solution (100 ml, 40 ml, 20 ml respectively) was diluted to 1 *l* with dd.H_2O and toluene (300 µl) was added.

Sodium phosphate working solution [20 mM Na_2HPO_4 with 0.03% (v/v) toluene]. Sodium phosphate stock solution (20 ml) was diluted to 1 *l* with dd.H_2O and toluene (300 µl) was added.

5.4.1.2 Procedure

Euthanasia on ten male Wistar rats (~4 months old) was performed by overdose inhalation of anaesthetic, followed by exsanguination. The skin was shaved with a scalpel blade until it was completely free of hair. The skin was removed using a scalpel blade, and subcutaneous tissue was removed from the skin. Small pieces of skin (~2 cm x 4 cm, 90 g) were snap frozen in liquid nitrogen and stored at -80°C.

Pieces of skin (90 g) were extracted with 0.9% (w/v) NaCl (3 x 1.5 *l*, 3 x 30 min) in a beaker that was mixed continually with a magnetic stirrer bar. The solution was filtered through cheesecloth and the insoluble debris extracted with ice-cold distilled water (2 x 1 *l*, 2 x 30 min). The tissue was resuspended in 500 mM acetic acid (2 x 1 *l*, 2 x 12 h) and stirred slowly. The solution was filtered through cheesecloth and the extraction repeated on the insoluble debris. The extracts were combined and centrifuged (7500 x g, 2 h, 4°C). Lipid was removed from the surface of the supernatant and the supernatant was removed gently with a peristaltic pump, taking care not to dislodge the pellet. The supernatant was dialysed against two changes of 5% (w/v) NaCl in 100 mM acetic acid (2 x 12 *l*, 2 x 12 h, 4°C) to precipitate the collagen. The collagen was pelleted by centrifugation (7500 x g, 30 min, 4°C) and the pellets were redissolved in 500 mM acetic acid (3 *l*) and dialysed against 500 mM acetic acid (5 *l*) overnight. The dialysis membrane was placed in a solution of 20 mM Na_2HPO_4 (5 *l*) and dialysed against a further three changes of buffer (20 *l* total) to reprecipitate the collagen. After centrifugation (7500 x g, 30 min, 4°C) the collagen pellets were redissolved in 500 mM acetic acid (2 *l*) and the collagen was reprecipitated by the addition of solid NaCl to 5% (w/v). The collagen was pelleted (7500 x g, 30 min, 4°C), washed once in 20% (w/v) NaCl (1 *l*), resuspended in 500 mM acetic acid (1 *l*) and stirred slowly overnight at 4°C. The solution was centrifuged (30000 x g, 30 min, 4°C), the supernatants removed and dialysed against 100 mM acetic acid (10 *l*, 12 h). The solution was concentrated against crushed PEG 20 kDa (12 h, 4°C) and lyophilised. The

lyophilised collagen was stored in ~10 mg aliquots at -20°C.

5.4.1.3 Results and Discussion

The above isolation method produced sufficient amounts of type I collagen for the development and optimisation of the MMP-8 zymogram. Although the procedure is relatively lengthy (~8 days), the high yield (~1g type I collagen/100 g starting material) and low cost of the method more than compensates for this.

5.4.2 SEM of type I collagen fibrils

The native structure of type I collagen cannot be assayed by assessing its biological function and, therefore, a number of techniques are required to assess the purity of the collagen fraction and to verify that the collagen still maintains its native tropohelical structure when incubated at physiological temperature and pH. To ensure that the purified collagen was not denatured (i.e. gelatin) and that it was still capable of fibril and fibre formation, SEM examination was used to investigate type I collagen gel formation at physiological temperature and pH.

In contrast to TEM, conventional SEM allows 3 dimensional visualisation of the sample topography down to a resolution of 10 nm. As for TEM, SEM requires a vacuum and a potential (10-15 kV) to accelerate electrons emitted from a tungsten filament and allow collision with the sample (Robinson and Gray, 1990). Low energy secondary electrons (2-5 eV) derived from inelastic scatter are drawn away from the sample to a scintillator placed near a Faraday cage of high potential. The electrons are collected, amplified and form an image that is projected onto a cathode ray tube screen. The image is constructed by progressive sweeping of the electron beam across the specimen in what is termed a raster pattern. An increased magnification is the result of decreasing the raster area (Robinson and Gray, 1990).

Sample preparation for SEM analysis involves four steps: fixation, dehydration, critical point drying and metal coating. Fixation regimes differ between cell types, but PMNLs in this study were fixed as for cryoultramicrotomy. Dehydration in an ethanol series of increasing concentration [30-100% (v/v)] follows fixation and is usually performed at room temperature despite solvent effects. Removal of ethanol to produce a fully desiccated sample is achieved by critical point drying (CPD).

The critical point of a compound refers to the combination of temperature and pressure at which the liquid/gas interphase disappears. At the critical point, all liquid undergoes a phase change

into gas with minimal surface to volume alteration. Carbon dioxide and Freon 13 are both suitable for CPD since they both have critical points that are easily attained. Carbon dioxide is the most popular and is used as a transitional fluid in CPD to replace the ethanol. After the liquid carbon dioxide has flooded the sample completely under high pressure and temperature and removed all trace of ethanol, the pressure is gently released to allow CO_2 vapourisation. The sample is kept in a desiccator until mounted and sputter coated. Recently, hexamethyldisilazane (Braet *et al.*, 1997) has been used as a transitional fluid instead of CO_2. After ethanol dehydration, cells are immersed in the hexamethyldisilazane solution (at room temp) and it is allowed to evaporate (~30 min). No specialised equipment is required; the method is less time-consuming and can be performed at room temperature.

Sputter coating involves deposition of a thin layer of gold:palladium (60:40) or carbon on the surface of the specimen to make it conductive. Gold is a popular choice since it does not oxidise over time. During coating, argon gas is introduced into a partially evacuated chamber ($1x10^{-3}$ Torr) of high potential and becomes ionised to gas plasma upon collision with oxygen molecules. The ionised plasma strikes a cathodic metal plate (usually gold) and releases metal particles. The gold is then deposited in a thin layer (~10 nm) onto the specimen. The now-conductive specimen is mounted on a metal stub and examined in an SEM.

5.4.2.1 Reagents

Collagen solubilising solution (50 mM acetic acid, pH 4.0). Distilled H_2O was made up to 100 ml in a volumetric flask. An aliquot (286 µl) was removed and replaced with an equal volume of acetic acid.

1 M NaOH. NaOH (4 g) was dissolved in dd.H_2O (~80 ml) and made up to 100 ml in a volumetric flask.

30, 70 and 90% (v/v) ethanol series solutions. Ethanol (30, 70 and 90 ml respectively) was diluted to 100 ml with dd.H_2O and kept at 4°C.

PBSG was prepared as described in Section 2.7.1.

5.4.2.2 Procedure

Type I collagen (4 mg) was dissolved in 50 mM acetic acid, pH 4.0 (1 ml). From previous experiments, it was calculated that 4 µl of 1 M NaOH is required to neutralise 100 µl of 50 mM

acetic acid. Collagen fibril formation was initiated by neutralising an aliquot of collagen solution (200 µl) with 1 M NaOH (8 µl). The solution was mixed thoroughly, but gently, with a micropipette tip and spread onto glass coverslips (5-50 µl solution per coverslip) that had been previously sonicated in ethanol and allowed to dry.

The coverslips were placed in Terasaki wells and the solutions were allowed to gel at 37°C for 10 min (Brodsky and Eikenberry, 1982). After this, PBSG (200 µl) was added to each well and allowed to incubate for a further 10 min. PMNLs were isolated from whole blood (Section 2.7.2) and an aliquot ($1x10^5$ cells) was added to the collagen-coated coverslips and allowed to adhere (30 min, 37°C). Glutaraldehyde [8 µl of a 25% (v/v) stock solution] was added per well and left overnight at 37°C. The fixed collagen fibrils were dehydrated though an ethanol series of increasing concentrations and left in 100% ethanol until CPD. After CPD, the coverslips were stuck on copper stubs with double-sided adhesive tape and colloidal graphite was 'painted' onto the underside of the coverslip and the stub to improve conductivity and decrease charging effects in the SEM chamber. The coverslips were sputter coated and stored in a desiccator until viewed.

5.4.2.3 Results and Discussion

From Figure 5.6, it is evident that the purified type I collagen retains its native conformation and that both fibril (Figure 5.6 A and B) and fibre (Figure 5.6 C) formation occurs at physiological pH and temperature. Together, these results prove that type I collagen was purified intact and that it was suitable for use as a substrate for type I collagenase (MMP-8) zymography. Adherent PMNLs did not seem to digest the collagen fibres, but exhibited some membrane ruffling, possibly due to activation by the collagen fibres (Figure 5.6 C).

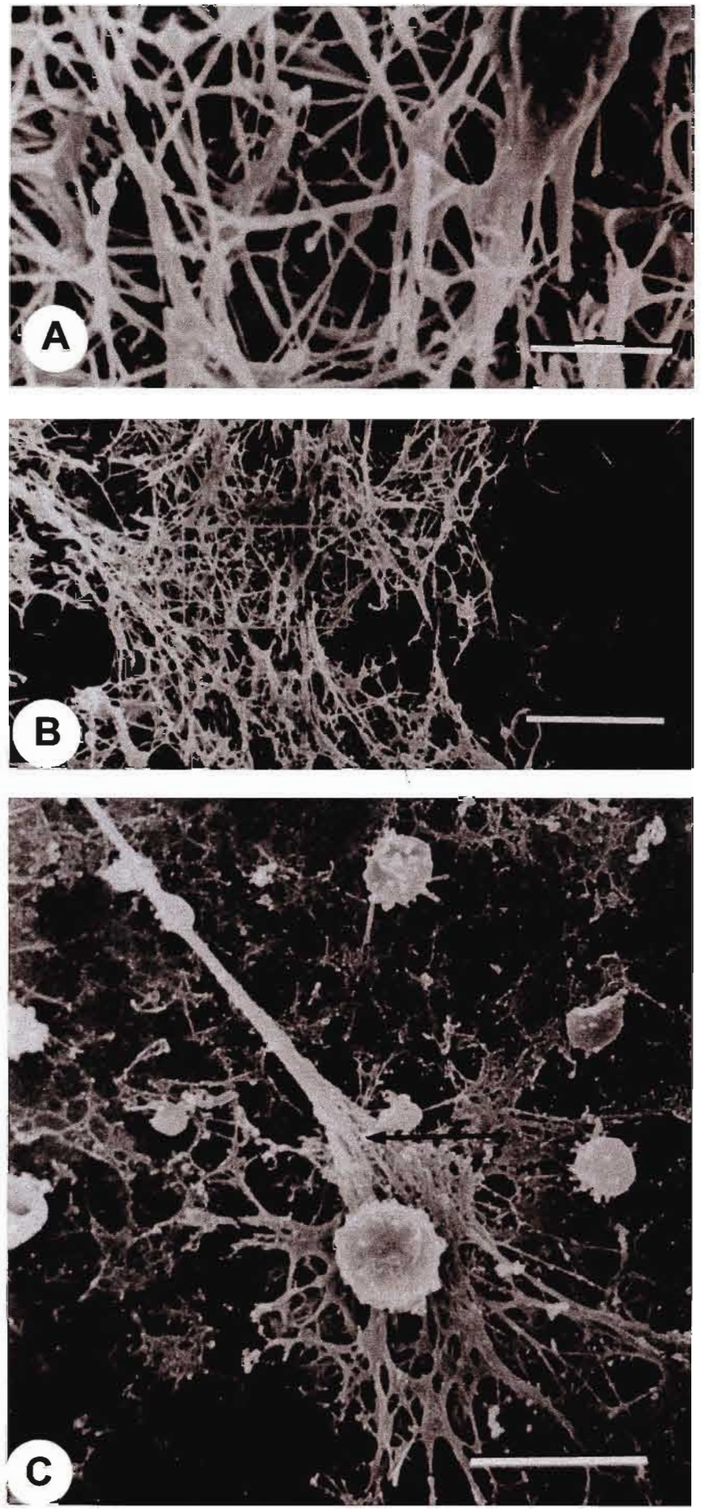

Figure 5.6 **SEM preparations of purified rat skin type I collagen in neutral solution to assess structural integrity.**

A and B), Type I collagen was neutralised with NaOH and allowed to form fibrils in PBSG. The collagen fibrils are intact and there appears to be no denaturation into gelatin. The collagen scaffolding is similar to that found in SEM preparations of stromal tissue. Bar = A), 2 µm; B), 10 µm. C), Autoassembly of fibrils into a collagen fibre. A PMNL rests on a collagen fibre and the component fibrils are also visible (arrow). Bar = 10 µm.

5.4.3 Electrophoretic analysis of purified type I collagen

Electrophoretic patterns were also used to ensure that the collagen fraction was free of other non-collagen contaminants and to verify the success of the purification. Although the fractions were freeze-dried and kept at -20°C, various reports indicate that long-term storage results in collagen degradation (Harris and Vater, 1980). For this reason, the integrity of purified type I collagen was regularly assessed by examining its electrophoretic patterning as degradation products are visible as low M_r bands in SDS-PAGE gels.

5.4.3.1 Reagents

The reagents used were prepared as described in Section 2.4.2.

5.4.3.2 Procedure

Lyophilised type I collagen (1 mg) was dissolved in 50 mM acetic acid (1 ml). Aliquots (8-40 µl, corresponding to 8-40 µg) were diluted with an equal volume of non-reducing treatment buffer and put aside to allow SDS interaction with the proteins (30 min, RT). The collagen samples were separated on a Tris-tricine SDS-PAGE gel with a 5% (w/v) running and 4% (w/v) stacking gel (Section 2.4.2.2).

5.4.3.3 Results and Discussion

The purified collagen produced the characteristic bands of monomeric α_1(I) and α_2(I) (both bands known as the α band ~100 and 110 kDa), α_1(I)α_2(I) heterodimer and $\alpha_1(I)_2$ homodimer (both bands known as the β band ~170 kDa) and the $[\alpha_1(I)]_2[\alpha_2(I)]$ heterotrimer (known as the γ band ~210 kDa). The patterning in Figure 5.7 is identical to those reported previously (Harris and Vater, 1980; Murphy *et al.*, 1980; Saari *et al.*, 1990) and, therefore, proves the purity of the final collagen fraction and reveals that no collagen degradation by endogenous rat collagenases occurred during purification.

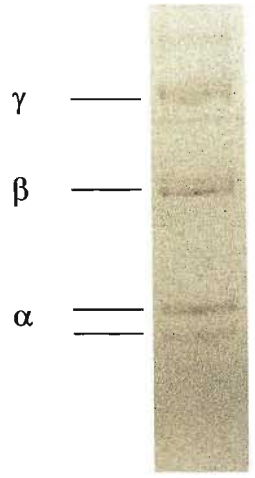

Figure 5.7 **Pure rat skin type I collagen purified according to Cawston and Barrett (1979).** Pure type I collagen (8 μg) was separated by Tris-tricine SDS-PAGE with a 4% stacking gel and 5% running gel, under non-reducing conditions and stained with Coomassie Blue. M_r's: γ, ~210 kDa; β, 170 kDa; α, 100 and 110 kDa.

5.4.4 Induction of PMNL granule exocytosis using the Ca^{2+}-ionophore, ionomycin

Previous work in the field of ionophore-stimulated PMNL granule release has shown that the release of the various PMNL granule populations can be controlled by altering the $[Ca^{2+}_{ex}]$ (Sengeløv *et al.*, 1993; Lollike *et al.*, 1995; Rosales and Ernst, 1997; Nüße *et al.*, 1998). The two most commonly used ionophores include A23187 (an antibiotic from *Streptomyces* spp.) and ionomycin (from *Streptomyces conglobatus*). Both ionophores form liposoluble complexes in the plasma membrane of cells and render them permeable to Ca^{2+} (Thomas, 1982). In this study, ionomycin was used as A23187 can transport Mg^{2+} in addition to Ca^{2+}, potentially complicating results if the intracellular Mg^{2+} concentration is altered (Thomas, 1982).

Granule mobilisation using a Ca^{2+} ionophore is useful in assessing the order of release as this method is receptor-independent as, although some receptor-bound ligands may induce granule release (by also increasing $[Ca^{2+}_i]$) in the accepted hierarchical order (see Table 1.2), others induce only partial release (e.g. C3b) and may, therefore, give the incorrect impression that a certain granule type is insensitive to $[Ca^{2+}_i]$ transients. The lack of fusion of granules containing proMMPs and TIMP-1 with the phagosome ingested via the IgG receptor implies one of two possible scenarios. Firstly, lack of fusion may be due to an insufficient increase in $[Ca^{2+}_i]$ to allow fusion of all granules with the phagosome. This is unlikely as MPO-containing azurophil

granules (that require high levels of Ca^{2+}_i for fusion) were shown to fuse with the phagosome (Figure 5.5). Secondly, the lack of fusion may be due to the signal transduction pathways specifically involved in phagocytosis of IgG-opsonised particles. In this case, as with phagocytosis of C3b-opsonised particles, only fusion of a few relevant granules may occur. Selectivity of granule fusion with the phagosome may be achieved by granule fusion proteins (such as v- and t-SNARES) and, therefore, increases in $[Ca^{2+}_i]$, although not sufficient to allow fusion with the phagosome, may still permit extracellular degranulation as all known granules are able to fuse with the plasma membrane to release their contents (Borregaard and Cowland, 1997).

To further the understanding of the regulation of the TIMP-1 vesicle release (along with proMMP-8 and -9-positive granules), PMNLs were isolated, permeabilised with ionomycin and the sequence of granule marker protein release was followed using a number of different assays. This information was anticipated to provide insight into the possible order of proMMP and TIMP-1 release relative to each other and be important for the understanding of proteolytic events involved in inflammation and chemotaxis. It was envisioned that once the optimal $[Ca^{2+}_{ex}]$ for TIMP-1 and proMMP-8 and -9 release was determined, the exact $[Ca^{2+}_i]$ sensitivities could subsequently be determined using commercially available fluorescent $[Ca^{2+}_i]$ indicators [e.g. indo-1FF (London *et al.*, 1996) or Fura-2/AM (Sengeløv *et al.*, 1993)].

The activation status of the MMPs was followed during $[Ca^{2+}_{ex}]$-induced exocytosis to determine whether any endogenous proMMP activators were present in the supernatant. Zymography is ideal for this purpose since both the pro- and active forms of the MMPs can be detected simultaneously (Davis, 1991; Kleiner and Stetler-Stevenson, 1994; Murphy and Crabbe, 1995; Gaudin *et al.*, 1997; Sørensen and Borregaard, 1999; Kolkenbrock *et al.*, 2000) and it was hoped that this new approach of using collagen zymography would be successful in demonstrating these characteristics in any MMP-8 released.

5.4.4.1 Reagents

Ionomycin stock solution (1 mM). Ionomycin (1 mg) was dissolved in anhydrous DMSO (1.34 ml), stored at 4°C and protected from light. For release assays, stock solution (10 µl) was diluted in DMSO (10 µl) to give a working concentration of 500 µM.

HNE substrate (MeOSuc-Ala-Ala-Pro-Val-AMC) stock solution (1 mM). The peptide substrate

(2 mg) was dissolved in anhydrous DMSO (3.19 ml), stored at 4°C and protected from light. Just before use, the substrate (60 µl) was diluted with dd.H_2O (540 µl) to give a final concentration of 100 µM.

AMC standard stock solution (10 mM). AMC (1.75 mg) was dissolved in anhydrous DMSO (1 ml), stored at 4°C and protected from light. To create working stock solutions of 100 and 25 µM, stock solution (10 µl and 2.5 µl of 10 mM) was diluted with anhydrous DMSO (990 µl and 997.5 µl respectively).

EDTA stock solution (10 mM). EDTA free acid (0.029 g) was diluted in dd.H_2O (9 ml), titrated to pH 7.4 with NaOH and made up to 10 ml. This solution was stored at -20°C.

HNE Buffer [200 mM Tris-HCl, 1 M NaCl, 0.1% (v/v) Brij 35, pH 8.5]. Tris (2.423 g) and NaCl (5.844 g) were dissolved in 90 ml dd.H_2O. Brij 35 [333 µl of 30% (v/v) stock solution] was added and the pH titrated to 8.5 with HCl. The solution was made up to 100 ml and stored at 4°C.

PMNL ionomycin resuspension buffer (10 mM HEPES, 140 mM NaCl, 5 mM KCl, 1 mM $MgCl_2$, 5 mM glucose, pH 7.4). HEPES (0.238 g), NaCl (0.818 g), KCl (0.037 g), $MgCl_2.6H_2O$ (0.02 g) and glucose (0.09 g) were dissolved in 90 ml dd.H_2O. The pH was titrated to 7.4 with HCl and the volume made up to 100 ml. The solution was autoclaved and kept at RT.

Calcium stock solution (containing 20 mM $CaCl_2$). This buffer is identical in composition and pH as the PMNL ionomycin resuspension buffer above, but contains 0.438 g $CaCl_2.6H_2O$/100 ml. This buffer was stored frozen at -20°C rather than autoclaved to avoid possible formation of $CaCO_3$ precipitates.

AEBSF stock solution (100 mM). AEBSF (0.024 g) was dissolved in dd.H_2O (1 ml) and stored at -20°C.

2 x Collagenase zymography buffer [200 mM Tris-HCl, 10 mM $CaCl_2$, 0.01% (v/v) Brij 35, 0.04% (w/v) NaN_3, pH 8.0]. Tris (12.114 g), $CaCl_2.6H_2O$ (1.10 g) and NaN_3 (0.2 g) were dissolved in dd.H_2O (450 ml) and Brij 35 [165 µl of a 30% (v/v) stock solution] was added. The

pH was titrated to 8.0 with HCl, made up to 500 ml and stored at 4°C.

Phosphate-buffered saline (PBS), pH 7.2. NaCl (8 g), KCl, (0.2 g), $NaH_2PO_4.2H_2O$ (1.15 g) and KH_2PO_4 (0.2 g) were dissolved in 950 ml dd.H_2O. The pH was titrated to 7.2 with NaOH, and made up to 1 *l*.

NaN_3-PBS. PBS was prepared as described above, except that NaN_3 was added to a final concentration of 1% (w/v).

PBS-Tween [0.1% (v/v)]. Tween® 20 (1 ml) was diluted to 1 *l* with PBS.

Blocking solution [0.5% (w/v) BSA in PBS] (BSA-PBS). BSA (0.5 g) was dissolved in PBS (100 ml).

Citrate-phosphate buffer (150 mM), pH 5.0. Citric acid solution (21.0 g citric acid.H_2O/*l*, 500 ml) was titrated with a solution of $NaH_2PO_4.2H_2O$ (35.6 g/*l*) to pH 5.0.

Substrate solution [0.05% (w/v) ABTS and 0.0015% (v/v) H_2O_2 in citrate-phosphate buffer]. ABTS (7.5 mg) and H_2O_2 [7.5 µl of a 30% (v/v) solution] were dissolved in citrate-phosphate buffer, pH 5.0 (15 ml) for each ELISA plate.

Peroxidase stopping buffer [0.01% (w/v) NaN_3 in citrate-phosphate buffer]. NaN_3 (0.1 g) was dissolved in citrate-phosphate buffer (100 ml).

Buffers for zymography, ECL and western blotting and alkaline phosphatase have previously been described (Sections 2.6.1, 2.8 and 3.5.1.1, respectively).

5.4.4.2 Procedure

PMNL isolation. PMNLs were isolated from whole blood (100 ml) (Section 2.7.2), counted ($5.53x10^6$/ml) and assessed for viability (>98% trypan blue exclusion).

Ionomycin permeabilisation and [Ca^{2+}_{ex}] titration. PMNLs [$2.21x10^7$ cells in ice-cold PMNL ionomycin resuspension buffer (4 ml)] were split into 8 aliquots (500 µl each) in sterile Eppendorf microfuge tubes and numbered 1-8. The tubes were recentrifuged and PMNLs

resuspended in various volumes of ice-cold ionomycin resuspension buffer and other test reagents added to give a final reagent volume of 500 µl as indicated in Table 5.5. For experiments specifically performed to determine TIMP-1 release, AEBSF and NaN_3 were included in the ionomycin resuspension buffer to a final concentration of 2 mM and 0.02% (w/v), respectively, to prevent TIMP-1 degradation by serine proteinases and ROS released from PMNLs.

Table 5.5 Method for the determination of Ca^{2+}-induced exocytosis in the presence of 1 µM ionomycin and increasing [Ca^{2+}_{ex}].

Tube number	1	2	3	4	5	6	7	8
Initial volume (µl)	489	497.8	496.5	495.2	494	491.5	486.5	474
Ionomycin (µl)	1	1	1	1	1	1	1	1
Stock EDTA (µl)	10	0	0	0	0	0	0	0
Stock Ca^{2+} (µl)	0	1.25	2.5	3.75	5	7.5	12.5	25
Final [Ca^{2+}_{ex}] (µM)	0	50	100	150	200	300	500	1000
No. moles ionomycin per cell	$1.81x10^{-16}$	$1.81x10^{-16}$	$1.81x10^{-16}$	$1.81x10^{-16}$	$1.81x10^{-16}$	$1.81x10^{-16}$	$1.81x10^{-16}$	$1.81x10^{-16}$
No. moles Ca^{2+}_{ex} per cell	0	$9.03x10^{-15}$	$1.81x10^{-14}$	$2.71x10^{-14}$	$3.61x10^{-14}$	$5.42x10^{-14}$	$9.03x10^{-14}$	$1.81x10^{-13}$
Final volume (µl)	500	500	500	500	500	500	500	500

PMNLs were incubated (20 min, 37°C) with gentle intermittent shaking and the reaction was terminated by placing the microfuge tubes on ice (1 min) and centrifuging (400 x g, 5 min). The supernatant fluid from each tube was removed and split into 9 aliquots [50 µl each containing $3.07x10^5$ cell equivalents (eq.)] and stored at -70°C until required for PMNL granule release assays, while the pellets were first analysed for alkaline phosphatase activity as described below. Once alkaline phosphatase activity had been assayed, the PMNL pellets from tubes 1-7 were discarded (since we were only interested in granule proteins released into the supernatant due to increasing [Ca^{2+}_{ex}]) while the pellet from tube 8 (the 'no calcium' control, i.e. 0 µM Ca^{2+}_{ex} + 500 µM EDTA) (after alkaline phosphatase assay) was resuspended in 500 µl of ionomycin resuspension buffer containing 0.2% (v/v) Triton X-100 and split into 9 aliquots (50 µl each; each aliquot containing $3.07x10^5$ cell eq.) and stored at -70°C. This was done in order to allow detection of the various unreleased (intracellular) granule marker proteins (HNE, lactoferrin, proMMP-8, proMMP-9, TIMP-1) by the methods described below (Sengeløv *et al.*, 1993).

Alkaline phosphatase colorimetry. Alkaline phosphatase was chosen as a marker to detect release of the secretory vesicles. Unlike other granule marker proteins, alkaline phosphatase (which is GPI-anchored) is not released into the supernatant fluid, but remains anchored to the plasma membrane and, hence, the PMNL pellet is required for assay. Exposed alkaline phosphatase is termed 'active' since its activity can be assayed directly, while unreleased alkaline phosphatase is termed 'latent' since its activity can only be assayed in the presence of detergent to allow substrate access (Kobayashi and Robinson, 1991; Edwards, 1994; Sengeløv, 1996; Sengeløv and Borregaard, 1999).

The PMNL pellets were resuspended in ionomycin resuspension buffer (to dilute $[Ca^{2+}_{ex}]$ and thereby avoid calcium phosphate precipitation in the alkaline phosphatase assay), repelleted and resuspended in alkaline phosphatase buffer lacking Triton X-100 (200 µl, 20 min, 37°C) to permit quantification of active (surface exposed) alkaline phosphatase and not latent (intracellular and unreleased) alkaline phosphatase. Upon completion of the assay, the cells were removed by centrifugation (1000 x g, 2 min) and the supernatants aspirated and added to microtitre plates (200 µl). Alkaline phosphatase activity was detected by measuring the absorbance of the liberated *p*NP at 405 nm in a Bio-Tek EL 307 ELISA plate reader.

HNE fluorimetry. Supernatant fractions from each $[Ca^{2+}_{ex}]$ level and the Triton X-100 'no calcium control' pellet extract (all 25 µl; $1.54x10^5$ cell eq.) were mixed with HNE buffer (125 µl) and allowed to equilibrate (10 min, 40°C) (Barrett, 1981). Substrate (50 µl) was added and the incubation was allowed to continue for a further 10 min in the dark. The solutions (200 µl) were then added to wells of a white opaque fluorimeter plate and enzyme activity was quantified (λ_{ex} = 360 nm, λ_{em} = 460 nm) by interpolating the fluorescence obtained from the test samples with standard AMC curves constructed in the range of 100-1000 pmoles (r = 0.997) and 500-5000 pmoles (r = 0.991) of AMC. Percentage release of HNE was calculated by dividing the fluorescence obtained in the supernatant by the sum of the fluorescence obtained from the supernatant and the Triton X-100 'no calcium' control PMNL pellet extract.

Lactoferrin ELISA. Supernatant fractions (40 µl) were diluted with NaN_3-PBS [760 µl containing AEBSF at a final concentration of 2 mM (200 µl of 100 mM stock solution/10 ml)] to prevent proteolytic degradation of lactoferrin by degranulated PMNL serine proteinases (cathepsin G, HNE, proteinase 3). Nunc Immuno Maxisorp F96 microtitre plate wells were

coated with the diluted fractions (100 µl, $3.07x10^4$ cell eq.) and incubated (2 h, 37°C). Uncoated areas of the wells were blocked with BSA-PBS (200 µl/well, 1 h, 37°C) and wells were washed three times with PBS-Tween (200 µl). Rabbit anti-lactoferrin IgG was added (1/1000 dilution in BSA-PBS, 100 µl/well, 2 h, 37°C), followed by HRPO-linked sheep anti-rabbit IgG secondary antibody (1/450 dilution in BSA-PBS, 120 µl/well, 1 h, 37°C). The wells were washed three times with PBS-Tween (200 µl) after each step. The ABTS HRPO substrate was added to the wells (150 µl/well), colour development was allowed to progress in the dark (10-30 min) and the absorbance read at 405 nm. Controls included contained either no primary antibody, no secondary antibody, no blocking agent or substrate only. The highest values obtained from any one of these controls were subtracted from the absorbances obtained in the test samples.

ProMMP-8 collagen zymography. Type I collagen (Section 5.2.1) (15 mg) was dissolved in 50 mM acetic acid, pH 4.0 (11.15 ml) with gentle stirring (~30 min, RT). Acrylamide stock solution (3.75 ml) was added to give a final concentration of 7.5%. The gel was polymerised as described in Section 2.4.1.2. Upon polymerisation, the gel-casting unit was disassembled and placed in 1 x Laemmli running gel buffer, pH 8.0 (prepared as described in Section 2.4.1.1, except the SDS was omitted to prevent collagen denaturation) until the pH of the running gel had increased sufficiently to allow anodic migration of protein samples (1-2 h, RT). The gel was reassembled and a 4% stacking gel cast (Section 2.4.1.2). Supernatant fractions from each $[Ca^{2+}_{ex}]$ level and the Triton X-100 'no calcium control' pellet extract were diluted 1:45 and 5 µl (~683 cell eq.) of each was mixed with an equal volume of non-reducing sample buffer and electrophoresed. The gels were disassembled, washed, incubated for zymography (in collagenase buffer as opposed to gelatinase buffer), stained and destained as described in Section 2.6.2.

ProMMP-9 gelatin zymography. Gelatin zymogram gels were prepared and run as described in Section 2.6.2. Samples for gelatin zymography were diluted and prepared as described for collagen zymograms above.

TIMP-1 western blot. A 10% Laemmli SDS-PAGE gel was cast as described in Section 2.4.1.2. Supernatant fractions from each $[Ca^{2+}_{ex}]$ level and the Triton X-100 'no calcium control' pellet extract (40 µl; $2.46x10^5$ cell eq.) were diluted with reducing treatment buffer (40 µl) and boiled

(5 min) before electrophoresis and blotting onto nitrocellulose (Section 2.8). The nitrocellulose membrane was dried (2 h, RT) and blocked with TEN containing 1% (w/v) gelatin (1 h, RT). The blot was probed with chicken anti-TIMP-1 IgY (between 10-50 µg/ml, 2 h, RT) and subsequently with alkaline phosphatase-conjugated goat-anti chicken IgG (1/5000, 1 h, RT), both diluted in 1% gelatin-TEN. The blot was developed with BCIP/NBT (Section 2.8.1.2) until distinct bands were visible.

Analysis of total granule protein release by SDS-PAGE and silver staining. Supernatant fractions from each [Ca^{2+}_{ex}] level and the Triton X-100 'no calcium control' pellet extract (10 µl; $6.15x10^4$ cell eq.) were diluted with reducing treatment buffer (10 µl) and boiled (5 min) before electrophoresis on a 12.5% Laemmli SDS-PAGE gel (Section 2.4.1.2). After electrophoresis, the gel was silver stained (Section 2.5.2.2).

5.4.4.3 Results and Discussion

Cytoskeletal disrupting agents (e.g. cytochalasins A, B, D) induce [Ca^{2+}_i] transients in the absence of Ca^{2+}_{ex} (Sengeløv *et al.*, 1993; Al-Mohanna *et al.*, 1997) and give rise to subsequent exaggerated responses to [Ca^{2+}_{ex}] due to non-specific priming (Sengeløv *et al.*, 1993), whereas ionomycin does not. Ionomycin was therefore chosen for use in this study. It was found, however, that increasing [Ca^{2+}_{ex}] leads to a trend in protein release that differed to that anticipated, i.e. protein release did not continually increase with increasing [Ca^{2+}_{ex}] or show one peak of release (Figure 5.8 E). A biphasic pattern of granule release has, however, previously been described in patch clamp analyses (Nüße *et al.*, 1998) which showed that the first phase of granule release consisted of granules with high affinity and low cooperativity for Ca^{2+}, while the subsequent phase was characterised by granules with low affinity and high cooperativity for Ca^{2+}. In the current study, a similar biphasic release was most evident (by examining protein release) at 100 and 200 µM Ca^{2+}_{ex} (Figure 5.8 E, lanes 3 and 5). Further increase in Ca^{2+}_{ex} beyond 200 µM does not appear to result in increased overall protein release (Figure 5.8 E, lanes 7 and 8).

Alkaline phosphatase was maximally released upon incubation with ionomycin alone (Table 5.5, tube 1) and, therefore, did not require exogenously added Ca^{2+} for mobilisation (results not shown). Mere insertion of ionomycin into the PMNL plasma membrane may cause a small [Ca^{2+}_i] spike due to release of Ca^{2+}_i from intracellular stores (the calciosomes) (Volpe *et al.*, 1988) and may have given rise to this phenomenon. Recent confocal microscopy studies

using chlortetracycline, an antibiotic and chelating agent that fluoresces upon binding Ca^{2+} (Caswell and Hutchinson, 1971), showed that the calciosomes reside near the periphery of the PMNL (Al-Mohanna *et al.*, 1997). The random insertion of ionomycin molecules into the plasma membrane and closely apposed calciosomes may have, therefore, given rise to the brief $[Ca^{2+}{}_i]$ spike resulting in secretory vesicle exocytosis. The observed complete exocytosis of secretory vesicles in this experiment does not reflect the observations of an earlier report (Sengeløv *et al.*, 1993) where it was estimated that only ~40% of the secretory vesicles (as identified by HSA) were released with ionomycin alone. This is probably due to differences in the conditions under which ionomycin-mediated granule release in the presence of $Ca^{2+}{}_{ex}$ occurred. Previous studies report total PMNL numbers and the molar concentration of $Ca^{2+}{}_{ex}$ added, but important information such as the final number of moles of $Ca^{2+}{}_{ex}$ and ionomycin available in proportion to the reported total number of PMNLs, was omitted. The theoretical number of moles of both ionomycin and $Ca^{2+}{}_{ex}$ per cell are, however, reported here (Table 5.5).

Addition of increasing amounts of $[Ca^{2+}{}_{ex}]$ resulted in release of HNE in two distinct peaks (Figure 5.8 A). This biphasic response consisted of a modest increase in HNE activity at 150 μM $Ca^{2+}{}_{ex}$ (in contrast to the observed decrease in protein staining in Figure 5.8. E, lane 4) followed by a more dramatic increase in activity that peaked at 500 μM $Ca^{2+}{}_{ex}$. At 500 μM $Ca^{2+}{}_{ex}$ (i.e. maximal release) approximately 52% of the total HNE activity was released into the extracellular medium. Again, as with alkaline phosphatase release, this is higher (by approximately two-fold) than that reported by Sengeløv *et al.* (1993) but is most probably due to the absolute number of moles of $Ca^{2+}{}_{ex}$ used (as explained above). The decrease in HNE release upon increasing $[Ca^{2+}{}_{ex}]$ from 500 to 1000 μM is unexpected, but a similar finding (i.e. inhibition of exocytosis at high $[Ca^{2+}{}_{ex}]$) has been reported in the patch clamp analyses of Nüße *et al.* (1998) and, unfortunately, remains unexplained. Rosales and Ernst (1997), who investigated Ca^{2+}-dependent secretion of granules in streptolysin O-permeabilised PMNLs, showed that annexins I and V can inhibit Ca^{2+}-mediated HNE release. High $[Ca^{2+}{}_{ex}]$ (between 500 and 1000 μM), annexins I and V may, therefore, be selectively recruited to the azurophil granule membranes to inhibit degranulation and, hence, HNE release.

In contrast to the phasic release of HNE, release of the specific granule marker, lactoferrin, seems to demonstrate a positive correlation with increasing $[Ca^{2+}{}_{ex}]$ (Figure 5.8 A). Lactoferrin release was initially sharp from 0-200 μM $Ca^{2+}{}_{ex}$, thereafter increasing gradually up to 1000 μM. A higher sensitivity of lactoferrin to $Ca^{2+}{}_{ex}$ relative to HNE is demonstrated by the

fact that the majority of lactoferrin was released prior to HNE at concentrations below 300 μM Ca^{2+}_{ex}. This observation reinforces the accepted order of granule release, i.e. the order of release is the reverse of synthesis and, therefore, the majority of lactoferrin-positive specific granules are released into the supernatant before HNE-positive azurophil granules (Table 1.2).

Both proMMP-8 and proMMP-9 were released at low [Ca^{2+}_{ex}] and even the Ca^{2+}_{i} spike induced by ionomycin insertion allowed minimal release of both proMMPs at 0 μM Ca^{2+}_{ex} (Figure 5.8 B and C, lane 1) (Sengeløv *et al.*, 1993). Due to the high sensitivity of zymography, the samples required several-fold dilution before optimal resolution of gelatinolytic bands was obtained. ProMMP-8 was released at a low $[Ca^{2+}]_{ex}$, and appears to have reached a maximum (indicated by the area for collagen degradation) at 500 μM, while proMMP-9 release appears to be maximal at 200-300 μM Ca^{2+}_{ex} (Figure 5.8 B and C, lanes 7 and 5-6, respectively). Although both proMMP-8 (band at ~75 kDa, Figure 5.8 B) and -9 (bands at 92, 125 and 220 kDa, Figure 5.8 C) were readily released in response to ionomycin alone and increasing [Ca^{2+}_{ex}], neither zymogen was activated throughout the duration of the assay. This finding is in agreement with Kolkenbrock *et al.* (2000) who concluded that none of the PMNL serine proteinases would significantly contribute to released proMMP activation *in vivo* since they only produced minimal (~1%) proMMP-9 activation *in vitro*. Although the collagen zymogram is theoretically specific for type I collagenases such as MMP-8, high concentrations of gelatinase have been reported to degrade intact type I collagen although this is not the preferred gelatinase substrate (Gogly *et al.*, 1998). This, therefore, explains the presence of weak collagenolytic activity for proMMP-9 (92 kDa) in the type I collagenase zymogram (Figure 5.8 B) in addition to the single broad band obtained for proMMP-8 [75-82 kDa - this broad band is most probably due to heterogeneity in the glycosylation of proMMP-8 (Mallya *et al.*, 1990)]. The resolution of the novel collagen zymogram used here proved adequate for the purpose of this study. Subsequent to this study, a similar collagen zymography method using another interstitial collagenase, MMP-1, was described by Gogly *et al.* (1998) and is reported to have a sensitivity limit of 100 ng. This method was attempted, but did not permit satisfactory collagen dissolution and, hence, the method described here was used instead.

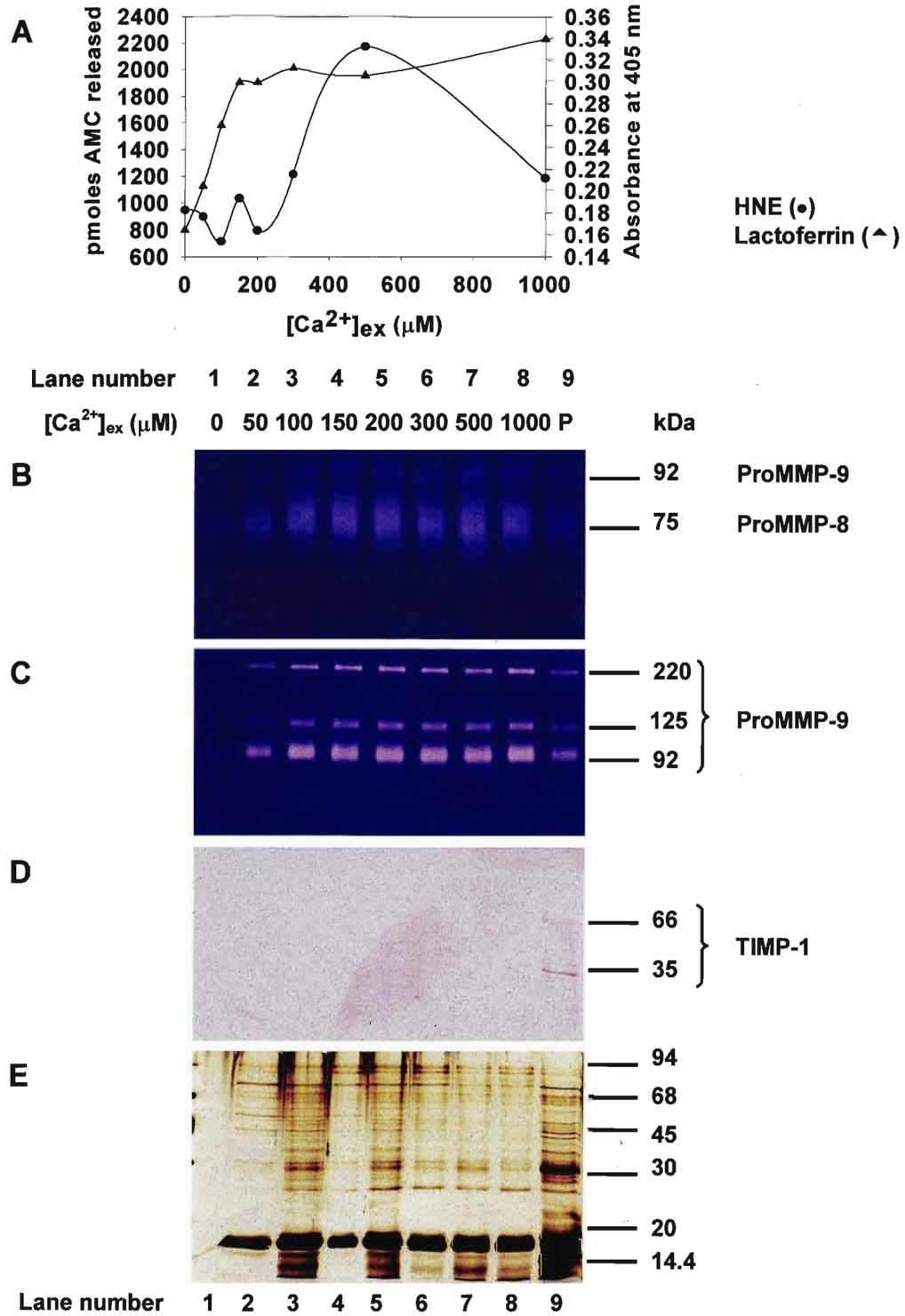

Figure 5.8 **Analysis of ionomycin-mediated Ca^{2+}-dependent PMNL granule exocytosis to assess the order of TIMP-1 release relative to other granule proteins.**

PMNLs were rendered permeable to Ca^{2+}_{ex} by incubation with the liposoluble Ca^{2+}-ionophore, ionomycin (1 μM), exposed to increasing $[Ca^{2+}_{ex}]$ (0-1000 μM) and the supernatants assayed for the presence of various granule marker proteins. Lane P (B-E), contains the Triton X-100 soluble PMNL pellet extract from the 'no calcium control' (0 μM Ca^{2+}_{ex} + 500 μM EDTA). A), HNE (azurophil granules) release was detected by fluorimetry and lactoferrin (specific granules) release was detected by indirect ELISA. B), 75-82 kDa proMMP-8 (specific granules) was detected by type I collagen zymography. Due to the high concentration of proMMP-9 in PMNLs and the weak collagenolytic activity of proMMP-9, some clearing is evident at 92 kDa. Neither proMMP-8 nor -9 were activated during ionomycin-induced Ca^{2+}-dependent granule exocytosis. C), proMMP-9 (specific and gelatinase granules) was detected by gelatin zymography. D), TIMP-1 release was detected by western blotting. Membranes were probed with chicken anti-TIMP-1 IgY (50 μg/ml) and detected with alkaline phosphatase-conjugated goat anti-chicken IgG (1/5000) and BCIP/NBT. No TIMP-1 was released under the range of $[Ca^{2+}_{ex}]$ employed, but remained in the cell pellet (lane P) in both a 66 kDa and 35 kDa form. E), Analysis of granule protein release by reducing SDS-PAGE and silver staining. Cell equivalents used for each assay: A), HNE ($1.54x10^5$); lactoferrin ($3.07x10^4$); B and C), proMMPs (683); D), TIMP-1 ($2.46x10^5$) and E), total protein ($6.15x10^4$).

In contrast to all the other PMNL granules, the release of which was assayed by detection of marker proteins, all of the TIMP-1 remained within the PMNL pellet (Figure 5.8 D, lane P). To ensure that the negative results for TIMP-1 release was not due to insufficient protein loading, each lane on the western blot was loaded with protein released from ~$2.46x10^5$ cell eq. This is considerably greater than that required for the detection of the other granule protein markers (see legend to Figure 5.8). In addition, to ensure that non-detection of TIMP-1 in the supernatants was not due to either limiting antibody or, conversely, excess antibody levels (which would cause a prozone effect), a dilution range of 10-50 μg/ml was employed and the blots were allowed to develop overnight to improve detection. In all cases, the only positive TIMP-1 bands (66 and ~35 kDa) obtained were from the Triton X-100 'no calcium control' PMNL pellet. The 66 kDa band corresponds to partially denatured TIMP-1 'complex' as described in Chapter 4, and the ~35 kDa band to monomeric TIMP-1. The observed apparent TIMP-1 M_r of 35 kDa is slightly higher than that previously obtained for the monomer after boiling and affinity chromatography (see Figure 4.1 D; Section 4.1.1) and may be due to incomplete solubilisation of TIMP-1 with SDS in the presence of excess Triton X-100 in the pellet. Previous experiments to investigate the detection limits of the chicken anti-TIMP-1 IgY have demonstrated that the antibody can detect less than 10 ng of pure rTIMP-1 by dot blot (results not shown). Therefore, the results should be reliable and any released TIMP-1 should have been detected. Although HNE and ROS may also be released into the supernatant, it is unlikely that TIMP-1 would be degraded as AEBSF and NaN_3 were included in the buffers to prevent proteolysis and oxidative degradation. From results seen in multiple replicate samples, it is interesting to note that with the chicken anti-TIMP-1 antibodies, the monomeric form of TIMP-1 appears to be more predominant in PMNL homogenates (Figure 5.8 D, lane P) compared to the 66 kDa form identified by the rabbit anti-TIMP-1 antibodies used in Chapter 4. This is possibly due to preferential recognition and binding of the chicken antibodies to monomeric TIMP-1, rather than suggesting that the monomeric form occurs in greater quantities than the 66 kDa form in resting PMNL homogenates. We are confident that the proportion of the 66 kDa form relative to the monomeric form of TIMP-1 seen in western blots of PMNL homogenates (Section 4.1.1) is reflective of the true *in vivo* situation, as this was also observed in the western ligand blot for TIMP-1 on PMNL homogenates (Section 4.2.2).

There appear to be four possible explanations for the observed lack of TIMP-1 degranulation: 1), the TIMP-1 vesicle may be insensitive to increases in $[Ca^{2+}_i]$ [this is supported by the non-

fusogenicity of the TIMP-1 vesicle with IgG-opsonised latex bead phagosomes (Section 5.2) where fusion is known to be predominantly regulated by Ca^{2+}_i]; 2), TIMP-1 release occurred but at levels that would not be physiologically relevant or detectable (i.e. would result in no significant inhibition of proteolytic degradation by released MMPs); and 3), the TIMP-1 vesicle is sensitive to [Ca^{2+}_i], but its release occurs at higher [Ca^{2+}_i] than that obtained with [Ca^{2+}_{ex}] = 1000 μM. Although higher [Ca^{2+}_i] may be non-physiological, previous reports (Demaurex *et al.*, 1994) have shown that Ca^{2+} influx occurs even at 10 mM Ca^{2+}_{ex}. TIMP-1 release may, therefore, be regulated by a specific (as yet unknown) receptor-mediated pathway that raises [Ca^{2+}_i] higher than that possible by ionomycin treatment and high [Ca^{2+}_{ex}] buffers. It is, however, felt that all the above explanations, except the first, are unlikely.

In conclusion, the ionomycin experiments suggest that the TIMP-1 vesicle differs from all other major granule populations (azurophil, specific, gelatinase, secretory) by exhibiting insensitivity to the greatest [Ca^{2+}_i] used in previous studies (Sengeløv *et al.*, 1993; Rosales and Ernst, 1997). Therefore, if the primary role of the TIMP-1 vesicle *in vivo* is to inhibit (or downregulate) MMP activity on the ECM during invasion and diapedesis, it must be regulated by a non-Ca^{2+}_i-requiring signal transduction pathway. The insensitivity of the TIMP-1 vesicle to [Ca^{2+}_i] as compared to the rapid release of both proMMPs to [Ca^{2+}_i] may be required to serve as a mechanism to avoid simultaneous release of both inhibitor and proteinase during invasion. This would allow fine regulation of MMP-mediated proteolysis.

Indeed it would be interesting to investigate whether TIMP-1 vesicle release could be stimulated (via a receptor-mediated pathway) by collagen or gelatin fragments produced by MMP activity as this could provide a novel feedback inhibition pathway for controlling excessive ECM destruction. A PMNL type I collagen receptor that binds chain-specific peptide fragments and induces the respiratory burst has been identified (Monboisse *et al.*, 1990) while another receptor that binds a peptide from the α3 chain of type IV collagen, resulting in downregulation of the respiratory burst and degranulation has also been described (Ziaie *et al.*, 1999). It is possible that a similar collagen-binding receptor may be responsible for mobilisation of the TIMP-1 vesicle and inhibition of MMP-mediated proteolysis. Future experiments investigating the effect of addition of collagen and gelatin fragments to PMNLs may help identify the mechanism(s) controlling TIMP-1 vesicle mobilisation.

5.5 Discussion

The PMNL contains at least four main populations of cytoplasmic granules that are under the control of regulated exocytosis and are mobilised, in part, by changes in $[Ca^{2+}_i]$. The azurophil and specific granules contain the majority of microbicidal proteins and enzymes for the phagocytic digestion and destruction of engulfed pathogens, whereas the gelatinase and the secretory vesicles contain extracellularly-relevant proteins and receptors. The protein contents of the latter two granule populations are not thought to play a direct role in pathogen destruction, but the secretory vesicle receptors are crucial for binding of opsonised pathogens (Edwards, 1994; Borregaard and Cowland, 1997).

The results from the current study further support the hypothesis that granule fusion events not only occur in a strict sequence, but that granule populations can be selectively excluded from, for example, the phagosome if their protein content serves no direct function. This granule fusion selectivity may allow the PMNL to accurately coordinate its two main *in vivo* functions: phagocytosis of microorganisms and possibly proteolytic cleavage of ECM components and also conserve granules during the process of fighting infection by avoiding complete degranulation events. Some leukocytes (e.g. mast cells) undergo complete granule release upon stimulation but are able to resynthesise populations after release (Roitt, 1994). Granule resynthesis does not appear to occur in the PMNL and it has, therefore, evolved a method of single granule or 'quantum' (phasic) release (Liou and Campbell, 1996; Owen and Campbell, 1999). The quantum/phasic release may conserve protein while simultaneously allowing transient protein activity (i.e. allowing a brief period of proteolysis before enzyme inhibition or degradation) and may account for why only a few granules are seen associated with cytoskeletal elements at any one time.

The results from this chapter support the above hypothesis and show that during IgG-mediated phagocytosis (which would mimic an opsonised pathogen), the secretory vesicles, the majority of lactoferrin-positive specific granules and the azurophil granules are targeted to the phagosome and fuse with it. However, the TIMP-1 vesicle, the gelatinase (MMP-9) granules and the majority of the proMMP-8-positive/lactoferrin-negative specific granules are excluded from fusing with the phagosome. Hence, the results show that the PMNL can exert fusogenic control during phagocytosis by only allowing granules with a direct microbicidal purpose to fuse with the phagosome, and does not sequentially degranulate all populations into the phagosome as Ca^{2+}_i levels increase during the course of phagocytosis. In this case, the release

of TIMP-1, proMMP-9 and, to a degree proMMP-8 into the phagosome, seem similarly regulated. The results obtained from the ionomycin experiments show that although proMMP-8 and proMMP-9-containing granules are excluded from the phagosome, they are both highly sensitive to increases in $[Ca^{2+}_i]$ and are readily degranulated (in a similar pattern) into the supernatant fluid, but TIMP-1 is apparently not released. Therefore, lack of fusion of proMMP-8 and -9 with the phagosome is not due to insensitivity to Ca^{2+}_i, but may be due to control exerted by membrane fusion proteins or cytoskeletal elements.

The fact that proMMP-9 was excluded from the phagosome while some proMMP-8 entered, possibly means that either these two granules may be differentially regulated, or that some proMMP-8 entered the phagosome due to its presence in some lactoferrin-positive specific granule populations. Some indication that movement of these granules may be related to the type of cytoskeleton to which they are associated, i.e. specific granules being associated with microtubules but proMMP-9-containing granules being associated with one of the other (as yet unidentifiable) cytoskeletal elements, is given by the studies on the cytoskeletal association of these granules. The fact that the TIMP-1 vesicle is associated with a cytoskeletal element which appears dissimilar to that to which proMMP-9 is associated, potentially explains why proMMP-9-containing gelatinase granules may be released in response to increased levels of Ca^{2+}_i while the TIMP-1 vesicle is apparently not. Further studies should include efforts to identify these cytoskeletal elements and could include EM immunolabelling, studies using signal transduction pathway inhibitors and cytoskeletal depolymerisation agents.

Although still not firmly established, the apparent fine control and selectivity of granule fusion during phagocytosis and extracellular release may have important consequences for strategies designed to assist in fighting infection and controlling inflammation. The fact that the PMNL regulates fusion of granules independently of each other, allows the potential prevention of extracellular release or mobilisation of certain granule populations, e.g. those containing MMPs, without compromising the fusion of other populations, e.g. those that are required for pathogen destruction. In the phagosome, this would be an ideal situation as the normal phagocytic function of PMNLs may potentially not be affected by specifically designed anti-inflammatory drugs if these were aimed at acting only on PMNLs and at inhibiting the release of MMPs or stimulating the release of TIMP-1.

Such drugs could target the specific differential regulation or interaction of the proMMP-9-

containing granules and the TIMP-1 vesicle with the cytoskeleton compared to that of the specific and azurophil granules. These differences may be exploited in the designing of future anti-inflammatory drugs that may have fewer side effects than the presently available synthetic MMP inhibitors. At present, these inhibitors carry the risk of disturbing the natural turnover of collagens that is essential for various natural and essential processes (see Table 1.3). An alternative strategy of preventing the release of certain granules would, therefore, be preferable.

Further investigations into the exact role of MMPs and TIMP-1 in the PMNL are also required. Whether the MMPs serve a direct role in degrading collagen during chemotaxis, or whether they are involved in degrading collagen (cleaved by other proteinases) to form chemotactic peptides is unknown. In addition, whether they are used mainly to downregulate the inhibitory action of serpins or whether they (MMP-9 in particular) play a role in cytokine (IL-1β) generation and, therefore, induce immune stem cell differentiation is also a question remaining to be addressed. The role of TIMP-1 and the *in vivo* existence and possible role of high M_r forms of TIMP-1 similarly require investigation.

CHAPTER 6

General Discussion

6.1 Introduction

The PMNL is a highly sophisticated professional phagocyte that is recruited to a site of infection to engulf foreign particles/organisms and to produce secondary inflammatory signals (cytokines, lipid mediators etc.). Unfortunately, the series of events proposed to occur post-diapedesis are largely theoretical and remain a mystery. This is largely due to the fact that extravasating, inflammatory PMNLs are difficult to isolate and, therefore, are difficult to study. The exact mechanism(s) whereby PMNLs migrate through tissue to the site of infection have not been fully established, although it is tempting to draw comparisons between the invasive movement of PMNLs with that observed in metastatic cells. Metastatic cells, like PMNLs, can both intra- and extravasate thereby gaining access to the vascular and lymph system and tissues and utilise proteinases to actively degrade components of the ECM in order to gain access to the tissue and establish secondary colonies (Mignatti and Rifkin, 1993; Chambers and Matrisian, 1997; Kim *et al.*, 1998).

6.2 MMPs and TIMPs in invasion

Since the mid 1970's, there has been an increasing interest in the role of MMPs in assisting cellular invasion through collagen, the predominant class of ECM structural proteins. Although there are more than 20 types of collagen that differ in tissue distribution, there is a specific MMP member available for initial cleavage of the intact fibrillar collagen species to allow denaturation into gelatin, thus making the collagens susceptible to the relatively non-specific gelatinases. In addition to the MMPs that degrade fibrillar collagens (interstitial collagenases), there are gelatinases (that prefer gelatin), stromelysins (that prefer proteoglycans and glycoproteins) and MT-MMPs (that are responsible for the extracellular activation of selected proMMP zymogens and processing of TNFα) (Matrisian, 1992; Stetler-Stevenson, 1999; Westermarck and Kähäri, 1999). Regulation of MMP gene expression tends to be cell specific, but regulation of enzymatic activity of the translated proteinase is effected via either α_2-M (in the bloodstream) or TIMPs. Four members of the TIMP family have been discovered to date, differing with respect to their tissue distributions and associations with MMP zymogens. They

all, however, inhibit active MMPs with similar efficiencies.

Apart from their proposed involvement in extravasation and tissue migration, MMPs are now thought to play roles throughout the entire tumour metastatic process, from primary tumour growth, through intravasation, extravasation to the initial and sustained growth of the secondary tumours (Chambers and Matrisian, 1997). The MMPs that have mainly been implicated in the invasive behaviour of a number of cell lines are the gelatinases (gelatinase A/MMP-2 and gelatinase B/MMP-9) (Lennarz and Strittmatter, 1991; Matrisian, 1992; Bernhard *et al.*, 1994; De Clerk *et al.*, 1994; Fujimoto *et al.*, 1994; Ray and Stetler-Stevenson, 1995; Yu *et al.*, 1996; Lee *et al.*, 1997; Nakahara *et al.*, 1997; Puyraimond *et al.*, 1999). Although the expression and release of MMPs has recently been shown to be upregulated in metastatic cells, the mechanism(s) of their extracellular activation have only recently been identified. In the case of MMP-2, an MT-MMP is responsible for cleaving the MMP pro-peptide and focusing the MMP activity to a particular area for degradation of ECM components (Yu *et al.*, 1996; Nakahara *et al.*, 1997; Hotary *et al.*, 2000).

ProMMP-9/gelatinase B/type IV collagenase has been previously identified in many cell types as well as PMNLs and is known to specifically cleave basement membrane type IV collagen in addition to denatured collagens (Mignatti and Rifkin, 1993; Fujimoto *et al.*, 1994; Murphy and Crabbe, 1995; Goetzl *et al.*, 1996). Since collagens are not components of foreign pathogens, it is assumed that the PMNL MMPs must be produced for the degradation of collagens during PMNL chemotaxis and migration into perivascular tissue. The type IV collagenase, MMP-9, may degrade the sheet-like basement membrane type IV collagen whereafter MMP-8 may cleave the stromal type I collagen. The denatured type I collagen may subsequently be degraded by MMP-9, providing a pathway within the ECM through which the PMNL could migrate.

MMPs are stored as zymogens in PMNLs and require activation in order to degrade appropriate substrates. The demonstration of a proMMP-9/TIMP-1 complex during proMMP-9 isolation (Triebel *et al.*, 1995) has previously indicated the possible existence of a proMMP-9/TIMP-1 heterodimeric complex. Our colocalisation studies support the existence of such a complex *in vivo*, as approximately 22.6% of the proMMP-9 localised by immunocytochemistry in PMNLs, occurs together with TIMP-1 in a discrete TIMP-1 vesicle subpopulation. These findings suggest that activation of proMMP-9 may be via a complex similar to that of the proMMP-2/TIMP-2/MT-MMP heterotrimeric complex seen in other cell types (Saito and Seiki, 1995;

Hotary *et al.*, 2000). Such a system may be responsible for either intracellular or extracellular activation of MMPs, however, a specific MT-MMP has, as yet, not been identified and the mechanism of *in vivo* proMMP activation remains unresolved.

The exclusion of the proMMPs (except low levels of proMMP-8) from the phagosome upon uptake of IgG-opsonised latex beads implies that proMMP-8 and –9 activation is not brought about intracellularly by MPO-derived HOCl or other ROS or serine proteinases released into the phagosome under these conditions.

At the conclusion of this study, the exact order and regulation of release of the TIMP-1 vesicle relative to that of the MMPs is still not understood. The TIMP-1 vesicle appears to be insensitive to increases in $[Ca^{2+}_i]$, unlike the MMP-containing granules, and possibly associates with a unique cytoskeletal element. Regulation of TIMP-1 release, therefore, seems distinct from that governing all other proteins and this is an extremely interesting finding of potentially vital importance for strategies aimed at regulation of release of TIMP-1 and, hence, the control of inflammation.

Since TIMP-1 is known to have many functions, besides that as an inhibitor, and has a unqiue structure similar only to a few bacterial protein toxins, one of the intriguing and puzzling findings of this study was the identification of the high M_r TIMP-1 form. The *in vivo* role of such a species is uncertain. It might represent a form of TIMP-1 that exists as a highly insoluble aggregate, like the high M_r cysteine proteinase inhibitor purified from epidermis (Fukuyama *et al.*, 1986). The questions of the solubility of the high M_r form of TIMP-1 and whether this may give rise to, or is a part of a mechanism responsible for the discrete and compact packaging of TIMP-1 during granule biogenesis, or whether this form relates directly to the *in vivo* role(s) of the inhibitor in PMNLs, remain unresolved. In addition, the question of whether the 66 kDa form is susceptible to ROS degradation like monomeric TIMP-1, or whether it is specially expressed at a low level to resist ROS damage and cleavage by enzymes such as HNE, remains similarly unknown. The finding that the 66 kDa form retains both binding and inhibitory function towards MMPs is interesting and further structural analysis of this form would be informative. The major question also remains as to whether this form is an artefact or not, as it was mainly detected in homogenates. It was, however, also found in plasma and sputa (results not reported). If it is an artefact, the possibility that the artefact is generated by oligonucleotide binding activity, previously reported for TIMP-1, is intriguing and it would be worthwhile

investigating this possibility as identification of the DNA sequence bound may give an indication of the other possible roles of TIMP-1.

6.3 The continued debate over the role of MMPs and TIMP-1 in PMNL invasion

Subsequent to the commencement of these studies, a report by Steadman *et al.* (1997), stated that human PMNLs do not degrade major basement membrane components during chemotaxis, while studies by Mackarel *et al.* (1999) and Betsuyaku *et al.* (1999) provided evidence that PMNLs do not use MMPs or serine proteinases during invasion. These studies reflected the opinions that had been raised earlier in SEM PMNL invasion experiments using human chorion membranes (Bakowski and Tschesche, 1992) and immunofluorescence studies in collagen gels (Mandeville *et al.*, 1997) and suggest that PMNLs rely predominantly (or rather, exclusively, as expressed by Steadman *et al.*, 1997) on mechanical deformation of ECM collagen fibres. Therefore, the above studies imply that PMNL migration may not be reliant on large scale degradation of ECM components or may not require degradation of the ECM at all.

However, despite many recent findings in ***in vitro*** model systems disputing the relevance of proteinases and, in particular, the MMPs in PMNL invasion, the dependence on MMPs to facilitate extravasation has been supported by ***in vivo*** work performed using intravital video microscopy (IVVM) of hamster cheek pouches (Oda *et al.*, 1995) and genetically deficient mice (Osiewicz *et al.*, 1999). IVVM studies provided evidence that PMNLs use MMPs to breach the venular basement membrane during chemotaxis induced by LTB_4 gradients. Addition of the hydroxamic acid-derived MMP inhibitor FN-439 (*p*-NH_2-Bz-Gly-Pro-D-Leu-D-Ala-NHOH) (IC_{50} MMP-8 = 1.3 μM; IC_{50} MMP-9 = 30 μM), significantly reduced ($p<0.05$) the PMNL count in the interstitium. The hamster cheek pouch system has many advantages over techniques employing denuded human umbilical vascular endothelial cells, Matrigel® (Steadman *et al.*, 1997), or simple collagen gels (Kuntz and Saltzman, 1997). Apart from being artefactual/artificial in nature, the *in vitro* systems cannot emulate the complex and dynamic homeostatic conditions and fluxes of various components (such as inhibitors) and various other signal transducing molecules maintained in a whole animal system and may, therefore, not accurately reflect the mechanism(s) of tissue infiltration and the role of proteinases in inflammation. The *in vivo* study of Oda *et al.* (1995), therefore, provides the most convincing evidence in favour of MMP-mediated proteolytic events during PMNL extravasation.

We believe that extensive proteolysis is unnecessary for PMNL invasion as only limited, single-

site cleavage of type I and IV collagens is required for the unwinding of collagen tropohelices. To assist PMNL passage through the ECM, we propose that PMNLs allow limited release of both MMP-8 and MMP-9 to effect such cleavage, and, subsequent timely release of TIMP-1 may play an important role in rapidly inhibiting and, hence, localising and controlling the extent of MMP activity. The location of TIMP-1, separate from its target enzymes, in a vesicle that may be differentially mobilised, would facilitate the fine regulation of such a proteolytic process. The release of a TIMP-1/proMMP-9 complex from the TIMP-1 vesicle subpopulation, where TIMP-1 binds to proMMP-9 at a site distant from its inhibitory domain, may be used specifically. The 'piggy-back' action of the enzyme/inhibitor complex would allow stabilisation of the proMMP during extracellular activation and allow brief enzyme activity before it is rapidly quenched.

Since the MMPs are known to exhibit high activity towards ECM collagens but by most accounts do not seem to be relevant in invasion, this then raises the question of why the PMNL synthesises and stores proMMPs, TIMP-1, HNE and α_1-proteinase inhibitor (Mason *et al.*, 1991) if such proteolysis and subsequent inhibition is not required. Do the proteinases and their inhibitors serve other functions? This has indeed been the case for HNE, which has been found to be responsible for defensin release from azurophil membranes to kill microorganisms, degradation of inhibitors (Okada *et al.*, 1988) and direct killing of microorganisms (Edwards, 1994), apart from its anticipated elastinolytic role. Similarly, MMP-9 has recently been found to possess a caspase-1-like activity in the processing of IL-1β (Schönbeck *et al.*, 1998) and active MMPs have been found to degrade α_1-proteinase inhibitor and α_1-antichymotrypsin (Desrochers *et al.*, 1992). It is, therefore, tempting to think that PMNL MMPs may serve non-collagenolytic roles *in vivo*.

6.4 Other possible roles for PMNL gelatinase?

The recent *in vivo* studies, which reported the hyper-resistance of TIMP-1-deficient mice to *Pseudomonas aeruginosa* corneal infections also seems to lend support to the notion that MMPs are essential for tissue invasion and bacterial killing by PMNLs (Osiewicz *et al.*, 1999). The authors found that mice deficient for TIMP-1 showed increased PMNL accumulation in the infected corneas, resulting in a reduction in the bacterial burden to a level 1600-fold lower than normal/wild-type mice. To prove that hyper-resistance to infection was PMNL-dependent, neutropenia (i.e. a reduction in the number of circulating PMNLs) was induced by cyclophosphamide, resulting in a 90% reduction in circulating PMNLs. The neutropenic mice

(both TIMP-1 deficient and wild-type) showed identical bacterial burdens, thereby indicating that resistance is PMNL-dependent. The resistance was shown to be MMP-dependent (and not due to loss of a TIMP-1 pleiotropic function) since treatment of TIMP-1-deficient mice with BB-94 (a relatively non-specific hydroxamate-based MMP inhibitor) gave rise to bacterial burdens similar to wild-type mice.

Since bacteria do not contain components which are degradable by MMPs, and TIMP-1 absence should not impede the invasion of PMNLs to the site of infection, it is tempting to hypothesise that the increased PMNL accumulation and subsequent killing of *P. aeruginosa* in corneas of TIMP-1-deficient mice may be due to MMP release and destruction of components of the complement cascade. Previous reports have demonstrated that PMNL MMPs are capable of cleaving both C1-inhibitor (the endogenous inhibitor of C1r and C1s) (Knäuper *et al.*, 1991) and the collagen-like domain of complement factor, C1q (Ruiz *et al.*, 1999). Cleavage of C1-inhibitor would permit activation and assembly of C1qrs on IgG-opsonised bacteria and thereby allow increased killing via the membrane attack pore-forming complex of the classical pathway of complement fixation. Bacterial killing via the membrane attack complex would increase the concentration of circulating PMNL chemoattractants such as C3a and C5a (Roitt, 1994). These anaphylatoxins induce vasodilation and improve delivery of PMNLs to the site of infection and, hence, would assist in the killing of microorganisms.

PMNLs, however, possess different receptors and killing of bacteria may be influenced by the receptor bound during phagocytosis. The receptor bound may be influenced by PMNL secretion of MMPs as PMNL MMP-induced cleavage of the collagen-like domain of C1q may result in the inhibition of complement assembly on complement-fixing IgG and, hence, increased uptake of IgG-opsonised bacteria via PMNL Fc receptors (FcγIIIRB/CD16b) rather than complement receptors. Since phagocytosis of bacteria via Fc receptors as opposed to complement receptors is known to result in full maturation of phagosomes, this may result in more efficient killing of bacteria (Joiner *et al.*, 1989). Some bacteria (such as *P. aeruginosa*), however, seem to evade destruction by phagocytosis by preventing maturation of the phagosome. This may be induced if increased uptake of bacteria occurs via the complement receptor and may, theoretically, occur if bacteria are able to either 1), prevent the release of MMPs (and MMP activity) on the C1q complement component, thereby allowing complement assembly and uptake via complement receptor rather than the IgG receptor or 2), such organisms may have evolved mechanisms for promoting the secretion of TIMP-1, thereby preventing MMP-mediated C1q destruction. This

would then favour the uptake of microorganisms via the complement receptor, resulting in the non-maturation of the phagosome and, hence, survival of the microorganism.

The results of Osiewicz *et al.* (1999) do not provide indisputable evidence for either of the three scenarios. Therefore, further investigations are required to identify the exact stage that MMPs are required for PMNL-mediated bacterial killing. Even so, it is interesting to note that none of the other TIMP members (TIMPs-2, -3 and -4) appear to substitute for TIMP-1 in the genetically deficient mice. The results from the study by Osiewicz *et al.* (1999) prove that TIMP-1 may be an important regulator of PMNL function. The discovery of the unique TIMP-1 vesicle and its apparent unique regulation in the current study implies that the PMNL may differentially release TIMP-1 versus MMP-8 and -9 in a yet unknown manner. It would, therefore, be useful to identify and elucidate these mechanism(s), as induction of TIMP-1 release during inflammation or arthritis may assist in decreasing MMP-mediated PMNL extravasation and tissue damage.

Although much is known about the kinetics of MMP-mediated collagenolysis and TIMP-mediated MMP inhibition *in vitro*, the formation of proteolytic microenvironments at cell focal contact points *in vivo* have the potential to exclude inhibitors and generate pH microenvironments different to the extracellular fluid (Boyer and Tannock, 1992). This makes extrapolation of *in vitro* data difficult. EM has an advantage over cell-free assays as it relies on observations made on the whole cell. Enzyme release and substrate degradation can be monitored to an extent. Unfortunately, it can only provide a static 'snap shot' of cell activity at a point in time and, therefore, cannot provide a fully continuous story. Acknowledgement of the limitations of various techniques, be they cell-free assays or real time kinetics, is important in elucidating the true sequences of events that occur during cell invasion. In addition, acknowledging that cellular cross-talk occurs *in vivo* and that multiple enzyme cascades may occur simultaneously, will guard against the temptation to oversimplify invasion mechanisms.

The current studies reported in this thesis have provided some answers to granule localisation of TIMP-1 and have also provided some assays and reagents necessary for the continuation of this work. The mechanism of regulated exocytosis and the precise mechanisms involved in invasive behaviour still remain unresolved. In addition to providing the basis for further PMNL cryoimmunocytochemistry work, MMP zymogram and TIMP reverse zymogram analyses and phagocytosis experiments, two important areas requiring immediate future investigation have

been highlighted: identification of the mechanism(s) of selective PMNL granule release and the definitive assessment of the roles of proteinases (or proteoglycanases) in PMNL tissue invasion. Investigations into the importance of phagocytic degradation of collagen by PMNLs, and the role of MMP-8 and -9 in such a process would also be of great interest.

6.5 Future areas of research

Identification of the mechanism(s) involved in maintaining PMNL granule selectivity by regulated exocytosis. Previous studies have demonstrated that the four major PMNL granule populations differ with respect to sensitivity to $[Ca^{2+}_i]$ (Lew *et al.*, 1984, 1986; Borregaard *et al.*, 1993; Sengeløv *et al.*, 1993). The known potential fusogen proteins present in the PMNL are shown in Table 6.1. It would be useful to thoroughly investigate the differences in phospholipid composition of the various granule populations (especially the TIMP-1 vesicle) as this may regulate the fusogen protein association and, hence, fusion events. This information would be potentially useful in understanding the regulation of granule fusion under different conditions (e.g. activation, phagocytosis, invasion etc.). Initial results obtained after examining granule phospholipids indicate that there are differences in membrane phospholipids (Borregaard *et al.*, 1993) although a complete analysis of all derivatives and populations has not been performed. In addition, an investigation into the phospholipid dynamics of the phagosome would be interesting due to the fact that a number of pathogens prevent phagosomal maturation by interfering with membrane recycling (de Chastellier and Thilo, 1997).

The identification of membrane phospholipids in PMNLs is more difficult than in other cell types since their lipids cannot be radiolabelled after purification of blood PMNLs as granule biogenesis has already terminated in mature PMNLs. Apart from extracting and labelling immature PMNLs from bone marrow, it would be impossible to isolate radioactive phospholipid for analysis using thin layer chromatography, gas chromatography or high performance liquid chromatography. Thin layer chromatographic detection of unlabelled or 'cold' lipids, is not sufficiently sensitive but a rapid detection system for unlabelled phospholipid derivatives has been described using ^{31}P nuclear magnetic resonance spectroscopy (Bredamante *et al.*, 1990). The different substituents attached to the phosphate group (e.g. ethanolamine, serine, choline, inositol) produce distinct peaks depending on their protecting or deprotecting characteristics on the phosphorus atom. In this manner, PI, PE, PS, PC, sphingosine and lysophosphatidylcholine have been resolved in blood plasma samples. To monitor the dynamics of phospholipid association with the phagosome, the latex bead compartment may also be isolated by a density

shift technique used by Pizou *et al.* (1994) and Kaufman *et al.* (1996) and the phospholipids analysed.

Identification of the apparently different cytoskeletal elements that may result in the differential release of MMP-9 and TIMP-1, and an investigation into the identity of fusion proteins associated with the TIMP-1 vesicle are required as information gained from these experiments may assist in our understanding of differential granule release patterns. A list of the fusion proteins identified to date are given in Table 6.1. As it is hypothesised that TIMP-1 synthesis occurs between metamyelocytic and terminal PMNL differentiation, it would be anticipated that fusion proteins such as those common to the gelatinase granules and secretory vesicles may be most relevant. Such investigations would be difficult, however, and therefore, the best approach would be to initially study the receptor-mediated TIMP-1 vesicle release using pharmaceutical cell signalling compounds which would activate the various known signalling pathways and, thereafter, deduce the pathway activated and the mechanism of regulation of TIMP-1 release.

Table 6.1 Potential protein mediators of PMNL granule fusion.

Intracellular location	Fusogenic proteins[†]	Potential target organelle(s)/cellular compartment/phospholipid[‡]
Cytosol	G3PDH[a]	PE,PA,PC
	Annexin I[b,c]	PA>PS,PI,F-actin,PLA_2
Azurophil granule	?	??
Specific granule	SCAMP[d]	?
	Annexin III[e]	PA>PS>>PI>PE
	Annexin XI[f]	PE,PS
	Rap1, Rap2[g]	Specific granules (cytochrome b_{558})
Gelatinase granule	SCAMP[d]	?
	VAMP-2[d]	Plasma membrane syntaxin 4
Secretory vesicle	SCAMP[d]	?
	VAMP-2[d]	Plasma membrane syntaxin 4
Plasma membrane	Syntaxin 4[d]	Vesicle-bound VAMP-2
	Annexin I (+)[b,c]	PA>PS,PI,F-actin,PLA_2
	Annexin III (+)[b,c]	PA>PS>>PI>PE
Phagosome	Annexin I[h]	PA>PS,PI,F-actin,PLA_2
	Annexin III[i]	PA>PS>>PI>PE

[†] SCAMP, secretory carrier membrane protein; VAMP, vesicle associated membrane protein; Rap, a Ras-related small GTPase.

[‡] PA, phosphatidic acid; PC, phosphatidylcholine; PE, phosphatidylethanolamine; PI, phosphatidylinositol; PS, phosphatidylserine; PLA_2, phospholipase A_2.

(+) Occurs during PMNL degranulation.

[a] Hessler *et al.*, 1998; [b] Rosales and Ernst, 1997; [c] Sjölin *et al.*, 1994; [d] Brummell *et al.*, 1995; [e] Le Cabec and Maridonneau-Parini, 1994; [f] Sjölin and Dahlgren, 1996; [g] Maridonneau-Parini and De Gunzburg, 1992; [h] Kaufman *et al.*, 1996; [i] Ernst, 1991.

Investigation of the role of MMPs in PMNL extravasation, ECM degradation and tissue infiltration. Many *in vitro* methods are available for tumour invasion studies include degradation of pure ECM components, degradation of basement membrane formed by cultured cells, degradation and invasion of an *in vitro* reconstituted matrix (e.g. Matrigel®), invasion through natural basement membrane (e.g. bovine lens capsule) and repopulation and invasion of deepithelialised xenotransplanted rat tracheas. All these methods have the drawback that they

are 'artificial' and, therefore, non-representative of an *in vivo* system. Two other methods exist that allow for invasion and detection of metastatic cells in chicken embryos or laboratory animals (such as nude mice) (Mignatti and Rifkin, 1993). Identification of the metastasised cells may be accomplished by incubating the cells in radioactive medium prior to the invasion assay, but this method does not distinguish live from dead cells and thus the efficiency of invasion cannot be accurately determined. In a recent report, Kim *et al.* (1998) described the use of PCR in detecting invasive cells in a chicken embryo system, which would possibly be most useful in the current investigation. The PCR technique comprises two primers that recognise and bind flanking regions of *Alu* elements - repetitive sequences found in human cells (comprising ~5% of the human genome), but absent in avian cells. Invasive test cells are introduced onto the upper chorioallantoic membrane (CAM) in a ~9 day old chicken embryo and are allowed to digest the interstitium and intravasate into the bloodstream. The invasive cells are transported throughout the embryo and may arrest and extravasate in the lower CAM at a site distant to that of the original application. The lower CAM is removed from the rest of the embryo and the total DNA is extracted (Figure 6.1). PCR is performed with the *Alu* primers, producing a ~220 bp amplicon that indicates the presence of human cells in the lower CAM - a phenomenon that could only occur if the cells actively degraded through the upper CAM, travelled through the bloodstream and extravasated in the lower CAM. In addition to a simple qualitative result obtained by the amplicon, quantification of the number of extravasated cells can also be performed by comparing the amplicon band intensity obtained from the DNA extracted from the lower CAM to those obtained from known starting numbers of test cells (e.g. 100 to 100000 cells).

A similar technique may be performed on PMNLs to establish which proteinases are involved in invasion. A chemoattractant may be used (in the lower CAM) to establish a gradient to allow directional PMNL migration into the bloodstream and arrest extravasation in the lower CAM. Detection of invasive PMNLs would be similarly established via the *Alu* PCR technique. The efficiency of a number of hydroxamate-derived MMP inhibitors in preventing PMNL invasion may be assessed. In such a system, the use of inhibitors to prevent tumour cell invasion in the chicken embryo system has already met with success (Kim *et al.*, 1998) and should be applicable to PMNL studies.

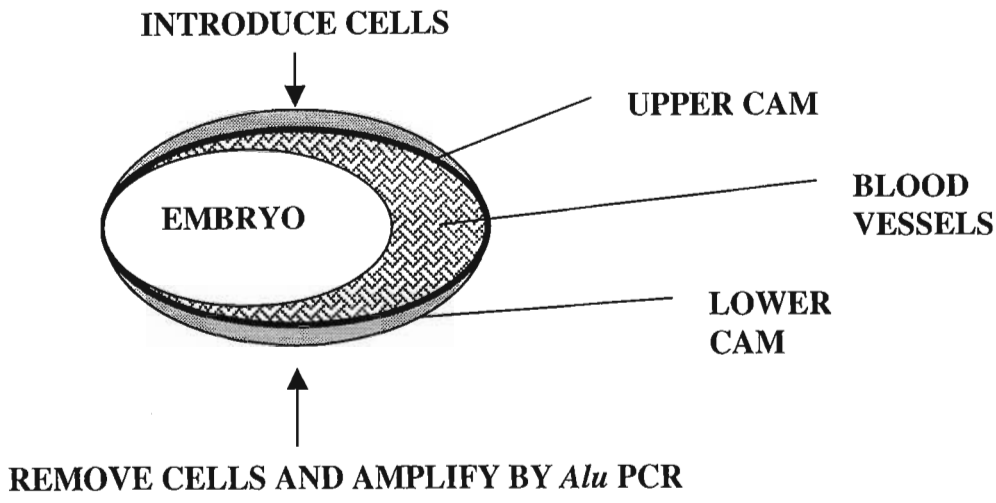

Figure 6.1 **Schematic representation of the chicken embryo model for assessment of cell invasion.**

A hole is made in the eggshell above the upper chorioallantoic membrane (CAM) and the cell sample is dispensed onto the upper CAM. Invasive cells digest the interstitium and enter the circulation of the embryo. Cells that subsequently arrest and invade into the lower CAM are identified by isolating the lower CAM and amplifying the DNA with *Alu* primers by PCR. Metastatic cells are identified by the appearance of a 220 bp PCR amplicon since avian DNA lacks *Alu* sequences.

Investigations of possible phagocytic uptake and intracellular digestion of type I collagen by PMNLs. In addition to extracellular release of proteinases, the PMNL might phagocytose collagen fibrils to degrade them intracellularly during invasion and inflammation. Phagocytic digestion of collagens has been observed in involution and osteoclast remodelling (Woessner, 1991) and may be a major and important mechanism by which PMNLs contribute to inflammation. The phagosome work performed in this thesis only reflects granule fusion selectivity during IgG-mediated phagocytosis and signalling and, hence, the selectivity of granule release into the phagosome may differ with differing opsonins (Joiner *et al.*, 1989). Preliminary work involving incubation of PMNLs with pure type I collagen have revealed that this induces the respiratory burst and that PMNLs contain type I collagen receptors (Monboisse *et al.*, 1990). Hence, phagocytosis via a type I collagen receptor-mediated pathway is possible. Phagocytic digestion of collagen may allow: 1), uninterrupted digestion of collagen by *active* MMPs in a compartment separate from extracellular inhibitors and 2), production of collagen fragments that, when released extracellularly, may act as chemoattractants (Terranova *et al.*, 1989) to signal more PMNLs to a particular site. In either case, if the proMMPs are targeted to

the phagosome upon ingestion of type I collagen, they may be activated and may subsequently be released into the extracellular fluid. To assess the role of phagosomal collagen breakdown by PMNLs, type I collagen has been purified and anti-type I collagen antibodies raised in chickens. Future experiments may involve the incubation of PMNLs in the presence of collagen fibrils and fibres and detection of collagen phagocytosis (via immunocytochemistry of ultrathin cryosections). ProMMP inclusion into the phagosome may be studied by gelatin and type I collagen zymography of latex bead phagosomes isolated by density centrifugation and type I collagen degradation may be assessed using western blotting of purified phagosomes and supernatant fluids to detect the characteristic ¾ and ¼ type I collagen fragments.

6.6 Applications of these studies for drug designing and treatment of inflammation

The similarity between the invasive nature of leukocytes (such as PMNLs) and cancer cells has the potential to provide insight into tissue invasion and the proteins and proteinases involved in this process. The designing of drugs to inhibit enzymes responsible for promoting cellular invasion requires careful consideration. Firstly, the drug should be enzyme-specific rather than class-specific. Although MMPs might be implicated in tumour invasion and possibly leukocyte invasion, the administration of broad spectrum MMP inhibitors to patients runs the risk of interfering with normal MMP-mediated events that are important to the individual (e.g. wound healing and immune response). The same would apply to other classes of proteinases since various members are crucial for the survival of normal body function (e.g. serine proteinases are responsible for a functional clotting cascade). Modern pharmaceuticals have provided a number of enzyme-specific synthetic proteinase inhibitors of low M_r and good solubility, but full elucidation of all possible *in vivo* functions of proteinases need to be completed before such inhibitors are administered. The multiple and seemingly unrelated (pleiotropic) functions of proteinases such as the gelatinases [IL-β converting activity, serpin degradation and now in the light of the Osiewicz study (Osiewicz *et al.*, 1999), possible function in facilitating the killing of microorganisms], cathepsins (e.g. mitogenic activity of cathepsin D) and proteinase inhibitors (TIMP-1 growth factor, anti-angiogenic and anti-apoptotic functions, α_1-proteinase inhibitor cysteine proteinase activity, cell growth inhibitory and microbicidal functions) highlights the need for further research into the exact enzymes and proteolytic cascades involved in invasion and other non-proteolytic pathways that might be inhibited. It is hoped that identification of unique and critical enzymes in these cascades would provide an opportunity for the specific and highly selective inhibition of invasion and metastasis of the tumour, without the risk of compromising the health of the patient and ultimately allowing surgical removal of the single

tumour mass. Continued research into the role of the MMPs by means of inhibitor trials in the *in vivo* chicken embryo model and further research into the mobilisation of the unique TIMP-1 vesicle are required to add to the knowledge gained so far regarding the granule location and regulation of MMPs and TIMPs in PMNLs.

REFERENCES

Absolom DR (1986). Basic methods for the study of phagocytosis. In: Immunochemical techniques Part J - Phagocytosis and cell mediated cytotoxicity. Methods in Enzymology vol. 132. (DiSabato G, Everse J, eds), Academic Press, Orlando, pp 95-115.

Adachi E, Hopkinson I, Hayashi T (1997). Basement membrane stroma relationships between collagen fibrils and the laminar densa. Int. Rev. Cytol. 173:73-156.

Allen LH, Aderem A (1996). Mechanisms of phagocytosis. Curr. Opin. Immunol. 8:36-40.

Albrecht E, Petty HR (1998). Cellular memory: Neutrophil orientation reverses during temporally decreasing chemoattractant concentrations. Proc. Natl. Acad. Sci. USA. 95:5039-5044.

Al-Mohanna FA, Pettit EJ, Hallett MB (1997). Does actin polymerisation status modulate Ca^{2+} storage in human neutrophils? Release and coalescence of Ca^{2+} stores by cytochalasins. Exp. Cell Res. 234:379-387.

Anderson RGW, Orci L (1988). A review of acidic intracellular compartments. J. Cell Biol. 106:539-543.

Anderson MM, Requena JR, Crowley JR, Thorpe SR, Heinecke JW (1999). The myeloperoxidase system of human phagocytes generates N^{ε}-(carboxymethyl)lysine on proteins: a mechanism for producing advanced glycation end products at sites of inflammation. J. Clin. Invest. 104:103-113.

Andrews PC, Krinsky NI (1986). Human myeloperoxidase and hemi-myeloperoxidase. In: Immunochemical techniques Part J - Phagocytosis and cell mediated cytotoxicity. Methods in Enzymology vol. 132. (DiSabato G, Everse J, eds), Academic Press, Orlando, pp 369-370.

Arvan P, Castle D (1998). Sorting and storage during secretory granule biogenesis: Looking backward and looking forward. Biochem. J. 332:593-610.

Avalos BR, Kaufman SE, Tomonaga M, Williams RE, Golde DW, Gasson JC (1988). K562 cells produce and respond to human erythroid potentiating activity. Blood. 71:1720-1725.

Babior BM (1999). NADPH oxidase: an update. Blood. 93:1464-1476.

Bainton DF (1973). Sequential degranulation of the two types of polymorphonuclear leukocyte granules during phagocytosis of microorganisms. J. Cell Biol. 58:249-264.

Bainton DF (1999). Distinct granule populations in human neutrophils and lysosomal organelles identified by immuno-electron microscopy. J. Immunol. Meth. 232:153-168.

Bainton DF, Ullyot JL, Farquhar GD (1971). The development of neutrophilic polymorphonuclear leukocytes in human bone marrow. J. Exp. Med. 134:907-934.

Bakowski B, Tschesche H (1992). Migration of polymorphonuclear leukocytes through human amnion membrane - A scanning electron microscopic study. Biol. Chem. Hoppe-Seyler. 373:529-546.

Barrett AJ (1981). Leukocyte elastase. In: Proteolytic Enzymes. Methods in Enzymology vol. 80 (Lorand L, ed), Academic Press, New York, pp 581-588.

Bentwood BJ, Henson PM (1980). The sequential release of granule constituents from human neutrophils. J. Immunol. 124:855-862.

Berger M, Medof ME (1987). Increased expression of complement decay-accelerating factor during activation of human neutrophils. J. Clin. Invest. 79:214-220.

Berger M, Wetzler E, August JT, Tartakoff AM (1994). Internalisation of type I complement receptor and *de novo* multivesicular body formation during chemoattractant-induced endocytosis in human neutrophils. J. Clin. Invest. 94:1113-1125.

Bergmann U, Michaelis J, Oberhoff R, Knäuper V, Beckmann R, Tschesche H (1989). Enzyme linked immunosorbent assays (ELISA) for the quantitative determination of human leukocyte collagenase and gelatinase. J. Clin. Chem. Clin. Biochem. 27:351-353.

Bernhard EJ, Gruber SB, Muschel RJ (1994). Direct evidence linking expression of matrix metalloproteinase 9 (92-kDa gelatinase/collagenase) to the metastatic phenotype in transformed rat embryo cells. Proc. Natl. Acad. Sci. USA. 91:4293-4297.

Bertaux B, Hornebeck W, Eisen AZ, Dubertret L (1991). Growth stimulation of human keratinocytes by tissue inhibitor of metalloproteinases. J. Invest. Dermatol. 114:447-456.

Betsuyaku T, Shipley JM, Liu Z, Senior RM (1999). Neutrophil emigration in the lungs, peritoneum, and skin does not require gelatinase B. Am. J. Respir. Cell Mol. Biol. 20:1303-1309.

Bielschowsky M (1902). Die Silberimpragnation der Axenzylinder. Centralblatt für Neurologie, Bd 21:579-584.

Birkedal-Hansen H (1987). Catabolism and turnover of collagens: Collagenases. In: Structural and contractile proteins Part D: Extracellular Matrix. Methods in Enzymology vol. 144 (Cunningham LW, ed), Academic Press, Orlando, pp 140-169.

Bischoff KM, Shi L, Kennelly PJ (1998). The detection of enzyme activity following sodium dodecyl sulfate-polyacrylamide gel electrophoresis. Anal. Biochem. 260:1-17.

Bjerrum OW, Nielsen H, Borregaard N (1989). Quantitative analysis of phospholipids and demonstration of plasmalogen in human neutrophil subcellular fractions by high-performance liquid chromatography. Scand. J. Clin. Lab. Invest. 49:613-622.

Blocker A, Giffiths G, Olivo J-C, Hyman AA, Severin FF (1998). A role for microtubule dynamics in phagosome movement. J. Cell Sci. 111:303-312.

Blocker A, Severin FF, Burkhardt JK, Bingham JB, Yu H, Olivo J-C, Scroer TA, Hyman AA, Griffiths G (1997). Molecular requirements for bi-directional movement of phagosomes along microtubules. J. Cell Biol. 137:113-129.

Blum H, Beier H, Gross HJ (1987). Improved silver staining of plant proteins, RNA and DNA in polyacrylamide gels. Electrophoresis. 8:93-99.

Bock JB, Scheller RH (1997). A fusion of new ideas. Nature. 387:133-135.

Bode W, Fernandez-Catalan C, Tschesche H, Grams F, Nagase H, Maskos K (1999). Structural properties of matrix metalloproteinases. Cell. Mol. Life Sci. 55:639-652.

Bokovsky J, Kennett RH (1987). Simple and rapid purification of monoclonal antibodies from cell culture supernatants and ascites fluid by hydroxylapatite chromatography on analytical and preparative scales. Hybridoma. 6:219-228.

Bollag DM, Edelstein SJ (1991). Protein methods. John Wiley and Sons, New York.

Borregaard N, Christensen L, Bjerrum OW, Birgens HS, Clemmensen I (1992). Identification of a highly mobilisable subset of human neutrophil intracellular vesicles that contain tetranectin and latent alkaline phosphatase. J. Clin. Invest. 90:86-90.

Borregaard N, Cowland JB (1997). Granules of the human neutrophilic polymorphonuclear leukocyte. Blood. 89:3503-3508.

Borregaard N, Lollike K, Kjeldsen L, Sengeløv H, Bastholm L, Nielsen MH, Bainton DF (1993). Human neutrophil granules and secretory vesicles. Eur. J. Haematol. 51:187-198.

Borregaard N, Miller LJ, Springer TA (1987). Chemoattractant-regulated mobilization of a novel intracellular compartment in human neutrophils. Science. 237:1204-1206.

Borregaard N, Sehested M, Nielsen BS, Sengeløv H, Kjeldsen L (1995). Biosynthesis of granule proteins in normal human bone marrow cells. Gelatinase is a marker of terminal neutrophil differentiation. Blood. 85:812-817.

Botos I, Scapozza L, Zhang D, Liotta LA, Meyer EF (1996). Batimastat, a potent matrix metalloproteinase inhibitor, exhibits an unexpected mode of binding. Proc. Natl. Acad. Sci. USA. 93:2749-2754.

Boujrad N, Ogwuegbu SO, Garnier M, Lee CH, Matrin BM, Papadopoulos V (1995). Identification of a stimulator of steroid hormone synthesis isolated from testis. Science. 268:1609-1612.

Boyer RF (1993). Modern Experimental Biochemistry (2nd Edition). The Benjamin/Cummings Publishing Co., California, USA.

Boyer MJ, Tannock IF (1992) Relation of intracellular pH to tumor cell lines: Influence of microenvironmental conditions. Cancer Res. 52:4441-4447.

Bradford MM (1976). A rapid and sensitive method for the quantitation of microgram quantities of protein utilising the principle of protein-dye binding. Anal. Biochem. 72:248-254.

Braet F, De Zanger R, Wisse E (1997). Drying cells for SEM, AFM and TEM by hexamethyldisilazane: A study on hepatic endothelial cells. J. Microsc. 186:84-87.

Branden C, Tooze J (1991). Introduction to protein structure. Garland Publishing Inc., New York, pp 113-127.

Bredamante S, Barchiesi E, Barenghi L, Zoppi F (1990). An alternative expeditious analysis of phospholipid composition in human blood plasma by ^{31}P NMR spectroscopy. Anal. Biochem. 185:299-303.

Breton-Gorius J, Mason DY, Buriot D, Vilde J-L, Griscelli C (1980). Lactoferrin deficiency as a consequence of a lack of specific granules in neutrophils from a patient with recurrent infections - Detection by immunoperoxidase staining for lactoferrin and cytochemical electron microscopy. Am. J. Path. 99:413-417.

Bretz U, Baggiolini M (1974). Biochemical and morphological characterisation of azurophil and specific granules of human neutrophilic polymorphonuclear leukocytes. J. Cell Biol. 63:251-269.

Brodsky B, Eikenberry, EF (1982). Characterisation of fibrous forms of collagen. In: Structural and Contractile Proteins, Part A - The Extracellular Matrix. Methods in Enzymology vol. 82, (Cunningham LW, Frederikson, DW, Eds), Academic Press, New York, pp 127-174.

Brown DA, Rose JK (1992). Sorting of GPI-anchored proteins to glycolipid-enriched membrane subdomains during transport to the apical cell surface. Cell. 68:533-535.

Brummell JH, Volchuk A, Sengeløv H, Borregaard N, Cieutat A-M, Bainton DF, Grinstein S, Klip A (1995). Subcellular distribution of docking/fusion proteins in neutrophils, secretory cells with multiple exocytic compartments. J. Immunol. 155:5750-5759.

Brusca JS, Radolf JD (1994). Isolation of integral membrane proteins by phase partitioning with Triton X-114. In: Aqueous two-phase systems. Methods in Enzymology vol. 228 (Walter H, Johansson G, eds), Academic Press, San Diego, pp 182-193.

Bu CH, Pourmotabbed T (1995). Mechanism of activation of human neutrophil gelatinase B. J. Biol. Chem. 270:18563-18569.

Burroughs SF, Devine DV, Browne G, Kaplan ME (1988). The population of paroxysmal nocturnal hemoglobinuria neutrophils deficient in decay-accelerating factor is also deficient in alkaline phosphatase. Blood. 71:1086-1089.

Cain TJ, Liu Y, Kobayashi T, Robinson JM (1995). Rapid purification of glycosylphosphatidylinositol-anchored alkaline phosphatase from human neutrophils after upregulation to the cell surface. J. Histochem. Cytochem. 41:1367-1372.

Campbell EJ, Campbell MA (1988). Pericellular proteolysis in the presence of proteinase inhibitors: effects of substrate opsonisation. J. Cell Biol. 106:667-676.

Campbell EJ, Cury JD, Shapiro SD, Goldberg GI, Welgus HG (1991). Neutral proteinases of human mononuclear phagocytes: Cellular differentiation markedly alters cell phenotype for serine proteinases, metalloproteinases, and tissue inhibitor of metalloproteinases. J. Immunol. 146:1286-1293.

Candiano G, Porotto M, Lanciotti M, Ghiggeri GM (1996). Negative staining of proteins in polyacrylamide gels with methyl trichloroacetate. Anal. Biochem. 243:245-248.

Cao J, Sato H, Takino T, Seiki M (1995). The C-terminal region of membrane type matrix metalloproteinase is a functional transmembrane signal required for progelatinase A activation. J. Biol. Chem. 270:801-805.

Caswell AH, Hutchinson JD (1971). Visualization of membrane bound cations by a fluorescent technique. Biochem. Biophys. Res. Comm. 42:43-49.

Caterina NCM, Windsor LJ, Yermovsky AE, Bodden MK, Taylor KB, Birkedal-Hansen H, Engler JA (1997). Replacement of conserved cysteines in human tissue inhibitor of metalloproteinases-1. J. Biol. Chem. 272:32141-32149.

Cawston TE, Barrett AJ (1979). A rapid and reproducible assay for collagenase using [1-^{14}C] acetylated collagen. Anal. Biochem. 99:340-345.

Cawston TE, Curry VA, Clark IM, Hazelman BL (1990). Identification of a new metalloproteinase inhibitor that forms tight-binding complexes with collagenase. Biochem. J. 269:183-187.

Cawston TE, Mercer E, Mooney C, Wright JK (1986a). Tissue inhibitor of metalloproteinases. In: Proteinases in inflammation and tumor invasion (Tschesche H, ed), Walter de Gruyter and Co., Berlin. p 189.

Cawston TE, Murphy G (1981). Mammalian collagenases. In: Proteolytic enzymes - Part C. Methods in Enzymology vol. 80 (Lorand L, ed), Academic Press, New York, pp 711-734.

Cawston TE, Murphy G, Mercer E, Galloway WA, Hazleman BL, Reynolds JJ (1983). The interaction of purified rabbit bone collagenase with purified rabbit bone metalloproteinase inhibitor. Biochem. J. 211:313-318.

Cawston TE, Noble DN, Murphy G, Smith AJ, Woodley C, Hazleman B (1986b). Rapid purifiaction of tissue inhibitor of metalloproteinases from human plasma and identification as a γ-serum protein. Biochem. J. 238:677-682.

Chambers AF, Matrisian LM (1997). Changing views of the role of matrix metalloproteinases in metastasis. J. Natl. Cancer. Inst. 89:1260-1270.

Chesler L, Golde DW, Bersch N, Johnson MD (1995). Metalloproteinase inhibition and erythroid potentiation are independent activities of tissue inhibitor of metalloproteinases-1. Blood. 86:4506-4515.

Cieutat A-M, Lobel P, August JT, Kjeldsen L, Sengeløv H, Borregaard N, Bainton DF (1998). Azurophilic granules of human neutrophilic leukocytes are deficient in lysosome-associated membrane proteins but retain the mannose 6-phosphate recognition marker. Blood. 91:1044-1058.

Clague MJ (1998). Molecular aspects of the endocytic pathway. Biochem. J. 336:271-282.

Clark RA, Borregaard N (1985). Neutrophils autoinactivate secretory products by myeloperoxidase-catalyzed oxidation. Blood. 65:375-381.

Cleland WW (1964). Dithiothreitol, a new protective agent for SH groups. Biochemistry. 4:480-482.

Cole AA, Chubinskaya S, Schumacher B, Huch K, Cs-Szabo G, Yao J, Mikecz K, Hasty KA, Kuettner KE (1996). Chondrocyte matrix metalloproteinase 8. Human articular chondrocytes express neutrophil collagenase. J. Biol. Chem. 271:11023-11026.

Collins SJ, Ruscett FW, Gallagher RE (1977). Continuous growth and differentiation of human myeloid leukemia cells in suspension culture. Nature. 270:347-350.

Cooper TW, Eisen AZ, Stricklin GP, Welgus HG (1985). Platelet-derived collagenase inhibitor: Characterisation and subcellular localization. Proc. Natl. Acad. Sci. USA. 82:2779-2783.

Copeland RA (1994). Reverse fluorescence staining of proteins in polyacrylamide gels using terbium chloride. Anal. Biochem. 220:218-219.

Cramer E, Pryzwansky KB, Villeval L-J, Testa U, Breton-Gorius J (1985). Ultrastructural localisation of lactoferrin and myeloperoxidase in human neutrophils by immunogold. Blood. 65:423-432.

Cuypers PA, Hermens WT, Hemker HC (1978). Ellipsometry as a tool to study protein films at liquid-solid interfaces. Anal. Biochem. 84:56-60.

Dahlgren C, Carlsson SR, Karlsson A, Lundqvist H, Sjölin C (1995). The lysosomal membrane glycoproteins Lamp-1 and Lamp-2 are present in mobilisable granules, but are absent from the azurophil granules of human neutrophils. Biochem. J. 311:667-674.

Dahlgren C, Follin P, Lundqvist H, Sjölin C (1993). Quantitative slot-blot chemiluminescence assay for determination of myeloperoxidase from human granulocytes. Anal. Biochem. 214:284-288.

Damiano V, Kucich U, Murer E, Laudenslager N, Weinbaum G (1988). Ultrastructural quantitation of peroxidase and elastase-containing granules in human neutrophils. Am. J. Pathol. 131:235-245.

Dauscher G (1981). Histochemical demonstration of heavy metals. A revised version of the sulphide method suitable for both light and electron microscopy. Histochem. 71:1-7.

Davis GE (1991). Identification of an abundant latent 94 kDa gelatin-degrading metalloprotease in human saliva which is activated by acid exposure: Implications for a role in digestion of collagenous proteins. Arch. Biochem. Biophys. 286:551-554.

De Chastellier C, Thilo L (1997). Phagosome maturation and fusion with lysosomes in relation to surface property and size of the phagocytic particle. Eur. J. Cell Biol. 74:49-62.

De Clerck YA, Shimada H, Taylor SM, Langley KE (1994). Matrix metalloproteinases and their inhibitors in tumor progression. In: Inhibition of matrix metalloproteinases: Therapeutic potential vol. 732 (Greenwald RA, Golub LM, eds), Annals New York Academy of Sciences, pp 222-232.

De Maio A (1994). Protein blotting and immunoblotting using nitrocellulose membranes. In: Protein blotting - A practical approach (Dunbar BS, ed). Oxford University Press, Oxford, pp 12-32.

De Mey J (1986). The preparation and use of gold probes. In: Immunocytochemistry: Modern

methods and applications, 2nd Ed (Polak JM, van Noorden S, eds), John Wright and Sons, Bristol, UK, pp 115-145.

Demaurex N, Monod A, Lew DP, Krause KH (1994). Characterisation of receptor-mediated and store-regulated Ca^{2+} influx in human neutrophils. Biochem. J. 297:595-600.

Denhardt DT, Feng B, Edwards DR, Cocuzzi ET, Malyakar UM (1993). Tissue inhibitor of metalloproteinases (TIMP; a.k.a EPA): Structure, control of expression and biological functions. Pharmac. Ther. 59:329-341.

Dennison C, Lovrien R (1997). Three phase partitioning: Concentration and purification of proteins. Protein Expression and Purification. 11:149-161.

Desjardins M, Nzala NN, Corsini R, Rondeau C (1997). Maturation of phagosomes is accompanied by changes in their fusion and size-selective acquisition of solute materials from endosomes. J. Cell Sci. 110:2303-2314.

Desnoyers S, Shah GM, Bourossa S, Poirier GG (1995). Rapid removal of non-specific background in silver-stained polyacrylamide gels. Anal. Biochem. 232:138-140.

Desrochers PE, Mookhtiar K, Van Wart HE, Hasty KA, Weiss SJ (1992). Proteolytic inactivation of α_1-proteinase inhibitor and α_1-antichymotrypsin by oxidatively activated human neutrophil metalloproteinases. J. Biol. Chem. 267:5005-5012.

Detmers PA, Zhou D, Powell D, Lichenstein H, Kelley M, Pironkova R (1995). Endotoxin receptors (CD14) are found with CD16 (FcγRIII) in an intracellular compartment of neutrophils that contains alkaline phosphatase. J. Immunol. 155:2085-2095.

Devarajan P, Mookhtiar K, Van Wart HE, Berliner N (1991). Structure and expression of the cDNA encoding human neutrophil collagenase. Blood. 77:2731-2738.

Dewald B, Bretz U, Baggiolini M (1982). Release of gelatinase from a novel secretory compartment of human neutrophils. J. Clin. Invest. 70:518-525.

Dewald B, Rindler-Ludwig R, Bretz U, Baggiolini M (1975). Subcellular localisation and heterogeneity of neutral proteinases in neutrophilic polymorphonuclear leukocytes. J. Exp. Med. 141:709-723.

Diakonova M, Gerke V, Ernst J, Liautard J-P, van der Vusse G, Griffiths G (1997). Localisation of five annexins in J774 macrophages and on isolated phagosomes. J. Cell Sci. 110:1199-1213.

Docherty AJP, Lyons A, Smith BJ, Wright EM, Stephens PE, Harris TJR, Murphy G, Reynolds JJ (1985). Sequence of human tissue inhibitor of metalloproteinases and its identity to erythroid-potentiating activity. Nature. 318:66-69.

Dransfield I, Buckle AM, Savill JS, McDowall A, Haslett C, Hogg N (1994). Neutrophil apoptosis is associated with a reduction in CD16 (FcγRIII) expression. J. Immunol. 153:1254-1263.

Drouin L, Overall CM, Sodek J (1988). Identification of matrix metalloproteinase inhibitor (TIMP) in human parotid and submandibular saliva: partial purification and

characterisation. J. Periodont. Res. 23:370-377.

Dubochet J, Lepault J, Freeman R, Berriman JA, Homo JC (1982). Electron microscopy of frozen water and aqueous solutions. J. Microsc. 128:219-237.

Dunbar BS (1994). Introduction and basic setup for protein transfer. In: Protein blotting - A practical approach (Dunbar BS, ed). Oxford University Press, Oxford, pp 5-9.

Durrant I, Fowler S (1994). Chemiluminescent detection systems for protein blotting. In: Protein blotting - A practical approach (Dunbar BS, ed). Oxford University Press, Oxford, pp 141-152.

Dustin P (1978). Microtubules. Springer-Verlag, Berlin, pp 295-298.

Edwards SW (1994). Biochemistry and physiology of the neutrophil. Cambridge University Press, Cambridge.

Egesten A, Breton-Gorius J, Guichard J, Gullberg U, Olsson I (1994). The heterogeneity of azurophil granules in neutrophil promyelocytes: Immunogold localization of myeloperoxidase, cathepsin G, elastase, proteinase 3, and bacterial permeability increasing protein. Blood. 83:2985-2989.

Elliott E, Dennison C, Fortgens PH, Travis J (1995). Paraformaldehyde fixation of neutrophils for immunolabeling of granule antigens on cryoultrasections. J. Histochem. Cytochem. 43:1019-1023.

Ellouz F, Adam A, Ciorbaru R, Lederer E (1974). Minimal structural requirements for adjuvant activity of bacterial peptidoglycan derivatives. Biochem. Biophys. Res. Comm. 59:1317-1325.

English WR, Puente XS, Freije JMP, Knäuper V, Amour A, Merryweather A, López-Otín C, Murphy G (2000). Membrane type 4 matrix metalloproteinase (MMP-17) has tumour necrosis factor-α convertase activity but does not activate proMMP-2. J. Biol. Chem. 275:14046-14055.

Englund PT (1993). The structure and biosynthesis of glycosylphosphatidylinositol protein anchors. Ann. Rev. Biochem. 62:121-138.

Ernst JD (1991). Annexin III translocates to the periphagosomal region when neutrophils ingest opsonised yeast. J. Immunol. 146:3110-3114.

Ey PL, Prowse SJ, Jenkin CR (1978). Isolation of pure IgG1, IgG2a, IgG2b immunoglobulins from mouse serum using protein A-Sepharose. Biochemistry. 15:429-436.

Fadeel B, Åhlin A, Henter J-I, Orrenius S, Hampton MB (1998). Involement of caspases in neutrophil apoptosis: Regulation by reactive oxygen species. Blood. 92:4808-4818.

Feng D, Nagy JA, Pyne K, Dvork HF, Dvorak AM (1998). Neutrophils emigrate from venules by a transendothelial cell pathway in response to fMLP. J. Exp. Med. 187:903-915.

Ferguson MAJ (1989). Identification of glycosylphosphatidylinositol anchors by fatty acid labelling. In: Post-translational modification of proteins by lipids - a laboratory manual (Brodbeck U, Bordier C, eds). Springer-Verlag, Berlin-Heidelberg. p 2.

Fernandez-Patron C, Hardy E, Sosa A, Seoane J, Castellanos L (1995). Double staining of Coomassie Blue-stained polyacrylamide gels by imidazole-sodium dodecyl sulfate-zinc reverse staining: Sensitive detection of Coomassie Blue-undetected proteins. Anal. Biochem. 224:263-269.

Field MC, Menon AK (1993). Glycolipid anchoring of cell surface proteins. In: Lipid modification of proteins (Schlesinger MJ, ed). CRC Press, Boca Raton, pp 84-134.

Flower DR (1996). The lipocalin protein family: Structure and function. Biochem. J. 318:1-14.

Fosang AJ, Last K, Knäuper V, Neame PJ, Murphy G, Hardingham TE, Tschesche H, Hamilton JA (1993). Fibroblast and neutrophil collagenases cleave at two sites in the cartilage aggrecan interglobular domain. Biochem. J. 295:273-276.

Fosang AJ, Last K, Neame PJ, Murphy G, Knäuper V, Tschesche H, Hughes CE, Caterson B, Hardingham TE (1994). Neutrophil collagenase (MMP-8) cleaves at the aggrecanase site E^{373}-A^{374} in the interglobular domain of cartilage aggrecan. Biochem. J. 304:347-351.

Fouret P, Du Bois RM, Bernaudin J-F, Takahashi H, Ferrans VJ, Crystal RG (1989). Expression of the neutrophil elastase gene during human bone marrow cell differentiation. J. Exp. Med. 169:833-845.

Foxman EF, Campbell JJ, Butcher EC (1997). Multistep navigation and the combinatorial control of leukocyte chemotaxis. J. Cell Biol. 139:1349-1360.

Freund J (1956). The mode of action of immunological adjuvants. Adv. Tuberc. Res. 7:130-148.

Freund J, McDermott K (1942). Sensitisation to horse serum by means of adjuvants. Proc. Soc. Exp. Biol. Med. 49:548-553.

Fujimoto N, Hosakawa N, Iwata K, Okada Y, Hayakawa T (1994): A one step sandwich enzyme immunoassay for human matrix metalloproteinase 9 using monoclonal antibodies. In Inhibition of matrix metalloproteinases: Therapeutic potential vol. 732 (Greenwald RA, Golub LM eds). Annals of the New York Academy of Sciences, p 359.

Fukuyama K, Toku S, Nakano S, Epstein WL (1986). Distribution and solubilisation of a high molecular mass cysteine proteinase inhibitor from rat epidermis. In: Cysteine proteinases and their inhibitors (Turk V, ed), Walter de Gruyter and Co., Berlin, pp 685-692.

Gabriel O, Gersten DM (1992). Staining for enzyme activity after gel electrophoresis. Anal. Biochem. 203:1-21.

Garwicz D, Lindmark A, Persson A-M, Gullberg U (1998). On the role of proform conformation for processing and intracellular sorting of human cathepsin G. Blood. 92:1415-1422.

Gaudin P, Berthier S, Barro C, Zaoui P, Morel F (1997). Proteolytic potential of human neutrophil membranes. Eur. J. Cell Biol. 72:345-351.

Geisow MJ, Aitken A (1989). Gas or pulsed liquid phase sequence analysis. In: Protein sequencing - a practical approach, (Findlay JBC, Geisow MJ, eds), IRL Press, Oxford, pp 85-98.

Gershoni JM, Palade GE (1982). Electrophoretic transfer of proteins from sodium dodecyl sulfate-polyacrylamide gels to a positively charged membrane filter. Anal. Biochem. 131:1-15.

Gerst JE (1999). SNAREs and SNARE regulators in membrane fusion and exocytosis. Cell. Mol. Life Sci. 55:707-734.

Glenny AT, Pope CG, Waddington H, Wallace U (1926). Immunological notes. J. Pathol. 29:31-40.

Goetzl EJ, Banda MJ, Leppert D (1996). Matrix metalloproteinases in immunity. J. Immunol. 156:1-4.

Gogly B, Groult N, Hornebeck W, Godeau G, Pellat B (1998). Collagen zymography as a sensitive and specific technique for the determination of subpicogram levels of interstitial collagenase. Anal. Biochem. 255:211-216.

Goldberg GI, Strongin A, Collier IE, Genrich LT, Marmer BL (1992). Interaction of 92-kDa type IV collagenase with the tissue inhibitor of metalloproteinases prevents dimerization, complex formation with interstitial collagenase, and activation of the proenzyme with stromelysin. J. Biol. Chem. 267:4583-4591.

Goli UB, Fields GB, Van Wart HE (1992). Synthetic triple helical models for the collagen cleavage site in interstitial collagens. Matrix Suppl. 1:71-72

Gomez DE, Alonso DF, Yoshiji H, Thorgeirsson UP (1997). Tissue inhibitors of metalloproteinases: Structure, regulation and biological functions. Eur. J. Cell Biol. 74:111-123.

Grant GA, Goldberg GI, Wilhelm SM, He C, Eisen AZ (1992). Activation of extracellular matrix metalloproteases by proteases and organomercurials. Matrix Suppl. 1:217-223.

Green GDJ, Kembhavi AA, Davies ME, Barrett AJ (1984). Cystatin-like proteinase inhibitors from human liver. Biochem. J. 218:939-946.

Griffiths G (1993). Fine structure immunocytochemistry. Springer-Verlag, Berlin Heidelberg, Germany.

Grignon DJ, Sakr W, Toth M, Ravery V, Angulo J, Shamsa F, Pontes JE, Crissman JC, Fridman R (1996). High levels of tissue inhibitor of metalloproteinases-2 (TIMP-2) expression are associated with poor outcome in invasive bladder cancer. Cancer Res. 56:1654-1659.

Guedez L, Stetler-Stevenson WG, Wolff L, Wang J, Fukushima P, Mansoor A, Stetler-Stevenson M (1998). *In vitro* suppression of programmed cell death of B-cells by tissue inhibitor of metalloproteinase-1. J. Clin. Invest. 102:2002-2010.

Gullberg U, Andersson E, Garwicz D, Lindmark A, Olsson I (1997). Biosynthesis, processing and sorting of neutrophil proteins: Insight into neutrophil granule development. Eur. J.

Haematol. 58:137-143.

Gurvich AE, Drizlikh GI (1964). Use of antibodies on an insoluble support for specific detection of radioactive antigens. Nature. 5:648-649.

Hackam DJ, Rotstein OD, Sjolin C, Schreiber AD, Trimble WS, Grinstein S (1998). v-SNARE-dependent secretion is required for phagocytosis. Proc. Natl. Acad. Sci. USA. 95:11691-11696.

Hampton MB, Kettle AJ, Winterbourn CC (1998). Inside the neutrophil phagosome: Oxidants, myeloperoxidase, and bacterial killing. Blood. 92:3007-3017.

Handley DA (1989). The development and application of colloidal gold as a microscopic probe. In: Colloidal gold: Principles, methods and applications vol. 1 (Hayat MA,ed), Academic Press, San Diego, pp 1-8.

Hanson RD, Hohn PA, Popescu NC, Ley TJ (1990). A cluster of haematopoietic serine proteinase genes is found on the same chromosomal band as the human alpha/delta T-cell receptor locus. Proc. Natl. Acad. Sci. USA. 87:960-963.

Harada A, Takei Y, Kanai Y, Tanaka Y, Nonaka S, Hirokawa N (1998). Golgi vesiculation and lysosome dispersion in cells lacking cytoplasmic dynein. J. Cell Biol. 141:51-59.

Haralson MA, Hassell JR (1995). The extracellular matrix - an overview. In: Extracellular Matrix: A Practical Approach, (Haralson MA, Hassell JR, eds), Oxford University Press, Oxford, pp 12-30.

Harlow E, Lane D (1988). Antibodies - a laboratory manual, Cold Spring Harbour Laboratories, p 509.

Harris ED, Vater CA (1980). Methodology of collagenase research: Substrate preparation, enzyme activation and purification. In: Collagenase in normal and pathological connective tissues (Woolley DE, Evanson JM, eds), John Wiley and Sons, Chichester, UK, pp 37-63.

Hasty KA, Pourmotabbed TF, Goldberg GI, Thompson JP, Spinella DG, Stevens RM, Mainardi CL (1990). Human neutrophil collagenase. J. Biol. Chem. 265:11421-11424.

Hatanaka M, Seya T, Matsumoto M, Hara T, Nonaka M, Inoue N, Takeda J, Shimizu A (1996). Mechanisms by which the surface expression of the glycosylphosphatidyl inositol-anchored complement complement regulatory proteins decay accelerating factor (CD55) and CD59 is lost in human leukemia cell lines. Biochem. J. 314:969-976.

Hayakawa T, Yamashita K, Tanzawa K, Uchijima E, Iwata K (1992). Growth promoting activity of tissue inhibitor of metalloproteinases-1 (TIMP-1) for a wide range of cells. FEBS Lett. 298:29-32.

Hessler RJ, Blackwood RA, Brock TG, Francis JW, Harsh DM, Smolen JE (1998). Identification of glyceraldehyde-3-phosphate dehydrogenase as a Ca^{2+}-dependent fusogen in human neutrophil cytosol. J. Leuk. Biol. 63:331-336.

Heusel JW, Hanson RD, Silverman GA, Ley TJ (1991). Structure and expression of a cluster of human haematopoietic serine proteinase genes found on chromosome 14q11.2. J. Biol.

Chem. 266:6152-6158.

Hibbs MS, Bainton DF (1989). Human neutrophil gelatinase is a component of specific granules. J. Clin. Invest. 84:1395-1402.

Hibbs MS, Hasty KA, Seyer JM, Kang AH, Mainardi CL (1985). Biochemical and immunological characterisation of the secreted forms of human neutrophil collagenase. J. Biol. Chem. 260:2493-2500.

Hoffstein S, Weissmann G (1978). Microfilaments and microtubules in Ca^{2+} ionophore-induced secretion of lysosomal enzymes from human polymorphonuclear leukocytes. J. Cell Biol. 78:769-781.

Horisberger M (1989). Quantitative aspects of labelling colloidal gold with proteins. In: Immunogold labelling in cell biology (Verkleij AJ, Leunissen JLM, eds), CRC Press, Florida, pp 50-59.

Horobin RW (1990). An overview of the theory of staining. In: Theory and practice of histological techniques, (Bancroft JD, Stevens A, eds), Churchill Livingstone, Edinburgh, pp 93-105.

Hotary K, Allen E, Punturieri A, Yana I, Weiss SJ (2000). Regulation of cell invasion and morphogenesis in a three-dimensional type I collagen matrix by membrane-type matrix metalloproteinases 1, 2, and 3. J. Cell Biol. 149:1309-1323.

Huang W, Meng Q, Suzuki K, Nagase H, Brew K (1997). Mutational study of the amino-terminal domain of human tissue inhibitor of metalloproteinases-1 (TIMP-1) locates an inhibitory region for matrix metalloproteinases. J. Biol. Chem. 272:22086-22091.

Hummel KM, Penheiter AR, Gathman AC, Lilly WW (1996). Anomalous estimation of protease molecular masss using gelatin-containing SDS-PAGE. Anal. Biochem. 233:140-142.

Ingham KC (1990). Precipitation of proteins with polyethylene glycol. In: Guide to protein purification. Methods in Enzymology vol. 182 (Deutscher MP, ed), Academic Press, London, pp 301-308.

Ito A, Sato T, Iga T, Mori Y (1990). Tumour necrosis factor bifunctionally regulates matrix metalloproteinase and tissue inhibitor of metalloproteinase (TIMP) production by human fibroblasts. FEBS Lett. 269:93-95.

Itoh Y, Nagase H (1995). Preferential inactivation of tissue inhibitor of metalloproteinase-1 that is bound to the precursor of matrix metalloproteinase 9 (progelatinase B) by human neutrophil elastase. J. Biol. Chem. 270:16518-16521.

Jaconi MEE, Lew DP, Carpentier J-L, Magnusson KE, Sjögren M, Stendahl O (1990). Cytosolic free calcium elevation mediates the phagosome-lysosome fusion during phagocytosis in human neutrophils. J. Cell Biol. 110:1555-1564.

Johnson AG, Gaines S, Landy M (1956). Studies on the O antigen of *Salmonella typhosa* V. Enhancement of antibody response by the purified lipopolysaccharide. J. Exp. Med. 103:225-246.

Joiner KA, Ganz T, Rotrosen D (1989). Purification and characterisation of neutrophil phagosomes containing *Salmonella typhimurium*: The use of endogenous iodination to identify components involved in phagosome formation. J. Cell Biol. 109:2771.

Jones J, Morgan BP (1995). Apoptosis is associated with reduced expression of complement regulatory molecules, adhesion molecules and other receptors on polymorphonuclear leukocytes: functional relevance and role in inflammation. Immunology. 86:651-660.

Jost CR, Gaillard ML, Fransen JAM, Daha MR, Ginsel LA (1991). Intracellular localisation of glycosylphosphatidyl inositol-anchored CD67 and FcRIII (CD16) in affected neutrophil granulocytes of patients with paroxysmal nocturnal hemoglobinuria. Blood. 78:3030-3036.

Jost CR, Huizinga TWJ, de Goede R, Fransen JAM, Tetteroo PAT, Daha MR, Ginsel LA (1990). Intracellular localisation and *de novo* synthesis of FcRIII in human granulocytes. Blood. 75:144-151.

Katanaev VL, Wymann MP (1998). GTPγS-induced actin polymerisation *in vitro*: ATP and phosphoinositide-independent signalling in Rho-family proteins and a plasma membrane-associated guanine nucleotide exchange factor. J. Cell Sci. 111:1583-1594.

Kaufman M, Leto T, Levy R (1996). Translocation of annexin I to plasma membranes and phagosomes in human neutrophils upon stimulation with opsonised zymosan: Possible role in phagosome function. Biochem. J. 316:35-42.

Kim J, Yu W, Kovalski K, Ossowski L (1998). Requirement for specific proteases in cancer cell intravasation as revealed by a novel semiquantitative PCR-based assay. Cell. 94:353-362.

Kjeldsen L (1995). Gelatinase granules in human neutrophils. Eur. J. Haematol. Suppl. 56:9-29.

Kjeldsen L, Bainton DF, Sengeløv H, Borregaard N (1993a). Structural and functional heterogeneity among peroxidase-negative granules in human neutrophils: Identification of a distinct gelatinase containing granule subset by combined immunocytochemistry and subcellular fractionation. Blood. 82:3183.

Kjeldsen L, Bainton DF, Sengeløv H, Borregaard N (1994). Identification of Neutrophil gelatinase-associated lipocalin as a novel matrix protein of specific granules in human neutrophils. Blood. 83:799-807.

Kjeldsen L, Bjerrum OW, Askaa J, Borregaard N (1992). Subcellular localisation and release of human neutrophil gelatinase, confirming the existence of separate gelatinase-containing granules. Biochem. J. 287:603-610.

Kjeldsen L, Johnsen AH, Sengeløv H, Borregaard N (1993b). Isolation and primary structure of NGAL, a novel protein associated with human neutrophil gelatinase. J. Biol. Chem. 268:10425-10432.

Kjeldsen L, Sengeløv H, Borregaard N (1999). Subcellular fractionation of human neutrophils on Percoll density gradients. J. Immunol. Methods. 232:131-143.

Kleijmeer MJ, Morkowski S, Griffith JM, Rudensky AY, Geuze HJ (1997). Major histocompatibility complex class II compartments in human and mouse B lymphoblasts represent conventional endocytic compartments. J. Cell Biol. 139: 639-649.

Kleine T, Bartsch S, Bläser J, Schnierer S, Triebel S, Valentin M, Gote T, Tschesche H (1993). Preparation of active recombinant TIMP-1 from *Escherichia coli* inclusion bodies and complex formation with the recombinant catalytic domain of PMNL-collagenase. Biochemistry. 32:14125-14129.

Kleiner DE, Stetler-Stevenson WG (1994). Quantitative zymography: Detection of picogram quantities of gelatinases. Anal. Biochem. 218:325-329.

Knäuper V, Triebel S, Reinke H, Tschesche H (1991). Inactivation of human plasma C1-inhibitor by human PMN leukocyte matrix metalloproteinases. FEBS Lett. 290:99-102.

Knäuper V, Wilhelm SM, Seperack PK, DeClerck YA, Langley KE, Osthues A, Tschesche H (1993). Direct activation of human neutrophil procollagenase by recombinant stromelysin. Biochem. J. 295:581-586.

Knight CG, Willenbrock F, Murphy G (1992). A novel coumarin-labelled peptide for sensitive continuous assays of the matrix metalloproteinases. FEBS Lett. 296:263-266.

Ko Y-G, Thompson GA (1995). Purification of glycosylphosphatidylinositol-anchored proteins by modified Triton X-114 partitioning and preparative gel electrophoresis. Anal. Biochem. 224:166-172.

Kobayashi T, Robinson JM (1991). A novel intracellular compartment with unusual secretory properties in human neutrophils. J. Cell Biol. 113:743-756.

Kolkenbrock H, Zimmermann J, Burmester G-R, Ulbrich N (2000). Activation of progelatinase B by membranes of human polymorphonuclear granulocytes. Biol. Chem. 381:49-55.

Kostoulas G, Hörler D, Nuggi A, Cash B, Baici A (1997). Electrostatic interactions between leukocyte elastase and sulfated glycosaminoglycans: Physiological implications. Biol. Chem. 378:1481-1489.

Kuntz RM, Saltzman WM (1997). Neutrophil motility in extracellular matrix gels: Mesh size and adhesion affect speed of migration. Biophys. J. 72:1472-1480.

Laemmli UK (1970). Cleavage of structural proteins during assembly of the head of bacteriophage T4. Nature. 227:680-685.

Langanger G, De Mey JR (1989). Detection of cytoskeletal proteins in cultured cells at the ultrastructural level. In: Immunogold labelling in cell biology (Verkleij AJ, Leunissen JLM, eds), CRC Press, Florida, pp 336-354.

Le Cabec V, Cowland JB, Calafat J, Borregaard N (1996). Targeting of proteins to granule subsets is determined by timing and not by sorting: the specific granule protein NGAL is localised to azurophil granules when expressed in HL-60 cells. Proc. Natl. Acad. Sci. USA. 93:6454-6457.

Le Cabec V, Maridonneau-Parini I (1994). Annexin 3 is associated with cytoplasmic granule in neutrophils and translocates to the plasma membrane in activated cells. Biochem. J.

303:481-487.

Leco KJ, Apte SS, Taniguchi GT, Hawkes SP, Khokha R, Schultz GA, Edwards DR (1997). Murine tissue inhibitor of metalloproteinases-4 (*Timp-4*): cDNA isolation and expression in adult mouse tissues. FEBS Lett. 401:213-217.

Lee AY, Akers KT, Collier M, Li L, Eisen AZ, Seltzer JL (1997). Intracellular activation of gelatinase A (72-kDa type IV collagenase) by normal fibroblasts. Proc. Natl. Acad. Sci. USA. 94:4424-4429.

Lefebvre V, Vaes G (1989). The enzymatic evaluation of procollagenase and collagenase inhibitors in crude biological media. Biochim. Biophys. Acta. 992:355-361.

Lefebvre V, Vaes G (1992). The assay of procollagenase and collagenase inhibitors in crude biological media. Matrix Suppl. 1:326-327.

Lehrer RI, Ganz T (1990). Antimicrobial polypeptides of human neutrophils. Blood. 76:2169-2181.

Lelievre Y, Bouboutou R, Boiziau J, Faucher D, Achard D, Cartwright T (1990). Low molecular weight, sequence based, collagenase inhibitors selectively block the interaction between collagenase and TIMP (Tissue inhibitor of metalloproteinases). Matrix. 10:292-299.

Lennarz WJ, Strittmatter WJ (1991). Cellular functions of metallo-endoproteinases. Biochim. Biophys. Acta. 1071:149-158.

Leunissen JLM, De Mey JR (1989). Preparation of gold probes. In: Immunogold labelling in cell biology (Verkleij AJ, Leunissen JLM, eds), CRC Press, Florida, pp 4-16.

Lew PD, Monod A, Waldvogel FA, Dewald B, Baggiolini M, Pozzan T (1986). Quantitative analysis of the cytosolic free calcium dependency of exocytosis from three subcellular compartments in intact human neutrophils. J. Cell Biol. 102:2197-2204.

Lew PD, Wollheim CB, Waldvogel FA, Pozzan T (1984). Modulation of cytosolic-free calcium transients by changes in intracellular calcium buffering capacity: Correlation with exocytosis and O_2 production in neutrophils. J. Cell Biol. 99:1212-1220.

Li G, Fridman R, Kim H-RC (1999). Tissue inhibitor of metalloproteinase-1 inhibits apoptosis of human breast epithelial cells. Cancer Res. 59:6267-6275.

Lichte A, Kolkenbrock H, Tschesche H (1996). The recombinant catalytic domain of membrane-type matrix metalloproteinase-1 (MT1-MMP) induces activation of progelatinase A and progelatinase A complexed with TIMP-2. FEBS Lett. 397:277-282

Liou TG, Campbell EJ (1996). Quantum proteolysis resulting from release of single granules by human neutrophils - A novel, nonoxidative mechanism of extracellular proteolytic activity. J. Immunol. 157:2624-2631.

Liou W, Geuze HJ, Slot JW (1996). Improving structural integrity of cryosections for immungold labeling. Histochem. Cell Biol. 106:41-58.

Lisanti MP, Rodriguez-Boulan E (1990). Glycophospholipid membrane anchoring provides

clues to the mechanism of protein sorting in polarized epithelial cells. Trends. Biol. Sci. 15:113-118.

Lollike K, Borregaard N, Lindau M (1995). The exocytic fusion pore of small granules has a conductance similar to an ion channel. J. Cell Biol. 129:99-104.

London RE, Levy LA, Murphy E (1996). US Patent 5.516.911.

Losch U, Schranner I, Wanke R (1986). The chicken egg, an antibody source. J. Vet. Med. B. 33:609-619.

Low MG, Futerman AH, Ackermann KE, Sherman WR, Silman I (1987). Removal of covalently bound inositol from *Torpedo* acetylcholinesterase and mammalian alkaline phosphatases by deamination with nitrous acid. Biochem. J. 241:615-619.

Lowry OH, Rosenbrough NJ, Farr AL, Randall RJ (1951). Protein measurement with the Folin phenol reagent. J. Biol. Chem. 193:265-275.

Mackarel AJ, Cottell DC, Russell KJ, Fitzgerald MX, O'Connor CM (1999). Migration of neutrophils across pulmonary endothelial cells is not blocked by matrix metalloproteinase or serine protease inhibitors. Am. J. Respir. Cell Mol. Biol. 20:1209-1219.

Mainardi CL, Dixit SN, Kang AH (1980). Degradation of type IV (basement membrane) collagen by a proteinase isolated from human polymorphonuclear leukocyte granules. J. Biol. Chem. 255:5435-5441.

Makowski GS, Ramsby ML (1996). Calibrating gelatin zymograms with human gelatinase standards. Anal. Biochem. 236:353-356.

Mallya SK, Mookhtiar KA, Gao Y, Brew K, Dioszegi M, Birkedal-Hansen H, van Wart HE (1990). Characterisation of 58-kilodalton human neutrophil collagenase: Comparison with human fibroblast collagenase. Biochemistry. 29:10628-10634.

Mandeville JTH, Lawson MA, Maxfield FR (1997). Dynamic imaging of neutrophil migration in three dimensions: Mechanical interactions between cells and matrix. J. Leuk. Biol. 61:188-200.

Maquoi E, Frankenne F, Baramova E, Munuat C, Sounni NE, Remacle A, Noël A, Murphy G, Foidart J-M (2000). Membrane type 1 matrix metalloproteinase-associated degradation of tissue inhibitor of metalloproteinase 2 in human tumour cell lines. J. Biol. Chem. 275:11368-11378.

Maridonneau-Parini I, de Gunzburg J (1992). Association of rap1 and rap2 proteins with the specific granules of human neutrophils. J. Biol. Chem. 267:6396-6402.

Mason DY, Cramer EM, Massé J-M, Crystal R, Bassot J-M, Breton-Gorius J (1991). $Alpha_1$-antitrypsin is present within the primary granules of human polymorphonuclear leukocytes. Am. J. Pathol. 139:623-628.

Matrisian LM (1992). The matrix-degrading metalloproteinases. BioEssays. 14:455-463.

Mazzieri R, Masiero L, Zanetta L, Monea S, Onisto M, Garbisa S, Mignatti P (1997). Control

of type IV collagenase activity by components of the urokinase-plasmin system: A regulatory mechanism with cell-bound reactants. EMBO J. 16:2319-2332.

Mercer E, Cawston TE, de Silva M, Hazleman BL (1985). Purification of a metalloproteinase inhibitor from human rheumatoid synovial fluid. Biochem. J. 231:505-510.

Michaelis J, Vissers MCM, Winterbourn CC (1992). Cleavage of α_1-antitrypsin by human neutrophil collagenase. Matrix. Suppl. 1:80-82.

Mignatti P, Rifkin DB (1993). Biology and biochemistry of proteinases in tumor invasion. Physiol. Rev. 73:161-195.

Miyamoto Y, Akaike T, Alam MS, Inoue K, Hamamoto T, Ikebe N, Yoshitake J, Okamoto T, Maeda H (2000). Novel functions of human α_1-proteinase inhibitor after *S*-nitrosylation: inhibition of cysteine protease and antibacterial activity. Biochem. Biophys. Res. Comm. 267:918-923.

Moeremans M, Daneels G, Van Dijk A, Langanger G, De Mey J (1984). Sensitive visualisation of antigen-antibody reactions in dot and blot immune overlay assays with immunogold and immunogold/silver staining. J. Imm. Meth. 74:353-360.

Mollinedo F, Nakajima M, Llorens A, Barbosa E, Callejo S, Gajate C, Fabra A (1997). Major colocalisation of the extracellular-matrix degradative enzymes heparanase and gelatinase in tertiary granules of human neutrophils. Biochem. J. 327:917-923.

Monboisse J-C, Bellon G, Randoux A, Dufer J, Borel J-P (1990). Activation of human neutrophils by type I collagen. Biochem. J. 270:459-462.

Moorewood CR, Elliott E, Dennison C, Bruton AG (1992). Further modification of the LKB 7800 series KnifeMaker for improved reproducibility in breaking 'cryo' knives. J. Microsc. 168:111-114.

Murphy G (1992). Dissociation of tissue inhibitor of metalloproteinases (TIMP) from enzymes complexes yields fully active inhibitor. Matrix Suppl. 323-324.

Murphy G, Bretz U, Baggiolini M, Reynolds JJ (1980). The latent collagenase and gelatinase of human polymorphonuclear leukocytes. Biochem. J. 192:517-525.

Murphy G, Crabbe T (1995). Gelatinases A and B. In: Proteolytic Enzymes - Aspartic and Metallo Peptidases. Methods in Enzymology vol. 248, (Barrett AJ, ed), Academic Press, San Diego, pp 470-484.

Murphy G, Reynolds JJ, Bretz U, Baggiolini M (1977). Collagenase is a component of the specific granules of human polymorphonuclear leucocytes. Biochem. J. 162:195-200.

Murphy G, Reynolds JJ, Bretz U, Baggiolini M (1982). Partial purification of collagenase and gelatinase from human polymorphonuclear leukocytes. Biochem. J. 203:209-221.

Murphy G, Willenbrock F (1995). Tissue inhibitors of matrix metalloendopeptidases. In: Proteolytic Enzymes - Aspartic and Metallo Peptidases. Methods in Enzymology vol. 248 (Barrett AJ, ed), Academic Press, San Diego, pp 496-509.

Murzin AG (1993). OB (oligonucleotide/oligosaccharide binding)-fold: Common structural and

functional solution for non-homologous sequences. EMBO J. 12:861-867.

Musil D, Zucic D, Turk D, Engh RA, Mayr I, Huber R, Popovic T, Turk V, Towatari T, Katunuma N, Bode W (1991). The refined 2.15 Å X-ray crystal structure of human liver cathepsin B: the structural basis for its specificity. EMBO J. 10:2321-2330.

Nabi IR (1999). The polarization of the motile cell. J. Cell Sci. 112:1803-1811.

Nagai K, Katori M (1988). Possible changes in the leukocyte membrane as a mechanism of leukocyte adhesion to the venular walls induced by leukotriene B_4 and fMLP in the microvasculature of the hamster cheek pouch. Int. J. Microcirc. Clin. Exp. 7:305-314.

Nagase H, Itoh Y, Binner S (1994). Interaction of α_2-macroglobulin with matrix metalloproteinases and its use for identification of their active forms. In: Inhibition of matrix metalloproteinases: Therapeutic Potential vol. 732 (Greenwald RA, Golub LM eds). Annals New York Academy of Sciences, pp 294-302.

Nagayama M, Sakamoto S, Sakamoto M (1984). Mouse bone collagenase inhibitor: Purification and partial characterisation of the inhibitor from mouse calvaria cultures. Arch. Biochem. Biophys. 228:653-659.

Nakahara H, Howard L, Thompson EW, Sato H, Seiki M, Yeh Y, Chen W-T (1997). Transmembrane/cytoplasmic domain-mediated membrane type 1-matrix metalloprotease docking to invadopodia is required for cell invasion. Proc. Natl. Acad. Sci. USA. 94:7959-7964.

Nemoto E, Nakamura M, Shoji S, Horiuchi H (1997). Circulating promyelocytes and low levels of CD16 expression on polymorphonuclear leukocytes accompany early-onset periodontitis. Infect. Immun. 65:3906-3912.

Netzel-Arnett S, Mallya SK, Nagase H, Birkedal-Hansen H, Van Wart HE (1991). Continuously recording fluorescent assays for five human matrix metalloproteinases. Anal. Biochem. 195:86-92.

Nüße O, Serrander L, Lew DP, Krause K-H (1998). Ca^{2+}-induced exocytosis in individual human neutrophils: High- and low-affinity granule populations and submaximal responses. EMBO J. 17:1279-1288.

Oda T, Katori M, Hatanaka K, Nagai Y (1995). Inhibition of neutrophil migration by a selective inhibitor of matrix metalloproteinase: analysis by intravital microscopy. Mediators of Inflammation. 4:133-137.

Oda T, Katori M, Hatanaka K, Yamashina S (1992). Five steps in leukocyte extravasation in the microcirculation by chemoattractants. Mediators of Inflammation. 1:403-410.

Ogata Y, Enghild JJ, Nagase H (1992). Matrix metalloproteinase 3 (stromelysin) activates the precursor for the human matrix metalloproteinase 9. J. Biol.Chem. 267:3581-3584.

O'Grady RL, Nethery A, Hunter N (1984). A fluorescent screening assay for collagenase using collagen labeled with 2-methoxy-2,4-diphenyl-3(2H)-furanone. Anal. Biochem. 140:490-494.

Ohlsson K (1980). Polymorphonuclear leukocyte collagenase. In: Collagenase in normal and

pathological connective tissues (Woolley DE, Evanson JM, eds), John Wiley and Sons, Chichester, UK, pp 209-222.

Okada Y, Watanabe S, Nakanishi I (1988). Inactivation of tissue inhibitor of metalloproteinases by neutrophil elastase and other serine proteases. FEBS Lett. 229:157-160.

Okumura Y, Sato H, Seiki M, Kido H (1997). Proteolytic activation of the precursor of membrane type 1 matrix metalloproteinase by human plasmin. FEBS Lett. 402:181-184.

Oliver GW, Leferson JD, Stetler-Stevenson WG, Kleiner DE (1997). Quantitative reverse zymography: Analysis of picogram amount of metalloproteinase inhibitors using gelatinase A and B reverse zymograms. Anal. Biochem. 244:161-166.

Opendakker G, Masure S, Proost P, Billiau X, van Damme J (1991). Natural human monocyte gelatinase and its inhibitor. FEBS Lett. 284:73-78.

Oren A, Taylor JMG (1995). The subcellular localization of defensins and myeloperoxidase in human neutrophils: Immunocytochemical evidence for azurophil granule heterogeneity. J. Lab. Clin. Med. 125:340-347.

Osiewicz K, McGarry M, Soloway PD (1999). Hyper-resistance to infection in TIMP-1-deficient mice is neutrophil-dependent but not immune cell autonomous. Ann. NY. Acad. Sci. 878:494-496.

Osthues A, Knäuper V, Oberhoff R, Reinke H, Tschesche H (1992). Isolation and characterisation of tissue inhibitors of matrix metalloproteinases (TIMP-1 and TIMP-2) from human synovial fluid. FEBS Lett. 296:16-19.

Owen CA, Campbell EJ (1999). The cell biology of leukocyte-mediated proteolysis. J. Leuk. Biol. 65:137-150.

Owen CA, Campbell MA, Sannes PL, Boukedes SS, Campbell EJ (1995). Cell surface-bound elastase and cathepsin G on human neutrophils: A novel, non-oxidative mechanism by which neutrophils focus and preserve catalytic activity of serine proteinases. J. Cell Biol. 131:775-789.

Park HI, Ni J, Gerkema FE, Liu D, Belozerov VE, Sang QA (2000). Identification and characterisation of human endometase (matrix metalloproteinase-26) from endometrial tumour. J. Biol. Chem. Published online ahead of print as manuscript M002349200 (www.jbc.org).

Pedersen TL, Yong K, Pedersen JO, Hansen NE, Dano K, Plesner T (1996). Impaired migration *in vitro* of neutrophils from patients with paroxysmal nocturnal haemoglobinuria. Br. J. Haematol. 95:45-51.

Pei D (1999a). Identification and characterisation of the fifth membrane-type matrix metalloproteinase, MT5-MMP. J. Biol. Chem. 274:8925-8932.

Pei D (1999b). Leukolysin/MMP-25/MT6-MMP: a novel matrix metalloproteinase specifically expressed in the leukocyte lineage. Cell Research. 9:291-303.

Pember SO, Kinkade JM (1983). Differences in myeloperoxidase activity from neutrophilic polymorphonuclear leukocytes of differing density: Relationship to selective exocytosis of distinct forms of the enzyme. Blood. 61:1116-1124.

Peng SX, Strojnowski MJ, Hu JK, Smith BJ, Eichhold TH, Wehmeyer KR, Pikul S, Almstead NG (1999). Gas chromatographic and mass spectrometric analysis of hydroxylamine for monitoring the metabolic hydrolysis of metalloprotease inhibitors in rat and human microscomes. J. Chromatog. B. 724:181-187.

Peppin GJ, Weiss SJ (1986). Activation of the endogenous metalloproteinase, gelatinase, by triggered human neutrophils. Proc. Natl. Acad. Sci. USA. 83:4322-4326.

Pertoft H, Laurent TC, Låås T, Kågedal L (1978). Density gradients prepared from colloidal silica particles coated with polyvinylpyrrolidone (Percoll). Anal. Biochem. 88:271-274.

Pike RN, Dennison C (1989). Protein fractionation by three phase partitioning (TPP) in aqueous/t-butanol mixtures. Biotech. Bioeng. 33:221-228.

Pizou V, Desjardins M, Bucci C, Parton RG, Zerial M (1994). Localisation of Rap 1a and Rap 1b proteins with the late endocytic/phagocytic compartments and Rap 2a with the Golgi complex. J. Cell Sci. 107:1661-1670.

Polson A, Coetzer T, Kruger J, von Maltzen E, van der Merwe KJ (1985). Improvement in the isolation of IgY from the yolk of eggs laid by immunised hens. Immunol. Invest. 14:323-327.

Polson A, Potgieter GM, Largier JF, Mears EGF, Joubert FJ (1964). The fractionation of protein mixtures by linear polymers of high molecular mass. Biochem. Biophys. Acta. 82:463-475.

Pryzwansky KB, Breton-Gorius J (1985). Identification of a subpopulation of primary granules in human neutrophils based upon maturation and distribution. Lab. Invest. 53:664-671.

Pryzwansky KB, MacRae EK, Spitznagel JK, Cooney MH (1979). Early degranulation of human neutrophils: Immunocytochemical studies of surface and intracellular phagocytic events. Cell. 18:1025-1033.

Puyraimond A, Weitzman JB, Babiole E, Menashi S (1999). Examining the relationship between the gelatinolytic balance and the invasive capacity of endothelial cells. J. Cell Sci. 112:1283-1290.

Rabinovitch M (1995). Professional and non-professional phagocytes: an introduction. Trends Cell Biol. 5:85-87.

Rabinowitz S, Horstmann H, Gordon S, Griffiths G (1992). Immunocytochemical characterisation of the endocytic and phagolysosomal compartments in peritoneal macrophages. J. Cell Biol. 116:95-112.

Ray JM, Stetler-Stevenson WG (1995). Gelatinase A activity directly modulates melanoma cell adhesion and spreading. EMBO J. 14:908-917.

Read SM, Northcote DH (1981). Minimisation of variation in the response to different proteins of the Coomassie Blue dye-binding assay for protein. Anal. Biochem. 116:53-64.

Ree AH, Flørenes VA, Berg JP, Maelandsmo GM, Nesland JHM, Fodstad Ø (1997). High levels of messenger RNA for tissue inhibitors of metalloproteinases (TIMP-1 and TIMP-2) in primary breast carcinomas are associated with development of distant metastases. Clin. Cancer Res. 3:1623-1628.

Rice WG, Ganz T, Kinkade JM, Selsted ME, Lehrer RI, Parmley RT (1987). Defensin-rich dense granules of human neutrophils. Blood. 70:757-765.

Ritter LM, Garfield SH, Thorgeirsson UP (1999). Tissue inhibitor of metalloproteinases-1 (TIMP-1) binds to the cell surface and translocates to the nucleus of human MCF-7 breast carcinoma cells. Biochem. Biophys. Res. Comm. 257:494-499.

Robbins AR, Ward RD, Oliver C (1995). A mutation in glyceraldehyde 3-phosphate dehydrogenase alters endocytosis in CHO cells. J. Cell Biol. 130:1093-1104.

Roberts IM (1975). Tungsten coating - a method of improving glass microtome knives for cutting ultrathin sections. J. Microsc. 103:113-119.

Robinson G, Gray T (1990). Electron microscopy 1: Theoretical aspects and instrumentation. In: Theory and practice of histological techniques (Bancroft JD, Stevens A, eds), Churchill Livingston, Edinburgh, pp 509-523.

Robinson JM, Karnovsky ML, Karnovsky MI (1982). Glycogen accumulation in polymorphonuclear leukocytes, and other intracellular alterations that occur during inflammation. J. Cell Biol. 95:933-941.

Roitt IM (1994). Essential Immunology (8^{th} Edition). Blackwell Scientific Publications, Oxford, UK.

Roos D, de Boer M (1986). Purification and cryopreservation of phagocytes from human blood. In: Immunochemical Techniques Part J - Phagocytosis and Cell-mediated Cytotoxicity. Methods in Enzymology vol. 132 (DiSabato G, Everse J, eds), Academic Press, Orlando, pp 225-241.

Rosales JL, Ernst JD (1997). Calcium-dependent neutrophil secretion: Characterisation and regulation by annexins. J. Immunol. 159:6195-6202.

Rothwell SW, Nath J, Wright DG (1989). Interaction of cytoplasmic granules with microtubules in human neutrophils. J. Cell Biol. 108:2313-2326.

Ruiz S, Henschen-Edman AH, Nagase H, Tenner AJ (1999). Digestion of C1q collagen-like domains with MMPs-1, -2, -3 and -9 defines the sequence involved in the stimulation of neutrophil superoxide production. J. Leuk. Biol. 66:416-422.

Russ C, Callegaro I, Lanza B, Ferrone S (1983). Purification of IgG monoclonal antibodies by caprylic acid precipitation. J. Imm. Meth. 65:269-271.

Saari H, Suomalainen K, Lindy O, Konttinen YT, Sorsa T (1990). Activation of latent human neutrophil collagenase by reactive oxygen species and serine proteases. Biochem. Biophys. Res. Comm. 171:979-987.

Saito H, Minamiya Y, Kitamura M, Saito S, Enomoto K, Terada K, Ogawa J-I (1998). Endothelial myosin light chain kinase regulates neutrophil migration across human

umbilical vein endothelial monolayer. J. Immunol. 161:1533-1540.

Saito H, Seiki M (1995). Membrane-type matrix metalloproteinases (MT-MMPs) in tumour metastasis. J. Biochem. 119:209-215.

Salo T, Sorsa T, Lauhio A, Konttinen YT, Ainamo A, Kjeldsen L, Borregaard N, Ranta H, Landevirta J (1994). Matrix metalloproteinases, their endogenous inhibitors, and microbial activators in gingival crevicular fluid and saliva of HIV (+) subjects. In: Inhibition of matrix metalloproteinases: Therapeutic potential vol. 732 (Greenwald RA, Golub LM eds), Annals of the New York Academy of Sciences, p 476.

Savill JS, Wyllie AH, Henson JE, Walport MJ, Henson PM, Haslett C (1989). Macrophage phagocytosis of aging neutrophils in inflammation: Programmed cell death in the neutrophil leads to recognition by macrophages. J. Clin. Invest. 83:865-870.

Schägger H, von Jagow G (1987). Tricine sodium dodecyl sulfate polyacrylamide gels for the separation of proteins in the range from 1 to 100 kDa. Anal. Biochem. 166:368-379.

Schettler A, Thorn H, Jokusch BM, Tschesche H (1991). Release of proteinases from stimulated polymorphonuclear leukocytes: Evidence for subclasses of the main granule types and their association with cytoskeletal components. Eur. J. Biochem. 197:197-201.

Schneider P, Ferguson MAJ (1995). Microscale analysis of glycosylphosphatidylinositol structures. In: Lipid modification of Proteins. Methods in Enzymology vol. 250 (Casey RJ, Buss JE, eds), Academic Press, San Diego, pp 614-619.

Schönbeck U, Mach F, Libby P (1998). Generation of biologically active IL-1β by matrix metalloproteinases: A novel caspase-1-independent pathway of IL-1β processing. J. Immunol. 161:3340-3346.

Schwartz MA, Ven Kataraman S, Libby A, Mookhtiar K, Mallya S, van Wart HE, Birkedal-Hansen H (1992). Sulfur-based inhibitors for MMPs. Matrix Suppl. 1:309-310.

Segal AW, Dorling J, Coade S (1980). Kinetics of fusion of the cytoplasmic granules with phagocytic vacuoles in human polymorphonuclear leukocytes. J. Cell Biol. 85:42-59.

Segal AW, Gelsow M, Garcia R, Harper A, Miller R (1981). The respiratory burst of phagocytic cells is associated with a rise in vacuolar pH. Nature. 290:406-409.

Sengeløv H (1996). Secretory vesicles of human neutrophils. Eur. J. Haematol. Suppl. 57:7-24.

Sengeløv H, Borregaard N (1999). Free-flow electrophoresis in subcellular fractionation of human neutrophils. J. Immunol. Meth. 232:145-152.

Sengeløv H, Follin P, Kjeldsen L, Lollike K, Cahlgren C, Borregaard N (1995). Mobilisation of granules and secretory vesicles during *in vivo* exudation of human neutrophils. J. Immunol. 154:4157-4165.

Sengeløv H, Kjeldsen L, Borregaard N (1993). Control of exocytosis in early neutrophil activation. J. Immunol. 150:1535-1543.

Sengeløv H, Voldstedlund M, Vinten J, Borregaard N (1998). Human neutrophils are devoid of

the integral membrane protein caveolin. J. Leuk. Biol. 63:563-566.

Shabani F, McNeil J, Tippett L (1998). The oxidative inactivation of tissue inhibitor of metalloproteinase-1 (TIMP-1) by hypochlorous acid (HOCl) is suppressed by anti-rheumatic drugs. Free Rad. Res. 28:115-123.

Shapiro SD, Fliszar CJ, Broekelmann TJ, Mecham RP, Senior RM, Welgus WG (1995). Activation of the 92-kDa gelatinase by stromelysin and 4-aminophenylmercuric acetate. J. Biol. Chem. 270:6351-6356.

Shipley JM, Doyle GAR, Fliszar CJ, Ye Q-Z, Johnson LL, Shapiro SD, Welgus HG, Senior RM (1996). The structural basis for the elastinolytic activity of the 92-kDa and 72-kDa gelatinases. J. Biol. Chem. 271:4335-4341.

Sitte P, Neumann K, Edelmann L (1989). Cryosectioning according to Tokuyasu vs. rapid freezing, freeze-substitution, and resin embedding. In: Immunogold labelling in cell biology (Verkleij AJ, Leunissen JLM, eds), CRC Press, Florida, pp 64-94.

Sjölin C, Dahlgren C (1996). Isolation by calcium-dependent translocation to neutrophil specific granules of a 42 kDa cytosolic protein, identified as being a fragment of annexin XI. Blood. 87:4817-4823.

Sjölin C, Stendahl O, Dahlgren C (1994). Calcium-induced translocation of annexins to subcellular organelles of human neutrophils. Biochem. J. 300:325-330.

Sloane BF, Sameni M, Cao L, Berquin I, Rozhin J, Ziegler G, Moin K, Day N (1994). Alterations in processing and trafficking of cathepsin B during malignant progression. In: Biological functions of Proteases and Inhibitors (Katunuma N, Suzuki K, Travis J, Fritz H, eds), Japan Scientific Societies Press, Tokyo, pp 131-147.

Slot JW, Geuze HJ (1984). Gold markers for single and double immunolabeling of cryosections. In: Immunolabeling for Electron Microscopy (Polak JM, Varndell IM, eds), Elsevier Press, Oxford, UK, p 129.

Slot JW, Geuze HJ (1985). A new method of preparing gold probes for multiple labelling cytochemistry. Eur. J. Cell Biol. 38:87-93.

Slot JW, Posthuma G, Chang LY, Crapo JD, Geuze HJ (1989). Quantitative assessment of immunogold labelling in cryosections. In: Immunogold labelling in cell biology (Verkleij AJ, Leunissen JLM, eds), CRC Press, Florida, pp 136-156.

Smith PK, Krohn RI, Hermanston GT, Mallia AK, Gartner FH, Provenzano MD, Fijimoto EK, Goeke NH, Olson BJ, Klenk DC (1985). Measurement of protein using bicinchoninic acid. Anal. Biochem. 150:76-85.

Sørensen O, Borregaard N (1999). Methods for quantitation of human neutrophil proteins, a survey. J. Immunol. Meth. 232:179-190.

Sorsa T, Ding Y, Salo T, Lauhio A, Teronsen O, Ingman T, Ohtani H, Andoh N, Takeha S, Konttinen YT (1994). Effects of tetracyclines on neutrophil, gingival, and salivary collagenases: A functional and Western blot assessment with special reference to their cellular sources in periodontal diseases. In: Inhibition of matrix metalloproteinases: Therapeutic potential vol. 732 (Greenwald RA, Golub LM eds), Annals New York

Academy of Sciences, pp 112-131.

Springman EB, Angleton EL, Birkedal-Hansen H, Van Wart HE (1990). Multiple modes of activation of latent human fibroblast collagenase: Evidence for the role of a Cys^{73} active-site zinc complex in latency and a 'cysteine switch' mechanism for activation. Proc. Natl. Acad. Sci. USA. 87:364-368.

Steadman R, St John PL, Evans RA, Thomas GJ, Davies M, Heck LW, Abrahamson DR (1997). Human neutrophils do not degrade major basement membrane components during chemotactic migration. Int. J. Biochem. Cell Biol. 395:993-1004.

Stetler-Stevenson WG (1999). Matrix metalloproteinases in angiogenesis: a moving target for therapeutic intervention. J. Clin. Invest. 103:1237-1241.

Stricklin GP, Hoidal JR (1992). Oxidant-mediated inactivation of TIMP. Matrix Suppl. 1:325.

Stricklin GP, Welgus WG (1983). Human skin fibroblast collagenase inhibitor. J. Biol. Chem. 258:12252-12258.

Suzuki K, Watanabe T, Sakurai S-I, Ohtake K, Kinoshita T, Araki A, Fujita T, Takei H, Takeda Y, Sato Y, Yamashita T, Araki Y, Sendo F (1999). A novel glycosylphosphatidyl inositol-anchored protein on human leukocytes: A possible role for regulation of neutrophil adherence and migration. J. Immunol. 162:4277-4284.

Takigawa M, Nishida Y, Suzuki F, Kishi J-I, Yamashita K, Hayakawa T (1990). Induction of angiogenesis in chick yolk-sac membrane by polyamines and its inhibition by tissue inhibitors of metalloproteinases (TIMP and TIMP-2). Biochem. Biophys. Res. Comm. 171:1264-1271.

Takizawa T, Robinson JM (1993). Combined immunocytochemistry and enzyme cytochemistry on ultra-thin cryosections: A new method. J. Histochem. Cytochem. 41:1635-1639.

Takizawa T, Saito T, Robinson JM (1998). Freeze-fracture cytochemistry: A new method combining immunocytochemistry and enzyme cytochemistry on replicas. J. Histochem. Cytochem. 46:11-18.

Talbot DC, Brown PD (1996). Experimental and clinical studies on the use of matrix metalloproteinase inhibitors for the treatment of cancer. Eur. J. Cancer. 32A:2528-2533.

Tapper H (1996). Out of the phagocyte or into its phagosome: Signalling to secretion. Eur. J. Haematol. 57:191-201.

Terranova VP, Maslow D, Marcus G (1989). Directed migration of murine and human tumour cells to collagenase and other proteinases. Cancer Res. 49:4835-4841.

Thomas MV (1982). Techniques in Calcium Research. Academic Press, London, pp 15-17.

Tokuyasu KT (1978). A study of positive staining of ultrathin frozen sections. J. Ultrastruct. Res. 63:287-307.

Tokuyasu KT (1980). Immunochemistry on ultrathin frozen sections. Histochem. J. 12:281-303.

Tokuyasu KT (1986). Application of cryoultamicrotomy to immunocytochemistry. J. Microsc. 143:139-149.

Towbin H, Staehlin T, Gordon J (1979). Electrophoretic transfer of proteins from acrylamide gels to nitrocellulose sheets: Procedure and some applications. Proc. Natl. Acad. Sci. USA. 76:4350-4353.

Triebel S, Blaser J, Gote T, Pelz G, Schuren E, Schmitt M, Tschesche H (1995). Evidence for the tissue inhibitor of metalloproteinases-1 (TIMP-1) in human polymorphonuclear leukocytes. Eur. J. Biochem. 231:714-719.

Tschesche H, Knäuper V, Krämer S, Michaelis J, Oberhoff R, Reinke H (1992). Latent collagenase and gelatinase from human neutrophils and their activation. Matrix Suppl. 1:245-255.

Udenfriend S, Kodukula K (1995). How glycosylphosphatidylinositol-anchored membrane proteins are made. Ann. Rev. Biochem. 64:563-591.

Uitto V-J, Firth JD, Nip L, Golub LM (1994). Doxycycline and chemically modified tetracyclines inhibit gelatinase A (MMP-2) gene expression in human keratinocytes. In: Inhibition of matrix metalloproteinases: Therapeutic potential vol. 732 (Greenwald RA, Golub LM eds), Annals of the New York Academy of Sciences, pp 365-371.

Van Oss, CJ (1986). Phagocytosis: An overivew. In: Immunochemical Techniques Part J - Phagocytosis and Cell-mediated Cytotoxicity. Methods in Enzymology vol. 132 (DiSabato G, Everse J, eds), Academic Press, Orlando, pp 3-15.

Volpe P, Krause K-H, Hashimoto S, Zorzato F, Pozzan T, Meldolesi J, Lew PD (1988). "Calciosome", a cytoplasmic organelle: The inositol 1,4,5 trisphosphate-sensitive Ca^{2+} store of nonmuscle cells? Proc. Natl. Acad. Sci. USA. 85:1091-1095.

Walcheck B, Moore KL, McEver RP, Kishimoto TK (1996). Neutrophil-neutrophil interactions under hydrodynamic shear stress involve L-selectin and PSGL-1. J. Clin. Invest. 98:1081-1087.

Wang X, Fu X, Brown PD, Crimmin MJ, Hoffman RM (1994). Matrix metalloproteinase inhibitor BB-94 (batimastat) inhibits human colon tumour growth and spread in a patient-like orthotopic model in nude mice. Cancer Res. 54:4726-4728.

Wang Y, Russo TA, Kwon O, Chanock S, Rumsey SC, Levine M (1997). Ascorbate recycling in human neutrophils: Induction by bacteria. Proc. Natl. Acad. Sci. USA. 94:13816-13819.

Watson RWG, Redmond HP, Wang JH, Condron C, Bouchier-Hayes D (1996). Neutrophils undergo apoptosis following ingestion of *Escherichia coli*. J. Immunol. 156:3986-3992.

Weaver VM, Fischer AH, Peterson OW, Bissell MJ (1996). The importance of the microenvironment in breast cancer progression: recapitulation of mammary tumorigenesis using a unique human mammary epithelial cell model and a three-dimensional culture assay. Biochem. Cell Biol. 74:833-851.

Weibel ER (1979). Stereological Methods vol. 1: Practical methods for biological morphometry, Academic Press, London, UK, p 9.

Weiss SJ (1989). Tissue destruction by neutrophils. New Engl. J. Med. 320:365-376.

Welgus HG, Stricklin GP (1983). Human skin fibroblast collagenase inhibitor: Comparative studies in human connective tissues, serum and amniotic fluid. J. Biol. Chem. 258:12259-12264.

Westermarck J, Kähäri V-M (1999). Regulation of matrix metalloproteinase expression in tumour invasion. FASEB J. 13:781-792.

Woessner JF (1991). Matrix metalloproteinases and their inhibitors in connective tissue remodelling. FASEB J. 5:2145-2154.

Woessner JF (1994). The family of matrix metalloproteinases. In: Inhibition of matrix metalloproteinases: Therapeutic Potential vol. 732 (Greenwald RA, Golub LM eds). Annals New York Academy of Sciences, pp 11-21.

Xu SY, Varslon M, Engstràm A, Peterson CGB, Venge P (1994). Purification and characterization of a human neutrophil lipocalin (HNL) from the secondary granules of human neutrophils. Scan. J. Clin. Lab. Invest. 54:365-368.

Yamashita K, Takahashi A, Kobayashi S, Hirata H, Mesner PW, Kaufmann SH, Yonehara S, Yamamoto K, Uchiyama T, Sasada M (1999). Caspases mediate tumour necrosis factor alpha-induced neutrophil apoptosis and downregulation of reactive oxygen production. Blood. 93:674-685.

Yao J, Baecher-Allan CM, Sharon J (2000). Serpins identified as cell growth inhibitors in human plasma. Mol. Cell Biol. Res. Comm. 3:76-81.

Yu AE, Hewitt RE, Kleiner DE, Stetler-Stevenson WG (1996). Molecular regulation of cellular invasion - role of gelatinase A and TIMP-2. Biochem. Cell Biol. 74:823-831.

Zhao W-Q, Li H, Yamashita K, Guo X-K, Hoshino T, Yoshida S, Shinya T, Hayakawa T (1998). Cell cycle accumulation of tissue inhibitor of metalloproteinases-1 (TIMP-1) in the nuclei of human gingival fibroblasts. J. Cell Sci. 111:1147-1153.

Ziaie Z, Fawzi A, Bellon G, Monboisse J-C, Kefalides NA (1999). A peptide of the α3 chain of type IV collagen protects basement membrane against damage by PMN. Biochem. Biophys. Res. Comm. 261:247-250.

Zor T, Selinger Z (1996). Linearisation of the Bradford protein assay increases its sensitivity: Theoretical and experimental studies. Anal. Biochem. 236:302-308.

Zsigmondy R (1925). Das Kolloidale Gold. Akademische Verlagsgesellschaft, MBH, Leipzig.

PUBLICATIONS

THE JOURNAL OF BIOLOGICAL CHEMISTRY
Vol. 275, No. 36, Issue of September 8, pp. 28308–28315, 2000
Printed in U.S.A.

Neutrophil Tissue Inhibitor of Matrix Metalloproteinases-1 Occurs in Novel Vesicles That Do Not Fuse with the Phagosome*

Received for publication, March 17, 2000, and in revised form, June 16, 2000
Published, JBC Papers in Press, June 26, 2000, DOI 10.1074/jbc.M002263200

Brendon Price‡, Clive Dennison‡, Harald Tschesche§, and Edith Elliott‡¶

From the ‡School of Molecular and Cellular Biosciences, Department of Biochemistry, University of Natal, Pietermaritzburg, Scottsville 3209, Natal, South Africa and the §Department of Biochemistry, Faculty of Chemistry, University of Bielefeld, Bielefeld 33615, Germany

The human neutrophil granule location of precursors of matrix metalloproteinases (MMPs), MMP-8 and -9, has been established, but that of the tissue inhibitor of matrix metalloproteinases-1 (TIMP-1) has not. In this study, labeling for TIMP-1, pro-MMP-8, pro-MMP-9, and established granule marker proteins reveals that TIMP-1 is mainly located in distinct oval, electron translucent organelles, a little larger than azurophil granules. A lack of labeling for the fluid phase endocytic marker, bovine serum albumin-gold, the lysosome-associated membrane protein markers, and for glycosylphosphatidylinositol-linked proteins, which are enriched in secretory vesicles, indicates the non-endosomal, non-lysosomal, and non-secretory nature of this organelle. Density gradient cofractionation with the least dense, secretory population and some pleomorphism of the organelle suggest it is a "vesicle" rather than a "granule" population. Colocalization with pro-MMP-9 or pro-MMP-8, in minor subpopulations, suggests that TIMP-1 vesicle biogenesis occurs between metamyelocytic and terminal differentiation and before secretory vesicle synthesis. Pulse-chased IgG-coated latex beads and immunolabeling show that specific and azurophil granules fuse with the phagosome whereas TIMP-1 and pro-MMP-9-containing organelles do not. This suggests that these play no role in phagosomal destruction of IgG-opsonized bacteria. Separate localization and colocalization of these proteins may, however, facilitate fine regulation of extracellular proteolysis.

Protease-assisted tumor invasion is thought to be regulated by the balance of proteases and inhibitors released at the invasion front (1). Similarly, the complement of neutrophil granule proteases and inhibitors and their order of release may be important in invasion, inflammation and anti-infection processes. Due to their strong activity against type IV and stromal type I collagen, both neutrophil collagenases, matrix metalloproteinases-8 and -9 (MMP-8[1] and MMP-9), may play a role in basement membrane invasion and inflammation (2–4). In the bloodstream, MMP activity is regulated by α_2-macroglobulin (5) and members of the tissue inhibitor of matrix metalloproteinase (TIMP) family (6–8). In tissues, however, the TIMPs may play the predominant role as α_2-macroglobulin (720 kDa) may be too large to gain access to many pericellular spaces.

TIMP-1 was recently shown by protein purification, sequencing, mRNA isolation, and immunofluorescence staining to be present in neutrophil granules (4), but the identity of the TIMP-1-containing organelle, and its possible role, have not been previously described.

Three major neutrophil granule populations (azurophil, specific, and gelatinase granules) and a secretory vesicle population, defined by specific marker proteins and distinctive "granular" shape or pleomorphic, "vesicular" shapes, are synthesized at defined stages of neutrophil maturation (9). Since the expression of each set of granule markers peaks at defined stages of neutrophil maturation (2, 10–17), it is possible that the expression or non-expression of granule marker protein genes during biogenesis of a particular granule type may determine the marker composition of a particular granule (18, 19). Furthermore, minor subpopulations, which contain marker proteins for more than one granule type, may arise during overlapping expression of marker proteins as the expression of one "granule-specific" marker protein begins and another decreases (10–15).

In mature neutrophils, granule release seems to occur largely in the reverse order to that of synthesis (and granule density), although this may also depend on the nature of the inducing stimulus (20). The most dense azurophil granules are synthesized first and are the last to be released (15, 21–24). Conversely, the least dense secretory vesicles are synthesized last and are released first (14). Secretory vesicles contain extracellular matrix receptors (2, 9, 14) that are important for rolling, endothelial attachment, diapedesis, and basement membrane traversal (25). These (and most other secretory vesicle proteins) are membrane-associated via a glycosylphosphatidylinositol linkage (GPI anchor) (26, 27) and are exposed on the cell surface via exocytosis. As would be anticipated, their extracellular release occurs before that of other granules, as diapedesis and membrane-traversal without extracellular matrix receptors would be impossible. The time of synthesis and

* This work was supported by grants from the Research Fund of the University of Natal and the National Research Foundation (South African Foundation for Research Development), by Wissenschaft und Technologie Cooperation Grant on Leukocyte Proteins Grant 396KOA6A from the Forschungzentrum Jülich, Germany, and by Deutsche Forschungsgemeinschaft, Bonn, Special Research Program SFB 549 (Project A05). The costs of publication of this article were defrayed in part by the payment of page charges. This article must therefore be hereby marked "*advertisement*" in accordance with 18 U.S.C. Section 1734 solely to indicate this fact.

¶ To whom correspondence should be addressed: School of Molecular and Cellular Biosciences, Dept. of Biochemistry, University of Natal, Pietermaritzburg, Private Bag X01, Scottsville 3209, Natal, South Africa. Tel.: 27-33-2605455; Fax: 27-33-2605462; E-mail: elliott@unpsun1.cc.unp.ac.za.

[1] The abbreviations used are: MMP, matrix metalloproteinase; pro-MMP, precursor matrix metalloproteinase; TIMP(-1), tissue inhibitor of matrix metalloproteinase(-1); GPI, glycosylphosphatidylinositol; BSA, bovine serum albumin; MT1-MMP, membrane type matrix metalloproteinase-1; NBT, nitro blue tetrazolium; BCIP, 5-bromo-4-chloro-3-indolyl phosphate; PMSF, phenylmethylsulfonyl fluoride; PEG, polyethylene glycol; HSA, human serum albumin; IgY, chicken yolk immunoglobulin; TPP, three-phase partitioning; PBS, phosphate-buffered saline; LAMP, lysosome-associated membrane protein; PAGE, polyacrylamide gel electrophoresis; Tricine, *N*-[2-hydroxy-1,1-bis(hydroxymethyl)ethyl]glycine.

order of release of the TIMP-1 organelles, however, remain unknown.

Besides inhibiting MMPs, TIMPs have a number of other functions, such as erythroid cell potentiation, growth promotion, and antiapoptotic, differentiation-promoting, and angiogenesis-promoting activities (6, 7, 28–34). A TIMP-2/pro-MMP-2 heterodimer complex has also been reported to have a role in the binding of pro-MMP-2 to membrane-type MMP (MT1-MMP/MMP-14), resulting in activation and subsequent focusing of MMP-2 activity on the invadopodia of cancer cells (1, 35, 36), where it may facilitate invasion. A TIMP-1/pro-MMP-9 heterodimer has been identified during the isolation of pro-MMP-9 from neutrophils (4), and an unanswered question is whether this occurs *in vivo* and plays a specific role, or whether it is merely an isolation artifact.

In the present study, the intracellular localization of TIMP-1, and the role of MMPs and TIMPs in phagosomal digestion of opsonized particles were investigated. TIMP-1 was mainly located in distinct electron-translucent vesicles, slightly larger than azurophil granules, less dense than all but the secretory vesicles and lacking markers for known granules and for secretory vesicles, endosomes, and lysosomes. TIMP-1 also colocalized with pro-MMP-8 and pro-MMP-9 in minor vesicle subpopulations. Pro-MMP-9 and TIMP-1 were excluded from the phagosome during phagocytosis of IgG-opsonized latex beads, suggesting that they have no role in the phagosomal destruction of opsonized materials, such as bacteria. The possible implication of the largely separate and minor colocalization of TIMP-1, pro-MMP-8, and pro-MMP-9 in different neutrophil organelles, with regard to the invasive movement of neutrophils and the possible timing of synthesis of TIMP-1, is discussed.

EXPERIMENTAL PROCEDURES

Materials

Protein A-gold (5, 10, and 15 nm) was from the Department of Cell Biology, University of Utrecht, Utrecht, The Netherlands. Percoll, 2,2′-azino-di-(3-ethyl)-benzthiozolinesulfonic acid, RPMI 1640 medium, dimethyl sulfoxide (Me_2SO), nitro blue tetrazolium (NBT), 5-bromo-4-chloro-3-indolyl phosphate (BCIP), levamisole, alkaline phosphatase-conjugated goat anti-rabbit, goat anti-mouse IgG, and rabbit anti-lactoferrin antibodies were from Sigma. Microtiter plates were from Nunc (Roskilde, Denmark). Enhanced chemiluminescence (ECL) reagents, x-ray film, and 0.45-μm nitrocellulose membrane were from Amersham Pharmacia Biotech (Buckinghamshire, United Kingdom). Phenylmethylsulfonyl fluoride (PMSF) and polyethylene glycol (PEG) (6 and 20 kDa) were from Roche Diagnostics (Mannheim, Germany). Type I porcine gelatin (300 bloom) was from Merck (Darmstadt, Germany). Anti-TIMP-1 monoclonal antibody was from Calbiochem (La Jolla, CA). The sheep anti-rabbit horseradish peroxidase conjugate and the rabbit anti-human serum albumin (anti-HSA) IgG were gifts from Drs. Theresa Coetzer and Rory Morty, respectively, from the School of Molecular and Cellular Biosciences, University of Natal, Natal, South Africa. Rabbit anti-human TIMP-1, anti-pro-MMP-8, and anti-pro-MMP-9 (4, 37) were from the Department of Biochemistry, University of Bielefeld, Bielefeld, Germany. The rabbit anti-myeloperoxidase antibody was from Dakopatts (Glostrup, Denmark). Monoclonal ascites fluid lysosome-associated membrane protein -1 and -2 (LAMP-1 and LAMP-2) antibodies were from the Developmental Studies Hybridoma Bank, University of Iowa, Iowa City, IA.

Methods

Neutrophil Isolation—Human neutrophils were isolated on Percoll density gradients (38), erythrocytes lysed (39), cells resuspended in RPMI 1640 medium or phosphate-buffered saline (PBS; 140 mM NaCl, 3 mM KCl, 8 mM Na_2HPO_4, 1 mM KH_2PO_4, 0.5 mM $MgCl_2$, 1 mM $CaCl_2$, pH 7.3), tested for viability using trypan blue exclusion, and processed for subcellular fractionation or cryoultramicrotomy. For antibody characterizations, neutrophils were resuspended in PBS containing 1 M NaCl, 2 mM L-methionine, and 10% Me_2SO and snap-frozen in liquid nitrogen.

Protein Quantitation—Protein was quantitated using a modified Bradford assay (40).

Three-phase Partitioning (TPP) Enrichment of Sputum Pro-MMP-9—Sputum (20 ml) from a healthy individual was clarified (10,000 × *g*, 10 min, room temperature) and the supernatant fractionated using TPP (41) with incremental addition of ammonium sulfate (20%, 40%, 60%, and 80% (m/v)). Precipitates (15 μg) were dissolved in MMP buffer (42), separated on reducing SDS-PAGE (43), and processed for gelatin zymography (42) or silver-stained (44). The fraction showing most activity at about 92 kDa and with the least number of other contaminating proteins was probed for the presence of pro-MMP-9 by Western blotting (as described below) and saved for use in a Western ligand blot.

Production of Anti-GPI-anchored Protein Antibodies for Identification of Neutrophil Secretory Vesicles—Neutrophil transmembrane, GPI-anchored, and lipid-modified proteins were enriched by Triton X-114 phase partitioning (45). Translocation of GPI-anchored proteins from the detergent to the aqueous phase was effected by nitrous acid deamination (46). These proteins were analyzed by non-reducing PAGE, and for alkaline phosphatase activity (a marker for GPI-anchored secretory vesicle proteins). Active fractions were precipitated with 10 volumes of acetone (−20 °C, 1 h), resuspended in PBS, and used to raise antibodies in laying hens by inoculation of 25 μg of protein into the breast muscle, initially in Freund's complete adjuvant and subsequently in incomplete adjuvant at weeks 1, 3, and 6. Immunoglobulin (IgY) was isolated from 6-week egg yolks by PEG (6 kDa) precipitation (47) and tested for specificity using immunolabeling, specific labeling being anticipated to be limited to the inner membranes of electron-translucent secretory vesicles.

Western Blotting—The specificity of the majority of antibodies was established by Western blotting of the crude neutrophil homogenate (prepared as described below). Semipurified neutrophil homogenates and a Western ligand blot were used to confirm the specificity and form of TIMP-1 targeted by the anti-TIMP-1 antibody in crude homogenates.

Crude neutrophil homogenates were prepared by thawing snap-frozen neutrophils in the presence of 1 mM EDTA, 2 mM PMSF, and 1% NaN_3. These were centrifuged (10,000 × *g*, 20 min, 4 °C), the supernatants (~80 μg of protein/lane) separated on a 10% reducing Tris-Tricine SDS-PAGE (43) and blotted onto a nitrocellulose membrane (48). To dissociate high molecular weight forms of TIMP-1, homogenates were also lyophilized, resuspended in denaturation buffer (6 M guanidine-HCl, 500 mM Tris-HCl, 2 mM EDTA, pH 8.1), reduced and carboxymethylated (49), separated by SDS-PAGE, electrotransferred (as above), and probed with rabbit anti-TIMP-1 IgG (20 μg/ml).

TIMP-1 was semipurified from snap-frozen neutrophils (1 ml), thawed in the presence of proteinase inhibitors, by a combination of heat treatment (20 min, 85 °C), centrifugation (1000 × *g*, 10 min, room temperature), and heparin-agarose chromatography (50). The eluate was concentrated against PEG (20 kDa), precipitated using trichloroacetic acid and deoxycholic acid (51), pelleted (10,000 × *g*, 5 min, 4 °C), washed with cold acetone, and air-dried. Samples were resuspended in reducing buffer (30 μl) prior to SDS-PAGE separation, blotted (as above), and probed with rabbit anti-TIMP-1 IgG (20 μg/ml).

A crude TPP fraction showing a gelatinolytic band of about 92 kDa was similarly resolved by reducing SDS-PAGE, blotted, and probed with rabbit anti-pro-MMP-9 IgG (4 μg/ml).

Western Ligand Blot of Neutrophil Homogenates for TIMP-1—Blots of the variously treated crude neutrophil homogenates were incubated with a crude sputum pro-MMP-9 TPP fraction (identified by zymography and Western blotting) and subsequently labeled with anti-MMP-9 antibodies, as described above. TIMP-1 binds to pro-MMP-9 even after blotting (52), and, hence, any TIMP-1 forms present should be revealed by this method.

Endogenous neutrophil myeloperoxidase and alkaline phosphatase activities were quenched with 0.01% NaN_3 and 2 mM levamisole, respectively. Membranes were blocked with 3% nonfat milk in Tris-buffered saline (20 mM Tris-HCl, 200 mM NaCl, pH 7.4) and probed with primary antibodies and binding detected with either a horseradish peroxidase-coupled sheep anti-rabbit secondary antibody and ECL or an alkaline phosphatase-coupled goat anti-rabbit/anti-mouse antibody and a BCIP/NBT chromogenic detection system.

Subcellular Fractionation of Neutrophil Granules—Neutrophil granule fractionation was performed as described (10) with a few modifications. Neutrophils (10×10^6/ml) were resuspended in ice-cold relaxation buffer (100 mM KCl, 10 mM HEPES, 3 mM NaCl, 1 mM Na_2ATP, 3.5 mM $MgCl_2$, pH 7.3), disrupted by sonication, and centrifuged (365 × *g*, 15 min, 4 °C). The postnuclear supernatant (5 ml) was applied to a 35-ml four-layer discontinuous Percoll gradient (1.05/1.07/1.12/1.14 g/ml), containing 2.9 mM PMSF, and centrifuged (36,600 × *g*, 30 min, 4 °C). Granule fractions were collected in 29 aliquots of 1 ml each and assayed

for myeloperoxidase activity (azurophil granule fraction) (13, 53–55) or latent alkaline phosphatase activity (secretory vesicle and plasma membrane fraction) (56). Granule fractions were pooled on the basis of the presence of myeloperoxidase or alkaline phosphatase, or a lack of either activity (specific and gelatinase granules), designated α, γ, and β, respectively (23), and processed for cryoultramicrotomy and stereology (as described below).

Cryoultramicrotomy and Immunolabeling —Isolated neutrophils and pooled granule fractions were fixed (2% paraformaldehyde, 0.05% glutaraldehyde in 200 mM HEPES, pH 7.2) overnight at 4 °C. Residual aldehyde groups were quenched (20 mM glycine in PBS, pH 7.2), the cells pelleted (400 × *g*, 2 min, 4 °C), embedded in 10% gelatin, processed for cryoultramicrotomy (57, 58), and stored in liquid nitrogen.

Ultrathin cryosections (60–80 nm) cut on an RMC MT6000XL ultramicrotome at −100 °C were retrieved on 1.15 M sucrose/1% methylcellulose droplets (59), placed on carbon-coated, glow-discharged nickel grids (60), and whole cell sections double-labeled with rabbit antibodies against granule antigens (anti-myeloperoxidase (15 μg/ml), anti-lactoferrin (12.5 μg/ml), anti-pro-MMP-8 (10 μg/ml), anti-pro-MMP-9 (10 μg/ml), anti-TIMP-1 (25 μg/ml), and antibodies to the secretory vesicle antigen, albumin (10 μg/ml)) followed by protein A-gold, as described (57). Secretory vesicles are endocytic in origin (9), and, as albumin is also thought to be taken up only during the myeloid stage of differentiation (9), labeling for GPI-anchored proteins, enriched in the secretory vesicles, was also undertaken. LAMP-1 and LAMP-2 labeling was used to distinguish organelles of endosomal or lysosomal origin.

For LAMP-1 (ascites fluid diluted 1/120) and LAMP-2 (ascites fluid diluted 1/200) labeling, and labeling for GPI-anchored proteins (chicken IgY, diluted 10 μg/ml), an additional rabbit anti-mouse (1/500) or rabbit anti-chicken linker (10 μg/ml) antibody was also used prior to application of the protein A-gold probe. Sections were stained with neutral uranyl acetate-oxalate and sealed with acidic 0.2% uranyl acetate, 1.8% methylcellulose (58).

Neutrophil granule fractions were labeled for TIMP-1 and myeloperoxidase as described above.

Stereological and Statistical Analysis—Diameters of the various neutrophil granule populations were statistically estimated on sections of whole cells by measuring the mean diameter of multiple random sections of each population, using at least three micrographs with primary magnifications of 27,500 and 33,000 (57, 61), on a minimum of 11 granules, each granule type being defined by its content of a particular granule marker protein. If granules were not exactly spherical, the mean of two different diameters through the center was used. The diameters of dumbbell-shaped specific granules were not included in diameter estimations, and significant differences in diameter between the TIMP-1 vesicle and other granule types were established using one-sided Student's *t* tests. Diameter estimations were compared with those previously published (62) and those measured for density gradient granule fractions. Approximate mean profile areas were calculated for spherical organelles using the measured diameters. Labeling density for a particular antigen was assessed by counting the number of specific gold particles per granule/organelle/vesicle on a minimum of seven or more such organelles and expressed as gold particles/μm^2. Nonspecific (background) particles (on cytosol or nucleus) were counted and similarly expressed.

The degree of colocalization of a particular granule antigen with TIMP-1 was established by counting the number of gold probes, representing labeling that colocalizes with TIMP-1, relative to the total number of gold probes for that particular antigen on each micrograph (in a minimum of 15 granules containing the marker of interest), and expressing this as a percentage.

On granule fractions, diameters were estimated by measuring multiple random diameters of at least 10 vesicles labeling for myeloperoxidase or TIMP-1.

Visualization of the Lysosomal Compartment Using Pulse-Chase Labeling —BSA-gold colloids (14 ± 1.23 nm) were produced by the tannic acid/citrate method (63). Neutrophils in serum-free RPMI 1640 medium were pulsed with 14 nm gold (1:50 dilution; A_{520} = 0.552) for 1 h, washed thoroughly in fresh medium, chased for another 3 h (all at 37 °C), in order to label lysosomal compartments (64), before processing for cryoultramicrotomy and immunolabeling (as described).

Visualization of the Phagosomal Compartment Using IgG-opsonized Latex Beads —Human IgG was purified from serum by PEG (6 kDa) precipitation (65) and adsorbed to 1-μm amine-modified latex beads (~ 1 mg of IgG/50 μl of beads, overnight, 4 °C). The beads were washed with RPMI 1640 medium and diluted 1:200 in medium containing neutrophils. Phagocytosis was terminated at various time periods (0.5, 1, 2, 5, 10, 20, 30, and 60 min) by the addition of fixative, and the cells were processed for cryoultramicrotomy and immunolabeling (as described above).

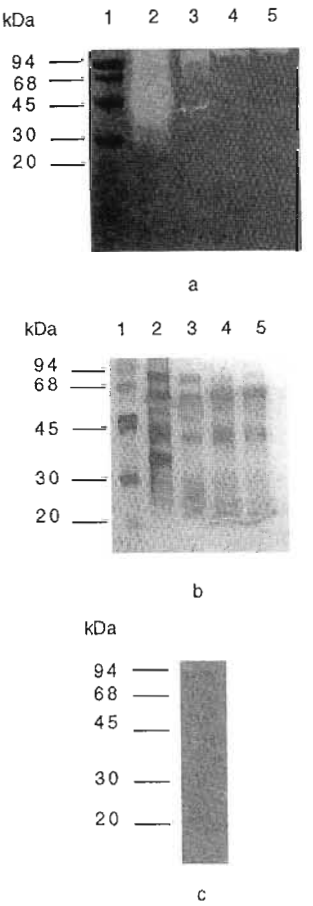

FIG. 1. **Gelatin zymography, silver staining and Western blotting analysis of TPP sputum fractions.** Aliquots of TPP fractionated sputum (15 μg/lane) were separated under non-reducing conditions on a 10% Tris-Tricine SDS-PAGE gel containing 1 mg/ml gelatin (*a*) and under reducing conditions without gelatin (*b*). *Lane 1*, M_r markers; *lane 2*, 0–20% $(NH_4)_2SO_4$; *lane 3*, 20–40% $(NH_4)_2SO_4$; *lane 4*, 40–60% $(NH_4)_2SO_4$; *lane 5*, 60–80% $(NH_4)_2SO_4$ fraction. Gels were stained with Coomassie Blue (*a*) or silver (*b*). The Western blot of the 60–80% $(NH_4)_2SO_4$ TPP fraction was probed with rabbit anti-MMP-9 IgG (4 μg/ml) (*c*) and detected with an alkaline phosphatase-conjugated secondary antibody and BCIP/NBT. Only the 92-kDa pro-MMP-9 is present in the fraction.

RESULTS

Purification of Pro-MMP-9 by TPP —TPP proved a quick, convenient method of fractionating pro-MMP-9 from sputum, a rich source of MMP-9 (66). Zymograms and silver-stained gels showed that the 60–80% $(NH_4)_2SO_4$ TPP fraction contained a distinctive 92-kDa gelatinolytic band (Fig. 1*a*, *lane 5*) and had the lowest number of contaminating proteins (Fig. 1*b*, *lane 5*). The presence of a 92-kDa pro-MMP-9 band was confirmed by probing a Western blot with an anti-pro-MMP-9 antibody (Fig. 1*c*). This preparation was used to confirm previously determined anti-pro-MMP-9 and anti-TIMP-1 antibody specificities (4, 37). The anti-pro-MMP-9 antibody appeared to be specific as it targeted none of the contaminating bands revealed by silver staining (Fig. 1*b*).

Preparation of Anti-GPI-anchored Protein Antibodies —The presence of alkaline phosphatase activity in the aqueous phase, after nitrous acid deamination of GPI anchors, indicated efficient cleavage of neutrophil GPI anchors. Chicken antibodies were successfully raised against these proteins, as they specifically labeled membranes of a distinctly electron translucent and highly pleomorphic secretory vesicle-like population (Fig. 6*a*).

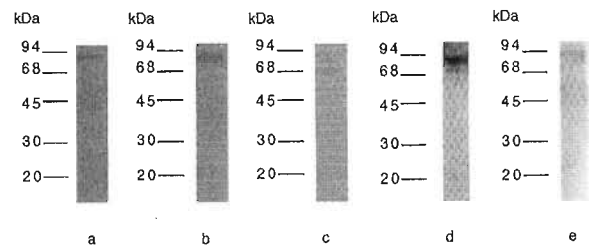

FIG. 2. **Western blots of neutrophil homogenates with antibodies against granule marker proteins and neutrophil MMPs.** Homogenates (~80 μg/lane) were separated by 10% Tris-Tricine SDS-PAGE under reducing conditions. The blotted proteins were probed with rabbit antibodies against: myeloperoxidase (25 μg/ml) (*a*), lactoferrin (50 μg/ml) (*b*), human serum albumin (20 ng/ml) (*c*), MMP-8 (10 μg/ml) (*d*), and MMP-9 (10 μg/ml) (*e*). Blots were developed chromogenically with BCIP/NBT (*a*, *b*, *d*, and *e*) or using ECL (*c*).

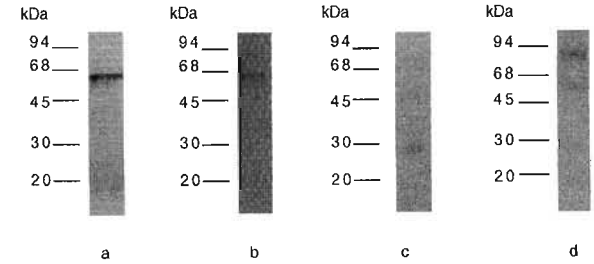

FIG. 3. **Western blots of neutrophil homogenates with antibodies against TIMP-1 and Western ligand blotting of neutrophil TIMP-1 with sputum pro-MMP-9.** Homogenates (~80 μg/lane) were separated by 10% Tris-Tricine SDS-PAGE under reducing conditions and probed with rabbit anti-TIMP-1 IgG (20 μg/ml) (*a–c*). Blots of untreated neutrophil homogenate (*a*), homogenate reduced, carboxymethylated, and denatured in guanidinium hydrochloride prior to SDS-PAGE and blotting (*b*), and homogenate boiled and passed through heparin-agarose and the eluate subjected to SDS-PAGE and blotting (see text for details) (*c*) are shown. A Western ligand blot of neutrophil homogenates with TPP-fractionated sputum pro-MMP-9 to verify the identity of the 66-kDa TIMP-1 species is also shown (*d*). The blotted neutrophil homogenate was incubated with pro-MMP-9, washed, and probed with rabbit anti-MMP-9 IgG (10 μg/ml). Blots were developed chromogenically with BCIP/NBT (*b* and *d*) or using ECL (*a* and *c*).

Western Blotting —The antibodies raised against the granule marker proteins myeloperoxidase, lactoferrin and albumin were specific as they targeted only antigens of the anticipated molecular weight in crude neutrophil homogenates (Fig. 2, *a–c*, respectively). The specificities of the pro-MMP-8, pro-MMP-9, and TIMP-1 antibodies were previously determined using pure antigen (52) or semipurified neutrophil homogenates (37) but the specificities and lack of cross-reactivity of the anti-pro-MMP-8 and anti-pro-MMP-9 antibodies were confirmed here using crude neutrophil homogenates (Fig. 2, *d* and *e*).

Characterization of the antibodies used to label neutrophil TIMP-1 revealed a 66-kDa band in crude neutrophil homogenates (Fig. 3*a*) instead of the anticipated 28–30 kDa. This result was confirmed, using a commercial specific monoclonal anti-TIMP-1 antibody (results not shown).

The high molecular weight TIMP-1-reactive protein did not dissociate after reduction with freshly made dithiothreitol and carboxymethylation, or in 6 M guanidine chloride (49) (Fig. 3*b*), or thawing in the presence of Me_2SO (67) and methionine (68). (Me_2SO and methionine (free radical scavengers) were used to prevent artifactual covalent complexes forming due to exposure to reactive oxygen species or myeloperoxidase-derived hypochlorous acid (69), during neutrophil homogenization or oxidative burst (70) (results not shown).)

In contrast, homogenates that were boiled, and passed through a heparin-agarose column, prior to SDS-PAGE and Western blotting, gave only a single band at 28–30 kDa, and no band at 66 kDa (Fig. 3*c*), indicating that the 66-kDa band obtained in the previous blots contained TIMP-1. Purified TIMP-1 samples have been reported to auto-aggregate during storage, and the high molecular weight form reported here may, therefore, represent an aggregate found at high concentration (71–73).

Western Ligand Blot of Crude Neutrophil Homogenates for TIMP-1—Immunolabeling for pro-MMP-9 after treatment of a blot of a crude neutrophil homogenate with partially purified sputum pro-MMP-9 revealed three bands of approximately 92, 66, and 30 kDa (Fig. 3*d*) instead of the single 92-kDa pro-MMP-9 band observed when probing the untreated homogenate (Fig. 2*e*). The ~92-kDa band probably represents the pro-MMP-9 already present in the neutrophil homogenate (Fig. 2*e*), while the 66-kDa band may represent an aggregate form of TIMP-1 revealed by its reaction with the added pro-MMP-9 (Fig. 3*d*), confirming previous results (Fig. 3, *a* and *b*). The 30-kDa band possibly corresponds to low amounts of monomeric TIMP-1, now visualized due to a signal amplification effect achieved after pro-MMP-9 binding to TIMP-1 (Fig. 3*d*). A faint 20-kDa band was visible in some blots and may represent pro-MMP-9 bound to unglycosylated TIMP-1 (74) (results not shown).

Subcellular Fractionation of Neutrophil Granules —Granules, from neutrophil homogenates, were separated into three distinct density gradient fractions designated α, β, and γ. Peroxidase activity and myeloperoxidase labeling was found in the most dense, α fraction that should contain the azurophil (myeloperoxidase-containing) granules (Fig. 4). Latent alkaline phosphatase activity and immunolabeling for TIMP-1 was found in the least dense, γ fraction that should contain the secretory vesicles and plasma membrane (Fig. 4).

Stereology and Immunolocalization of TIMP-1 Vesicles with Respect to Markers for Other Granules and the Endocytic/Lysosomal Pathway —In this study, the diameters measured for established granule populations compared favorably with those previously reported (12, 62). Labeling of neutrophil sections showed that TIMP-1 was mainly located in electron translucent organelles, on average slightly larger than the azurophil granules, significantly larger than other granule or vesicle populations, but significantly smaller than BSA-gold-containing lysosomes (Table I, Figs. 5–7). TIMP-1 showed no significant colocalization with azurophil markers in the electron-dense or electron-translucent, myeloperoxidase-labeling azurophil granules (Fig. 5*a*), as confirmed in sections of granule fractions (Fig. 4), and counts and statistical analysis done on whole cell sections (Table I).

Some colocalization of the specific granule marker, pro-MMP-8, with TIMP-1 was observed in electron-translucent organelles of various sizes (Fig. 5*c*), whereas specific granules labeling for lactoferrin and pro-MMP-8, or pro-MMP-8 only (3, 54, 75) were predominantly round and electron-dense (Fig. 5*b*) or dumbbell-shaped and electron-dense (Fig. 5*c*).

Colocalization of pro-MMP-9 with TIMP-1 was seen in electron translucent organelles about the size of TIMP-1 vesicles (Fig. 5*d* and Table I), whereas most pro-MMP-9-labeled granules (*i.e.* specific and gelatinase granules) (62, 76–78) were smaller (Table I), almost circular and electron-dense, with some dumbbell-shaped organelles (Fig. 5*d*). Separate localizations for TIMP-1 and pro-MMP-9 were, however, mainly seen. Less than a third of the pro-MMP-9 and slightly less than 15% of pro-MMP-8 colocalized with TIMP-1 (Table I).

Labeling for the secretory granule marker, human serum albumin (HSA) (9), showed no colocalization of HSA and TIMP-1 (Table I), but labeling density was low. Labeling for the GPI-anchored proteins, enriched in secretory vesicles, proved a more reliable marker for this organelle and confirmed that

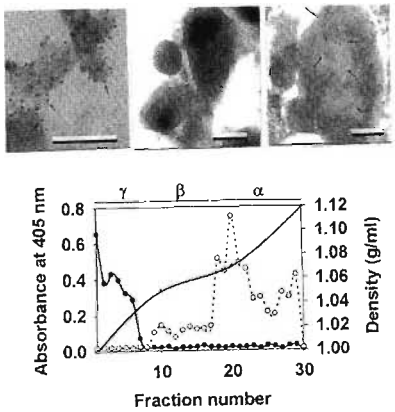

FIG. 4. **Determination of the relative density and content of TIMP-1 or myeloperoxidase in granule fractions.** Neutrophils were disrupted by sonication, postnuclear supernatants separated on a Percoll gradient (as described under "Experimental Procedures") and granule fractions pooled on the basis of the presence of alkaline phosphatase activity (γ fraction, secretory granule fraction) and myeloperoxidase activity (α fraction), or absence of both enzymes (β fraction). Latent alkaline phosphatase activity (γ fraction, *solid circle* and *solid line* on *graph*) was detected with a paranitrophenyl phosphate substrate and myeloperoxidase activity (α fraction, *open circle* and *dotted line* on *graph*) was detected with 2,2′-azino-di-(3-ethyl)-benzthiozoline-sulfonic acid/H_2O_2, both at 405 nm. A plot of the relative density is given by the *solid line* (*no circles*). Granules were processed for cryoultramicrotomy and labeled for TIMP-1 and myeloperoxidase TIMP-1 was found in the γ fraction (10 nm gold; *small arrow*), and myeloperoxidase was found in the α fraction (5 nm gold; *small arrow*). *Bars*, 200 nm.

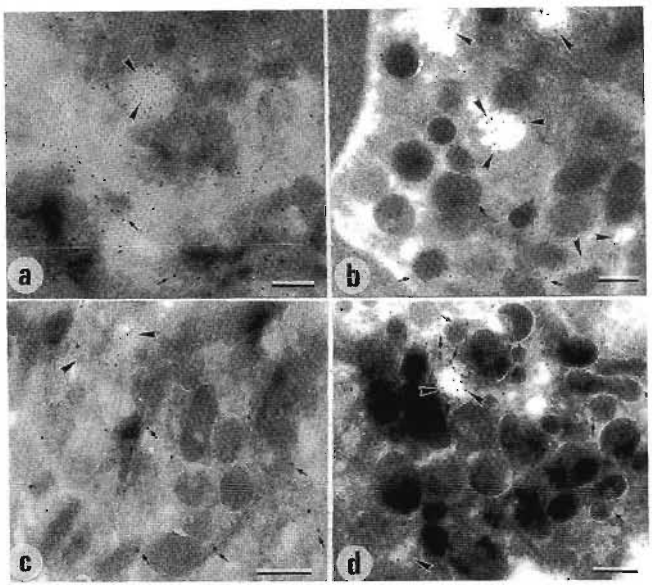

FIG. 5. **Immunolocalization of TIMP-1 with respect to markers for the azurophil (myeloperoxidase), specific (lactoferrin, pro-MMP-8, and pro-MMP-9), and gelatinase granules (pro-MMP-9) on thawed neutrophil cryosections.** Figure shows TIMP-1 (5 nm gold; *arrowheads*) and myeloperoxidase (10 nm; *small arrows*) (*a*), TIMP-1 (5 nm gold; *arrowheads*) and lactoferrin (10 nm gold; *small arrows*) (*b*), TIMP-1 (5 nm gold; *arrowheads*) and pro-MMP-8 (10 nm gold; *small arrows*) (*c*), and TIMP-1 (5 nm gold; *arrowheads*) and pro-MMP-9 (10 nm gold; *small arrows*). *Bars*, 200 nm.

TIMP-1 does not seem to occur in GPI-rich secretory vesicles (Fig. 6*a*).

On the basis of their lack of multilaminar or multivesicular shape (Figs. 5–7), and lack of labeling for LAMP antigens (76, 79) (Fig. 6*b*) or BSA-gold, after a long chase (Fig. 6*c*), large and small TIMP-1 vesicles do not appear to be lysosomes. Pleomorphic and smaller TIMP-1 organelles were mainly observed in thicker sections (Fig. 5*c* and 6, *a* and *c*).

Fractionated granules appear to have larger dimensions than those determined from sections (Table I). Organelles in

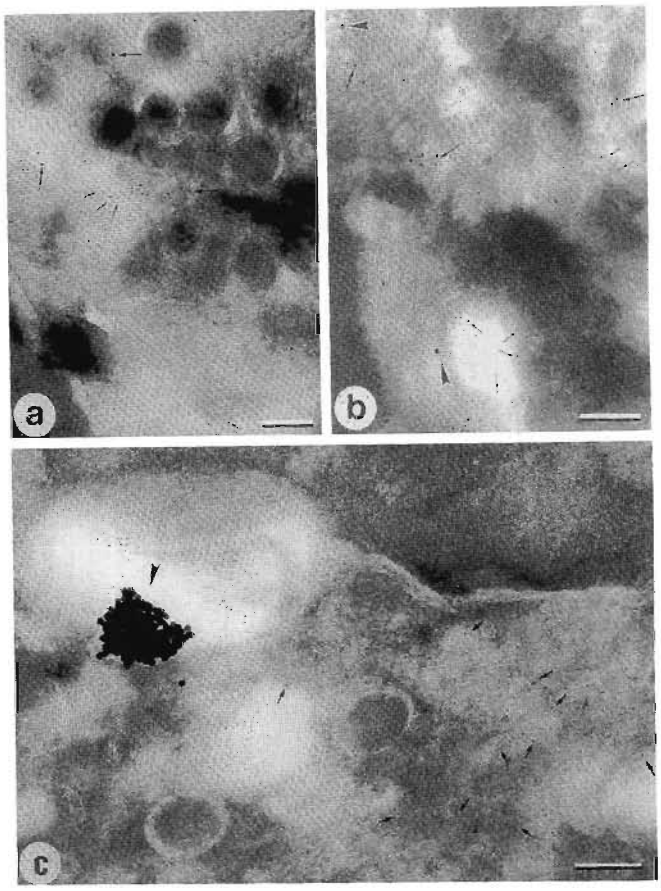

FIG. 6. **Immunolocalization of TIMP-1 with respect to secretory vesicle GPI-anchored proteins, LAMP-1, LAMP-2, and BSA-gold pulsed into the lysosome/late endosome organelle in thawed neutrophil cryosections.** Figure shows vesicle GPI-anchored proteins (5 nm gold; *smaller arrows*) and TIMP-1 (10 nm gold; *larger arrows*) (*a*), TIMP-1 (5 nm gold; *small arrows*), LAMP-1 (10 nm gold; *larger arrow*), and LAMP-2 (15 nm gold; *arrowhead*) (*b*), and TIMP-1 (5 nm gold; *arrow*) and BSA-gold pulse-chased into the lysosome/late endosome organelle (14 nm gold; *arrowhead*) (*c*). *Bars*, 200 nm.

the azurophil granule fraction (α fraction) ranged from 314–423 nm and the remaining fraction (β fraction) had an average diameter of 314 nm (Fig. 4). Osmotic swelling may be responsible for the increased dimensions and the apparent loss (from the γ fraction) of secretory vesicles and the larger TIMP-1 populations. Some secretory vesicle membranes (and/or plasma membranes) are present in this fraction as latent alkaline phosphatase activity is demonstrable. Only the smaller, pleomorphic, TIMP-1-labeled structures seem to survive the fractionation procedures and are present in this fraction, however (Fig. 4). These smaller TIMP-1 vesicles ranged in size from 50 to 120 nm and are of a considerably smaller size than the major TIMP-1 granule (266–350 nm) (Table I).

Visualization of Granule Fusion with Phagosomes —At least two of the known granules (azurophil and specific) fuse with phagosomes and deliver their contents. We therefore asked whether pro-MMP-8-, pro-MMP-9-, or TIMP-1-containing organelles also fused with the phagosomes, and in which order.

Experiments involving pulse-chased IgG-opsonized 1-μm latex beads, followed by immunocytochemistry on thawed cryosections, showed that the TIMP-1 vesicle and the gelatinase granules containing pro-MMP-9 do not fuse with the phagosome (results not shown). Complete phagosomal maturation is, however, indicated by the appearance of lactoferrin in the phagosome within 20 min (Fig. 7*b*), followed by myeloperoxidase after 1 h (Fig. 7*a*). Pro-MMP-8 was detected in the phagosome in trace amounts, presumably due to fusion of the

TABLE I
Stereological analysis of immunocytochemical labeling results

Marker protein	Granule population	Diameter[a]	Student's *t* value	Mean profile area	Gold particles/μm^2	Gold particles/μm^2 background	Gold particles per organelle/granule/vesicle[a]	Colocalization with TIMP-1[b]
		nm		μm^2				%
TIMP-1	TIMP-1[c]	266 ± 84 (15)		0.056 ± 0.005	334 ± 233	0	19 ± 13 (15)	100
Myeloperoxidase	Azurophil	237 ± 74 (17)	1.01[NS]* (30 *df*)	0.045 ± 0.004	205 ± 176	8	9 ± 8 (20)	0.9 (3/322)
Lactoferrin	Specific	161 ± 41 (11)	3.79** (24 *df*)	0.021 ± 0.008	650 ± 415	6	13 ± 9 (15)	3.5 (6/169)
Pro-MMP-8	Specific	168 ± 35 (11)	3.61** (24 *df*)	0.022 ± 0.005	127 ± 60	49	3 ± 1 (15)	14.5 (20/138)
Pro-MMP-9	Specific/gelatinase	133 ± 36 (11)	4.89** (24 *df*)	0.014 ± 0.004	214 ± 111	1	3 ± 2 (15)	22.6 (26/115)
Albumin	Secretory	ND[d]		ND[d]	ND[d]	0	2 ± 2 (10)	0 (0/46)
GPI proteins	Secretory	ND[d]		ND[d]	ND[d]	0	6 ± 3 (7)	1.4 (2/139)
LAMP-1 and	Multivesicular or multilaminar compartments	ND[d]		ND[d]	ND[d]	1	3 ± 1 (11)	0 (0/127)
LAMP-2		ND[d]		ND[d]	ND[d]	0	1 ± 0.5 (10)	0 (0/96)
BSA-gold	Lysosome	406 ± 200 (7)	2.35* (20 *df*)	0.13 ± 0.03	303 ± 142	2	39 ± 18 (10)	0 (0/406)

[a] Number in parentheses indicates the number of granules/vesicles/organelles over which estimations made.

[b] Colocalization was determined by expressing the number of gold particles counted for the labeling of a particular antigen colocalizing with TIMP-1 (y) as a percentage of the total number of gold particles counted for that antigen ($x + y$) and expressed as $y/(x + y) \times 100\%$ *e.g.* for myeloperoxidase, out of a total of 322 gold probes representing labeling for myeloperoxidase ($x + y$), only 3 of these (y) colocalize with TIMP-1 in a TIMP-1 vesicle.

[c] We propose that this organelle be named the TIMP-1 vesicle.

[d] ND, not determined. Diameter and mean profile area estimations for the secretory vesicles and LAMP-positive structures were not possible due to the highly pleomorphic nature of these vesicles/organelles.

[e] NS, *, ** Indicates that from one-sided Student's *t* tests, diameter differences of a particular granule with respect to the TIMP-1 vesicle are either nonsignificant (NS), or significant at the 5% (*) or the 1% (**) level for the various degrees of freedom (*df*).

FIG. 7. **Immunolocalization of TIMP-1 with respect to the azurophil granule marker myeloperoxidase and the specific granule marker, lactoferrin.** Figure shows labeling results after phagocytosis of 1-μm latex beads for the longest time period (1 h), myeloperoxidase (10 nm gold, *arrowhead*) entered the latex bead phagosome (*L*), while the electron translucent organelle containing TIMP-1 (5 nm gold, *small arrow*) still remained separate (*a*). At a shorter time (20 min), lactoferrin (10 nm gold, *arrowhead*) entered the latex bead phagosome (*L*) while the electron translucent organelle containing TIMP-1 (5 nm gold, *small arrow*) remained separate (*b*). The presence of myeloperoxidase in the phagosome (*L*) after the longest incubation time indicates that the phagosome has fully matured (*a*). *Bars*, 200 nm.

subpopulation of lactoferrin- and pro-MMP-8-positive specific granules (results not shown). Non-inclusion of TIMP-1, pro-MMP-9, and most of pro-MMP-8 into the phagosome is unlikely, therefore, to be due to partial or incomplete phagosomal maturation.

DISCUSSION

Neutrophil granule and vesicle proteins appear to be segregated into different granules and vesicle populations on the basis of their *in vivo* roles. This is thought to occur through the concurrent synthesis of groups of proteins of related function, at particular stages of neutrophil development (18, 19, 80). Thus, any colocalization of a protein of interest with granule or vesicle marker proteins of known *in vivo* function may provide clues to the function of that protein, its time of synthesis, and site of action (*i.e.* phagosomal or extracellular).

We have shown here that the major TIMP-1 vesicle population appears devoid of markers for the known major granule and vesicle types (9, 79). Discrete sorting into a separate vesicle population may occur by self-association into high molecular weight forms (71–73), as seen here, and "retention" in the Golgi (80). We propose, however, that the markers in the minor TIMP-1 subpopulations give an indication of the time of synthesis of the major TIMP-1 vesicle, and pointers to its function.

One TIMP-1 subpopulation contains minor amounts of the specific granule markers, lactoferrin and pro-MMP-8, which are synthesized during the intermediate, myelocytic to metamyelocytic, stage of differentiation. Slightly more pro-MMP-9, a gelatinase granule marker, synthesized during later differentiation from the metamyelocyte to the "band" stage (9, 80) is seen in another subpopulation. The TIMP-1 vesicles are devoid of markers for terminal differentiation, *i.e.* the secretory vesicle markers, albumin (9), and GPI-anchored proteins. Considering the markers present in the TIMP-1 subpopulations and the density and morphology of the major TIMP-1 vesicle, we speculate that TIMP-1 synthesis may occur after late metamyelocytic differentiation but before secretory vesicle synthesis, and possibly before synthesis of the gelatinase granule. The TIMP-1 organelles are more electron-translucent and pleomorphic than

most granules but resemble secretory vesicles, and we suggest that they should be similarly named "vesicles."

The compartmentalization of most of the TIMP-1 to a distinct vesicle, largely separated from pro-MMP-8 and pro-MMP-9, may allow the neutrophil to selectively degranulate TIMP-1, without releasing the pro-MMPs. Such a pool of free TIMP-1 could be released prior to pro-MMP degranulation, to provide sufficient extracellular TIMP-1 to control the extent of MMP activity. Alternatively, it could be released after pro-MMP degranulation and activation, allowing initial proteolysis and invasion to occur, but subsequently terminating proteolysis and limiting tissue damage.

The colocalization of TIMP-1 with varying amounts of pro-MMP-9 in a minor vesicle subpopulation may assist in a finer regulation of neutrophil-derived MMP proteolytic activity. Colocalization suggests that these proteins may be released as a heterodimer. As TIMP-1 binds to pro-MMP-9 at a site distant from its inhibitory binding site, pro-MMP-9 may be able, in effect, to carry TIMP-1 "piggy-back" to its site of action. Here, after pro-MMP-9 activation, the TIMP-1 could be responsible for the rapid local inhibition of MMP-9 and hence its limited action. Pro-MMP-8, released together with TIMP-1 (but uncomplexed to TIMP-1) may have a similar limited action.

During inflammation, neutrophils selectively release some granule populations and retain others, depending on the stimulus. Similarly, IgG-opsonized bacteria induce phagocytosis (2) and cause fusion of lactoferrin-containing specific granules, followed by azurophil granules, with the phagosome (81, 82). Our data suggest that the TIMP-1 vesicles and pro-MMP-9-containing gelatinase granules do not, however, fuse with the IgG-coated bead-containing phagosome. Therefore, TIMP-1 vesicles appear to be under a different fusogenic control than the azurophil and specific granules, perhaps differentially associated with the cytoskeleton, as has been described for the gelatinase granules and MMP-8-positive, lactoferrin-negative specific granules (13, 83).

The primary function of neutrophils is the phagocytic destruction of pathogens, a function for which they are equipped with a number of antibacterial toxins and peptides as well as a complex oxidative system. Aside from the pro-MMPs, the two other neutrophil proteinases (cathepsin G and human neutrophil elastase) have microbicidal functionalities independent of proteolysis (2). The fact that the TIMP-1 vesicle does not fuse with the phagosome implies that the TIMP-1 vesicle does not contain other proteins required for the phagocytic destruction of pathogens. Additionally, the fact that this vesicle and the pro-MMP-9-containing vesicles (and most of the MMP-8-positive specific granules) do not fuse with the phagosome suggests that the MMPs and TIMPs may have a strictly extracellular role.

The substrate specificities of MMP-8 and MMP-9 are largely limited to components of the extracellular matrix. Hence, the role of these two highly specific MMPs may be solely to proteolytically facilitate neutrophil passage through the basement membrane and underlying stroma. The exclusion of the MMPs (except for low levels of pro-MMP-8) from the phagosome also implies that pro-MMP-8 and pro-MMP-9 activation is not brought about intracellularly by myeloperoxidase-derived HOCl, other reactive oxygen species, or cathepsin G (68) released into the phagosome.

The long-standing hypothesis that neutrophils utilize proteases (MMPs and serine proteinases) during extravasation has been questioned (84, 85). Some groups report that neutrophils preferentially use physical mechanisms rather than proteolytic means of migration (84–86) as *in vitro* studies, using radiolabeled extracellular matrix components (85), have concluded that little proteolytic activity is involved in the invasion process. Others, using *in vitro* model systems (87) or whole animal systems (88), confirm the relevance of MMPs in neutrophil extravasation (87, 88) and secreted TIMP-1 in preventing invasion (89). We believe that extensive proteolysis is unnecessary for migration (89) as only limited, single-site cleavage of type I and IV collagens is required for the unwinding of the collagen tropohelices, to assist the passage of neutrophils through the extracellular matrix. We propose that neutrophils allow limited release of both MMP-8 and MMP-9 to effect such cleavage, and that the subsequent timely release of TIMP-1 may play an important role in rapidly inhibiting and hence localizing and controlling the extent of MMP activity. The location of TIMP-1, separate from its target enzymes, in a vesicle that may be differentially mobilized would facilitate the required fine regulation of such a proteolytic process.

In conclusion, the major TIMP-1 vesicle population described here differs from other neutrophil organelles on the basis of overall collective features such as marker colocalizations, size, shape, and non-fusogenicity with the phagosome. We thus conclude it is a novel neutrophil compartment. Both the separate location and colocalization of TIMP-1 with MMP-9 in this novel compartment and the mechanisms and manner of release that we have proposed may explain the limited proteolysis seen during neutrophil invasion.

Acknowledgment—We are grateful to Dr Gareth Griffiths for guidance, critical appraisal of this manuscript, and for many helpful suggestions.

REFERENCES

1. Yu, A. E., Hewitt, R. E., Kleiner, D. E., and Stetler-Stevenson, W. G. (1996) *Biochem. Cell Biol.* **74,** 823–831
2. Edwards, S. J. (1994) *Biochemistry and Physiology of the Neutrophil,* Cambridge University Press, Cambridge, United Kingdom
3. Murphy, G., Bretz, U., Baggiolini, M., and Reynolds, J. J. (1980) *Biochem. J.* **192,** 517–525
4. Triebel, S., Bläser, J., Gote, T., Pelz, G., Schüren, E., Schmitt, M., and Tschesche, H. (1995) *Eur. J. Biochem.* **231,** 714–719
5. Ishibashi, H., Hayashida, K., and Okubo, H. (1988) *Methods Enzymol.* **163,** 485–495
6. Denhardt, D. T., Feng, B., Edwards, D. R., Cocuzzi, E. T., and Malyantar, U. M. (1993) *Pharmacol. Ther.* **59,** 329–341
7. Gomez, D. E., Alonso, D. F., Yoshiji, H., and Thorgeirsson, U. P. (1997) *Eur. J. Cell Biol.* **74,** 111–123
8. Murphy, G., and Willenbrock, F. (1995) *Methods Enzymol.* **248,** 496–509
9. Borregaard, N., and Cowland, J. B. (1997) *Blood.* **89,** 3503–3508
10. Nitsche, M., Gabrijelcic, D., and Tschesche, H. (1990) *Biol. Chem. Hoppe-Seyler* **371,** 611–615
11. Oren, A., and Taylor, J. M. G. (1995) *J. Lab. Clin. Med.* **125,** 340–347
12. Rice, W. G., Ganz, T., Kinkade, J. M., Selsted, M. E., Lehrer, R. I., and Parmley, R. T. (1987) *Blood* **70,** 757–765
13. Schettler, A., Thorn, H., Jokusch, B. M., and Tschesche, H. (1991) *Eur. J. Biochem.* **197,** 197–201
14. Sengeløv, H. (1996) *Eur. J. Haematol. Suppl.* **58,** 7–24
15. Sengeløv, H., Follin, P., Kjeldsen, L., Lollike, K., Dahlgren, C., and Borregaard, N. (1995) *J. Immunol.* **154,** 4157–4165
16. Bainton, D. F., Ullyot, J. L., and Farquhar, G. D. (1971) *J. Exp. Med.* **134,** 907–934
17. Pryzwansky, K. B., and Breton-Gorius, J. (1985) *Lab. Invest.* **53,** 664–671
18. Fouret, P., Du Bois, R. M., Bernaudin, J.-F., Takahashi, H., Ferrans, V. J., and Crystal, R. G. (1989) *J. Exp. Med.* **169,** 833–845
19. Le-Cabec, V., Cowland, J. B., Calafat, J., and Borregaard, N. (1996) *Proc. Natl. Acad. Sci. U. S. A.* **93,** 6454–6457
20. Joiner, K. A., Ganz, T., and Rotrosen, D. (1989) *J. Cell Biol.* **109,** 2771–2782
21. Bentwood, B. J., and Henson, P. M. (1980) *J. Immunol.* **124,** 855–862
22. Borregaard, N., Christensen, L., Bjerrum, O. W., Birgens, H. S., and Clemmensen, I. (1992) *J. Clin. Invest.* **90,** 86–90
23. Borregaard, N., Lollike, K., Kjeldsen, L., Sengeløv, H., Bastholm, L., Nielsen, M. H., and Bainton, D. F. (1993) *Eur. J. Haematol.* **51,** 187–198
24. Lew, P. D., Wollheim, C., Waldvogel, F. A., and Pozzan, T. (1994) *J. Cell Biol.* **99,** 1212–1220
25. Oda, T., Katori, M., Hatanaka, K., and Yamashina, S. (1992) *Mediators Inflamm.* **1,** 403–410
26. Jost, C. R., Huizinga, T. W. J., de Goede, R., Fransen, J. A. M., Tetteroo, P. A. T., Daha, M. R., and Ginsel, L. A. (1990) *Blood* **75,** 144–151
27. Kobayashi, T., and Robinson, J. M. (1991) *J. Cell Biol.* **113,** 743–756
28. Chesler, L., Golde, D. W., Bersch, N., and Johnson, M. D. (1995) *Blood.* **86,** 4506–4515
29. Guedez, L., Courtemach, L., and Stetler-Stevenson, M. (1998) *Blood.* **92,** 1342–1349
30. Guedez, L., Stetler-Stevenson, W. G., Wolff, L., Wang, J., Fukushima, P.,

Mansoor, A., and Stetler-Stevenson, M. (1998) *J. Clin. Invest.* **102,** 2002–2010
31. Hayakawa, T., Yamashita, K., Tanzawa, K., Uchijima, E., and Iwata, K. (1992) *FEBS Lett.* **298,** 29–32
32. Patarca, R., and Haseltine, W. A. (1985) *Nature* **318,** 390
33. Takigawa, M., Nishida, Y., Suzuki, F., Kishi, J.-I., Yamashita, K., and Hayakawa, T. (1990) *Biochem. Biophys. Res. Commun.* **171,** 1264–1271
34. Zhao, W.-Q., Yamashita, K., Guo, X.-K., Hoshino, T., Yoshida, S., Shinya, T., and Hayakawa, T. (1998) *J. Cell Sci.* **111,** 1147–1153
35. Cao, J., Sato, H., Takino, T., and Seiki, M. (1995) *J. Biol. Chem.* **270,** 801–805
36. Sato, H., Takino, T., Okada, Y., Cao, J., Shinagawa, A., Yamamoto, E., and Seiki, M. (1994) *Nature* **370,** 61–65
37. Bergmann, U., Michaelis, J., Oberhoff, R., Knäuper, V., Beckmann, R., and Tschesche, H. (1989) *J. Clin. Chem. Clin. Biochem.* **27,** 351–353
38. Bøyum, A. (1976) *Scand. J. Immunol.* **5,** 9–107
39. Roos, D., and de Boer, M. (1986) *Methods Enzymol.* **132,** 225–241
40. Zor, T., and Selinger, Z. (1996) *Anal. Biochem.* **236,** 302–308
41. Dennison, C., and Lovrien, R. (1997) *Protein Express. Purif.* **11,** 149–161
42. Kleiner, D. E., and Stetler-Stevenson, W. G. (1994) *Anal. Biochem.* **218,** 325–329
43. Schägger, H., and von Jagow, G. (1987) *Anal. Biochem.* **166,** 368–379
44. Blum, H., Beier, H., and Gross, H. J. (1987) *Electrophoresis* **8,** 93–99
45. Ko, Y.-G., and Thompson, G. A. (1995) *Anal. Biochem.* **224,** 166–172
46. Low, M. G., Futerman, A. H., Ackermann, K. E., Sherman, W. R., and Silman, I. (1987) *Biochem. J.* **241,** 615–619
47. Polson, A., Coetzer, T., Kruger, J., von Maltzahn, E., and van der Merwe, K. J. *Immunol. Invest.* 14, 323–327
48. Towbin, H., Staehelin, T., and Gordon, J. (1979) *Proc. Natl. Acad. Sci. U. S. A.* **76,** 4350–4354
49. Matsudaira, P. T. (1989) *A Practical Guide to Protein and Peptide Purification for Microsequencing*, pp. 5–30, Academic Press, San Diego
50. Drouin, L., Overall, C. M., and Sodek, J. (1988) *J. Periodont. Res.* **23,** 370–377
51. Bollag, D. M., and Edelstein, S. J. (1991) *Protein Methods*, p. 173, Wiley-Liss Inc., New York
52. Osthues, A., Knäuper, V., Oberhoff, R., Reinke, H., and Tschesche, H. (1992) *FEBS Lett.* **296,** 16–19
53. Andrews, P. C., and Krinsky, N. I. (1986) *Methods Enzymol.* **132,** 369–370
54. Cramer, E., Pryzwansky, K. B., Villeval, J.-L., Testa, U., and Breton-Gorius, J. (1985) *Blood* **65,** 423–432
55. Egesten, A., Breton-Gorius, J., Guichard, J., Gullberg, U., and Olsson, I. (1994) *Blood* **83,** 2985–2989
56. Absolom, D. R. (1986) *Methods Enzymol.* **132,** 95–180
57. Griffiths, G. (1993) *Fine Structure Immunocytochemistry,* Springer-Verlag, Berlin
58. Tokuyasu, K. T. (1986) *J. Microsc.* **143,** 139–149
59. Liou, W., Geuze, H. J., and Slot, J. W. (1996) *Histochem. Cell Biol.* **106,** 41–58
60. Roberts, I. M. (1975) *J. Microsc.* **103,** 113–119
61. Weibel, E. R. (1979) *Stereological Methods: Practical Methods for Biological Morphometry*, Vol. 1, Academic Press, London
62. Kjeldsen, L., Bainton, D. F., Sengeløv, H., and Borregaard, N. (1993) *Blood* **82,** 3183–3191
63. Slot, J. W., and Geuze, H. J. (1985) *Eur. J. Cell Biol.* **38,** 87–93
64. Berger, M., Wetzler, E., August, J. T., and Tartakoff, A. M. (1994) *J. Clin. Invest.* **94,** 1113–1125
65. Polson, A., Potgieter, G. M., Largier, J. F., Mears, E. G. F., and Joubert, F. J. (1964) *Biochim. Biophys. Acta* **82,** 463–475
66. Davis, G. E. (1991) *Arch. Biochem. Biophys.* **286,** 551–554
67. Babbs, C. F., and Steiner, M. G. (1990) *Methods Enzymol.* **186,** 137–147
68. Weiss, S. J. (1989) *N. Engl. J. Med.* **320,** 365–376
69. Uesugi, M., Hayashi, T., and Jasin, H. E. (1998) *J. Immunol.* **161,** 1422–1427
70. Stricklin, G. P., and Hoidal, J. R. (1992) *Matrix Suppl.* **1,** 325
71. Cawston, T. E., Mercer, E., Mooney, C., and Wright, J. K. (1986) in *Proteinases in Inflammation and Tumor Invasion* (Tschesche, H., ed) pp. 189–201, Walter de Gruyter & Co., Berlin
72. Cawston, T. E., Noble, D. N., Murphy, G., Smith, A. J., Woodley, C., and Hazleman, B. (1986) *Biochem. J.* **238,** 677–682
73. Mercer, E., Cawston, T. E., De Silva, M., and Hazleman, B. L. (1985) *Biochem. J.* **231,** 505–510
74. Docherty, A. J. P., Lyons, A., Smith, B. J., Wright, E. M., Stephens, P. E., and Harris, T. J. R. (1985) *Nature* **318,** 66–69
75. Breton-Gorius, J., Mason, D. Y., Buriot, D., Vilde, J.-L., and Griscelli, C.(1980) *Am. J. Pathol.* **99,** 413–417
76. Borregaard, N., Sehested, M., Nielsen, B. S., Sengeløv, H., and Kjeldsen, L. (1995) *Blood* **85,** 812–817
77. Dewald, B., Bretz, U., and Baggiolini, M. (1982) *J. Clin. Invest.* **70,** 518–525
78. Kjeldsen, L., Johnsen, A. H., Sengeløv, H., and Borregaard, N. (1993) *J. Biol. Chem.* **268,** 10425–10432
79. Cieutat, A.-M., Lobel, P., August, T. J., Kjeldsen, L., Sengeløv, H., Borregaard, N., and Bainton, D. F. (1999) *Blood* **91,** 1044–1058
80. Gullberg, U., Andersson, E., Garwicz, D., Lindmark, A., and Olsson, I. (1997) *Eur. J. Haematol.* **58,** 137–143
81. Bainton, D. F. (1973) *J. Cell Biol.* **58,** 249–264
82. Segal, A. W., Dorling, J., and Coade, S. (1980) *J. Cell Biol.* **85,** 42–59
83. Rothwell S. W., Nath, J., and Wright, D. G. (1989) *J. Cell Biol.* **108,** 2313–2326
84. Mackerel, J. A., Cottell, D. C., Russell, K. J., Fitzgerald, M. X., and O'Connor, C. M. (1999) *Am. J. Respir. Cell Mol. Biol.* **20,** 1209–1219
85. Steadman, R., St John, P. L., Evans, R. A., Thomas, G. J., Davies, M., Heck, L. W., and Abrahamson, D. R. (1997) *Int. J. Biochem. Cell Biol.* **395,** 993–1004
86. Mandeville, J. T. H., Lawson, M. A., and Maxfield, F. R. (1997) *J. Leuk. Biol.* **61,** 188–200
87. Itoh, Y., and Nagase, H. (1995) *J. Biol. Chem.* **270,** 16518–16521
88. Oda, T., Katori, M., Hatanaka, K., and Nagai, Y. (1995) *Mediators Inflamm.* **4,** 133–137
89. Bakowski, B., and Tschesche, H. (1992) *Biol. Chem. Hoppe-Seyler* **343,** 529–546

CRYO-IMMUNOCYTOCHEMICAL LOCALISATION OF TIMP-1 WITH RESPECT TO PRO-MMPs AND GRANULE MARKER PROTEINS IN NEUTROPHILS

B. Price[§], E. Elliott[§], C. Dennison[§] and H. Tschesche[†]

[§]Department of Biochemistry, University of Natal, Pietermaritzburg and [†]Department of Biochemistry, University of Bielefeld, Germany

Mature neutrophils (PMNs) produce four major cytoplasmic granule populations (azurophilic, specific, gelatinase, secretory) at distinct stages of development. Each granule population is characterised by the presence of various enzymes, receptors and bactericidal proteins, many of which have previously been designated as markers.

The matrix metalloproteinases (MMPs) are a family of neutral Zn^{2+} and Ca^{2+}-dependent enzymes that show exceptional proteolytic activity against various collagens and basement membrane components[1]. The MMPs have hence been implicated in assisting the invasive activity of metastasising primary tumours and may be utilised by inflammatory neutrophils (PMNs)[2]. Active MMPs are inhibited by TIMPs (Tissue Inhibitors of Matrix metalloProteinases) which are known to be secreted by various cell populations such as fibroblasts, macrophages and lymphocytes. It has been proposed that a fine balance of MMPs and TIMPs is required for normal matrix turnover to take place[3]. It is important to establish the PMN granule localisation of proMMPs in relation to possible inhibitor(s) in order to devise strategies to control inflammatory invasive processes.

ProMMP-8 (type I collagenase) and proMMP-9 (type IV collagenase) have previously been localised to the specific (proMMP-8 & proMMP-9) and gelatinase (proMMP-9) granules and are processed into their active forms upon release into the extracellular environment during activation[4]. Northern blot analysis of blood PMN mRNA indicated the presence of a TIMP-1 transcript and it was hence hypothesised that PMNs may regulate their own collagenolytic activity[5].

PMN MMP-8 & 9 were isolated from blood and TIMP 1 & 2 from the synovial fluid of rheumatoid arthritis patients. Polyclonal antibodies against the purified proteins were raised in rabbits. Western blotting on homogenates of LymphoPrep blood PMN fractions and cultured U937 monocytes assessed the specificity and potential cross-reactivity of the antibodies. Isolated PMNs were fixed, processed for cryo-ultramicrotomy and thawed cryo-sections were double labelled for TIMP and either proMMPs or marker proteins. Antibody binding was detected with 5 and 10 nm protein A gold probes.

TIMP-1 was found in a distinct electron-translucent granule and co-localised with granules containing either human leukocyte elastase, proMMP-8, proMMP-9, and to a lesser extent, lactoferrin. Preliminary results also indicate the absence of TIMP-2 in PMNs. These results imply that TIMP-1 may be synthesised continually throughout PMN maturation and may serve to prevent uncontrolled tissue damage during inflammation or conversely, to assist enzyme activation.

References

1. Woessner, J. F. (1991) FASEB J. 5, 2145.
2. Bernhard, E. J., Gruber, S. B. & Muschel, R. J. (1994) Proc. Natl. Acad. Sci. USA 91, 4293.
3. Matrisian, L. M. (1992) BioEssays 14, 455.
4. Kjeldsen, L., Bjerrum, O. W., Askaa, J. & Boregaard, N. (1992) Biochem. J. 287, 603.
5. Triebel, S., Bläser, J., Gote, T., Pelz, G., Schüren, Schmitt, M. & Tschesche, H. (1995) Eur. J. Biochem. 231, 714.

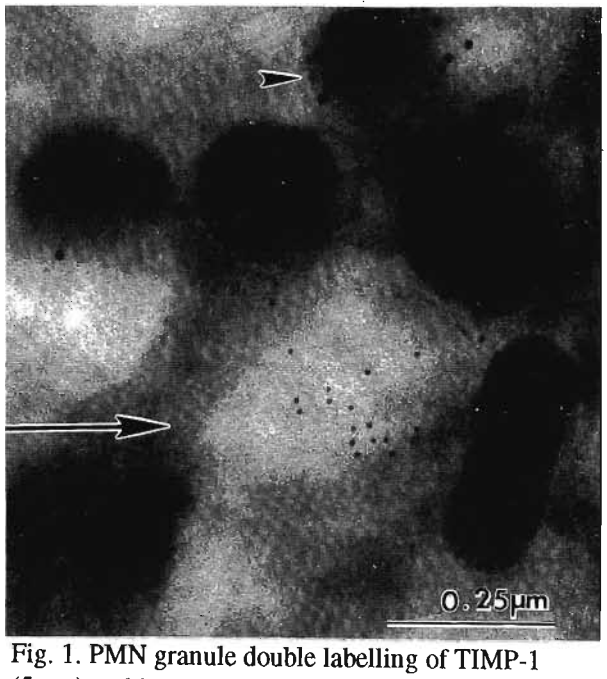

Fig. 1. PMN granule double labelling of TIMP-1 (5 nm) and lactoferrin (10 nm).